



Universitat
de les Illes Balears

DOCTORAL THESIS
2023

**COLORECTAL CANCER STUDY: NEW
BIOMARKERS RESEARCH IN DIFFERENT
SAMPLE TYPES.**

Marina Alorda Clarà



Universitat
de les Illes Balears

DOCTORAL THESIS

2023

**Doctoral Programme in Translational Research in
Public Health and High Prevalence Diseases**

**COLORECTAL CANCER STUDY: NEW
BIOMARKERS RESEARCH IN DIFFERENT
SAMPLE TYPES**

Marina Alorda Clarà

Thesis Supervisor: Jordi Oliver Oliver

Thesis Supervisor: Daniel Gabriel Pons Miró

Thesis tutor: Jordi Oliver Oliver

Doctor by the Universitat de les Illes Balears

Amb el vistiplau dels Directors

Dr. Jordi Oliver Oliver

Catedràtic d'Universitat

Dr. Daniel Gabriel Pons Miró

Professor Titular

Àrea de Bioquímica i Biologia Molecular
Dept. Biologia Fonamental i Ciències de la Salut

La interessada

Marina Alorda Clarà



Universitat
de les Illes Balears

Dr. Jordi Oliver Oliver, of Universitat de les Illes Balears

I DECLARE:

That the thesis titles *Colorectal cancer study: new biomarkers research in different sample types*, presented by Marina Alorda Clarà to obtain a doctoral degree, has been completed under my supervision.

For all intents and purposes, I hereby sign this document.

Signature

Palma de Mallorca, 05 May 2023



Universitat
de les Illes Balears

Dr. Daniel Gabriel Pons Miró, of Universitat de les Illes Balears

I DECLARE:

That the thesis titles *Colorectal cancer study: new biomarkers research in different sample types*, presented by Marina Alorda Clarà to obtain a doctoral degree, has been completed under my supervision.

For all intents and purposes, I hereby sign this document.

Signature

Palma de Mallorca, 05 May 2023

Als meus pares i a en Miquel

Las rosas tienen tanto pétalos como espinas, mi flor oscura. No debes creer que algo es débil porque parece delicado. Muéstrale al mundo tu valentía.

A la Caza de Jack el Destripador. Kerri Maniscalco

Agraïments

Para algunos la vida es galopar por un camino empedrado de horas, minutos y segundos. Yo, más humilde soy, y solo quiero que la ola que surge del último suspiro de un segundo me transporte mecido hasta el siguiente... així que, només puc dir moltes gràcies a totes les persones que m'han acompanyat dintre d'aquesta ona que ens ha estat transportant dintre el camí de la ciència durant aquests 5 anys.

En primer lloc, vull donar les gràcies als meus directors de tesi, el Dr. Jordi Oliver i el Dr. Dani Pons i la meva padrina jove, la Dra. Pilar Roca. Moltes gràcies Jordi per tenir sempre un moment per escoltar un problema, una paraula amable per transformar una llàgrima en una motivació i per tenir sempre solucions als problemes. Moltes gràcies Dani per tot, per tenir 5 minuts per escoltar-me (encara que es transformin en una hora i mitja), per mirar els *powerpoints* eterns amb resultats de PCR que més que resultats són problemes, per tota l'ajuda durant aquests 5 anys i, sobretot, per totes les rialles que hem compartit. Moltes gràcies Pilar per donar-me l'oportunitat de formar part d'aquest grup i de poder obrir-me un petit lloc a la ciència, a més de per tota l'ajuda durant aquest temps. No puc deixar de banda a la resta de professors del grup, el Dr. Jordi Sastre, la Dra. Lida Torrens i la Dra. Mercedes Nadal, que també han estat una part fonamental d'aquesta tesi. Moltes gràcies Jordi per tota l'ajuda durant aquests 5 anys, especialment la que em donares durant els moments més baixos, i també per totes les rialles i *cotilleos* que hem compartit, perquè que donen anys de vida. Moltes gràcies Lida per tota l'ajuda quan no entenia coses, quan tenia problemes dintre el lab i quan la feina em sortia per les orelles. Moltes gràcies Mercedes per tota la teva ajuda durant aquests darrers mesos.

Magdalena, Bel, Ana, Adamo i Emi, també vull agrair-vos totes les paraules d'ànims que m'heu donat durant tots aquests anys. Finalment, José Reyes, també vull agrair el teu recolzament durant aquests anys, ja que sempre has tingut una paraula amable, una rialla i un gran suport per a mi tant dintre de l'àmbit professional, com, sobretot, a l'àmbit personal.

Aquesta tesi no hauria estat possible sense la participació d'unes persones molt importants, els pacients voluntaris que han donat les seves mostres de forma altruista per ajudar a avançar en l'estudi del càncer de colon. Moltes gràcies, sense vosaltres no hauria estat possible.

Moltes gràcies a tot el personal del gabinet de digestiu de l'Hospital Comarcal d'Inca, especialment a na Petra i na Paulina, per tota l'ajuda amb la recollida de mostres.

Un gràcies molt gran per els tècnics de plataforma que han aconseguit les imatges més *guays* que podreu trobar aquí dins, les imatges de microscòpia. Moltes gràcies Guillem Ramis per la teva ajuda amb el microscopi confocal i per les xerradetes mentre esperàvem les imatges, Joan Cifre per la teva ajuda amb el microscopi de forces atòmiques i Toni Busquets per la teva ajuda amb el microscopi electrònic de transmissió i per les converses i rialles durant la *búsqueda y captura* de les vesícules. Finalment, gràcies Arne Fleischer per la teva ajuda amb els *arrays*. No puc oblidar els oficials de laboratori que ens acompanyen dia a dia, moltes gràcies Pep Miquel, Pep Sastre, Guillem, Xisco, Angel, Tolo, Manu i Javi, al personal de neteja i al personal de consergeria, moltes gràcies Macià, Juanma, Joan, Gemma, Aina i Andreu.

Moltes gràcies Marian per tota la teva ajuda amb les vesícules, sense tu no hauria estat possible, ets un sol! Moltes gràcies també al meu metge preferit de Són Llätzer, Guiem, per totes les xerradetes sobre funkos i perquè mai havia estat tant divertit anar a cercar mostres.

Moltes gràcies a totes les persones amb les que he compartit i segueixo compartint lab i despatxet. Margalida, moltes gràcies per totes les rialles que ens fas treure i per tota l'ajuda que m'has donat en aquesta darrera estirada. Maria Magdalena, moltes gràcies per totes les xerradetes i rialles de dematí prèvies a la feina, per tenir sempre un moment per escoltar-me, per comptar amb mi, per estar sempre pendent i preocupar-te de tot. Clara, moltes gràcies per el temps i *cotilleos* compartits. Sou fantàstiques. Gianluca, moltes gràcies per els teus "fins demà boniques" i per preocupar-te per la resta, ets un sol. Estela, *muchas gracias por todas las risas que compartimos, por todas las crisis que tuvimos que afrontar (y superamos) y por los momentos extremadamente divertidos que compartimos*. Dani, *gracias por ser una persona tan bonita y tener una sonrisa para todos*. Andrea, *eres un sol, ojalá los momentos estabulario fueran más de una vez por semana, porque son geniales*. Moltes gràcies Alba i Neus per aquests mesos compartits, tant de bo ens haguéssim conegut abans, sou uns amors. Rita, gràcies per tenir sempre un somriure per tothom. Raül, gràcies per preocupar-te per el benestar de tots. Toni, *tendríamos que dejarte poner más veces música en el labo, que al final alegre los experimentos, sigue teniendo ideas sin parar y sigue fluyendo, que así es más divertido, pero sobre todo disfruta de ser el más viejo del labo*. Pere, segueix posant el cor a tot el que fas, el món necessita més gent que estimi el que fa. Lucas, que ningú et llevi aquesta dolçor tan cuqui que tens. Les meves *supernenas*, Maria i Laura, gràcies per ser unes amigues fantàstiques, per seguir igual que quan estàvem tot el dia juntes encara que faci mesos que no ens veiem, per totes les rialles que vàrem compartir dintre d'aquestes parets i per les rialles que seguim compartint dintre les parets de ca'n joan de s'aigo. Neus, gràcies per trobar-li el costat positiu a tot, per tenir sempre un somriure a la cara encara que fora hi hagi tempesta i per ser una persona meravellosa. Mel, gràcies per les xerradetes a les 7 del matí, per les caminades contant-mos tota la vida que no hem pogut compartir, per tots els berenars, per les teves paraules, per el teu suport i, sobretot, per la teva amistat. Lida (siii, una altre vegada tu!! No esperaràs que hagués estat tan sosa!?!?!?) gràcies per tenir sempre mil moments per escoltar-me, gràcies per ser la millor companya de lectura del món, per tenir sempre un consell tant per la feina com per fora d'ella, i per ser la meva amiga; i ja saps, *compórtate con la confianza de un hombre blanco mediocre, pero con aún más confianza si es posible, porque tú no tienes nada de mediocre*, així que creu't ho, perquè ets una gran científica i el món ho ha de poder veure.

Moltes gràcies a tots els col·laboradors, TFGs i TFM's que han passat pel lab, perquè amb vosaltres cada dia s'aprèn una cosa nova.

Un gràcies infinit a les meves amigues i amics, Pris, Ana, Salo, Nerea, Estefy, Dani, Albert, Alicia, Quique, Marta, Mariangels, Juan i Andrea, perquè sempre sou allà per contar-vos tant una pena, com una alegria, per fer una berenadeta o un *soparigo*, per fer sa xerradeta o per contar *cotilleos* sense aturar, però sobretot, perquè m'ompliu el coret de felicitat. Sou com un cel ple de les estrelles més brillants.

Gracias Estefy por el diseño más bonito que podía tener de esta portada, el mundo tiene la necesidad de ver tu arte.

Gràcies a la meva gran família. A la meva família Alorda, Titi i Padrino, moltes gràcies per interessar-vos i per alegrar-vos per tot, però sobretot, gràcies per cuidar-me. Joan Pau i Toñi, Macu i Llorenç... vos podria agrair una vida de rialles i d'enfados, però tots sabem que per lo que més agraida vos estic, és per haver-me donat els nebots més meravellosos que mai podria haver desitjat, Sergi, Helena, Albert i Martín, sou com el dia més feliç que hagi viscut mai guardat dins el meu coret. Fàtima, moltes gràcies per interessar-te sempre per el que faig i viure-ho com si fos la cosa més interessant del món, tant de bo tothom tingués la teva curiositat. Pe, Padrina,

Antonieta... el món es queda petit per agrair-te tot el que se t'hauria d'agrair a diari, gràcies per el cor tan gran que tens, per cuidar de tothom, per l'alegria infinita que tens i per ser meravellosa, gràcies per ser la millor padrina del món. A la meva família Clarà, Magelí gràcies per la teva saviesa, les teves paraules i la teva companyia a les sessions científiques. Nen, gràcies per treure sempre el costat divertit a totes les coses, així la vida és més fàcil. Susana, gràcies per les teves paraules, el teu suport i la teva ajuda per mantenir el meu costat friki sempre en marxa. Sense els vostres corets això no hauria estat possible. Albert, gràcies per els teus *chistes* dolents i els teus jocs de paraules que, de tant en tant, em fan gràcia. David i Daniel, gràcies per ser un pilar bàsic per a la meva personalitat friki, *on your left*. A la meva família Enseñat, Fina i Biel, gràcies per tractar-me com una filla més, sou fantàstics i Aina, gràcies per deixar-me fer de germana gran. El dia que varen repartir la família, a mi em va tocar la millor.

Per alguna banda vaig llegir que *solo muere aquello que se olvida...* Iaia, Avi, Padrí, vos puc assegurar que vosaltres sereu infinits, esteu enganxats al meu cor com una pagellida a una roca. Tant de bo fóssiu aquí.

Bala, Baleta, Bebibala, gràcies per ser la millor cusseta del món i omplir el meu coret d'alegria cada vegada que et veig.

No puc xerrar de família i no mencionar als meus estimats i meravellosos pares. Madre, Padre, això no hauria estat possible sense vosaltres. La llista d'agraïments cap a vosaltres es podria fer eterna, així que ho resumiré en que trillions de gràcies per escoltar-me quan vos crit per telèfon plorant o quan vos cont que estic contenta perquè per fi ha anat bé l'experiment que tants de problemes m'estava donant, per el suport infinit que m'heu donat aquests 5 anys (i sempre) i per donar-me tot l'amor que una filla pot desitjar. Aquesta tesi també és vostra.

I per acabar, gràcies Miquel.

Ay mecachis, no m'he atrevit!!! Infinites infinitats de gràcies Miquel, gràcies per ser el meu suport i la meva felicitat, gràcies perquè *és nadal al meu cor, quan somrius content de veure'm i esclates a riure per sota el nas, però sobretot, perquè fas que vida antes que muerte, fuerza antes que debilidad, viaje antes que destino* tingui tot el sentit del multivers. Gràcies per ser com ets i per compartir la teva vida amb mi. T'estim

This thesis has been developed at the *Grup Multidisciplinar d'Oncologia Translacional* (GMOT) at the *Universitat de les Illes Balears*, that forms part of *Institut Universitari d'Investigació en Ciències de la Salut* (IUNICS) and *Institut d'Investigació Sanitària de les Illes Balears* (IdISBa). This study has been possible thanks to the research projects funded by *Fondo de Investigaciones Sanitarias del Instituto de Salud Carlos III* (PI14/01434) from the Spain Government cofounded with FEDER funds "*Una manera de hacer Europa*", by *Projectes Intramurals* from IdISBa (PRI20/15), in addition to the fundraising *Proyecto del Hospital Comarcal de Inca y la Universidad de las Islas Baleares* (CINUIB) from the *Fundació Universitat Empresa de les Illes Balears* (FUEIB). Moreover, the research group has also received funding from *Centro de Investigaciones Biomédicas en Red de Fisiopatología de la Obesidad y Nutrición* (CiberOBN, CB06/03). Finally, the PhD student has received a contract from *Conselleria de Fons Europeus, Universitat i Cultura* (AP_2021_004), IdISBa (SYN18/08), *Sociedad Española de Endoscopia Digestiva* (SEED19/01) and FUEIB (CINUIB).



Contents

Abbreviations	I
List of publications	I
Abstract	II
Resum	IV
Resumen	VI
1. Introduction	1
1.1. Epidemiology and etiology of colorectal cancer	5
1.2. Colorectal cancer classification	7
1.3. Tumoral microenvironment	7
1.4. Relationship between inflammation, angiogenesis, epithelial-mesenchymal transition, and metastasis.....	10
1.5. Mitochondrial functionality and oxidative stress.....	14
1.6. Colorectal cancer and phytoestrogens. The role of genistein	17
1.7. Diagnosis and biomarkers in colorectal cancer.....	19
1.8. Extracellular vesicles	21
2. Objectives and experimental approach	25
3. Materials and Methods	33
3.1. Samples	35
3.2. General procedures with cell culture	38
3.3. Methodology.....	41
4. Results	59
Manuscript 1. Antioxidant enzymes change in different non-metastatic stages in tumoral and peritumoral tissues of colorectal cancer.....	61
Manuscript 2. Inflammation-and metastasis-related proteins expression changes in early stages in tumor and non-tumor adjacent tissues of colorectal cancer samples	71
Manuscript 3. Isolation and characterization of extracellular vesicles in human bowel lavage fluid	87
Manuscript 4. Analysis of miRNAs and mRNAs expression in extracellular vesicles from bowel lavage fluid in colorectal cancer patients.....	101
Manuscript 5. High concentrations of genistein decrease cell viability depending on oxidative stress and inflammation in colon cancer cell lines.....	133
5. Recapitulation	155
6. Conclusions	161
7. References	165
8. Appendix	181

Manuscript 6. The phytoestrogen genistein affects inflammatory-related genes expression depending on the $Er\alpha/Er\beta$ ratio in breast cancer cells	183
Manuscript 7. Micronutrients selenomethionine and selenocysteine modulates the redox status of MCF-7 breast cancer cells	195
Manuscript 8. Xanthohumol reduces inflammation and cell metabolism in HT29 primary colon cancer cells	207
Manuscript 9. Use of omics technologies for the detection of colorectal cancer biomarkers	219

Abbreviations

18S: 18S ribosomal RNA

acMnSOD: Acetylated manganese superoxide dismutase

AFM: Atomic force microscopy

ATP: Adenosine triphosphate

B2M: Beta-2-microglobulin

BLF: Bowel lavage fluid

BSA: Bovine serum albumin

CAT: Catalase

COX2: Cyclooxygenase 2

CRC: Colorectal cancer

CXCL8: Interleukin 8

CXCR2: Interleukin 8 receptor

DMEM: Dulbecco's modified eagle's medium high glucose

DMSO: Dimethyl sulfoxide

ECM: Extracellular matrix

EcSOD: Extracellular superoxide dismutase

EGF: Epidermal growth factor

EMT: Epithelial-mesenchymal transition

ESCRT: Endosomal sorting complex required for transport

ESRRA and ERR α : Estrogen related receptor alpha

EVs: Extracellular vesicles

FBS: Fetal bovine serum

FOXO3: Forkhead box O3

GAPDH: Glyceraldehyde-3-phosphate dehydrogenase

GEN: Genistein

GPX1 and GPx: Glutathione peroxidase

GRd: Glutathione reductase

H₂O₂: Hydrogen peroxide

HC: High risk + cancer samples

HIF1 α : Hypoxia-inducible factor 1-alpha

HL: Healthy + low-risk samples

HPSE: Heparanase

IFN γ : Interferon gamma

IGF-1: Insulin-like growth factor 1

IKK: I κ B kinase

IL: Interleukin

IL10 and IL-10: Interleukin 10

IL1B and IL-1 β : Interleukin 1 beta

IL-4R: Interleukin 4 receptor

iNOS: Inducible nitric oxide

I κ B: Inhibitor of kappa B

miRNAs: MicroRNA

MMP9: Matrix metalloproteinase 9

mRNAs: Messenger RNA

mtDNA: Mitochondrial DNA

NF- κ B: Nuclear factor kappa B

NRF1: Nuclear respiratory factor 1

NRF2: Nuclear respiratory factor 2

NTA: Nanoparticle tracking analysis

O₂⁻: Superoxide anion

PINK1: PTEN-induced kinase 1

pI κ B: Inhibitor of kappa B phosphorylated

PPARG and PPAR γ : Peroxisome proliferator activated receptor gamma

PPARGC1A and PGC1 α : Peroxisome proliferator-activated receptor gamma coactivator 1-alpha

PPAR α : Peroxisome proliferator-activated receptor alpha

PSA: Ammonium persulfate

RNS: Reactive nitrogen species

ROS: Reactive oxygen species

SD: Standard deviation

SEM: Standard error of the mean

SOD1 and CuZnSOD: Copper-zinc superoxide dismutase

SOD2 and MnSOD: Manganese superoxide dismutase

SPSS: Statistical program for the social sciences software for windows

SSBP1 and mtSSB: Mitochondrial single stranded DNA binding protein 1

STAT: Signal transducer and activator of transcription

TBS-Tween: Tris buffer saline 0.05% Tween 20

TEM: Transmission electron microscopy

TEMED: N,N,N',N'-Tetramethyl ethylenediamine

TFAM: Transcription factor A

TGF β : Transforming growth factor beta

TNF and TNF α : Tumor necrosis factor alpha

VEGF: vascular endothelial growth factor

List of publications

This thesis has led to the following publications:

Gaya-Bover, A., Hernández-López, R., Alorda-Clara, M., de la Rosa, J. M. I., Falcó, E., Fernández, T., Company, M. M., Torrens-Mas, M., Roca, P., Oliver, J., Sastre-Serra, J. & Pons, D. G. (2020). **Antioxidant enzymes change in different non-metastatic stages in tumoral and peritumoral tissues of colorectal cancer.** *The International Journal of Biochemistry & Cell Biology*, 120, 105698. doi: 10.1016/j.biocel.2020.105698.

Alorda-Clara, M., Torrens-Mas, M., Hernández-López, R., Ibarra de la Rosa, J. M., Falcó, E., Fernández, T., Company, M. M., Sastre-Serra, J., Oliver, J., Pons, D. G., & Roca, P. (2022). **Inflammation-and Metastasis-Related Proteins Expression Changes in Early Stages in Tumor and Non-Tumor Adjacent Tissues of Colorectal Cancer Samples.** *Cancers*, 14(18), 4487. doi: 10.3390/cancers14184487.

Alorda-Clara, M., Reyes, J., Trelles-Guzman, M. G., Florido, M., Roca, P., Pons, D. G., & Oliver, J. (2023). **Isolation and Characterization of Extracellular Vesicles in Human Bowel Lavage Fluid.** *International Journal of Molecular Sciences*, 24(8), 7391. Doi: 10.3390/ijms24087391.

Alorda-Clara, M., Torrens-Mas, M., Morla-Barcelo, P. M., Roca, P., Sastre-Serra, J., Pons, D. G., & Oliver, J. (2022). **High Concentrations of Genistein Decrease Cell Viability Depending on Oxidative Stress and Inflammation in Colon Cancer Cell Lines.** *International journal of molecular sciences*, 23(14), 7526. doi: 10.3390/ijms23147526.

Furthermore, the following papers derived from the thesis are being prepared or being reviewed:

Analysis of miRNAs and mRNAs expression in extracellular vesicles from bowel lavage fluid in colorectal cancer patients

Moreover, during this thesis, the PhD student has been involved in collaborations leading to the papers presented in the appendix:

Pons, D. G., Vilanova-Llompart, J., Gaya-Bover, A., Alorda-Clara, M., Oliver, J., Roca, P., & Sastre-Serra, J. (2019). **The phytoestrogen genistein affects inflammatory-related genes expression depending on the ER α /ER β ratio in breast cancer cells.** *International journal of food sciences and nutrition*, 70(8), 941-949. doi: 10.1080/09637486.2019.1597025.

Pons, D. G., Moran, C., Alorda-Clara, M., Oliver, J., Roca, P., & Sastre-Serra, J. (2020). **Micronutrients selenomethionine and selenocysteine modulate the redox status of MCF-7 breast cancer cells.** *Nutrients*, 12(3), 865. doi: 10.3390/nu12030865.

Torrens-Mas, M., Alorda-Clara, M., Martínez-Vigara, M., Roca, P., Sastre-Serra, J., Oliver, J., & Pons, D. G. (2022). **Xanthohumol reduces inflammation and cell metabolism in HT29 primary colon cancer cells.** *International Journal of Food Sciences and Nutrition*, 73(4), 471-479. doi: 10.1080/09637486.2021.2012561.

Alorda-Clara, M., Torrens-Mas, M., Morla-Barcelo, P. M., Martinez-Bernabe, T., Sastre-Serra, J., Roca, P., Pons, D.G., Oliver, J. & Reyes, J. (2022). **Use of Omics Technologies for the Detection of Colorectal Cancer Biomarkers.** *Cancers*, 14(3), 817. doi: 10.3390/cancers14030817.



This thesis is presented as a research papers compendium previously published or accepted. Complete references of publications that forms part of the thesis nucleus and their quality index are:

Gaya-Bover, A., Hernández-López, R., Alorda-Clara, M., de la Rosa, J. M. I., Falcó, E., Fernández, T., Company, M. M., Torrens-Mas, M., Roca, P., Oliver, J., Sastre-Serra, J. & Pons, D. G. (2020). **Antioxidant enzymes change in different non-metastatic stages in tumoral and peritumoral tissues of colorectal cancer.** *The International Journal of Biochemistry & Cell Biology*, 120, 105698. doi: 10.1016/j.biocel.2020.105698. Impact factor (2021): 5.652 (Q2 in Biochemistry and Molecular Biology category and Q2 in Cell Biology category).

Alorda-Clara, M., Torrens-Mas, M., Hernández-López, R., Ibarra de la Rosa, J. M., Falcó, E., Fernández, T., Company, M. M., Sastre-Serra, J., Oliver, J., Pons, D. G., & Roca, P. (2022). **Inflammation-and Metastasis-Related Proteins Expression Changes in Early Stages in Tumor and Non-Tumor Adjacent Tissues of Colorectal Cancer Samples.** *Cancers*, 14(18), 4487. doi: 10.3390/cancers14184487. Impact factor (2021): 6.575 (Q1 in Oncology category).

Alorda-Clara, M., Reyes, J., Trelles-Guzman, M. G., Florido, M., Roca, P., Pons, D. G., & Oliver, J. (2023). **Isolation and Characterization of Extracellular Vesicles in Human Bowel Lavage Fluid.** *International Journal of Molecular Sciences*, 24(8), 7391. Doi: 10.3390/ijms24087391. Impact factor (2021): 6.208 (Q1 in Biochemistry and Molecular Biology category, and Q2 in Multidisciplinary Chemistry category).

Alorda-Clara, M., Torrens-Mas, M., Morla-Barcelo, P. M., Roca, P., Sastre-Serra, J., Pons, D. G., & Oliver, J. (2022). **High Concentrations of Genistein Decrease Cell Viability Depending on Oxidative Stress and Inflammation in Colon Cancer Cell Lines.** *International journal of molecular sciences*, 23(14), 7526. doi: 10.3390/ijms23147526. Impact factor (2021): 6.208 (Q1 in Biochemistry and Molecular Biology category, and Q2 in Multidisciplinary Chemistry category).



Colorectal cancer study: new biomarkers research in different sample types

Doctoral Thesis, Marina Alorda Clarà

Department of Fundamental Biology and Health Sciences, University of Balearic Islands, Palma, Spain

Abstract

Colorectal cancer is the third most common cancer worldwide and the second cause of cancer death, in fact, the 5-year survival decreases drastically across the stages. This decrease in survival in the advanced stages indicates the need of an early diagnosis. The new biomarker research is focused on the study of colorectal cancer tissues, but despite oxidative stress, inflammation, and the epithelial-mesenchymal transition are key processes for the development of this disease, their role in early stages is not well established yet. As well as the possibility of finding biomarkers in tumor tissues, these new biomarkers could be found in extracellular vesicles, because the extracellular vesicles are released from colorectal cancer cells since early stages. Moreover, these vesicles are delimited by a lipid bilayer that protects the extracellular vesicles content from degradation. Extracellular vesicles are found in most biological fluids, therefore could be found in bowel lavage fluid, which is an uncommon sample type acquired during colonoscopies with a huge potential as a colorectal cancer study sample. Finally, the main function of extracellular vesicles is to act as a communicator between cells. Diet is a factor risk of colorectal cancer since it participates in initiation and progression of colorectal cancer. Genistein, an isoflavone found in soybean, present an important effect in colorectal cancer, but the mechanism by which performs its action remains unclear.

For these reasons, the objectives of this thesis were: 1) to determine the changes in oxidative stress, inflammation, epithelial-mesenchymal transition, and metastasis related proteins in tumor and non-tumor adjacent tissues from patients with colorectal cancer in all the stages; 2) to analyze the bowel lavage fluid and its extracellular vesicles as a research sample for study and diagnosis of colorectal cancer; 3) to study the RNA content from extracellular vesicles isolated from bowel lavage fluid from colorectal cancer patients; 4) to determine the effect of genistein on oxidative stress, mitochondrial biogenesis, and inflammatory status in primary and metastatic colon cancer cell lines.

The obtained results indicate that early stages of colorectal cancer, especially stage II, present molecular characteristics that belong to advanced stages, which indicates the importance of early stages for the disease development and the possibility of using these changes as a source of possibly early biomarker of colorectal cancer. The non-tumor adjacent tissue presents an increase in inflammatory status across the stages, which could indicate a communication between both tissue types, which could be done by extracellular vesicles released by tumor cells. These extracellular vesicles can be isolated from bowel lavage fluid and can be used as a biomarker source, because its content can reflect the origin cell status. Furthermore, the content of extracellular vesicles from cancer patients is enriched in mRNAs and miRNAs, which participate in pathways related to oxidative stress and mitochondria, inflammation, proliferation, and cell death. Finally, all these mentioned pathways are modified by genistein to decrease cell viability in cells from primary and metastatic tumors in a different way.

In conclusion, the study of early stages of colorectal cancer allows an increase in the disease progression knowledge in addition to their function as a biomarker source, that can also be found in extracellular vesicles content, for diagnosis and prognosis of colorectal cancer to improve the survival of colorectal cancer patients.



Estudi del càncer de colon: recerca de nous biomarcadors en diferents tipus de mostra

Tesi Doctoral, Marina Alorda Clarà

Departament de Biologia Fonamental i Ciències de la Salut, Universitat de les Illes Balears, Palma, Espanya

Resum

El càncer colorectal és la tercera neoplàsia més comú al món i la segona causa de mort per càncer, de fet, la supervivència als 5 anys va disminuint dràsticament al llarg dels estadis d'aquesta malaltia. Aquesta disminució als estadis més avançats indica la necessitat d'un diagnòstic primerenc. La recerca de nous marcadors per al diagnòstic i pronòstic de la malaltia es centra en l'estudi dels teixits afectats per el càncer, però a pesar de que l'estrès oxidatiu, la inflamació i la transició epitel·li-mesènquima són processos clau per al desenvolupament d'aquesta patologia no es coneix bé el seu paper als estadis primerencs. A més de trobar aquests marcadors als teixits afectats, també es podrien trobar a les vesícules extracel·lulars, ja que s'alliberen per les cèl·lules del càncer colorectal des de estadis primerencs. A més, les vesícules estan delimitades per una bicapa lipídica que protegeix el seu contingut de la degradació. Aquestes vesícules es troben a la majoria de fluids del cos, per tant es podrien trobar a l'aspirat del lumen intestinal, que es una mostra poc coneguda que es recull durant les colonoscòpies i que té un gran potencial com a eina per a l'estudi d'aquest càncer. Finalment, la funció principal de les vesícules extracel·lulars és la comunicació entre cèl·lules. La dieta és un factor de risc per al càncer colorectal, ja que hi participa en l'inici i progressió. La genisteïna, una isoflavona dels aliments rics en soja, actua sobre el càncer colorectal, encara que com porta a terme la seva acció no està completament dilucidat.

Els objectius d'aquesta tesi varen ser: 1) determinar els canvis en l'estrès oxidatiu, inflamació, transició epitel·li-mesènquima i metàstasi a mostres de teixit tumoral i de teixit adjacent no tumoral de pacients afectats per càncer colorectal als diferents estadis de la malaltia; 2) analitzar l'aspirat intestinal i les vesícules extracel·lulars que conté com eina per a l'estudi i diagnòstic del càncer colorectal; 3) determinar i estudiar l'ARN contingut en les vesícules extracel·lulars aïllades de l'aspirat del lumen intestinal de pacients afectats per càncer colorectal; 4) determinar l'efecte de la genisteïna sobre l'estrès oxidatiu, la biogènesi mitocondrial i l'estat inflamatori sobre dues línies cel·lulars de càncer de colon.

Els resultats obtinguts indiquen que els estadis primerencs del càncer colorectal, especialment l'estadi II, presenten característiques moleculars pròpies d'estadis més avançats, la qual cosa indica la importància dels estadis primerencs per al desenvolupament de la malaltia i la possibilitat d'emprar aquests canvis com a font de marcadors primerencs del càncer colorectal. El teixit adjacent no tumoral presenta un increment en l'estat inflamatori al llarg dels diferents estadis, la qual cosa podria indicar una comunicació entre ambdós tipus de teixit, que pot ser gràcies a l'alliberament de les vesícules extracel·lulars per part de les cèl·lules tumorals. Aquestes vesícules poden ser aïllades de l'aspirat del lumen intestinal i emprades com a font de marcadors, ja que el seu contingut reflexa l'estat de la cèl·lula d'origen. A més, el seu contingut en ARN a pacients amb càncer es troba enriquit en vies relacionades amb l'estrès oxidatiu i la mitocòndria, la inflamació, la proliferació i la mort cel·lular, que es veuen modificats per la genisteïna per disminuir la viabilitat cel·lular de les cèl·lules de tumor primari i metastàtic.

En conclusió, l'estudi dels estadis primerencs del càncer colorectal permet un major coneixement de la progressió de la malaltia a més de la seva funció com a font de marcadors primerencs, que també poden ser trobats al contingut de les vesícules extracel·lulars, per al diagnòstic i pronòstic del càncer colorectal, que és clau per millorar la supervivència dels pacients afectats per aquesta malaltia.



Estudio del cáncer colorrectal: búsqueda de nuevos biomarcadores en diferentes tipos de muestra

Tesis Doctoral, Marina Alorda Clarà

Departamento de Biología Fundamental y Ciencias de la Salud, Universidad de las Islas Baleares, Palma, España

Resumen

El cáncer colorrectal es la tercera neoplasia más común en el mundo y la segunda causa de muerte por cáncer, de hecho, la supervivencia a los 5 años disminuye a lo largo de los estadios de la enfermedad. Esta disminución indica la necesidad de un diagnóstico temprano. La búsqueda de nuevos marcadores para el diagnóstico y pronóstico de esta enfermedad está muy centrada en el estudio de los tejidos afectados por el cáncer, pero a pesar de que el estrés oxidativo, la inflamación y la transición epitelio-mesénquima son procesos clave para el desarrollo de esta patología no se conoce bien su papel en los estadios tempranos. Además de encontrar estos marcadores en los tejidos afectados, también se podrían encontrar en las vesículas extracelulares, ya que son liberadas por las células del cáncer colorrectal desde estadios tempranos. Además, las vesículas están delimitadas por una bicapa lipídica que protege su contenido de la degradación. Estas vesículas se encuentran en la mayoría de los fluidos del cuerpo, por tanto, se podrían encontrar en el aspirado del lumen intestinal, una muestra poco conocida que se recoge durante las colonoscopias y que tiene un gran potencial como herramienta para el estudio del cáncer colorrectal. Finalmente, la función principal de las vesículas extracelulares es la comunicación entre células. La dieta es un factor de riesgo para el cáncer colorrectal, ya que participa en su iniciación y progresión. La genisteína, una isoflavona de los alimentos ricos en soja, actúa sobre el cáncer colorrectal, aunque el mecanismo todavía no está completamente dilucidado.

Los objetivos de esta tesis fueron: 1) determinar los cambios en el estrés oxidativo, inflamación, transición epitelio-mesénquima y metástasis en muestras de tejido tumoral y tejido adyacente no tumoral de pacientes afectados por cáncer colorrectal en los diferentes estadios de la enfermedad; 2) analizar el aspirado intestinal y las vesículas extracelulares que contiene como herramienta para el estudio y diagnóstico del cáncer colorrectal; 3) determinar y estudiar el ARN contenido en las vesículas extracelulares aisladas del aspirado del lumen intestinal de pacientes afectados por cáncer colorrectal; 4) determinar el efecto de la genisteína sobre el estrés

oxidativo, la biogénesis mitocondrial y el estado inflamatorio sobre dos líneas celulares de cáncer de colon.

Los resultados obtenidos indican que los estadios tempranos del cáncer colorrectal, especialmente el estadio II, presentan características moleculares propias de estadios más avanzados, lo que indica la importancia de los estadios tempranos en el desarrollo de la enfermedad y la posibilidad de usarlos como fuente marcadores tempranos del cáncer colorrectal. El tejido adyacente no tumoral presenta un incremento en el estado inflamatorio a lo largo de los estadios, lo que podría indicar una comunicación entre ambos tipos de tejido, que podría ser dada gracias a la liberación de las vesículas extracelulares por parte de las células tumorales. Estas vesículas pueden ser aisladas del aspirado del lumen intestinal y usadas como fuente de biomarcadores, ya que su contenido refleja el estado de la célula de origen. Además, su contenido en ARN en pacientes con cáncer se encuentra enriquecido en vías relacionadas con el estrés oxidativo y mitocondria, la inflamación, la proliferación y la muerte celular, procesos modificados por la genisteína para disminuir la viabilidad celular de células de tumor primario y metastásico.

En conclusión, el estudio de los estadios tempranos del cáncer colorrectal permite un mayor conocimiento de la progresión de la enfermedad además de su función como biomarcadores tempranos, que también pueden ser encontrados en el contenido de las vesículas extracelulares, para el diagnóstico y pronóstico del cáncer colorrectal, que es clave para mejorar la supervivencia de los pacientes afectados por esta enfermedad.

1. Introduction

Cancer is a disease including more than 100 types of cancer [1]. Tumorigenesis is the progressive transformation of normal cells to cancer cells due to the acquisition of different genetic alterations that produce several advantages in growth, and physiological alterations, which allow avoiding the antitumoral defense [1]. In order to acquire these changes, the cell develops new capacities that allow the survival, proliferation and dissemination of tumor cells [2]. These new capacities are hallmarks and tumoral cell benefits from the enabling characteristics to acquire them [2].

The first hallmark classification by Hanahan and Weinberg included six hallmarks [1], but the last classification already includes 10 hallmarks and 4 enabling characteristics (Figure 1) [3], which are [2,3]:

- Sustained proliferative signaling: tumor cells lose growth signaling control and acquire chronic proliferation.
- Growth suppressors evasion: tumor cells avoid negative regulation of proliferation, which is based on tumoral suppressor genes that control cellular growth and proliferation, and activate senescence and apoptosis.
- Cell death resistance: tumor cells avoid apoptosis by losing tumoral suppressor function, increasing antiapoptotic regulators expression and survival signaling, or inhibiting death signaling pathways.
- Enabled replicative immortality: tumor cells lose the limited number of cycles of growth and division, to achieve unlimited replicative potential.
- Angiogenesis induction: new tumor-associated vasculature allows tumor cells to get oxygen and nutrients, and to eliminate CO₂ and metabolic residues.
- Invasion and metastasis activation: tumor cells present shape and attachment alterations, that are achieved by the alteration of molecular adhesion related genes, and the increase of inflammation and an adhesion molecule associated to cellular migration during embryogenesis.
- Energy metabolism reprogramming: the sustaining of proliferative signaling induces the modification of energy metabolism to achieve enough energy for growth and division, for this, tumor cells limit their energetic metabolism to glycolysis. In addition, some tumoral cells have two populations, the hypoxic cells

use glucose and release lactate, and the better oxygenated cells use the lactate as energy source.

- Immune destruction evasion: solid tumors present immune evasion, that avoid their detection by immune system.
- Unlocked phenotypic plasticity: cancer cells avoid phenotypic plasticity restriction, resulting in evasion of terminal differentiation state.
- Senescent cells: senesce stimulates tumor development and malign progression.
- Genome instability and mutation: cancer cells increase DNA mutations, which is generally regulated by the DNA repair mechanisms.
- Tumor-promoting inflammation: tumors present immune system cells infiltration, that allows tumorigenesis and progression.
- Non-mutational epigenetic reprogramming: cancer cells get mutations in genes that control organization, modulation, and maintenance of chromatin structure, and in genes that regulate gene expression.
- Polymorphic microbiomes: microbiome polymorphic variability between individuals has an impact of cancer phenotype.

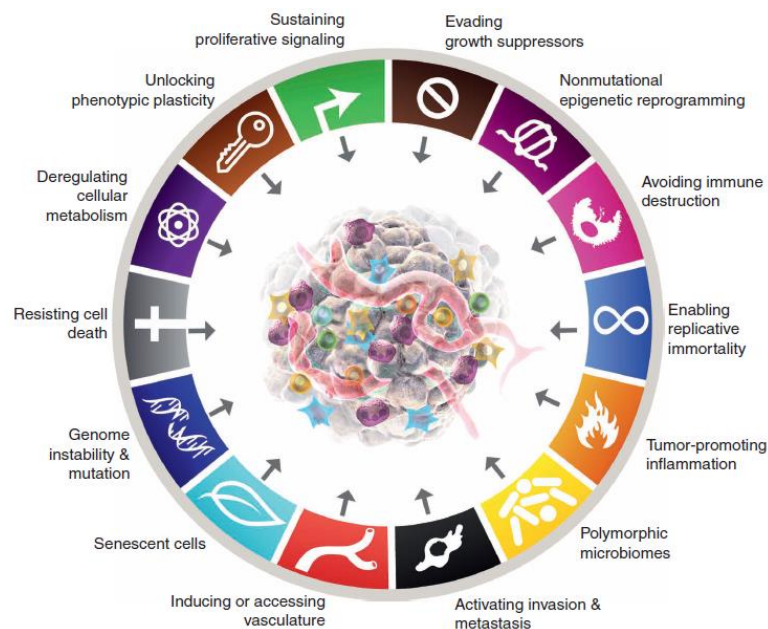


Figure 1. Hallmarks and enabling characteristics of cancer. Adapted from Hanahan, 2022 [3].

1.1. Epidemiology and etiology of colorectal cancer

Colorectal cancer (CRC) is the third most common cancer worldwide, being the second most prevalent and the second cause of cancer death [4]. The highest CRC incidence is in North America, Europe and Oceania, and the lowest CRC incidence is in Africa (Figure 2), despite this, the highest CRC mortality is in Asia and Europe (Figure 3) [4].

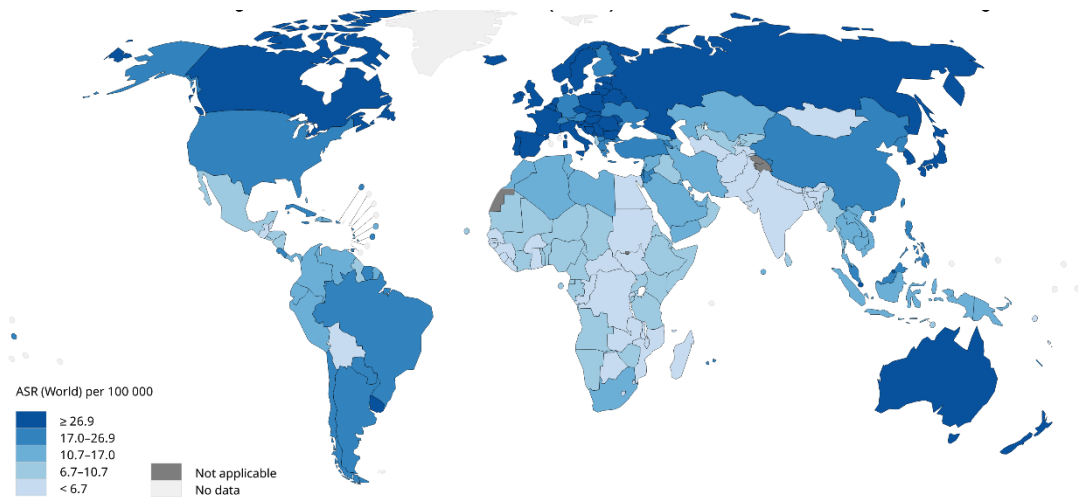


Figure 2. Estimated age-standardized incidence rates worldwide in 2020, including both sexes and all ages. Adapted from GLOBOCAN [4].

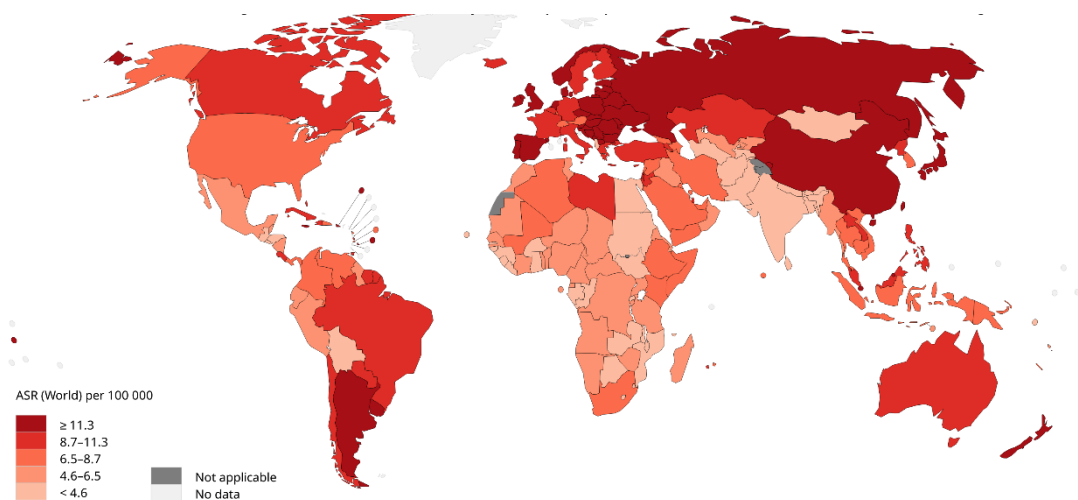


Figure 3. Estimated age-standardized mortality rates worldwide in 2020, including both sexes and all ages. Adapted from GLOBOCAN [4].

There are some risk factors that increase the probability to suffer CRC, such as smoking, alcohol, obesity, diabetes mellitus type 2, diet, inflammatory bowel disease, relatives with CRC, ingest of red meat, and sedentarism [5,6]. Despite this, there are some preventive factors for CRC, such as milk intake, ingest of whole grains, fresh fruit and

vegetables, calcium, fiber, vitamin D, aspirin, and probiotics [5,7]. Finally, as the CRC has anatomical heterogeneity, the probability of suffering CRC depends on bowel location [6].

There are 3 CRC types: sporadic (70%), hereditary (5%), and familial (25%) [6]. The sporadic CRC is characterized by APC and KRAS mutations, polyps formation, and loss of TP53 [6]. The hereditary CRC is divided into two types: polyposis, which is caused by the accumulation of a huge number of potentially malign polyps; and hereditary non-polyposis CRC, which is caused by mutations in DNA repair systems and is the main cause of Lynch syndrome [6]. Finally, the familial CRC is caused by inherited mutations [6].

The loss of genomic and epigenomic stability is the main cause of CRC, because produces epigenetic alterations and mutations accumulation in tumoral suppressor genes and oncogenes [5]. The most common alterations in CRC are in APC, catenin-beta 1, KRAS, BRAF, SMAD4, TGF β receptor 2, TP53, and PI3K catalytic subunit α genes, among others, and DNA methylation modifications, such as CpG islands hypermethylation of promoters that silence tumoral suppressor genes, hypomethylation of repeated genetic elements that give rise to genomic instability or oncogene activation [5]. The genomic instability is caused by three elements: chromosomal instability, microsatellite instability and CpG island methylator phenotype [6]. Chromosomal instability is an imbalance of chromosome number caused by alterations in chromosomes segregation, telomere disfunction and DNA damage [6]. Microsatellite instability is a loss of DNA repair systems, due to an inactivation of mismatch repair genes expression, such as MLH1, MSH2, MSH6, PMS1 and PMS2 [6]. Finally, CpG island methylator phenotype is an hypermethylation of oncogenes promoters, that produces gene silencing and protein expression loss [6]. The main evolution from normal epithelial cell to adenocarcinoma is the appearance of a polyp in an aberrant crypt, that evolves to early adenoma, then to advanced adenoma and finally progress to CRC in 10 to 15 years [5]. Despite all of this, in the past few years, it has been discovered that some genomic aberrations, the non-coding RNA, the intestinal microbiome, the dysbiosis, and the relation between microbiome and diet can influence the appearance of CRC [6].

1.2. Colorectal cancer classification

CRC can be classified by the TNM classification, where T indicates the size of primary tumor and the invasion extension, N indicates the presence or absence of metastasis in the regional lymph nodes, and M indicates the presence or absence of distant metastasis [8]. According to primary tumor extension, CRC can be divided into four stages, from I to IV, being the stages I, II and III non-metastatic stages and IV the metastatic stage [8]. In stage I, tumor grows and invades mucosa and muscular layer without node dissemination; in stage II, tumor continue growing from the muscular layer to the adjacent structures without node dissemination; in stage III, tumor invades near organs and, in stage IV, tumor spreads to other body parts through lymph nodes and blood vessels (Figure 4) [8].

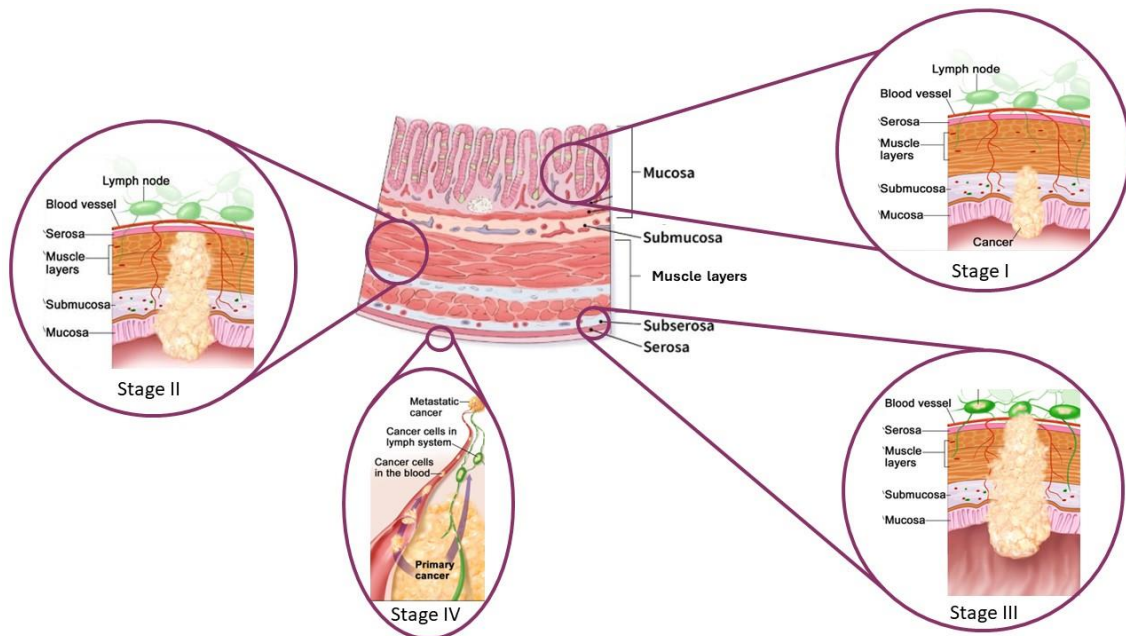


Figure 4. Colorectal cancer stages (I-IV) according to primary tumor extension. Created and adapted from American Cancer Society and Virginia Oncology Associates [9,10].

1.3. Tumoral microenvironment

Tumoral cells are surrounded by non-malignant cells that are bonded between them and to the extracellular matrix (ECM), forming the tumoral microenvironment [11]. Tumoral microenvironment is formed by tumor-infiltrating cells, tumor vasculature, ECM, and ECM-associated molecules [12]. Cells from tumoral microenvironment participate in tumoral initiation, growth, invasion, metastasis, and drug resistance [11]. Despite this, tumoral cells and microenvironment cells interact with each other to

achieve enabling characteristics in the tumoral cells, such as genetic and epigenetic alterations [12].

Tumor-infiltrating cells (Figure 5) are a group of cells which are recruited by inflammation and soluble chemoattractants within solid tumors to promote inflammation and tumoral growth [13]. Tumor-infiltrating cells are a heterogeneous group formed by different cell types [12–15]:

- Tumor-associated macrophages: monocytes recruited to the tumor by a decrease in IL-12 and an increase in IL-10 in the tumoral microenvironment, that can differentiate to tumor-associated macrophages and polarize to two states: M1, with anti-tumoral properties, and M2, main component of tumor-associated macrophages which promotes tumoral growth, ECM remodeling, epithelial-mesenchymal transition (EMT), metastasis, and immune evasion.
- Myeloid-derived suppressor cells: immature myeloid cells that avoid adaptive immune response.
- Mast cells: these cells release proangiogenic factors and growth factors to induce angiogenesis, in addition to release proteases to remodel ECM for tumoral growth and metastasis.
- Cancer-associated fibroblasts: main component of the stroma, these fibroblasts release growth factors to induce tumoral growth and metastasis, in addition to release chemokines, proteases and ECM components to stimulate proliferation, migration, invasion, metastasis, immunosuppression and survival.
- TIE-2-expressing monocytes: main population of monocytes, these cells induce tumoral growth and angiogenesis.
- Neutrophils: neutrophils release oncostatin M to induce vascular endothelial growth factor (VEGF) release from tumoral cells and induce angiogenesis, also produce immune evasion increasing the release of matrix metalloproteinase 9 (MMP9) that promotes an inhibition of T cells proliferation through the activation of transforming growth factor β (TGF β), in addition to degrade basal membrane increasing tumor mobility and extravasation.
- Dendritic cells: the mechanism by how dendritic cells promote invasion is not clear yet.

- Platelets: participate in tissular reparation, endothelial function, tumoral progression, metastasis, and angiogenesis.
- Mesenchymal stem cells: induce tumoral growth and metastasis through their immunosuppressive activity and pro-angiogenic properties.
- Natural killer: the presence or absence of TGF β in the tumoral microenvironment produces an inhibition or activation of their action above tumoral cells, respectively.
- Regulatory T cells: induce immunosuppression and metastasis.
- Cytotoxic T cells: their activity is suppressed to induce immune evasion.

Tumor vasculature (Figure 5) is affected by endothelial cells [14]. In presence of hypoxia, hypoxia-inducible factor 1-alpha (HIF1 α) is increased, inducing the expression of VEGF, basic fibroblast growth factor, and platelet-derived growth factor in tumoral cells, and promoting angiogenesis [13]. Finally, ECM (Figure 5) is a tridimensional structure that participates in cellular migration, differentiation, and proliferation, in addition to act as a cytokine and growth factor niche [13]. ECM has a wide variety of functions, such as cellular-cellular adhesion, signaling, proliferation, immune evasion, and metastasis [14], and it has several ECM-associated molecules: laminin, collagen, fibronectin, proteoglycans, hyaluronan, integrins, matrix metalloproteases, mucin, osteopontin, and galectin [13].

An important factor is the presence of TGF β , since it presents the TGF β paradox, for which, in healthy tissues, TGF β inhibits epithelial growth but in cancer tissues induces tumoral cell progression [15]. Among the functions of TGF β stand out control tissue development, proliferation, differentiation, apoptosis, and homeostasis, in addition to promote tumor-stroma interaction and induce malign phenotype, and the differentiation of mesenchymal stem cells to cancer-associated fibroblasts to create a positive feedback secreting TGF β and perpetuate malign phenotype [15]. It has been seen that long non-coding RNA (lncRNA) can modulate endothelial cells from the stroma, promoting tumoral progression and affecting angiogenesis and metastasis, in addition to modulate cancer stem cells renewal [16]. Finally, microRNA (miRNAs) from CRC cancer cells can be regulated by tumoral microenvironment, since it induces

epigenetics and enzymatic mechanisms that modulate miRNAs processing and producing CRC induction [12].

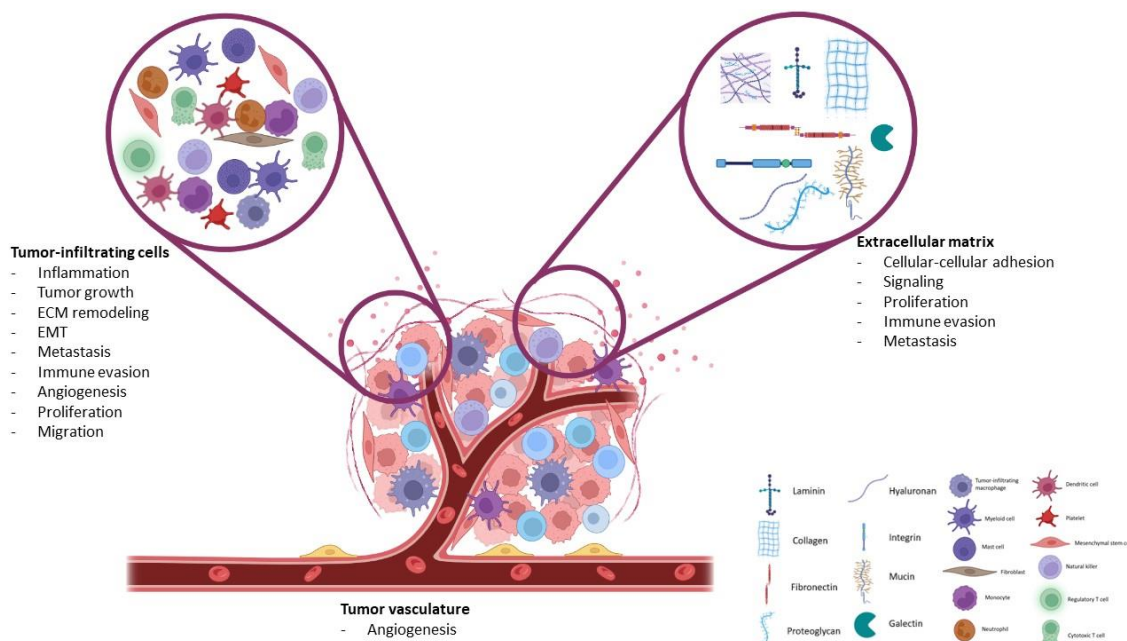


Figure 5. Schematic representation of tumoral microenvironment. Created by Biorender.

1.4. Relationship between inflammation, angiogenesis, epithelial-mesenchymal transition, and metastasis

Inflammation is a physiological process that when becomes chronic can induce malignant transformation to the surrounding tissues [17]. This inflammation is generated by the release of cytokines and chemokines and the activation of inflammation-related pathways, thus promoting all phases of cancer, due to the fact that the cytokine network created can recruit immune system cells, promoting the release of more cytokines creating a positive feedback that will allow survival, growth, proliferation, differentiation, activation of immune cells and migration of tumoral and stromal cells [17,18].

Nuclear factor kappa B (NF- κ B) is a very important transcription factor in inflammation, because is activated in all cell types, where can regulate the expression of proliferation genes, the immune and inflammatory response, and can contribute to some diseases, such as cancer [19]. To carry on its activity, NF- κ B needs to be at the nucleus, but in normal conditions is retained into the cytosol, where is bound to inhibitor of kappa B (I κ B) forming a dimer, blocking the NF- κ B translocation to the nucleus [19]. I κ B is phosphorylated by I κ B kinase (IKK), then is ubiquitinated and degraded into the

proteasome, releasing NF- κ B, allowing its dimerization and translocating it into the nucleus, where act as transcription factor of genes related to immune response, inflammation and growth cell, such as tumor necrosis factor α (TNF α), interleukin-1 β (IL-1 β), IL-8, cyclooxygenase 2 (COX2), inducible nitric oxide (iNOS), interferon gamma (IFN γ) and IL-6 [19,20]. There are two pathways for NF- κ B activation, and both of them are based on the degradation of two inhibitors by IKK [19]: the canonical pathway, which is activated by TNF α , IL-1 β , toll like receptors and virus, is based on the degradation of I κ B by phosphorylation by IKK and promotes the transcription of innate immunity and cell survival; the non-canonical pathway, which is activated by TNF receptor superfamily members, allows the degradation of p100, which is an inhibitor of RelB, one of the dimers that formed NF- κ B, granting the dimerization of NF- κ B and consequent translocation to the nucleus, where will induce the expression of lymphoid organogenesis genes and maintain the malignant phenotype [19]. On the other hand, NF- κ B can also be modulated by peroxisome proliferator activated receptor gamma (PPAR γ), which has anti-inflammatory properties, for this, PPAR γ can repress NF- κ B, nuclear factor of activated T cells, signal transducer and activator of transcription (STAT) and activator protein 1 genes in front of inflammation stimuli [20,21]. PPAR γ can block the NF- κ B translocation to the nucleus by bounding the subunit p65 of NF- κ B and avoiding the I κ B degradation by the proteasome, in both mechanisms, NF- κ B is retained in the cytosol being unable to regulate the expression of the inflammatory-related genes [20]. Furthermore, IL-4 can decrease the degradation of I κ B, also avoiding the NF- κ B translocation and, consequently, its action [22]. As previously described, NF- κ B regulates the expression of inflammatory-related genes, such as IL-1 β , that promotes cellular proliferation, differentiation, immunity and inflammatory response [23]; IL-6, which is produced when IL-1, IL-17 and TNF α are increased and regulates immune response, hematopoiesis and inflammation [23]; TNF α participates in inflammation and allows tissue destruction and renewal, because can destroy blood vessels when it is present in high concentrations but also induce angiogenic factors and if these high concentrations are chronic, can promote tumoral growth [24], in addition, it has been seen that TNF α can induce heparanase expression, that degrades extracellular matrix, allowing the release of proinflammatory cytokines and promotes the transcription of TNF α and IL-1 β [25]; and COX2, which also can be increased by IL-1 β through p38 MAP

kinase, the main function of COX2 is to form prostaglandin 2, that increases proliferation, invasiveness, mitogenesis and the expression of VEGF and platelet-derived growth factor, allowing angiogenesis, furthermore, COX2 can also increase reactive oxygen species (ROS) and MMP9 levels promoting metastasis, decreases arachidonic acid reservoirs decreasing cell differentiation and apoptosis, and promotes immunosuppression [26,27].

Angiogenesis is the capability to develop new blood vessels from pre-existing blood vessels to initiate and maintain tumors, promote metastasis and obtain oxygen and nutrients to the tumor, since the main activator of angiogenesis is hypoxia [28]. The increase of hypoxia in tumor cells promote the release of cytokines and HIF1 α , that activates the expression of VEGF [28]. There are two principal VEGFs: VEGF-A, that initiates, maintains and promotes angiogenesis; and VEGF-B, that has a dual role in front of angiogenesis, because can stimulate endothelial cell proliferation and vascular growth, in addition to help in vessel survival during disease, but on the other hand, it can also inhibit tumoral growth and angiogenesis [29,30]. Inflammation and angiogenesis are a very related processes, since the increase in NF- κ B promotes the increase of COX2 expression levels and, subsequently, the promotion of angiogenesis by increasing the VEGF expression levels [26,27]. In addition to the increase of VEGF expression, COX2 also increases MMP9 expression levels, promoting metastasis [26]. MMP9 is a matrix metalloproteinase, an endopeptidase that can act degrading de ECM and is related to angiogenesis, invasion and metastasis [31]. The main function of MMP9 is to degrade type IV collagen from the basal membrane, this protein is secreted as a zymogen and then is cleaved for activation and regulated by tissue inhibitors of MMP [31]. MMP9 is related to invasion and metastasis, due to the release of growth factors, signaling factors and the angiogenesis induction that is achieved by the ECM degradation [31]. In addition to be increased by COX2, MMP9 can also be upregulated by heparanase, which is an endo- β -glycosidase that cleaves heparan sulfate chains, degrading the ECM, promoting changes in tissue remodeling, migration and promoting inflammation, angiogenesis and metastasis [25]. An increase of heparanase levels allows cellular dissemination and the formation of a vascular network that will grant primary tumor growth and the acquisition of new metastatic invasive cells [25].

Inflammation is a process involved in first phases of tumor formation, as well as the EMT [18], which is a physiological mechanism in the development for which the epithelial cells transdifferentiate to mesenchymal cells through the loss of contact inhibition and the transformation of keratin into vimentin filaments [32,33]. These changes promote migration, matrix remodeling capacity, apoptosis resistance and molecular and morphological transformations [32]. In addition, EMT present hallmarks, such as the acquisition of fibroblast morphology, the increase of mesenchymal markers and extracellular matrix components, the decrease in epithelial markers and cytoskeleton components, and the increase and translocation to the nucleus of transcription factors [32]. These changes increase the capacity of migrate, invade and apoptosis resistance [32]. The EMT is characterized by an increase in vimentin, fibronectin, N-cadherin and integrin and a decrease in E-cadherin, cytokeratin, desmoplakin, claudin and occludin [32,33]. There are some transcription factors that regulate the EMT, such as Snail, Slug, Twist and ZEB [34]. NF- κ B, TNF α , TGF β , Wnt, Notch and growth factors can increase the expression of Snail 1 and 2, which decrease claudin and E-cadherin expression and increase vimentin, fibronectin and MMP expression, and decrease cell adhesion and polarity, respectively, increasing migration and invasion [34,35]. TGF β , IL-1 β and Wnt can also increase the expression of ZEB, which reduces polarity and increases the expression of vimentin and N-cadherin [18,34]. An hypoxia situation with an increase of HIF1 α can induce the expression of Twist1, which also decreases E-cadherin and increases N-cadherin, promoting a decrease in cell adhesion and an increase in cell motility [34]. Additionally, in cell culture studies it has been seen that some miRNAs, such as miR-200c, can affect the EMT by increasing the levels of N-cadherin, vimentin and Twist1 and decreasing the levels of E-cadherin [32]. Finally, inflammation can affect the EMT, because NF- κ B and STAT3, activated by IL-6, can increase the proliferation and mobility of metastatic cells, affecting migration and invasion [33,35]. Furthermore, an inflammatory status release proteases that can degrade the ECM, enhancing invasion and extravasation of cancer cells [35]. In addition to this, TAMs can produce growth factors (HGF, EGF, TGF, PDGF) and proinflammatory cytokines (IL-1 β , IL-6, TNF α) that can induce angiogenesis, immunosuppression, rupture of ECM and EMT [18]. Furthermore, in cell culture, the macrophages M2 induce morphology changes, a decrease in E-cadherin and an increase in vimentin, MMP and invasiveness [18].

1.5. Mitochondrial functionality and oxidative stress

Mitochondria are bioenergetic and biosynthetic cellular organelles that use cytoplasmic substrate to carry out fatty acid oxidation, Krebs cycle, electron transport chain and respiration to produce amino acids, lipids, nucleotides and NADPH [36]. In addition, mitochondria are responsible for adenosine triphosphate (ATP) production, cell cycle control, programmed cell death, proliferation, and cellular signaling [37]. Mitochondria are formed by two membranes that delimit intermembrane space and mitochondrial matrix [37]. The outer mitochondrial membrane participates in signaling, connects mitochondria to other organelles, and maintains the balance between cellular metabolic requirements and mitochondrial capacity [37]. The inner mitochondrial membrane needs membrane transporters because it is highly impermeable to ions and molecules, is a very extensive membrane formed by mitochondrial cristae, where are located the electron transport chain complexes, and the main function is to form ATP [37]. Finally, there is the mitochondrial matrix, where take place Krebs cycle, anaplethoric and cataplethoric reactions, part of urea cycle, transamination reactions, and where the complex II of electron transport chain is located [37].

Mitochondrial biogenesis is the process by which new mitochondria are generated, and it is very linked to mitophagy, because when one mitochondria is destroyed, a new one is generated [38]. Generally, mitochondrial biogenesis is reduced in cancer [38,39], but is increased in CRC, because in this cancer there is an increase of mitochondrial single-strand DNA binding protein (mtSSB), which regulates mitochondrial DNA (mtDNA) replication and produces cellular growth, survival and mitochondrial biogenesis in CRC [39]. In addition to the participation of mitochondrial biogenesis in cancer, it has been seen the existence of oncocyctomes, which are benign tumors with a huge content of damaged mitochondria with a lot of DNA mutations [36].

mtDNA is a small circular DNA formed by 16569 base pairs, which contains 37 genes for two ribosomal acid nucleic, 22 transfer RNA and 13 subunits from the oxidative phosphorylation system [40]. The mtDNA replication can be done during all cell cycle, not only in S phase [40]. Mitochondrial homeostasis is maintained by the coordination between mitochondrial biogenesis and mitophagy [41]. Mitochondrial biogenesis is induced by the activation of transcription factors that act in mitochondrial genes and

upregulate the local transcription of mitochondrial proteins [41]. First step in mitochondrial biogenesis is the mtDNA transcription, that starts with the activation of peroxisome proliferator-activated receptor gamma coactivator 1-alpha (PGC1 α) by deacetylation or phosphorylation to stimulate nuclear transcription factors, such as nuclear respiratory factor 1 and 2 (NRF1, 2), and estrogen related receptor alpha (ERR α), in addition to increase transcription factor A (TFAM) expression, which is the final effector of transcription and replication of mtDNA [41], mtSSB also participates in mtDNA replication [39]. After that, nuclear DNA codifies for specific translation factors, such as initiation factors 1 and 2, elongation factors Tu, Ts, and G1, translational release factor 1-like and the recycling factors, promoting translation [41]. The mitochondrial proteins codified by nuclear DNA are synthesized in the cytosol as pre-protein and present an amino terminal cleavage targeting signaling to import and assembly them [41]. Mitochondrial protein levels are regulated by translational activator of cytochrome c oxidase 1, that binds to mtDNA [41]. Mitophagy is done when mitochondrial fusion (reorganization of the matrix content from a damage mitochondria with a healthy one) and mitochondrial fission (division of damage material to the new mitochondria) do not work correctly, and promotes the damage mitochondria degradation [40]. PTEN-induced kinase 1 (PINK1) is located in the outer mitochondrial membrane from damage mitochondria marking them for degradation, then recruits Parkin, which in turn activates ubiquitin ligase E3, for ubiquitinate proteins from the outer mitochondrial membrane and produce mitophagy [40].

PGC1 α is the main regulator of mitochondrial biogenesis and a coactivator member of the family PGC, that promotes mitochondrial proteins synthesis and regulates the energetic metabolism by transcription factors regulation, such as NRF1 and 2, peroxisome proliferator-activated receptor alpha (PPAR α) and TFAM [42]. In normal conditions, PGC1 α function varies according to the energetic metabolism of the tissue, because if tissue has an aerobic metabolism, for example, in the base of the colonic crypts, PGC1 α increases antioxidant enzymes production, but if tissue presents a low aerobic metabolism, for example in villi, PGC1 α increases mitochondrial biogenesis, giving a ROS accumulation, that will end in apoptosis [42]. In normal conditions, an increase of PGC1 α produces an increase of specificity protein 1, which in turn increases

the expression of acyl-CoA binding protein, inducing an increase of cell proliferation and a decrease of apoptosis mediated by ROS [42]; in addition, PGC1 α regulates the gene expression of pathways that convert glucose in fatty acids, promoting the tumoral growth [42]; finally, an increase of PGC1 α and PGC1 β increase mitochondrial biogenesis [42].

Despite the importance of PGC1 α in mitochondrial biogenesis, there are other factors that are important for this process: TFAM participates in mtDNA transcription and replication, NRF1 and 2 keep the integrity of mitochondrial genome and regulate mtDNA transcription, polymerase γ participates in mtDNA replication and reparation, Pol β participates in mtDNA maintenance and reparation through its interaction with an helicase (TWINKLE), mtSSB and TFAM, and the primase PrimPol, that participates in mtDNA and nuclear DNA maintenance and reparation, and synthetizes de novo DNA [40].

As previously mentioned, in the inner mitochondrial membrane are located the complexes from the electron transport chain, which is formed by 5 multienzymatic complexes (I, II, III, IV and ATPase) and hydro- and lipo-soluble compounds that allow the electrons transfer through the complexes until the final acceptor, the O₂ [37]. This transfer generates a proton flux from the mitochondrial matrix to the intermembrane space, generating an electrochemical gradient through the inner mitochondrial membrane [37]. This electron transport releases energy that can be used for ATP production or thermoregulation [37]. Oxidative stress is the result of the disbalance between the free radical production and their elimination by the antioxidants [43]. ROS are the main cause of oxidative stress and are generated in the electron transport chain [37,43], despite this, ROS can be generated by autooxidation, photochemicals and enzymatic reactions [44]. The antioxidant mechanisms for remove ROS can be divided into enzymatic and non-enzymatic:

- Enzymatic mechanisms: SOD, that can be copper-zinc superoxide dismutase (CuZnSOD, present at the cytosol), manganese superoxide dismutase (MnSOD, present at the mitochondrial matrix) and extracellular superoxide dismutase (EoSOD), and reduce two superoxide anions (O₂⁻) to hydrogen peroxide (H₂O₂) and molecular oxygen; catalase, that reduces H₂O₂ into water; glutathione

peroxidase (GPx), that reduces H_2O_2 into water through the oxidation of glutathione; glutathione reductase, that reduces the glutathione disulfide into glutathione in presence of NADPH; peroxiredoxin, reduces the alkyl hydroperoxide and H_2O_2 into alcohol or water; thioredoxin, that reduces H_2O_2 to water and molecular oxygen in presence of NADPH [37,43,45].

- Non-enzymatic mechanisms: glutathione, vitamin C and D, ascorbic acid, lipoic acid, and α -tocopherol [43,45].

ROS can affect the structure and function of cell, also increase mutations and damage in DNA, produce genomic instability, DNA strand breakage, cross-linking of aberrant DNA, genome hypermethylation because reduce the expression and activity of DNA mismatch repair genes and increase the expression of methyltransferases, and finally, can activate proliferation and survival pathways [43]. These changes can induce neoplastic transformation and it has been seen that oxidative stress participate in all three cancer phases: initiation, because ROS produce mutations and alterations in DNA structure, promoting damage; promotion, due to the fact that ROS increase cellular proliferation and decrease apoptosis, block cell-cell communication, and modify second messengers systems; progression, because ROS can induce more alterations in DNA [43]. According to localization and concentration, ROS present a dual role in front of tumoral cells survival, because ROS can increase proliferation, survival and migration or can induce senescence and cell death [43]. Tumoral cell proliferation is regulated by ROS, because proliferation pathways such as MAPK/AP-1 and NF- κ B are affected by it, for example, H_2O_2 degrade I κ B, activating NF- κ B [43]. Finally, ROS can react with the group thiol from the catalytic protease domain of MMP9, allowing its invasive and metastatic capacity [43].

1.6. Colorectal cancer and phytoestrogens. The role of genistein

Phytoestrogens are heterocyclic non steroid phenols derived from plants that can act as estrogens agonists, in both ways structurally and functionally, in mammals [46]. In addition to the estrogen-like effects, phytoestrogens present antiproliferative effects, since phytoestrogens can be metabolized by intestinal bacteria and form metabolites similar to estrogens that prevent cancer [46], and can induce apoptosis [47]. Finally, phytoestrogens present a protective effect in front a huge variety of diseases, such as

cardiovascular disease, menopause symptoms, osteoporosis, and cancer [46]. There are six different types of phytoestrogens: isoflavones, that can be found in soy, legumes, clover, and peanuts, and form part of this group the genistein, quercetin, daidzein and glycitein; lignans, that can be found in seed, fruit, vegetables, whole grains, tee, and coffee; enteroglycans, lignans that can be metabolized to enteroglycans to be absorbed; coumestans, which can be found in soybean, clover, legumes, and fodder; lactones, which are not easy to find in common diet; and equol, lignans and daidzein can be metabolized into equol by bacteria, for this, equol can be found in animal origin products [46,48]. Phytoestrogens activity can be done by two mechanisms: genomic mechanisms, by which the phytoestrogen interacts with enzymes and receptors to cross the membrane and to induce transcription of estrogen responsive genes; non-genomic mechanisms, such as tyrosine kinase, DNA topoisomerase and angiogenesis inhibitions, and present antioxidant activity, to produce apoptosis [46,49].

Daily intake of phytoestrogens varies according to the zone, having the highest intake the Asiatic countries (39-47 mg/day) and the lowest intake de Western countries (1-2 mg/day) [50]. It has been seen that a high consumption of phytoestrogens is related to a lower risk of suffering CRC, specifically soy-rich products, in fact, until a few years ago, Asia was the continent with the lowest CRC incidence, but this has changed due to the westernization of the Asiatic diet and the introduction of soy products into the Western diet [46,47,49,50].

Genistein (GEN, 4',5,7-trihydroxyisoflavone, Figure 6) is a phytoestrogen from isoflavone group, that is present in soy with a concentration of 0.2-1 mg/g [46,51] and was isolated for the first time in 1899 [52]. GEN present antioxidant, anti-inflammatory, anti-cancer and proapoptotic properties [51], in addition to the capacity of cell cycle modulation, chemopreventive activity [53], and mitochondrial function and dynamics regulation [54].

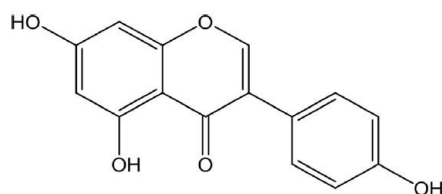


Figure 6. Chemical structure of genistein. Adapted from Luo, et al., 2014 [51].

GEN can bind to the estrogen receptor, inhibit tyrosine kinase and DNA topoisomerase II, in addition to downregulate PI3K/Akt pathway, alter cell cycle, induce apoptosis by increasing proapoptotic genes (caspase 3 and 9, PARP) and downregulating Bcl2 gene [55,56], and decrease the union of NF- κ B to the DNA through increase the I κ B dephosphorylation and upregulate I κ B- α expression, regulating the inflammatory response and producing an antitumoral effect [51,52]. The role of GEN in front of ROS is not well established yet, since GEN can act as a prooxidant by increasing ROS [55] at high concentrations [54], but it has been seen that GEN can act as antioxidant by scavenging ROS and reactive nitrogen species (RNS) [52,56], but it seems to be concentration and cellular type dependent [54]. GEN can modulate mitochondrial function, because GEN can maintain the bioenergetic status, control redox balance, induce mitochondrial biogenesis and cell death, but there is a lack of information about how GEN modifies these pathways and how regulates mitochondrial redox biology [54]. Finally, GEN stimulates normal cells division in addition to decrease cancer cells proliferation, GEN also inhibits angiogenesis, avoiding the capture of nutrients and oxygen for the tumor, furthermore, the GEN metabolites also present anticancer properties, but the mechanism is not established yet [56].

CRC can be affected by GEN, it has been seen that GEN can induce apoptosis in CRC cell culture through the inhibition of NF- κ B pathway [51], the inhibition of Insulin-like growth factor 1 (IGF-1) and PI3K/Akt pathway [53], and the increase of ROS [57]. GEN also inhibits cell proliferation by EGF inhibition, which in turn activates forkhead box O3 (FOXO3) [58]. Furthermore, GEN promotes cell cycle arrest in G₂/M activating ATM/p53, p21 and GADD45 α and downregulating CDK1 and cdc25A expression [53,58]. In addition, GEN can regulate gene transcription by epigenetics mechanisms [53]. Finally, GEN can revert EMT suppressing Notch1/NF- κ B/Slug/E-cadherin pathway [59].

1.7. Diagnosis and biomarkers in colorectal cancer

Nowadays, CRC diagnosis is done in late states of the disease, so the patients present a low survival rate [60,61]. For this fundamental reason, the screening program for CRC had been started to increase the diagnosis in early stages and reduce mortality. The gold standard for CRC screening is the fecal occult blood test [62], but there are other techniques that are used as screening, such as colonoscopy, flexible sigmoidoscopy,

guaiac fecal occult blood testing, fecal immunochemical testing, carcinoembryonic antigen in plasma and serum, and fecal calprotectin [62,63]. Despite the existence of CRC screening, there are different diagnostic techniques for patients that present symptoms. The most common techniques are the image-based, being the gold standard the colonoscopy, but positron emission tomography, computerized tomography and nuclear magnetic resonance are also used [64]. In addition to image techniques, blood tests are also very common, for example the carcinoembryonic antigen, the CA19-9 and the TAG-72 presence in plasma and tissular polypeptide specific antigen in serum [64], and the fecal analysis, such as the hemoglobin presence in stool and the study of DNA mutations, because of the stability of DNA in stool [64].

The last few years, the study of new biomarkers for CRC is growing due to the new sample types that can be used for this diagnostic, but despite the huge number of new biomarkers, there not very common in clinical use:

- Breath samples: the study of biomarkers in breath is done by volatolomics, that is based on the difference in volatile compounds that are released with breath between healthy patients and patients, in fact, different volatile compounds have been found to be higher in CRC patients [65–68].
- Urine samples: despite to be a non-invasive technique, is not very used, but it has been seen that CRC patients present an increase of mutations in KRAS [69], in addition to the existence of different metabolite panels for CRC diagnostic [70–72], and differences in protein content of exosomes from CRC patients [73].
- Stool samples: stools are a very studied non-invasive samples, in fact, it is known that CRC patients present a high number of DNA methylations [74–78]. There are different panels to determine CRC: miRNAs panel [79], lnc RNAs panel [80] and proteins panel [81]. It has been seen that patients with CRC present changes in metabolome [82–85], in addition to histone modifications, changes in microbiome and volatile organic compounds [86]. Finally, stool exosomes from CRC patients present an increase of two specific proteins, CD147 and A33 [87].
- Blood samples: this is a very used sample, because blood can be divided into plasma and serum, which increases the biomarker study. It has been seen that CRC patients present mutations in KRAS, APC and TP53 [88,89]. For this sample

type, it has been designed panels to determine CRC presence, based on proteins [90–94], messenger RNA (mRNAs) [88,90,95], and miRNAs [88,96–98], in addition to present changes in metabolome [99–101] and glycome [102–104].

- Bowel lavage fluid samples: this is a very unknown sample type but with a lot of potential, in fact, it has been seen that patients with CRC present an increase of KRAS, p53, TGFBR2 and APC mutations [105,106], and an increase of methylations in miR-124-3, LOC386758, SFRP1 and syndecan-2 [107,108]. It has been seen changes in microbiome, because CRC patients present *Bacteroides fragilis* [109], an increase in proteobacteria and fusobacteria and a decrease in firmicutes [110].
- Tissue samples: this is the most invasive and used sample type along time, in fact, there is a huge number of different panels to determine patients with CRC, the most common are mRNA panels [111] and protein panels [112,113]. Despite these panels, CRC patients present a lot of changes in the glycome when this is compared to healthy patients [104,114–120].

1.8. Extracellular vesicles

The minimal information for studies of extracellular vesicles (EVs) defines the EVs as “particles naturally released from the cell that are delimited by a lipid bilayer and cannot replicate” [121]. EVs present a diameter of 30 – 1000 nm [122], being the exosomes the particles released during an endocytic process of multivesicular bodies [123] with a diameter less than 100 nm [122], the microvesicles the particles formed by gemmation through the plasma membrane outside [123] with a diameter of 100 – 1000 nm, and the apoptotic bodies with a diameter of 500 – 3000 nm [124]. Furthermore, the EVs can be classified as large oncosomes, which are any EV released from cancer cells with an oncogenic content; migrosomes, that are oval structures bind to migratory cells membrane; ectosomes, that are similar to microvesicles; exosomes; and exomeres, which are EVs with a diameter less than 50 nm, without lipid bilayer and with no knowledge of their biogenesis [125]. EVs can be found in basically all the biological fluids [126], for example urine, blood, breast milk, saliva, bronchoalveolar aspirate, cerebrospinal fluid, exudates, pleural effusion, ascites, amniotic fluid, sperm, nasal secretion, lymph, tears and aqueous humor [121,124,127–129].

The main components of the lipid bilayer are: ceramide, cholesterol, sphingomyelins, phosphoglycerides, glycosphingolipids, phosphatidyl serine, phosphatidyl ethanolamine, mannose, N-linked glycans, polylactosamine, sialic acid [123]. Furthermore, it is possible to find cytosol proteins, from endosomal compartments and from plasma membrane: tetraspanins (CD9, CD63, CD81, CD82; small transmembrane proteins with four transmembrane segments and two extracellular loops), Tsg101, endosomal sorting complex required for transport-3 (ESCRT-3) binding protein to ALIX, Rab GTPases, SNARE, flotillins, annexin, clathrin and platelet derived growth factor receptors [123,130]. These proteins can be used as EVs markers [123]. The lipid bilayer takes care of the content protection in front of RNases and proteases, in addition to act as drug carrier during therapy [127]. Furthermore, the lipid bilayer protects the EVs from exterior contamination, and allow their stabilization [131]. An important advantage of EVs is that present a high sensibility and specificity when are used as biomarkers, in addition to their non-invasive isolation, due to its presence in body fluids [131]. On the other hand, EVs present some disadvantages, such as the need of a first isolation step, because the isolation techniques are long, expensive, hard and can present contamination [131].

The process of EVs formation can give to a different content [123]. Exosomes are formed in plasma membrane during endocytosis (Figure 7) [127,128]. First, an early endosome matures to late endosome or multivesicular bodies through the gemmation of endosomal vesicle membrane [127,128]. The membrane of multivesicular bodies form intraluminal vesicles, which are the exosomes [124]. The exosomes incorporate cytosolic content and transmembrane and peripheral proteins that are incorporated to the membrane that invaginates [132], in addition to membrane specific domains, mRNA, miRNA, proteins and DNA [128]. This content can be introduced inside exosomes through two mechanisms: ESCRT-dependent, in cooperation with ALIX and Tsg101: ESCRT-0 bind ubiquitinated molecules to introduce them into exosomes, then, ESCRT-I, II and III act during the intraluminal vesicles formation [124,128]; ESCRT-independent: heparanase cleaves the heparan sulfate, stimulating the acquisition of exosomes markers, such as CD63, tetraspanins participate in the selective loading of exosomal content and the adhesion of exosomes to target cells [124,128]. miRNAs can be loaded

into the exosomes by the sumoylation of heteronuclear ribonucleoprotein A2B1, because this allows the recognition of small sequences of four nucleotides (GGAG) [124,128]. After the loading of the exosomes, the multivesicular bodies can be merged with lysosomes to be degraded or can be merged with plasma membrane, releasing the exosomes [124,128]. Sphingomyelinase participates in the EVs release, and CD9, CD63 and CD81 in the endosomal vesicle trafficking [132].

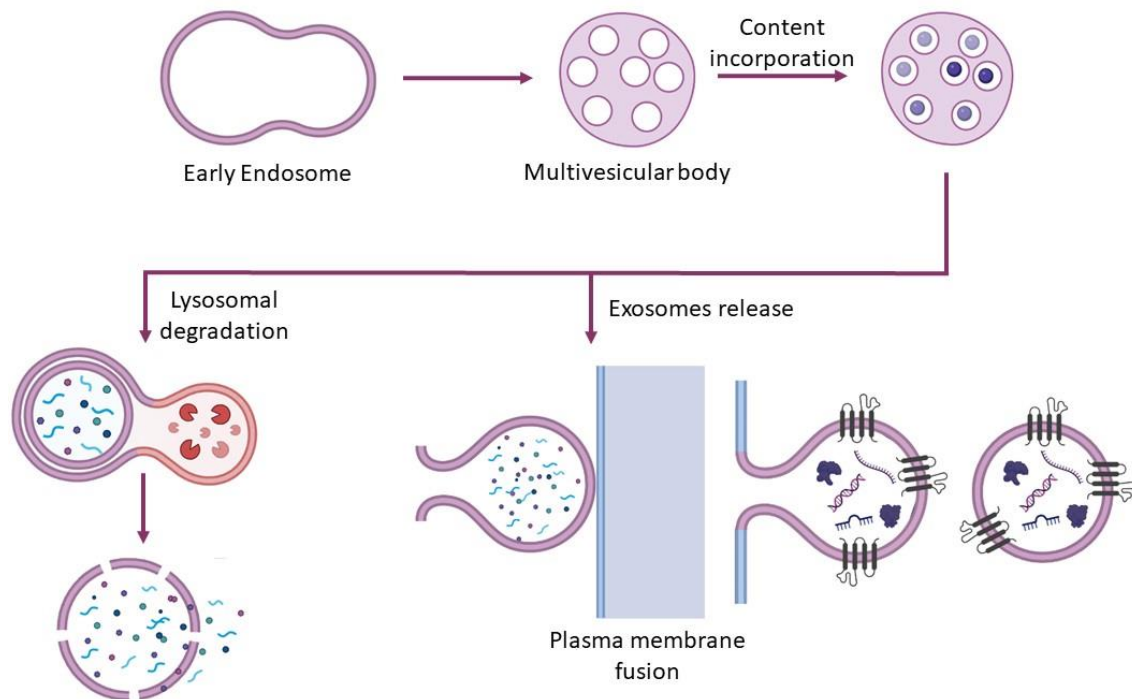


Figure 7. Exosomes formation during endocytosis. Created by Biorender.

It has been described that cell donor phenotype is reflected in the EVs content [122]. The EVs content is formed by endosomal membrane proteins, like annexin and flotillin, that facilitate transport and membrane fusion, in addition to tetraspanins [128], different kinds of proteins, such as signalization proteins, receptors, cytoskeleton proteins, lipids, DNA and different RNA types, like mRNA, miRNA and lncRNA [122]. Due to the fact that the EVs content forms part of tumor-derived cells genome, transcriptome and secretome, it contains oncoproteins, tumoral suppressor proteins, transcriptional regulators, tumoral suppressor genes with mutations, miRNAs related to metastasis, and proteins related to apoptosis, cell cycle, cellular signaling, oxidative stress, focal adhesions and cellular motility [122].

The main function of EVs is communication between cells and distant organs, due to their union to the membrane receptors in target cells and the consequent activation of signaling cascade, EVs also participate in debris and waste products removal, immune response, inflammatory processes, tissue reparation, and development and differentiation of stem cells [124,133]. Finally, EVs present an important role in carcinogenesis, because transmit the signal from tumoral cells to the microenvironment, in addition to modify the microenvironment [126], EVs also participate in tumor vasculature and angiogenesis, reorganize the extracellular matrix and cytoskeleton [122,124,126,133], activate survival and tumoral expansion signaling pathways, allow immune evasion [122,123,128], promote formation, progression, invasion and metastasis [126,127], and finally, participate in the establishment of premetastatic niche and drug resistance [123,127].

2. Objectives and experimental approach

The elaboration of this doctoral thesis has been part of three different projects developed at the *Grup Multidisciplinar d'Oncologia Translacional* (GMOT) at the *Institut Universitari d'Investigació en Ciències de la Salut* (IUNICS) from the *Universitat de les Illes Balears* (UIB) and the *Institut d'Investigació Sanitària de les Illes Balears* (IdISBa). The first project was *Hacia un diagnóstico personalizado en el cáncer colorrectal: influencia del metabolismo energético y estrés oxidativo en la respuesta al tratamiento* (PI14/01434), whose principal objective was to determine and to evaluate different energetic metabolism and oxidative stress key parameters as prognosis biomarkers in colorectal cancer (CRC) patients. The second project was *Influencia del metabolismo energético y la inflamación en la metástasis y la resistencia al tratamiento en el cáncer de colon* (PRI20/15), where the principal objectives were to compare the energetic metabolism, epithelial-mesenchymal transition, and inflammation between primary tumoral colon cancer cells and metastatic colon cancer cells; to study the energetic metabolism and oxidative stress in colon cancer stem cells by colonosphere formation and their implications in progression, metastasis and treatment response of this type of cancer; and finally, determine key parameters related to energetic metabolism, oxidative stress, and inflammation in different stages of CRC patients tissue samples. Finally, the third project was *Proyecto del Hospital Comarcal de Inca y la Universidad de las Islas Baleares* (FUEIB – CINUIB), whose principal objective was to develop a non-invasive system, based on the detection of bowel lavage fluid (BLF) and stool biomarkers, for CRC determination.

CRC is the third most common cancer worldwide, being the second cause of cancer death [4]. The overall 5-year survival for stage I is about 90%, for stage II approximately 70%, for stage III nearly 60%, and for stage IV less than 10% [60,61]. Therefore, an early diagnosis of CRC is necessary. Nowadays, CRC screening is active in the Balearic Islands for healthy people in an age range between 55 and 69 years, to decrease the late diagnosis rate of this disease. The gold standard technique for CRC screening is the fecal occult blood test (FOB), and if this test has a positive result, the patient must undergo a colonoscopy, which is a very invasive technique. Despite this, FOB test presents a high rate of false positive results so the determination of new early CRC biomarkers could improve the early diagnosis of this cancer and the overall survival of these patients

[63,64,134,135]. For this reason, the study of CRC tissues is very important, since these tissues can present new biomarkers in early stages to improve early diagnostic. It is known that oxidative stress is very altered in CRC, but the mechanism by which this oxidative stress affects to early stages is not well established yet. Despite this, it is known that oxidative stress alters signaling pathways by disturbing the expression and/or activity of different transcription factors, stimulating proliferation, invasion, and protection from apoptosis [44,45]. On the other hand, previous studies in our research group demonstrated that non-tumor adjacent tissue plays an important role in tumor progression [136,137], as well as presents an aberrant pattern of gene expression and structural alterations compared to tumor tissue [138–140]. For these reasons, as a first objective, our aim was to analyze the expression of antioxidant enzymes and proteins related to oxidative stress modulation in both tumor and non-tumor adjacent tissues in stages I, II, and III from CRC patients' samples, and to determine if these proteins could be biomarkers for non-metastatic stages in CRC. To achieve this goal, all these proteins were determined by Western blot, and the overall survival for high and low MnSOD or MnSOD/SIRT3 expression levels in tissue samples was studied by Kaplan-Meier survival curves. The results and conclusions generated with these experiments are shown in **Manuscript 1**.

Results obtained in Manuscript I demonstrate the importance of studying early stages for the progression of CRC, so considering the changes that occur in parameters that affect all the colorectal phases or advanced phases, such as inflammation and EMT respectively, could show changes in the early phases that have not been taken into account until now. Inflammation is a physiologic process that, when becomes chronic, can induce malignant transformation in surrounding tissues [17]. Furthermore, inflammation participates in all CRC phases [18], leading to cell survival, immunosuppression, tumor growth, proliferation, differentiation, angiogenesis, EMT, and metastasis [17,24,35]. Precisely, EMT is a process that appears at advanced cancer stages allowing epithelial cells to acquire a mesenchymal phenotype, as well as achieving the capacity to migrate, invade, and metastasize [141]. For these reasons, as a second objective, our purpose was to analyze the expression of inflammatory, EMT, and metastasis-related proteins in both tumor and non-tumor adjacent tissues in all

stages (I, II, III, IV) from CRC patient's samples, to better understand the relationship between these processes and to find new biomarkers. To achieve it, all those proteins were determined by Western blot, and the relapse-free survival for low or high Vimentin or VEGF-B expression levels in tissue samples was studied by a bioinformatic study using Kaplan-Meier survival curves. The results and conclusions generated with these experiments are shown in **Manuscript 2**.

Results obtained in Manuscripts I and II about tumor and non-tumor adjacent tissue samples from CRC patients demonstrate the relevance of early stages, specifically stage II, in addition to the importance of the non-tumor adjacent tissue. These results in tumor and non-tumor adjacent tissue could be due to cellular communication. This cellular communication can be achieved by extracellular vesicles (EVs), that can also present new possible biomarkers, due to the protection of these molecules for further analysis. Minimal information for studies of EVs (MISEV2018) defines EVs as “particles naturally released from the cell that are delimited by a lipid bilayer and cannot replicate”, and it has been seen that CRC cells release them since early stages [121]. EVs are characterized by a long half-life, easiness to obtain, and presence in high concentrations in several tissues and corporal fluids, including non-invasive samples. Furthermore, the lipid bilayer stabilizes the macromolecules content of EVs, and avoids their degradation, and these macromolecules cargo can reflect tumor status [63,142,143]. Finally, EVs main function is to participate in the transport of molecules to target cells, communicating cells, and they participate in most cancer phases [126,127,142,144,145]. For these reasons, EVs can be used as a diagnostic tool for CRC. BLF is obtained during colonoscopies as a result of irrigating the injured area in colon with saline serum to enrich it with injury area cells [146]. This type of sample presents some advantages in front of other samples, such as low bacterial and food interference, easiness to handle, less variability due to water presence, and less protein degradation [146]. Despite there are few studies using this sample for the identification of CRC biomarkers [105,108,110,147,148], this is a barely used sample type that has a lot of potential both to better understand CRC and to find new biomarkers [146]. For these reasons, as a third objective, our goal was to use BLF as a research tool for study and diagnosis of CRC through the isolation and study of EVs from this sample. To achieve it, the EVs were

isolated by ultracentrifugation and characterized by atomic force microscopy, transmission electron microscopy, and nanoparticle tracking analysis. The presence of tetraspanins, EVs markers, was determined by Western blot, the RNA cargo was studied by messenger RNA (mRNA) and microRNA (miRNA) arrays, and the obtained results were studied using the Softwares R and Transcriptome Analysis Console. Finally, the functions and the interrelationship between differentially expressed mRNA and miRNA were studied. The results and conclusions generated with these experiments are shown in **Manuscript 3** and **Manuscript 4**.

Until now, the highest incidence of CRC was in European countries, but lately, the number of cases has increased in Asia due to changes in diet, which is now more westernized [149]. Asia has the highest intake of soy-derived products, and, for this reason, presents a high intake of genistein (GEN), a phytoestrogen found in soybean [52]. Previous studies in our research group had demonstrated that GEN treatment on breast cancer cells can induce apoptosis and cell cycle arrest depending on ER α /ER β ratio, in addition to be beneficial for breast cancer cells with low ER α /ER β ratio due to the improvement in mitochondrial functionality and the decrease in reactive oxygen species (ROS) production and proinflammatory-related genes expression [150–153]. Moreover, previous studies in our research group also demonstrated that polyphenols, such as resveratrol and xanthohumol, can affect CRC acting as a prooxidant and producing cell death in metastatic cell lines and acting as an antioxidant in primary cell lines [154–157]. It has been seen that GEN can affect CRC, but the mechanism by how GEN affects it remains unclear [52,58]. Despite this, GEN has a dual role in front of oxidative stress, which participates in the beginning and progression of CRC [43], since it can act as an antioxidant [52], but at high concentrations can act as a prooxidant [55,158,159]. In addition, GEN also affects cell bioenergetics [54], but its role in mitochondrial biogenesis, which is compromised in cancer development, is not established yet [36]. Finally, GEN can also modulate inflammation [53], which is a key factor for tumoral growth, angiogenesis, epithelial-mesenchymal transition (EMT), and metastasis [17]. For these reasons, as a fourth objective, our goal was to analyze the effect of a high concentration GEN treatment in oxidative stress, mitochondrial biogenesis, and inflammation in two colon cancer cell lines: HT29, a primary and

moderately differentiated cell line, and SW620, a metastatic and poorly differentiated cell line. To achieve it, several parameters were studied as follows: cell viability was determined by Hoechst 33342, H₂O₂ production by Amplex® Red Hydrogen Peroxide/Peroxidase Assay kit, cell cycle analysis by flow cytometry, gene and/or protein expression levels of antioxidant enzymes, the expression of mitochondrial biogenesis regulators and inflammation-related genes were studied by real-time PCR and/or Western blot, and finally, the nuclear translocation of NF-κB and actin cytoskeleton remodeling were studied by confocal microscopy. The results and conclusions generated with these experiments are shown in **Manuscript 5**.

The investigations conducted in the present thesis were developed under the supervision of Dr. Jordi Oliver Oliver and Dr. Daniel Gabriel Pons Miró from *Grup Multidisciplinar d'Oncologia Translacional*. The execution of this work has been possible thanks to the research projects financed by the *Instituto de Salud Carlos III, Gobierno de España, co-financed by fondos FEDER – Unión Europea “Una manera de hacer Europa”* (PI14/01434 awarded the year 2014), *Projectes Intramurals IdISBa* (PRI20/15 awarded the year 2020), and the fundraising from *Fundació Universitat Empresa de les Illes Balears* (FUEIB; CINUIB), including all the donors that participated in the fundraising. Furthermore, the research group has also received funding from *Ciber Fisiopatología de la Obesidad y la Nutrición* (Ciberobn; CB06/03), from the *Instituto de Salud Carlos III*. To carry on the tumor and non-tumor adjacent tissues from CRC patients experiments (PI14/01434), the researchers received help from *Hospital Universitari Son Llàtzer*, in addition to the pathological anatomy service from the hospital. Finally, to carry out the BLF experiments (FUEIB – CINUIB), the researchers received help from digestive service from the *Hospital Comarcal d'Inca*.

3. Materials and methods

3.1. Samples

3.1.1. Cell culture

3.1.1.1. Colon cancer cell lines characteristics

HT29 cell line was purchased at *American Type Culture Collection* (ATCC-HTB-38). This cell line was isolated from a primary tumor from a 44-year-old Caucasian female with colorectal adenocarcinoma. The morphology is epithelial and has a subcultivation ratio of 1:3 to 1:8 from 2 to 3 times per week.

SW620 cell line was purchased at *American Type Culture Collection* (ATCC-CCL-227). This cell line was isolated from a lymph node from a 51-year-old Caucasian male with Dukes C colorectal cancer. The morphology is epithelial and has a subcultivation ratio of 1:2 to 1:10 from 2 to 3 times per week.

3.1.2. Tumoral tissue

3.1.2.1. Inform consent and Declaration of Helsinki

All participant patients have received the patient information sheet about the research project, and they have signed an informed consent according to *World Medical Association Declaration of Helsinki* when medical research involves humans. The study was approved by the *Comité d'Ètica de la Investigació de les Illes Balears* (IB 2431/14 PI, 26/11/2014).

3.1.2.2. Colorectal tumor and non-tumor adjacent tissue

Tissues were collected from *Biobanc de Hospital Universitari Son Llàtzer*, for 5 years (2005-2010), and maintained at -80 °C until their processing. A total of 57 patients were included in the study and samples were divided into stages (I, II, III and IV) and into tissue types (tumor tissue and non-tumor adjacent tissue). In stage I, 9 samples were included (3 females and 6 males), 17 samples were included in stage II (8 females and 9 males), 19 samples were included in stage III (12 females and 7 males), and 12 samples (3 females and 9 males) were included in stage IV. The histological examen and the classification by TNM staging system were done by a pathologist.

3.1.2.3. *Patients' characteristics*

Patients of both sexes without comorbidity were included in the study, additionally, patients did not receive chemotherapy or radiotherapy before surgery. The age average was 70.7 years and SD was 11.0, where female age average was 69.9 ± 10.6 and range 50-88 and male age average was 71.4 ± 11.3 and range 51-95. Clinicopathological features of patients included in the study are shown in Table 1.

Table 1. Clinicopathological features of patient's samples included in the study.

Age	BMI	Stage	TNM	Histological grade	Tumor location	Metastasis
78	25.6	I	T2N0M0	-	-	No
56	-	I	T1N0MX	G2	Sigmoid colon	No
59	-	I	T2N0MX	G1	Sigmoid colon and rectum	No
83	28.2	I	T2N0M0	G2	Descending and rectum	Yes (local and lung)
79	-	I	T2N0MX	G2	Descending	No
65	-	I	T2N0M0	G3	Ascending	No
64	-	I	T2N0MX	G2	Descending	No
56	-	I	T2PN0M0	G1	Descending	No
60	-	I	T1N0MX	G1	-	No
77	25.5	IIA	T3BN0MX	G3	Right colon at hepatic angle	No
78	29.7	IIA	T3N0MX	G2	Rectum - sigmoid union	No
70	22.6	IIA	PT3BN0M0	G2	Rectum	No
67	26.7	IIA	T3CN0M0	G2	Rectum – sigmoid union	No
60	-	IIA	T3(M)N0MX	G1	Ascending	No
74	-	IIA	T3BN0MX	G3	Ascending	No
72	-	IIA	T3N0MX	G1	Descending	No
50	-	IIA	T3CPN0M0	G2	Descending	No
88	-	IIA	T3N0M0	G1	Sigmoid	No
81	20.8	IIA	T3PN0M0	G2	Descending	No
64	23.1	IIC	T4N0MX	G3	Transverse	No
67	41.9	IIA	T3BN0MX	G1	Transverse	Local
63	30.3	IIA	T2-T3N0	G2	-	No

Materials and methods

54	29.4	IIC	T4N0M0	G3	Sigmoid	No
66	-	IIA	T3N0MX	G1	Rectum	Lung
72	25.8	IIA	PT3PN0M0	G1	-	No
73	31.6	IIA	T3N0MX	G2	Caecum	No
81	24.2	IIIB	T3BN1M0	G1	Transverse	No
82	26.3	IIIB	T3N1M0	G2	Ascending – Caecum	No
50	25.5	IIIC	T4BPN2M0	G2	Sigmoid	No
67	24.9	IIIC	T3N2BM0	G3	Ascending	No
70	22.1	IIIA	T2N1M0	G2	Rectum	No
51	22.6	IIIC	T4BN2M0	G2	Sigmoid	No
69	27.6	IIIB	T3N1M0	G3	Ascending	No
83	24.7	IIIB	T3N2M0	G3	Ascending	No
75	-	IIIB	T3BN1M0	G2	Descending	No
75	-	IIIB	T3CN2M0	G2	Sigmoid	No
57	-	IIIC	T4BN1M0	G2	Descending	No
83	-	IIIC	T4N2MX	G2	Ascending	
95	-	IIIB	T3N2MX	G2	Ascending - Transverse	Local
89	-	IIIB	T3N2Mx	G1	Ascending	-
57	-	IIIC	T4bN1Mx	G2	Descending	Local
84	19.2	IIIC	ET4N2M0	G2	-	Local
79	23.8	IIIC	PT4PN2M0	G3	Descending	-
85	-	IIIB	T3N1MX	G2	Descending	-
68	33.6	IIIB	T3N2MX	G3	Ascending	-
92	-	IVA-B	T3N2M1	G2	Transverse - Sigmoid	Yes
83	-	IVA-B	T3BN2MX	G3	Ascending - Caecum	Yes
63	24.4	IVA-B	T2PN2PM1	-	Descending - Rectum	Yes
78	33.5	IVA-B	T3PN1M1	G1	Hepatic angle	Yes
52	23.4	IVA-B	T3N1M1	-	Sigmoid	Yes
80	23.6	IVA-B	T4N2M1	G2	Sigmoid	Yes
55	20.3	IV-B	T4PN2M1	G3	Ascending	Yes
76	23.4	IVA-B	T3N1M1	G2	Ascending	Yes
67	34.2	IVA-B	T3PN2M1	G3	Ascending	Yes
74	18.8	IVA-B	PT4PN0M	G3	Rectum	Yes
65	32.9	IV	T3N2M1	G2	Sigmoid - Rectum	Yes
95	27.9	IV	T3N2M1	G2	Ascending - Transverse	Yes

3.1.3. Bowel lavage fluid (BLF)

3.1.3.1. Inform consent and Declaration of Helsinki

All participant patients have received the patient information sheet about the research project, and they have signed an informed consent according to *World Medical Association Declaration of Helsinki* when medical research involves humans. The study was approved by the *Comité d'Ètica de la Investigació de les Illes Balears* (IB 3833/19 PI).

3.1.3.2. Sample acquisition

Days prior colonoscopy, patients received the information about colonoscopy and the information sheet about the research project. 48 hours before colonoscopy, patients had to reduce fiber, fat and gas intake, and 8 hours before colonoscopy patients drunk 3 liters of a polyethylene glycol solution to clean the bowel lumen. Colonoscopies were done at endoscopy unit from *Hospital Comarcal d'Inca* with anesthesia sedation. BLF was collected with saline solution (0.9% NaCl) applied directly above the injury area in the mucosa through endoscope flushing channel, then was aspirated and retained at the polyp trapping basket of the endoscope, which avoids the mixture with non-affected zones fluids, and finally was stored at -80 °C until processing. A total of 217 patients were included in this study and samples were divided according to pathology: without pathology (healthy samples; N=49), with polyps (divided into low- and high- risk of suffering CRC, N=73 and N=34, respectively), and cancer samples (N=61). Low-risk corresponds to 1 or 2 tubular adenomatous lesions with low grade dysplasia and serrated lesions without dysplasia, all less than 10 mm; high-risk corresponds to 3 or more tubular adenomatous lesions with low grade dysplasia less than 10 mm, at least one adenomatous lesion with villous component, high grade dysplasia or more than 10 mm, at least one serrated lesion with dysplasia or more than 10 mm [160]).

3.2. General procedures with cell culture

3.2.1. Maintenance and culture

All cell lines used present a biosecurity level 1, for this reason, all the experiments were done at sterile environment, in a biosecurity cabin type II, and following the basic regulations for cell culture.

Cells were cultured with Dulbecco's Modified Eagle's Medium High Glucose (DMEM, L0109-500, Biowest), with stable Glutamine, 25 mM HEPES and without Sodium Pyruvate and supplemented with 1% Penicillin-Streptomycin (L0018-100, Biowest) and 10% Fetal Bovine Serum (FBS, S181B-500, Biowest). Cells were maintained at 37 °C and in a 5% CO₂ atmosphere.

The general protocol for subculture cells is the following: cells were seeded in a 100 mm-well plate and, when confluence arrived at 70-80%, were cultured into another 100 mm-well plate as follows. DMEM medium was removed and 1 mL of sterile PBS pH 7.4 (137 mM NaCl, 2.7 mM KCl, 10 mM Na₂HPO₄, and 2 mM KH₂PO₄) was added to eliminate medium remains. Then, 1 mL of 0.25% Trypsin-EDTA (T4049, Sigma-Aldrich) was added to detach cells and incubated for 5 minutes at 37 °C and 5% CO₂ atmosphere. Next, the Trypsin-EDTA was inactivated with 3 mL of DMEM medium, and cells were transferred to another 100 mm-well plate at the necessary number of cells.

3.2.2. Freezing and thawing cells

Cells were frozen when there was an 80-90% of confluency. First, DMEM medium was removed, and 1 mL of sterile PBS pH 7.4 was added to eliminate medium remains. For cells detachment, 1 mL of 0.25% Trypsin-EDTA was added for 5 minutes at 37 °C and 5% CO₂ atmosphere and then, was inhibited with 3 mL of DMEM medium. The 4 mL obtained were centrifugated at 1600 rpm for 5 minutes, and supernatant was removed. After that, 3 mL of PBS were added to the pellet and the centrifugation was repeated. Finally, supernatant was removed, and pellet was resuspended in 1 mL of frozen solution (10% dimethyl sulfoxide [DMSO] in FBS) and transferred into a cryovial properly labeled. Cryovials were saved into Mr. Frostie™ (Thermofisher) with 2-propanol at -80 °C for, at least, 4 hours, then was stored into liquid nitrogen tank.

For cell thawing is necessary work fast, because the 10% DMSO can affect the cells. First, 13 mL of DMEM medium at 37 °C were used to transfer frozen cells to a new tube, which then was centrifugated at 1600 rpm for 5 minutes. Supernatant was removed and pellet was resuspended in 4 mL of DMEM medium. After that, it was transferred to a 60 mm-well plate overnight and next day, cells were cultivated into a 100 mm-well plate.

3.2.3. Mycoplasma detection

If culture contamination is suspected, mycoplasma detection is necessary, and can be done with Mycoplasma Detection Kit-Quick Test (B39032, Bimake.com), following manufacturer's protocol. When cell culture is contaminated by mycoplasma, some metabolites from mycoplasma are released to cell culture medium, so the presence of these metabolites produces a color shift, turning green. Briefly, 40 μ L of Reaction Buffer A were added to each well, then, 10 μ L of negative control (non-used medium), or cells (medium that was 48 hours in contact with cells) or positive control were added to each well, and plate was shaken and incubated at room temperature for 5 minutes. After that, 40 μ L of Reaction Buffer B were added to each well, and plate was shaken and incubated at room temperature for 4 minutes. Finally, 5 μ L of Stop Solution were added and plate was shaken. In the next 30 minutes, sample color can turn into green, indicating mycoplasma contamination or can remain as negative control, indicating no mycoplasma contamination.

If our cell culture is contaminated, is necessary clean the laboratory and discard the contaminated cell culture.

3.2.4. Cell Treatment

HT29 and SW620 cell lines were seeded and treated, the following day, at 70-80% of confluency with genistein (GEN, G6649-25MG, Sigma-Aldrich) at different concentrations depending on the methodology used for 48 hours.

GEN was diluted in 100% DMSO to a final concentration of 100 mM, then was consecutively diluted in DMEM medium to achieve final concentrations for treatments. For Cell Viability and Hydrogen Peroxide (H_2O_2) Production determinations, cells were treated with increasing concentrations (1, 5, 50 and 100 μ M) of GEN with 0.1% DMSO as the vehicle, and the control vehicle-cells were treated with 0.1% DMSO for 48 hours. For further experiments (Gene Expression, Mitochondrial DNA, Cell Cycle, Protein Levels, NF- κ B Translocation into the Nucleus, and Actin Cytoskeleton Remodeling determinations), cells were treated only with 100 μ M GEN with 0.1% DMSO as the vehicle, and the control vehicle-treated cells were treated with 0.1% DMSO for 48 hours.

3.3. Methodology

3.3.1. Fluorometric determinations

3.3.1.1. Cell viability determination by Hoechst

A total of 5×10^4 HT29 cells and 4×10^4 SW620 cells were seeded in each well in a 96-well plate. After GEN treatment, medium was removed, and cells were washed with sterile PBS pH 7.4. Then, 1 mg/mL Hoechst (in ethanol) was diluted 1/200 in PBS, to achieve a 5 μ g/mL Hoechst solution, cells were incubated with 100 μ L of this solution for 5 minutes at 37 °C. Finally, fluorescence was measured with FLx800 microplate reader, set at excitation wavelength of 350 nm and emission wavelength of 455 nm.

3.3.1.2. Hydrogen peroxide (H_2O_2) production determination by Amplex Red

A total of 5×10^4 HT29 cells and 4×10^4 SW620 cells were seeded in each well in a 96-well plate. After GEN treatment, H_2O_2 production was determined using an Amplex Red Hydrogen Peroxide/Peroxidase Assay Kit (A22188, Fisher Scientific). Briefly, medium was removed, and cells were washed with sterile PBS pH 7.4. Then, cells were incubated with 100 μ L of Krebs – Ringer (145 mM NaCl, 4.86 mM KCl, 0.54 mM $CaCl_2$, 1.22 mM $MgSO_4$, 5.5 mM Glucose, 5.7 mM Sodium Phosphate pH 7.4) with 0.1 U/mL horseradish peroxidase and 50 μ M Amplex Red reagent for 1 hour at 37 °C. During the hour, fluorescence was measured with FLx800 microplate reader, set at excitation wavelength of 570 nm and emission wavelength of 585 nm. The maximum slope of the increase in the fluorescence was detected within 30 minutes of exposure to reagents. The number of viable cells determined by Hoechst 33342, as previously described, was used to normalize the obtained results.

3.3.2. Extracellular vesicles (EVs) isolation by ultracentrifugation

BLF samples were centrifugated at 2,000 xg for 15 minutes at 4 °C to eliminate debris and cellular components. After that, 8 mL of sterile PBS (500 mM NaCl, 167 mM $NaH_2PO_4 \cdot 2H_2O$, 333 mM Na_2HPO_4) pH 7.5 were added to 4 mL of BLF and centrifugate at 2,000 xg for 10 minutes and 4 °C to remove debris and finally, supernatants were centrifugated at 2,000 xg for 10 minutes and 4 °C to eliminate large particles. After that,

supernatants were centrifugated at 100,000 xg for 1 hour and 4 °C to precipitate EVs. The resulting pellets were suspended in 100 µL of sterile PBS pH 7.5.

3.3.3. Gene expression determination

3.3.3.1. RNA isolation

For cell culture, a total of 1.5×10^6 HT29 cells and 2.1×10^6 SW620 cells were seeded in each well in 6-well plate. After GEN treatment, total RNA was isolated using Tri Reagent (T9424, Sigma-Aldrich) following the manufacturer's protocol. Briefly, 1 mL of Tri Reagent was added to the wells in order to scrape the cells and then was incubated for 5 minutes at room temperature. After that, 200 µL of chloroform were added to each sample, shook vigorously, and incubated for 15 minutes at room temperature. For phase separation, samples were centrifugated at 12,000 xg for 15 minutes at 4 °C. Then, 500 µL of isopropanol were added to aqueous phase, mixed, and incubated for 10 minutes at room temperature, followed by a centrifugation at 12,000 xg for 10 minutes at 4 °C. Supernatants were removed and pellets were washed with 1 mL of cold 75% ethanol, mixed, and centrifugated at 7,500 xg for 5 minutes at 4 °C. Finally, supernatants were removed, and pellets were dried under vacuum for 10 minutes and resuspended with 50 µL of RNase-free water. A BioSpec-nano spectrophotometer was used to quantify the total RNA amount, set at wavelength of 260 nm. The RNA quality was checked by 260/280 and 260/230 ratios.

For the EVs isolated from BLF used for mRNA array, total RNA was isolated using Tri Reagent LS (T3934, Sigma-Aldrich) following the manufacturer's protocol. Briefly, 750 µL of Tri Reagent were added to EVs samples and let it for 5 minutes at room temperature. After that, 200 µL of chloroform were added and incubated for 15 minutes at room temperature, followed by a centrifuge of 12,000 xg for 15 minutes and 4 °C. After centrifugation, three phases were differentiated. Then, 500 µL of isopropanol were added to the aqueous phase and it was incubated overnight at -20 °C for a better RNA precipitation. After the incubation, samples were centrifugated at 12,000 xg for 8 minutes at 4 °C and the resulting pellets were washed with cold 75% ethanol and centrifugated at 7,500 xg for 5 minutes at 4 °C. Supernatants were discarded and pellets were dried in the vacuum for 10 minutes. Finally, RNA was resuspended in 20 µL of

RNase-free water and quantified using a BIO-TEK PowerWave XS spectrophotometer at wavelength of 260 nm. The RNA quality was checked by 260/280 ratio.

For the EVs isolated from BLF used for array validation, total RNA was isolated using miRNeasy Mini Kit (217004, Qiagen), following manufacturer's protocol, to increase RNA integrity. Briefly, 700 μ L of QIAzol Lysis Reagent were added to EVs pellet to resuspend EVs and, after that, were homogenized by vortexing for 10 seconds. All samples were stored at -80 °C until RNA isolation was done. Samples were incubated 5 minutes at room temperature and then, 140 μ L of chloroform were added prior to an incubation of 3 minutes and a centrifuge of 12,000 xg for 15 minutes at 4 °C. After centrifugation, three phases were differentiated and aqueous phase was transferred to a new collection tube, where 525 μ L of 100% ethanol were added and mixed. Then, 700 μ L of sample were transferred into a RNeasy Mini column in a 2 mL collection tube, columns were centrifugated at 8,000 xg for 15 seconds at room temperature and the flow-through was discarded. This step was repeated with the remainder sample. After that, 700 μ L of Buffer RWT were added to the RNeasy Mini column, centrifugated at 8,000 xg for 15 seconds at room temperature and the flow-through was discarded. Then, 500 μ L of Buffer RPE were added to the RNeasy Mini column, centrifugated at 8,000 xg for 15 seconds at room temperature and the flow-through was discarded. Following, 500 μ L of Buffer RPE were added to the RNeasy Mini column, centrifugated at 8,000 xg for 2 minutes at room temperature and the flow-through was discarded. Next, the RNeasy Mini column was placed in a new 2 mL collection tube and centrifugated at 12,000 xg for 1 minute at room temperature. Finally, the RNeasy Mini column was placed in a 1.5 mL collection tube, 30 μ L of RNase-free water were added and it was centrifugated at 8,000 xg for 1 minute at room temperature to elute RNA. A BioSpec-nano spectrophotometer was used to quantify the total RNA amount, set at wavelength of 260 nm. The RNA integrity was checked by 260/280 and 260/230 ratios.

3.3.3.2. Reverse transcription

For GEN treated cell lines, reverse transcription was done as follows: 1 μ g of the total RNA was reverse transcribed to cDNA. First, RNA from samples suffered a denaturalization for 1 minute at 90 °C and then, 5 μ L of mix (2 μ L Buffer 5x, 2 μ L of 2.5 mM mix dNTPs, 0.5 μ L of 10 U RNase inhibitor, 0.5 μ L of 2.5 μ M random hexamers, and

0.5 µL of 100 U/ml reverse transcriptase) were added to each sample. Finally, samples were incubated 50 minutes at 37 °C, then 15 minutes at 70 °C and finally, at 4 °C. Each cDNA was diluted 1/10 and cDNA aliquots were frozen at -20 °C.

For EVs, reverse transcription was done as follows: 300 ng of the total RNA was reverse transcribed to cDNA. First, RNA samples were denaturalized for 1 minute at 90 °C. Next, the reverse transcription reagents were added to the sample (1 µL of 50 µM random hexamers [10609275, Fisher Scientific], 1 µL of 10 mM dNTPs Mix [100 mM dGTP Solution 10218-014, 100 mM dTTP Solution 10219-012, 100 mM dATP Solution 10216-018, 100 mM dCTP Solution 10217-016, Fisher Scientific], 1 µL of 20 U/µL RNase Out [10615995, Fisher Scientific], 2 µL of 0.1 M DTT, 4 µL of Buffer 5x and 1 µL of 200 U/µL M-MLV [10338842, Fisher Scientific]), and incubated at 25 °C for 10 minutes, then at 37 °C for 50 minutes, after at 70 °C for 15 minutes and finally, at 4 °C. cDNA aliquots were frozen at -20 °C after 1/10 dilution in RNase-free water.

3.3.3.3. Real-time PCR

A LightCycler 480 System II rapid thermal cycler (Roche Diagnostics, Basel, Switzerland) with SYBR Green technology was used to carry out the real-time PCR, 7.5 µL of mix were added to each well (2.1 µL of RNase-free water, 0.2 µL of forward and reverse primers each, and 5 µL of SYBR Green TB Green™ Premix Ex Taq™ [RR420A, Laboratorios Conda]) and 2.5 µL of each sample were added to each mix-containing well. The first step in the amplification program was a preincubation for achieve the denaturation of the template cDNA (5 minutes, 95 °C), then 40 cycles of denaturation (10 seconds, 95 °C), followed by annealing (10 seconds, primer-specific temperature, shown in Table 2) and elongation (12 seconds, 72 °C). For each gene was loaded a negative control without cDNA in the real-time PCR. For GEN treated cell lines experiments, the expression of beta-2-microglobulin (*B2M*) was used as housekeeping gene. Genes, primers, and annealing temperatures used are shown in Table 2.

Table 2. Primers sequences and their respective annealing temperatures and accession number.

Gene	Forward primer (5'-3') Reverse primer (5'-3')	Annealing temperature (°C)	Accession number
<i>B2M</i>	5'-TTT CAT CCA TCC gAC ATT GA-3' 5'-Cgg CAg gCA TAC TCA TCT TT-3'	54	NM_004048
<i>SOD2</i>	5'-CgT gCT CCC ACA CAT CAA TC-3' 5'-TgA ACg TCA CCg Agg AgA Ag-3'	64	BT006967
<i>SOD1</i>	5'-TCA ggA gAC CAT TgC ATC ATT-3' 5'-CgC TTT CCT gTC TTT gTA CTT TCT TC-3'	64	NM_000454
<i>CAT</i>	5'-CAT CgC CAC ATg AAT ggA TA-3' 5'-CCA ACT ggg ATg AgA ggg TA-3'	61	NM_001752
<i>GPX1</i>	5'-gCg gCg gCC Cag TCg gTg TA-3' 5'-gAg CTT ggg gTC ggT CAT AA-3'	61	M21304
<i>PPARGC1A</i>	5'-TCA gTC CTC ACT ggT ggA CA-3' 5'-TgC TTC gTC gTC AAA AAC Ag-3'	60	AF106698
<i>ESRRA</i>	5'-TCg CTC CTC CTC TCA TCA TT-3' 5'-Tgg CCA AAC CCA AAA ATA AA-3'	52	NM_004451
<i>TFAM</i>	5'-gTg gTT TTC ATC TgT CTT ggC-3' 5'-ACT CCg CCC TAT AAg CAT CTT-3'	60	BT019658
<i>SSBP1</i>	5'-TgT gAA AAA ggg gTC TCg AA-3' 5'-Tgg CCA AAg AAg AAT CAT CC-3'	60	AF277319
<i>TNF</i>	5'-AAg CCT gTA gCC CAT gTT gT-3' 5'-ggA CCT ggg AgT AgA TgA ggT-3'	58	NM_000594
<i>IL1B</i>	5'-TCg CCA gTg AAA TgA Tgg CT-3' 5'-ggT Cgg AgA TTC gTA gCT gg-3'	58	BT007213
<i>CXCL8</i>	5'-ggC ACA AAC TTT CAg AgA CAg CAg-3' 5'-gTT TCT TCC Tgg CTC TTg TCC TAG-3'	66	AK311874
<i>CXCR2</i>	5'-AgT TCT Tgg CAC gTC ATC gT-3' 5'-CCC CTg AAg ACA CCA gTT CC-3'	57	M68932
<i>HPSE</i>	5'-gCA AAC TgC TCA ggA CTg gA-3' 5'-gCT gAC CAA CAT CAg gAC CA-3'	60	AF084467
<i>IL10</i>	5'-ACA TCA Agg CgC ATg TgA AC-3' 5'-CAC ggC CTT gCT CTT gTT TTC-3'	60	M57627
<i>PPARG</i>	5'-gAg CCC AAg TTT gAg TTT gC-3' 5'-CTg TgA ggA CTC Agg gTg gT-3'	61	BT007281
<i>mtDNA</i>	5'-CgT gAC TCC TAC CCC TCA CA-3' 5'-ATC ggg TgA TAg CCA Ag-3'	60	NM_025230.5

18S	5'-ggA CAC ggA CAg gAT TgA CA-3'	60	NR_146119.1
	5'-ACC CAC ggA ATC gAg AAAGA		

3.3.4. Mitochondrial DNA determination

3.3.4.1. DNA isolation

A total of 1.5×10^6 HT29 cells and 2.1×10^6 SW620 cells were seeded in each well in 6-well plate. After GEN treatment, total DNA was isolated by using Tri Reagent (T9424, Sigma-Aldrich) following the manufacturer's protocol. Briefly, the remaining aqueous phase was removed, and 300 μ L of 100% ethanol were added, mixed by inversion, incubated for 3 minutes at room temperature and centrifugated at 2,000 xg for 5 minutes at 4 °C. Supernatants were saved in another tube for a future protein isolation and pellets were washed twice with 1 mL of 0.1 M trisodium citrate in 10% ethanol, incubated for 30 minutes at room temperature, and centrifugated at 2,000 xg for 5 minutes at 4 °C. After washes, pellets were resuspended with 1 mL of 75% ethanol, incubated 20 minutes at room temperature, and centrifugated at 2,000 xg for 5 minutes at 4 °C. Finally, pellets were dried under vacuum for 10 minutes, resuspended with 100 μ L of 8 mM NaOH, and centrifugated at 12,000 xg for 10 minutes at 4 °C. Supernatants were transferred to a new tube and a BIO-TEK PowerWave XS spectrophotometer was used to quantify de DNA amount, set at wavelength of 260 nm. The DNA integrity was checked by 260/280 ratio.

3.3.4.2. Real-time PCR

A total amount of 5 ng of DNA was carried out into a real-time PCR, as previously described, and the expression of NADH dehydrogenase subunit 4 as mitochondrial DNA (*mtDNA*) was analyzed, using the expression of *18S* as housekeeping gene. Genes, primers, and annealing temperatures used are shown in Table 2.

3.3.5. Cell cycle determination by flow cytometry

A total of 9×10^5 HT29 cells and 8×10^5 SW620 cells were seeded in each well in 6-well plate. After GEN treatment, cells were harvested with trypsin-EDTA and fixed in 1mL of cold 100% methanol, fixation was done drop by drop with simultaneously shaking gently. Fixed cells were incubated at -20 °C overnight and centrifugated at 600 xg for 5

minutes, discarding the supernatant. Before the analysis of DNA staining, cells were incubated at room temperature in the dark for 30 minutes with 500 μ L of working reagent (5 mg/mL RNase 100x and 1mg/mL propidium iodide 20x in sterile PBS pH 7.4). Flow cytometry experiments were performed using a Beckton-Dickinson FACSVerse flow cytometer, and the results were analyzed with FACSuite v1.0.6 Software.

3.3.6. Protein concentration determination

3.3.6.1. BCA method

BCA method (Pierce® BCA Protein Assay kit, 23225, Thermo Scientific™) was used to determine protein concentration of GEN treated cell lines, due to the protein solvent, which interferes with Bradford method. This method is based on the Cu^{2+} reduction to Cu^+ by proteins present on the sample, then, Cu^+ reacts with BCA (green) turning into purple, in a proportional way to protein concentration. This determination was done following manufacturer's protocol. Briefly, 2 mg/mL BSA was diluted in protein solvent (RIPA buffer: 50 mM Tris-HCl, pH 7.5, 150 mM NaCl, 0.1% SDS, 0.5% deoxycholate, 1% Triton X-100, 1 mM EDTA) as follows in Table 3 and was used as a pattern. 10 μ L of pattern or sample were added to each well and 200 μ L of BCA Reagent (Reagent A:Reagent B in a 50:1 proportion) were added to pattern and samples wells. Then, the plate was shaken for 30 seconds and incubated at 37 °C for 30 minutes covered from light. Finally, BIO-TEK PowerWave XS spectrophotometer was used to measure absorbance, that was set at a wavelength of 562 nm.

Table 3. BCA pattern made with 2 mg/mL BSA diluted in protein solvent, and mg/mL BSA.

	Vial A	Vial B	Vial C	Vial D	Vial E	Vial F	Vial G	Vial H
μ L diluent	0	125	325	175	325	325	325	400
μ L BSA	300 stock	375 stock	325 stock	175 vial B	325 vial C	325 vial E	325 vial F	0
mg/mL BSA	2.000	1.500	1.000	0.750	0.500	0.250	0.125	0

3.3.6.2. Bradford method

Bradford method [161] was used to determine protein concentration of tumor and non-tumor adjacent tissues, EVs isolated from BLF samples and BLF samples. This method is based on Coomassie blue reagent, which presents brown color in acid media, but when

contacts with proteins, brown turns blue in a direct proportional way to protein concentration. Briefly, 2 $\mu\text{g}/\mu\text{L}$ BSA was diluted in protein solvent (homogenization buffer [20 mM Tris pH 7.4, 250 mM Saccharose, 2 mM EGTA, 40 mM KCl, 1 mM MPSF, 1 mM Na_3VO_4 , 10 μM Pepstatin, and 10 μM Leupeptin] and PBS, respectively) with a final concentration of 0.5 $\mu\text{g}/\mu\text{L}$ and was used as a pattern (Table 4). 5 μL of sample were added to each well and 300 μL of Bradford Reagent (50 mL of 96% ethanol (v/v), 100 mg of Coomassie Brilliant Blue, 100 mL of 85% H_3PO_4 , screed until 1 L with double distilled H_2O) were added to pattern and samples wells. Finally, BIO-TEK PowerWave XS spectrophotometer was used to measure absorbance, that was set at a wavelength of 540 nm.

Table 4. Bradford pattern made with 2 $\mu\text{g}/\mu\text{L}$ BSA diluted in protein solvent with a final concentration of 0.5 $\mu\text{g}/\mu\text{L}$.

	Well 1	Well 2	Well 3	Well 4	Well 5	Well 6
μL BSA 0.5 $\mu\text{g}/\mu\text{L}$	0	1	2	3	4	5
μg BSA	0	0.5	1.0	1.5	2.0	2.5

3.3.7. Protein levels determination by Western blot

3.3.7.1. Sample acquisition

For GEN treated cell lines, a total of 8×10^5 HT29 cells and 8×10^5 SW620 cells were seeded in each well in 6-well plate. After GEN treatment, cells were harvested in PBS with a scraper, and centrifugated at 600 xg for 5 minutes. The pellet was dissolved in 200 μL of RIPA buffer with protease inhibitors (Halt protease and phosphatase inhibitor single-use cocktail, EDTA-free 100X, 78443, Thermo Scientific™). Then, cells were sonicated with Vibra Cell Ultrasonic Processor 75185 on ice in three cycles of 25W for 10 seconds with an interval of 5 seconds between each pulse and 40% of amplitude. After that, cells were centrifugated at 14,000 xg for 10 minutes. The supernatant was recovered, and the protein amount was quantified by BCA method, as previously described.

Frozen tumor and non-tumor adjacent tissues were homogenized in a proportion 1:10 (w/v) in homogenization buffer (20 mM Tris pH 7.4, 250 mM Saccharose, 2 mM EGTA and 40 mM KCl) with polytron (T10 basic, IKA-Werke 6 mbH, Staufen, Germany). After

that, homogenates were sonicated with Vibra Cell Ultrasonic Processor 75185 on ice in two cycles of 25 W for 5 seconds with an interval of 5 seconds between pulses and 40% of amplitude. Finally, homogenates were centrifugated at 600 xg for 10 minutes at 4 °C and supernatant was recovered. Protease and phosphatase inhibitors (1 mM PMSF, 1 mM NaF, 10 µM Pepstatin, 10 µM Leupeptin and 1 mM Na₃VO₄) were added to the supernatant. Protein levels were quantified by Bradford method, as previously described.

EVs isolated from BLF samples and BLF samples were directly quantified by Bradford method, as previously described.

Protein from EVs isolated from BLF samples was isolated by using Tri Reagent LS, following the manufacturer's protocol. Briefly, the supernatants saved during DNA isolation were incubated with 1 mL of 2-propanol at room temperature for 10 minutes and centrifugated at 12,000 xg for 10 minutes at 4 °C. The supernatants were discarded, and precipitates were washed three times with 2 mL of 0.3 M guanidine hydrochloride in 95% ethanol, incubated at room temperature for 20 minutes and centrifugated at 7,500 xg for 5 minutes at 4 °C. After the three washes, 2mL of 100% ethanol was added to the precipitates and incubated at room temperature for 20 minutes, followed by a centrifugation at 7,500 xg for 5 minutes and 4 °C. Next, protein pellets were air dried for 15 minutes, dissolved in 100 µL of 1% SDS and incubated overnight at -20 °C, if samples were not resuspended, there were incubated at 55 °C for two hours and agitation. After that, samples were centrifugated at 10,000 xg for 10 minutes and 4 °C and supernatant was transferred to a new tube. Finally, protein was quantified by BCA method, as previously described.

3.3.7.2. Sample preparation

For all SDS-PAGE carried out for GEN treated cells, 20 µg of total protein was loaded in each well and GAPDH was used as loading control; for all SDS-PAGE carried out for tumor and non-tumor adjacent tissues, 25 µg of total protein was loaded in each well and a sample consisting of a mixture of stages I-IV tumor and non-tumor adjacent tissues was loaded to allow comparison between gels; for all SDS-PAGE carried out for EVs, 5 µg of total protein was loaded in each well; for all SDS-PAGE carried out for BLF – protein, 10

μg was loaded in each well. Load buffer 4x (0.25 M Tris-HCl pH 6.8, 10% SDS (v/v), 40% glycerol (v/v), 0.1% bromophenol blue (w/v) and fresh 10% β -mercaptoethanol for all experiments, except EVs isolated from BLF) was added to each sample and boiled for 5 minutes.

3.3.7.3. Electrophoresis SDS-PAGE

Proteins were separated by electrophoresis in acrylamide/bisacrylamide (30/1) gels, which are formed by a 3% acrylamide/bisacrylamide (30/1) zone (stacking) and 8%-15% acrylamide/bisacrylamide (30/1) zone (resolving), depending on the protein size (composition is shown in Table 5).

Table 5. Composition of two acrylamide/bisacrylamide (30/1) 1.5 mm Mini Gel.

	Stacking		Resolving		
	3%	8%	10%	12%	15%
Tris-SDS pH 8.8	0 mL	10 mL	10 mL	10 mL	10 mL
Tris-SDS pH 6.8	5 mL	0 mL	0 mL	0 mL	0 mL
30% Acrylamide	1 mL	5.4 mL	6.7 mL	8 mL	10 mL
Deionized water	4 mL	4.6 mL	3.3 mL	2 mL	0 mL
20% Ammonium persulfate (PSA)	30 μL	100 μL	100 μL	100 μL	100 μL
N,N,N',N'-Tetramethyl ethylenediamine (TEMED)	20 μL	30 μL	30 μL	30 μL	30 μL

Polymerized gels were put on a Mini-PROTEAN Tetra Vertical Electrophoresis Cell (Bio-Rad) and 10x Tris/Glycine/SDS Buffer was added (1610772, Bio-Rad). First step of electrophoresis was at 80 V for 20 minutes, to allow samples to enter to the resolving zone, followed by 150 V for approximately 50 minutes, depending on the resolving gel.

3.3.7.4. Semi-dry electrotransfer

After electrophoresis SDS-PAGE, proteins were electrotransferred, by a semi-dry electrotransfer, on a 0.2 μm nitrocellulose membrane (1704159, Bio-Rad), using the Trans-blot Turbo Transfer System (Bio-Rad) at 1.3 A, 25 V, 1.5 mm Gel for 10 minutes. Then, membranes were blocked with 5% non-fat powdered milk in Tris Buffer Saline Tween (TBS-Tween; 20.08 mM Tris-base, 79.92 mM Tris-HCl and 750 mM NaCl pH 7.5, containing 0.05% Tween-20) or 5% BSA in TBS-Tween, for non-phosphorylated and

phosphorylated proteins, respectively, during 1 hour at room temperature and agitation.

3.3.7.5. Immunodetection

After blocking, membranes were washed with TBS-Tween and incubated overnight at 4 °C in agitation with primary antibody (5% BSA and 0.05% Sodium Azide in TBS-Tween). The primary antibodies used, and their respective dilutions are shown in Table 6.

Table 6. Primary antibodies, their respective dilutions, and commercial references.

	Dilution	Reference
CuZnSOD	1:1,000	574597, Calbiochem
MnSOD	1:500	30080, Santa Cruz
GPx	1:500	133160, Santa Cruz
Catalase	1:1,000	219010, Calbiochem
GAPDH	1:1,000	365062, Santa Cruz
pIκB	1:1,000	cs2859, Cell Signaling
IκB	1:1,000	cs4814, Cell Signaling
IFNγ	1:1,000	9657, Abcam
PPARγ	1:200	sc-7196, Santa Cruz
IL-4R	1:1,000	sc-28361, Sant Cruz
COX2	1:1,000	PA1211, Boster Biological
Heparanase	1:500	232817, Abcam
MMP9	1:1,000	cs13667, Cell Signaling
Vimentin	1:500	sc-373717, Santa Cruz
E-cadherin	1:200	sc-8426, Santa Cruz
N-cadherin	1:100	sc-393933, Santa Cruz
VEGF-B	1:500	cs2463, Cell Signaling
CD9	1:1,000	Ts9, 10626D, ThermoFisher
CD63	1:5,000	Ts63, ab59479, Abcam
α-Tubulin	1:500	sc-5286, Santa Cruz
GAPDH	1:1,000	sc-365062, Santa Cruz

Finally, membranes were washed with TBS-Tween and incubated with horseradish peroxidase-conjugated secondary antibody (2% non-fat powdered milk or BSA in TBS-

Tween) for 1 hour (2 hours for VEGF-B) at room temperature and agitation. The secondary antibodies used, and their respective dilutions are shown in Table 7.

Table 7. Secondary antibodies, their respective dilutions, and commercial references.

	Dilution	Reference
Anti-Rabbit	1:10,000 and 1:5,000 for VEGF-B	A9169, Sigma-Aldrich
Anti-Mouse	1:10,000 and 1:2,000 for GPx	A9044, Sigma-Aldrich
Anti-Sheep	1:10,000	A3415, Sigma-Aldrich

After secondary antibody incubation, membranes were washed with TBS-Tween and TBS, to avoid Tween interferences with detection, and then Clarity™ Western ECL Substrate (170-5061, Bio-Rad) was used to detect the immunoreactivity. Chemidoc™ XRS densitometer (Bio-Rad) was used to acquire chemiluminescent signal and, finally, the Quantity One Software (Bio-Rad) was used to analyze the results. Vimentin, VEGF-B, E-cadherin, and N-cadherin chemiluminescent signal was detected with the ImageQuant LAS 4000 mini Biomolecular Imager (GE Healthcare, Spain). CD9 and CD63 chemiluminescent signal was detected with ChemiDoc™ Imaging System (Bio-Rad).

3.3.8. Confocal microscopy

3.3.8.1. Immunocytofluorescence of NF-κB translocation into the nucleus

NF-κB cellular translocation was studied by immunocytofluorescence. A total of 5×10^5 cells of each cell line were seeded on a glass coverslip inside 6-well plate prior to GEN treatment, then cells were washed with PBS-T (0.1% Tween 20) and then were fixed with 50 μ L of 4% paraformaldehyde in PBS pH 7.4 for 10 minutes at room temperature. After that, cells were washed with cold PBS three times. Permeabilization was carried out with 1 mL of 0.25% Triton X-100 in PBS for 10 minutes at room temperature, and then cells were washed with PBS for 5 minutes three times. Then, cells were blocked with 1 mL of 1% BSA and 22.52 mg/mL glycine in PBS-T for 30 minutes at room temperature. After blocking, cells were incubated with 50 μ L of NF-κB primary antibody 1:50 (sc-372, Santa Cruz Biotechnology) with 1% BSA in PBS-T during 1 hour in a humidified chamber at room temperature. After incubation, cells were washed with PBS for 5 minutes three times and incubated with 50 μ L of anti-rabbit secondary antibody 1:100 (Alexa fluor 555,

A-21429, Invitrogen) with 1% BSA in PBS-T for 1 hour in a humidified chamber at room temperature in the dark. Before the DNA staining, cells were washed with PBS for 5 minutes three times. For the DNA staining, cells were incubated with 50 μ L of 1 μ g/mL Hoechst 33342 (B2261, Sigma-Aldrich) in PBS for 1 minute at room temperature in the dark and then washed with PBS. Finally, coverslip was mounted with a drop of DAKO Fluorescent Mounting Medium (S3023, DAKO) and incubated overnight at room temperature in the dark. The fluorescence was monitored with a Leica TCS-SPE Confocal Microscope, using 63x immersion oil (147 N.A.) objective lens. Fluorescence emission was 555 nm.

3.3.8.2. Actin cytoskeleton remodeling

A total of 5×10^5 cells of each cell line were seeded on a glass coverslip inside 6-well plate prior to GEN treatment, the, cells were washed with PBS and then were fixed with 50 μ L of 4% paraformaldehyde in PBS pH 7.4 for 10 minutes at room temperature. After that, cells were washed with PBS three times and were stained with 50 μ L of 0.1 mg/mL Phalloidin–Tetramethylrhodamine B isothiocyanate (1:1000, P1951, Sigma-Aldrich) for 1 hour at 37 °C. After staining, cells were washed with PBS three times and, for the DNA staining, cells were incubated with 50 μ L of 10 mg/mL DAPI (1:1000, D9542, Sigma-Aldrich) for 10 minutes at room temperature, and then washed with PBS three times. Finally, coverslip was mounted with a drop of DAKO Fluorescent Mounting Medium and incubated overnight at room temperature in the dark. The fluorescence was monitored with a Leica TCS-SPE Confocal Microscope, using 63x immersion oil (147 N.A.) objective lens. Fluorescence emission wavelength was 570 nm and fluorescence excitation wavelength was 532 nm.

3.3.9. Extracellular vesicles characterization

3.3.9.1. Western blot

The presence of EVs in a sample is demonstrated by the presence of some tetraspanins in their surface, such as CD9 and CD63. The presence of these tetraspanins CD9 and CD63 was determined by Western blot, as previously described. Primary and secondary antibodies are shown in Tables 6 and 7, respectively.

3.3.9.2. Nanoparticle Tracking Analysis (NTA)

The EVs size and concentration were analyzed using Nanosight NS3000 (Malvern Instruments, Malvern, USA). Samples were diluted 1:100, 1:500, and 1:1,000 in a 1 mL of final volume before analysis. Then, samples were recorded with a laser at a wavelength of 532 nm and sCMOS camera. Finally, data was analyzed with NTA 3.2 Dev Build 3.2.16 Software.

3.3.9.3. Atomic Force Microscopy (AFM)

50 μ L of EVs were added to a freshly cleaved Muscovite mica surface (NanoAndMore GmbH, Germany) for 10 minutes, washed with 2.5 mL of deionized water and dried with nitrogen. After that, EVs were observed in the atomic force microscope (Veeco, Oyster Bay, N, USA) in tapping model and aluminum coated silicon probe tips (HQ:NSC35/Al BS, Mikromasch, Lady's Island, SC, USA). Height and amplitude of the samples were recorded at 512 pixels x 512 pixels at a scanning rate of 1 Hz, and processed with NanoScope Image Software (v5.10, Veeco, Metrology, NY, USA).

3.3.9.4. Transmission Electron Microscopy (TEM)

50 μ L of EVs were mixed with 50 μ L of 4% formaldehyde (1:1; F8775, Sigma-Aldrich) and 10 μ L of this mix were fixed on copper Formvar-Carbon coated grids (01801, Iesmat, Madrid, Spain) for 20 minutes. In order to fix EVs on the grids, a 100 mm-well plate was covered by film paper, then, the sample was added to the film paper and the grid was putted on the top of the drop, this method was used for all the following steps. After the incubation, grids were washed with 100 μ L of sterile and filtrate PBS three times and incubated with 1% glutaraldehyde (G-7526, Sigma-Aldrich) for 5 minutes. Finally, grids were washed with 100 μ L of deionized water eight times, for 2 minutes each drop. Previous steps were done at fume hood, that was previously cleaned, and sample was processed in duplicates. For keeping the samples, a 100 mm-well plate was covered by filter paper and the grids were stored inside until the staining at room temperature. To visualized samples, grids were stained with 20 μ L of 2% phosphotungstic acid for 1 minute, washed with 20 μ L of deionized water for 1 minute and finally, air dried. Images were taken with transmission electron microscope Talos F200i (ThermoFisher) at 20 kV and 50 kV.

3.3.10. mRNA Array

3.3.10.1. mRNA Array

mRNA Array of EVs isolated from BLF was done with Clariom S Human mRNA Array (902917, Applied Biosystems). Samples were divided into 3 pools of each sample type, where control samples had 6 samples per pool, low – risk samples 5 samples per pool, high – risk samples 6 samples per pool, and cancer samples 3 samples per pool.

3.3.10.2. Transcriptome Analysis Console (TAC) and bioinformatics

The .cel files were processed using the R/*oligo* [162] v1.54.1 package in R 4.0.2. mRNA data were scaled to Z-score using the R/*scale* command. All genes with an absolute Z-Ratio over 1.5 and a Student's T-Test below 0.05 were considered as differentially expressed genes (DEG). The t-Distributed Stochastic Neighbor Embedding (t-SNE) algorithm was employed to represent the distribution of the samples using the R/*Rtsne* v0.15 package. Hierarchical clustering was represented by employing the R/*gplots* v.3.1.1 package. The pathway enrichment in mRNA was calculated with the R/*GOfuncR* v.1.8.0. The miRNA-mRNA pairs with inverse expression were obtained using the R/*multiMiR* [163] v.1.12.0 package. All genes in each GO term were retrieved using the R/*biomaRt* [164] v.2.46.3 package. The networks of miRNA-mRNA pairs with inverse expression were obtained with the tool miRNA interaction from *Transcriptome Analysis Console* (TAC 4.0.2.15, Applied Biosystems). Finally, the differential gene expression analysis in Tumor and Normal tissues of interest genes was determined using the TNMplot tool [165]. For the comparison between tumor and normal tissue, the TN-plot tool was used, using the non-paired tumor and normal tissues in colon tissue with gene chip data, finally, the statistical test used was Mann-Whitney U test with a statistical significance cutoff of $p < 0.05$; in addition, for mRNA signature the Gene Signature Analysis tool was used in colon tissue with gene chip data, and the statistical test used was Kruskal-Wallis test with a statistical significance cutoff of $p < 0.05$.

3.3.11. miRNA Array

3.3.11.1. miRNA Array

miRNA Array of EVs isolated from BLF was done with GeneChip™ miRNA 4.0 Array (902412, Applied Biosystems). Samples were divided into 3 pools of each sample type, where control samples had 6 samples per pool, low – risk samples 5 samples per pool, high – risk samples 6 samples per pool, and cancer samples 3 samples per pool.

3.3.11.2. Transcriptome Analysis Console (TAC) and bioinformatics

The .cel files were processed using the R/*oligo* [162] v1.54.1 package in R 4.0.2. miRNA data were scaled to Z-score using the R/*scale* command. All genes with an absolute Z-Ratio over 1.5 and a Student's T-Test below 0.05 were considered as differentially expressed genes (DEG) and differentially expressed miRNAs. The t-Distributed Stochastic Neighbor Embedding (t-SNE) algorithm was employed to represent the distribution of the samples using the R/*Rtsne* v0.15 package. Hierarchical clustering was represented by employing the R/*gplots* v.3.1.1 package. The pathway enrichment in miRNAs was computed using the miRNA Enrichment Analysis and Annotation Tool (*miEAA*) [166], and the enrichment in mRNA was calculated with the R/*GOfuncR* v.1.8.0. The miRNA-mRNA pairs with inverse expression were obtained using the R/*multiMiR* [163] v.1.12.0 package. All genes in each GO term were retrieved using the R/*biomaRt* [164] v.2.46.3 package. The networks of miRNA-mRNA pairs with inverse expression were obtained with the tool miRNA interaction from *Transcriptome Analysis Console* (TAC 4.0.2.15, Applied Biosystems). Finally, the differential gene expression analysis in tumor and normal tissues of interest genes found increased in HC samples was determined using the TNMplot tool [165]. For the comparison between tumor and normal tissue, the TN-plot tool was used, using the non-paired tumor and normal tissues in colon tissue with gene chip data, finally, the statistical test used was Mann-Whitney U test with a statistical significance cutoff of $p < 0.05$; in addition, for mRNA signature the Gene Signature Analysis tool was used in colon tissue with gene chip data, and the statistical test used was Kruskal-Wallis test with a statistical significance cutoff of $p < 0.05$ [165].

3.3.12. Kaplan – Meier survival curves

Relapse-free survival and overall survival were assessed for 585 colon cancer patients from GSE39582 dataset [167,168]. Statistical Program for the Social Sciences software for windows (SPSS, version 24.0; SPSS Inc., Chicago, IL) was used to perform survival curves using Kaplan – Meier curves survival analysis and Log Rank test for statistical significance, which was set at $P < 0.05$. Patients were divided into stages (I, II, III and IV) and low or high MnSOD, MnSOD/Sirt3 ratio, Vimentin and VEGF-B tissue expression levels.

3.3.13. Statistical Analysis

3.3.13.1. Boxplot Analysis

Statistical Program for the Social Sciences software for Windows (SPSS, version 25.0; SPSS Inc., Chicago, IL) was used to perform all the Boxplot analysis to discard the outliers, with minimal statistical significance at $P < 0.05$.

3.3.13.2. Student's t-test

SPSS software for Windows (version 25.0; SPSS Inc., Chicago, IL) was used to perform all the GEN treated cell cultures analysis. Student's t-test was used to analyze the differences between control and treated cells with minimal statistical significance at $P < 0.05$. All results are presented as mean values \pm standard error of the mean (SEM).

3.3.13.3. Two-way ANOVA

SPSS software for Windows (version 25.0; SPSS Inc., Chicago, IL) was used to perform all the tumor and non-tumor adjacent tissues statistical analyses. Two-way ANOVA was used to analyze differences between tissues and stages. Student's t-test was used to analyze differences between stages or tissues in proteins with an interactive effect found by the two-way ANOVA, with minimal statistical significance at $P < 0.05$. All results are presented as box-plot graphs and relativized to the mean of non-tumor adjacent tissue stage I samples, which was set as 100%.

3.3.13.4. Shapiro-Wilk test

After discarding outliers, SPSS software for Windows (version 25.0; SPSS Inc., Chicago, IL) was used to determine the normality of all BLF-related samples, with minimal statistical significance at $P < 0.05$.

3.3.13.4. One-way ANOVA

After Shapiro-Wilk test results, SPSS software for Windows (version 25.0; SPSS Inc., Chicago, IL) was used to perform some of BLF-related samples analysis (NTA results, *B2M* Ct values from EVs isolated from BLF). One-way ANOVA was used to analyze differences between the different groups in parametric results, with minimal statistical significance at $P < 0.05$. All results are presented as mean values \pm SD.

3.3.13.5. Kruskal-Wallis test

After Shapiro-Wilk test results, SPSS software for Windows (version 25.0; SPSS Inc., Chicago, IL) was used to perform some of BLF-related samples analysis (RNA, DNA, Protein and BLF protein concentrations, *B2M* Tm values, and NTA concentration all from EVs isolated from BLF). Kruskal-Wallis test was used to analyze differences between the different groups in non-parametric results, with minimal statistical significance at $P < 0.05$. All results are presented as mean values \pm SD.

4. Results

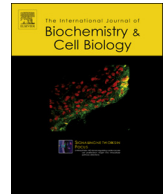
Antioxidant enzymes change in different non-metastatic stages in tumoral and peritumoral tissues of colorectal cancer.

Gaya-Bover, A., Hernández-López, R., Alorda-Clara, M., de la Rosa, J. M. I., Falcó, E., Fernández, T., Company, M. M., Torrens-Mas, M., Roca, P., Oliver, J., Sastre-Serra, J. & Pons, D. G. (2020). *The International Journal of Biochemistry & Cell Biology*, 120, 105698.



Contents lists available at ScienceDirect

International Journal of Biochemistry and Cell Biology

journal homepage: www.elsevier.com/locate/biociel

Antioxidant enzymes change in different non-metastatic stages in tumoral and peritumoral tissues of colorectal cancer

Auba Gaya-Bover^{a,b}, Reyniel Hernández-López^{a,b}, Marina Alorda-Clara^a, Javier M. Ibarra de la Rosa^{b,e}, Esther Falcó^{b,e}, Teresa Fernández^{b,e}, Maria Margarita Company^{b,d}, Margalida Torrens-Mas^{a,b}, Pilar Roca^{a,b,c}, Jordi Oliver^{a,b,c}, Jorge Sastre-Serra^{a,b,c,*}, Daniel Gabriel Pons^{a,b}

^a Grupo Multidisciplinar de Oncología Traslacional, Institut Universitari d'Investigació en Ciències de la Salut (IUNICS), Universitat de les Illes Balears, Palma de Mallorca, E-07122 Illes Balears, Spain

^b Instituto de Investigación Sanitaria de las Islas Baleares (IdISBa), Hospital Universitario Son Espases, edificio S, Palma de Mallorca, E-07120, Illes Balears, Spain

^c Ciber Fisiopatología Obesidad y Nutrición (CB06/03), Instituto Salud Carlos III, Madrid, Spain

^d Clínica Rotger, Palma de Mallorca, 07012, Islas Baleares, Spain

^e Hospital Son Llätzer, Palma de Mallorca, 07198, Illes Balears, Spain

ARTICLE INFO

Keywords:

Colorectal cancer
Tumour tissue
Non-tumour adjacent tissue
Antioxidant enzymes
Oxidative stress
Manganese superoxide dismutase

ABSTRACT

Antioxidant defences and oxidative stress are related to development, progression and malignancy of colorectal cancer. However, their role in early stages of cancer remains unknown. More and more recent studies have revealed that non-tumour adjacent tissue is not a normal tissue. Thus, our aim was to analyse protein levels of MnSOD (Manganese Superoxide Dismutase), acMnSOD (Acetylated Manganese superoxide Dismutase), SIRT3 (Sirtuin 3), CuZnSOD (Copper Zinc Superoxide Dismutase), CAT (Catalase), GPx (Glutathione Peroxidase), and GRd (Glutathione Reductase) both in tumour and non-tumour adjacent tissue from colorectal cancer patients by western blot. Non-tumour adjacent tissue seemed to have higher levels of antioxidant enzymes that detoxify hydrogen peroxide compared to tumour tissue. In contrast, tumour tissue had higher levels of MnSOD and acMnSOD. Furthermore, most of the proteins analysed showed significant differences between stage I and II in both non-tumour adjacent and tumour tissue. This could indicate that antioxidant enzymes, especially MnSOD, play a crucial role in early stages of colorectal cancer in both tissues, so they could be analysed as novel biomarkers to improve colorectal cancer diagnosis.

1. Introduction

Colorectal cancer (CRC) is the third most commonly diagnosed cancer in men and the second in women. Every year 1.1 million new CRC cases are detected, and 551,269 deaths occurred in 2018 (Bray et al., 2018). Mortality of this cancer has decreased due to an early detection through colonoscopy and screenings (Nishihara et al., 2013). However, there is a demanding need for specific biomarkers to detect CRC at early stages (Lee et al., 2018).

CRC can be classified into different stages attending to the extension of the tumour. Stage I is called cancer *in situ*, as the tumour has only invaded the submucosa; in stage II, the tumour has grown into other

nearby tissues or organs, although it has not invaded any lymph node or blood vessels. Stage III tumours have grown through the wall of the colon and are attached to other nearby tissues or organs already spreading to lymph nodes and blood vessels. Finally, stage IV is known as metastatic (“Colorectal Cancer Stages”).

In the last decade, there is growing evidence that oxidative stress may influence CRC progression (Simone et al., 2011). Oxidative stress is a situation caused by an imbalance between Reactive Oxygen Species (ROS) production and antioxidant defences in cells. Both exogenous and endogenous factors can cause ROS production, but complex I and III of electron transport chain and NADPH oxidases are the main source of ROS (Barja de Quiroga, 1999; Guzy and Schumacker, 2006; Lambeth,

Abbreviations: CRC, Colorectal Cancer; MnSOD, Manganese Superoxide Dismutase; acMnSOD, Acetylated Manganese superoxide Dismutase; SIRT3, Sirtuin 3; CuZnSOD, Copper Zinc Superoxide Dismutase; CAT, Catalase; GPx, Glutathione Peroxidase; GRd, Glutathione Reductase

* Corresponding author at: Grupo Multidisciplinar de Oncología Traslacional, Institut Universitari d'Investigació en Ciències de la Salut (IUNICS), Universitat de les Illes Balears, Palma de Mallorca, E-07122, Illes Balears, Spain.

E-mail address: jorge.sastre@uib.es (J. Sastre-Serra).

<https://doi.org/10.1016/j.biociel.2020.105698>

Received 1 July 2019; Received in revised form 20 December 2019; Accepted 20 January 2020

Available online 22 January 2020

1357-2725/ © 2020 Elsevier Ltd. All rights reserved.

2004). These molecules are highly reactive and can cause DNA mutations, leading to genomic instability and epigenomic changes causing a downregulation of tumour suppressor genes and an upregulation of oncogenes (Ushijima, 2005; Wu and Ni, 2015). Furthermore, ROS can change redox status in cells and alter signalling pathways influencing the expression and/or the activity of different transcription factors. This way, ROS stimulate proliferation, invasion and protection from apoptosis of cancer cells (Galadari et al., 2017; Sainz et al., 2012). Nevertheless, too high levels of ROS can trigger apoptosis (Redza-Dutordoir and Averill-Bates, 2016; Ricci et al., 2008).

To counteract ROS effects, cells rely on antioxidant defences. SIRT3 (Sirtuin 3, SIRT3, SIR2L3, EC: 3.5.1.-) is a NAD⁺ dependent deacetylase involved in oxidative stress. SIRT3 induces a crucial antioxidant response, activating MnSOD (Manganese Superoxide Dismutase, SOD2, EC:1.15.1.1), and electron transport chain complexes by deacetylation (Ahn et al., 2008; Alhazzazi et al., 2013; Kincaid and Bossy-Wetzel, 2013; Ozden et al., 2011; Tao et al., 2010). MnSOD and CuZnSOD (Copper Zinc Superoxide Dismutase, SOD1, EC: 1.15.1.1) detoxify superoxide anion into hydrogen peroxide. Superoxide anion is by far more reactive than hydrogen peroxide, but it has a very short half-life and it is not able to reach other spaces in the cell. Nevertheless, hydrogen peroxide has longer half-life and can reach other cell compartments. For these reasons, hydrogen peroxide can cause more damage in cells and its accumulation could cause serious consequences. GPx (Glutathione Peroxidase, GPx EC: 1.11.1.9) and Catalase (Catalase, CAT, EC: 1.11.1.6) are antioxidant enzymes that detoxify hydrogen peroxide into molecular oxygen, decreasing oxidative stress (Winterbourn, 2013).

Recent evidence has determined that a tumour could present the behavior of a complete organ, which consist of stromal non-tumour cells apart from tumour cells which can communicate and influence each other promoting tumour progression and invasion (Egeblad et al., 2010). Furthermore, Sanz-Pamplona et al. and other authors have established that non-tumour adjacent tissue of tumour has an aberrant expression in comparison with normal tissues and may have some structural alterations (D'Alessio et al., 2019; Ganci et al., 2017; Huang et al., 2016; Sanz-Pamplona et al., 2014).

There are few studies that have compared redox status between the central part of tumour and the non-tumour adjacent tissue through different stages in some types of cancer, although the knowledge about this issue is limited (Cancer et al., 2001; Santandreu et al., 2008). Antioxidant proteins levels and their role in CRC in early stages have not been well established yet. For these reasons, our aim was to analyse antioxidant enzymes and proteins related to oxidative stress modulation in CRC biopsies both in tumour and non-tumour adjacent tissues of stages I, II, III, avoiding metastatic effects of stage IV, and determine whether these proteins could be potential biomarkers for non-metastatic stages in CRC.

2. Materials and methods

2.1. Patients and tissue samples

This study was carried out on a group of 44 patients which were selected according to the following criteria: patients of both sexes without comorbidity in stage I, II and III of CRC were included. These patients had not been treated by radio- or chemotherapy before taking the samples: non-tumour adjacent and tumour tissue. Samples originating from Biobank of Hospital Son Llàtzer were taken by surgery between the years 2005-2010. All patients signed an informed consent before surgery and this study was conducted in accordance to "World Medical Association Declaration of Helsinki" when medical research involves humans. The time between diagnosis and surgery varied from a minimum of four days to a maximum of one and a half month. All CRC primary tumours were adenocarcinomas histological type distributed in 9 samples of stage I (6 males and 3 females), 16 samples of stage II (8 males and 8 females), and 19 samples of stage III (9 males and 10

females). Men average age was 71.1 (SD 12.66; Range: 51–95) and women average age was 68.07 (SD 11.04; Range 50–88). Characteristics and information of the patients are shown in Supplementary Table I.

Samples consist of frozen tissues of tumour specimens and non-tumour adjacent tissue, which was taken away from tumour border. Then, these tissues were histologically examined. Samples were classified by a pathologist according to Gleason score or TNM staging system.

2.2. Sample preparation for protein determinations

Approximately 100 mg of frozen tissue samples were homogenized with a polytron (T10 basic, IKA-Werke GmbH, Staufen, Germany) in 1:10 ratio (w:v) in homogenization cold buffer containing 20 mM Tris pH 7.4; 250 mM sucrose; 2 mM EGTA; 40 mM KCl. Homogenates were sonicated twice at 25 W with an interval of 85 s between both pulses. Finally, homogenates were centrifuged at 600xg during 10 min at 4 °C. Then protease inhibitors were added (10 µM Leupeptin, 10 µM Pepstatin, 1 mM PMSF and 1 mM Na₃VO₄). Supernatant was recovered, and protein content was determined by Bradford method (Bradford, 1976).

2.3. Sample preparation for protein determinations

Protein levels of MnSOD, CuZnSOD, acMnSOD, CAT, SIRT3, GPx, Grd (Glutathione reductase, GSR, EC: 1.8.1.7), were determined by using standard western blotting technique. Equal protein amount was added of each sample, corresponding to 25 µg of protein for all the proteins analysed. Proteins were separated on 8 %–16 % Criterion TM TGX Stain-Free TM Precast Gel (Bio-Rad Laboratories), and electrotransferred during 30 min to 0.2 µm nitrocellulose membrane (Bio-Rad Laboratories) using the Transblot turbo transfer system (Bio-Rad Laboratories). Then, membranes were blocked with 5 % non-fat powdered milk in Tris buffered saline-Tween (TBS-T, Tris buffered saline, pH 7.5 with 0.05 % (v/v) Tween-20 (Sigma Aldrich)). After that, membranes were twice quick washed and then two washes of 10 min were done with TBS-T. Once membranes were washed, primary antibodies (TBS-T, 0.05 % (w/v) sodium azide and 5 % w/v BSA were added to membranes, which were incubated overnight at 4 °C with the following antibodies and their respective dilutions against the following proteins: MnSOD SOD2 1:500 Santa Cruz Biotechnology Cat# sc-30080, RRID:AB_661470; acetylated MnSOD acMnSOD 1:1000 Abcam, Cat#137037, RRID:AB_2784527, SIRT3 1:500 Cell Signaling Technology Cat# 2627, RRID:AB_2188622 Cu/ZnSOD 1:500 Millipore Cat# 574597, RRID:AB_2255005; CAT 1:1000 Millipore Cat# 219010, RRID:AB_2071738, GPx 1:1000 Millipore Cat# ST1000, RRID:AB_2112416 and Grd 1:500 Santa Cruz Biotechnology Cat# sc-133245, RRID:AB_2295121. After incubation, membranes were washed and incubated 1 h at room temperature with the following horseradish peroxidase-conjugated secondary antibodies: anti-rabbit, anti-sheep, anti-mouse A9169, A3415 and A9044 respectively, Sigma-Aldrich, USA prepared at 1:10,000 dilution TBS-T, 2 % (w/v) non-fat powdered milk). Protein bands were detected by Immuno-Star © Western Chemiluminescent Kit Western blotting detection systems (Bio-Rad Laboratories). Chemiluminescent signal was acquired with Chemidoc XRS densitometer (Bio-Rad Laboratories). To confirm loading of protein in the gel, TGX Stain-Free Precast Gel was used as total carried control. Also, to make a comparison between gels a sample of tumour tissues from all stages of CRC (Mix) was loaded as control. Two samples of the same mix were loaded in each gel.

2.4. Kaplan-Meier survival curves

Overall survival was assessed for 560 colon cancer patients from the dataset GSE39582 of PROGeneV2 prognostic database [dataset] (Goswami and Nakshatri, 2014; Marisa et al., 2013). Survival curves

were generated using Kaplan Meier curves and analysed with log rank test to check for statistical significance. Patients were divided into high and low MnSOD, also called SOD2, expression levels and high and low MnSOD expression levels/SIRT3 expression levels ratio by selecting 50 % bottom and top of the median. The analysis was performed including all patients and analysing overall survival. Afterwards, logrank test was used to check statistical significance set at $p < 0.05$.

2.5. Statistical analysis

Fold Change [$\log_2(\text{tumour tissue protein expression levels}/\text{non-tumour adjacent tissue protein expression levels})$] and box-plot of the expression of each protein are represented graphically, showing distribution of the data, and the X inside the box represents the mean. The Statistical Program for the Social Sciences software for Windows (SPSS, version 24.0; SPSS Inc, Chicago, IL) was used for statistical analysis. All results are relativized to the mean of stage I peritumoral tissue. The differences between both tissues of all stages were analysed by Student's *t*-test and differences between stages in each tissue were analysed by one-way ANOVA and then DMS post hoc test. Statistical significance was set at $p < 0.05$.

3. Results

3.1. Differences between tumour and non-tumour adjacent tissue of antioxidant enzymes levels

To determine differences between tumour and non-tumour adjacent tissue, the fold change ratio was calculated and is shown in Fig. 1. Fold change was calculated as $\log_2(\text{tumour tissue}/\text{non-tumour adjacent tissue})$. Fold change representation showed that MnSOD and acMnSOD proteins were higher in tumour tissue in all stages compared to non-tumour adjacent tissue. CAT, GPx and GRd were higher expressed in non-tumour adjacent tissue compared to tumour tissue. CAT was higher in non-tumour adjacent tissue in stage II; GPx presented a higher expression in non-tumour adjacent tissue in stages I and III. Non-tumour adjacent tissue showed higher levels of GRd than tumour tissue in all stages.

3.2. Antioxidant protein expression levels

The protein expression levels of MnSOD, acMnSOD, SIRT3, CuZnSOD, CAT, GPx and GRd were analysed in non-tumour adjacent tissue and tumour tissue of samples from non-metastatic colorectal cancer stages (I, II and III).

In Figs. 2 and 6 the expression levels of CuZnSOD, CAT, Gpx, and Grd are shown. As it can be noted, there was a statistically significant increase of CuZnSOD both in tumour and peritumoral tissue in stage II compared to stage I. Non-tumour adjacent tissue of stage II presented an increase of CAT, GPx and GRd with respect to stage I non-tumour adjacent tissue. Furthermore, stage III non-tumour adjacent tissue also showed higher levels of CAT and GPx compared to stage I. Tumour

tissue from stage II and III had an increase of GPx compared to stage I.

The protein levels of SIRT3, MnSOD, acMnSOD are shown in Figs. 3 and 6. The antioxidant protein SIRT3 did not show any statistical differences in non-tumour adjacent tissue. However, in tumour tissue there was a decrease of SIRT3 in stage II and III with respect to stage I. Total MnSOD levels presented no differences in tumour tissue although there was an increase from stage I to stage II in non-tumour adjacent tissue. In agreement with SIRT3 results, acMnSOD levels did not show any differences in non-tumour adjacent tissue, and there was a statistically significant increase in stages II and III related to stage I in tumour tissue. However, acMnSOD was higher in tumour tissue than in non-tumour adjacent tissue. We calculated the acMnSOD/MnSOD ratio to indirectly determine the proportion of active MnSOD. According to these results, acMnSOD/MnSOD ratio showed no differences in non-tumour adjacent tissue, but this ratio increased from stage I to stage III in tumour tissue. Related to SIRT3 and MnSOD levels, there was an increase in MnSOD/SIRT3 ratio in tumour tissue compared to non-tumour adjacent tissue. Furthermore, due to the tendency of SIRT3 levels to decrease in stage II from non-tumour tissue and the increase in MnSOD in this stage, stage II non-tumour tissue had the highest value of MnSOD/SIRT3 ratio. There was also an increase in tumour tissue of stage II compared to stage I. In order to show more clearly the relation between SIRT3 and acMnSOD, we also calculated acMnSOD/SIRT3 ratio. The difference between both tissues were even higher than the differences observed in only acMnSOD levels, while tumour tissue of stages II and III also presented higher levels compared to stage I as seen in acMnSOD levels.

To try to determine by an indirect way the accumulation of hydrogen peroxide, MnSOD/CAT and MnSOD/GPx ratios were calculated and are shown in Fig. 4. In both cases the ratio value was higher in tumour tissue with respect to non-tumour adjacent tissue in all stages. MnSOD/CAT ratio tended to increase from stage I to stage III in non-tumour adjacent tissue. However, there was an opposite tendency in MnSOD/GPx ratio. In tumour tissue MnSOD/CAT ratio tended to increase from stage I to stage III, but MnSOD/GPx tended to decrease until stage III.

3.3. MnSOD levels and MnSOD/SIRT3 ratio are related to overall survival of colorectal cancer patients

To try to correlate our results with other patient datasets, we performed some bioinformatic analyses. We determined by GSE39582 dataset the relation between MnSOD levels and MnSOD/SIRT3 ratio with overall survival of CRC patients. These results are shown in Fig. 5 and indicate that the higher MnSOD and MnSOD/SIRT3 ratio values, the lower overall survival of patients. The ratio of the other analysed proteins was not statistically significant (data not shown).

4. Discussion

We have shown that non-tumour adjacent tissue of CRC seemed to have higher levels of antioxidants enzymes that detoxify hydrogen

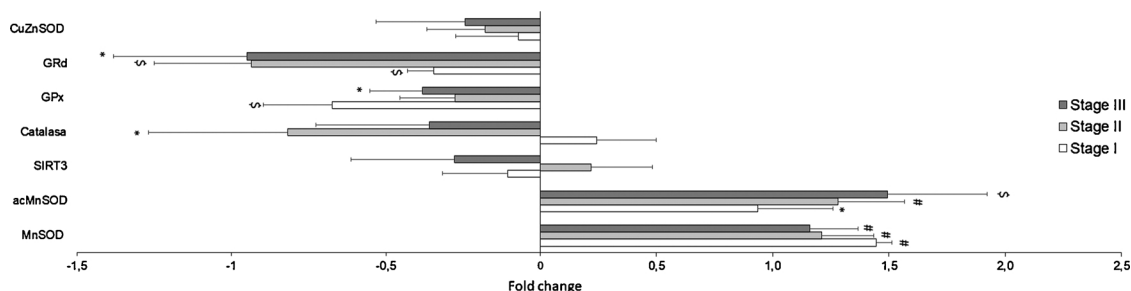


Fig. 1. Fold Change representation $\log_2(\text{Tumour tissue}/\text{Non-Tumour adjacent tissue})$ of all proteins analyzed (MnSOD, acMnSOD, SIRT3, Catalase, GPx, GRd and CuZnSOD). *t*-test (*) indicates that mean of fold change is different to 0 for each stage. (*) $p < 0.05$; (\$) $p < 0.01$; (#) $p < 0.001$.

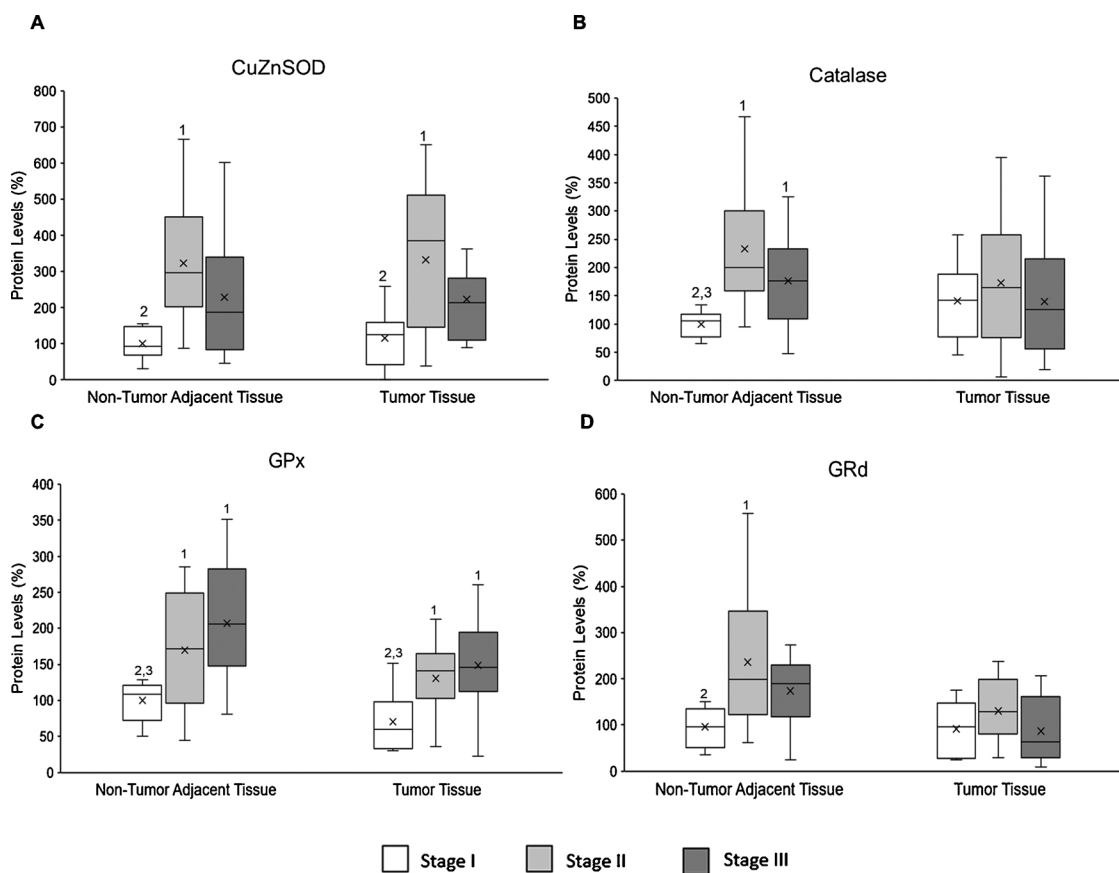


Fig. 2. Box-plot of protein expression levels. (A) CuZnSOD. (B) Catalase. (C) GPx. (D) GRd. Stage I non-tumour adjacent tissue is taken as control. ANOVA ($p < 0.05$): 1 indicates that is different from stage I, 2 indicates that is different from stage II and 3 indicates that is different from stage III, in both tissues. All experimental groups are relativized to Stage I non-tumour adjacent tissue.

peroxide in comparison to tumour tissue. In contrast, tumour tissue showed higher levels of MnSOD and acMnSOD than non-tumour adjacent tissue. Furthermore, changes in non-tumour adjacent tissue were found mainly between stage I and II in most of proteins analysed. Tumour tissue also showed a tendency to have higher levels of antioxidant enzymes in stage II compared to stage I. This could indicate that there may be an increase of the response against oxidative stress in the stage II of tumour tissue.

Oxidative stress in CRC has not been widely studied in non-metastatic stages. Our main results indicate that there was a higher expression of MnSOD in tumour tissue, an enzyme which produces hydrogen peroxide, in comparison to peritumoral tissue. Other studies have obtained similar results of SOD expression in CRC and in laryngeal carcinoma, and others correlate poorer prognosis with an increased MnSOD expression (Kacakci et al., 2009; Mayo et al., 2018; Piecuch et al., 2016; Toh et al., 2000). At the same time, there were higher levels of the antioxidant enzymes which detoxify hydrogen peroxide, mainly GPx and CAT, in non-tumour adjacent tissue compared to tumour tissue.

SIRT3 is a mitochondrial deacetylase that activates MnSOD by deacetylation (Tao et al., 2010). As it can be noted, tumour tissue had higher levels of acMnSOD than non-tumour adjacent tissue and tumoural tissue of stages II and III had higher levels of acMnSOD than stage I. However, SIRT3 levels were not different between both tissues, and stages II and III of tumoural tissue had lower levels of SIRT3 than stage I. As a result, acMnSOD/SIRT3 ratio was much higher in tumoural tissue than non-tumour adjacent tissue, and differences between the three stages of tumoural tissue were maintained. Thus, the levels of acMnSOD and SIRT3 were correlated in tumour tissue but not between both tissues. In tumour tissue there were higher levels of MnSOD, although the

degree of acetylation was also higher, suggesting an inactivation of this protein (Ozden et al., 2011; Torrens-Mas et al., 2018). Some datasets established that those patients showing a higher MnSOD/SIRT3 ratio presented a poorer prognosis (Goswami and Nakshatri, 2014). As we have analysed only the protein levels, it could be possible that MnSOD could be stabilized despite being inactive or lower expressed by SIRT3. There are some studies in cultured cell lines and *in vivo* mouse models that have revealed that MnSOD is also regulated by Cdks. These proteins phosphorylate MnSOD and it cannot be degraded. This way, hydrogen peroxide can be accumulated and stimulate the transition from G₂ to M phases (Candas and Li, 2014). Thus, maintaining high levels of MnSOD could be a possible strategy of tumour cells to enhance cellular proliferation.

According to our results, enzymes detoxifying hydrogen peroxide were downregulated in tumour tissue in comparison to non-tumour adjacent tissue. This could produce an accumulation of hydrogen peroxide which is more harmful than other oxygen radical species because of its ability to easily move throughout cellular compartments (Winterbourn, 2013). Other studies have also reported that CAT is downregulated in lung tumour tissue in comparison with normal tissue (Cancer et al., 2001). The glutathione consumption and recycling system, GPx and GRd, was also downregulated in tumour tissue compared to non-tumour adjacent tissue in all stages which is in agreement with a study showing that the activity of GRd is lower in control patients in comparison to those with CRC (Gopčević et al., 2013). A downregulation of glutathione consumption and recycling system results in an accumulation of hydrogen peroxide. Thus, oxidative stress may increase, which could enhance the progression of cancer. In fact, higher oxidative stress in the centre of tumour has been reported in glioma and CRC (Santandreu et al., 2008; Strzelczyk et al., 2012).

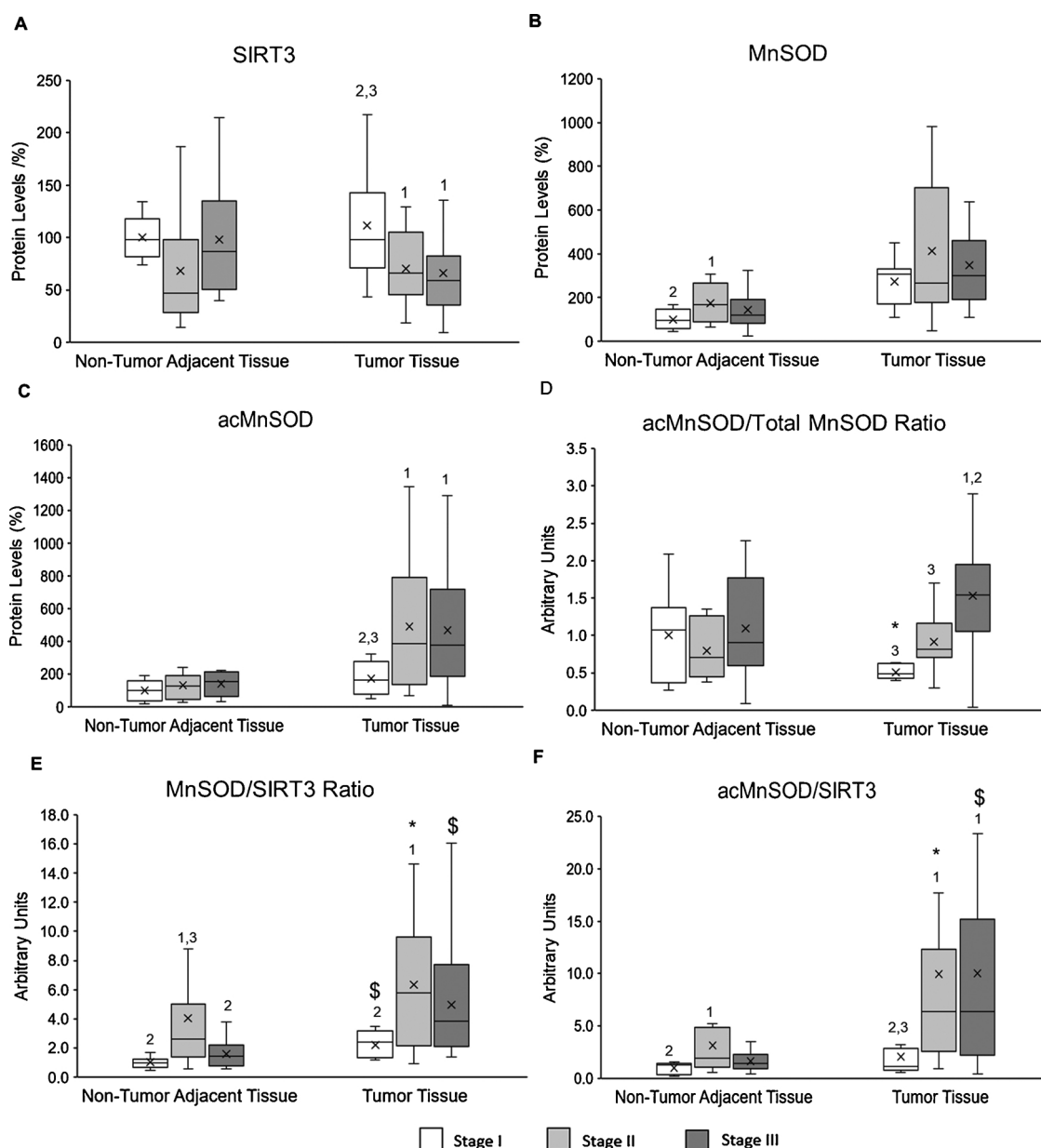


Fig. 3. Box-plot of protein expression levels. (A) SIRT3. (B) MnSOD. (C) acMnSOD. (D) acMnSOD/MnSOD ratio. (E) MnSOD/SIRT3. (F) acMnSOD/SIRT3. Stage I non-tumour adjacent tissue is taken as control. ANOVA ($p < 0.05$): 1 indicates that is different from stage I, 2 indicates that is different from stage II and 3 indicates that is different from stage III, in both tissues. In figure E and F, *t*-test. (*) $p < 0.05$; (\$) $p < 0.01$; (#) $p < 0.001$. All experimental groups are relativized to Stage I non-tumour adjacent tissue.

Interestingly, there was an important change from stage I to stage II in most of the proteins analysed. This could reflect the progression of the tumour in early stages both in non-tumour adjacent tissue and tumour tissue. From stage I to stage II the tumour becomes quite bigger (“Colorectal Cancer Stages”). As the tumour grows its centre becomes hypoxic. Some studies have established that even with proper mitochondrial functionality conditions, hypoxia can enhance anion superoxide production (Guzy and Schumacker, 2006; Solaini et al., 2010). Thus, stage II, where there could be an increase of hypoxia, there was an increase in MnSOD levels and MnSOD/CAT and MnSOD/GPx ratio, increasing hydrogen peroxide production, and consequently oxidative stress would increase. However, while a lot of studies have determined that SIRT3 is activated by stress, we would expect an increase of this protein in stage II (Kincaid and Bossy-Wetzel, 2013; Ozden et al., 2011; Tseng et al., 2013). Nevertheless, this protein also stimulates mitochondrial biogenesis. In fact, some researchers have determined that,

in hypoxic conditions, cancer cells decrease mitochondrial biogenesis in order to avoid high amount of superoxide anion production and thus, higher oxidative stress (LaGory et al., 2015).

In contrast, stage III showed the lowest values of MnSOD/GPx ratio, a fact that could be indicating higher hydrogen peroxide detoxification capacity according to other studies (Miar et al., 2015). There were few differences between stage II and III, which could be due to a hypoxic adaptation.

Non-tumour adjacent tissue suffered also an evolution regarding antioxidant defences. There were higher levels of some antioxidant enzymes in stages II and III compared to stage I such as MnSOD, GPx, CAT, and GRd. This implies that the non-tumour adjacent tissue could also progress with malignancy. In fact, more and more researchers are reporting that tumour can act as a whole organ, which can communicate with its environment, even with the whole organism (Egeblad et al., 2010). Moreover, it has been reported that non-tumour adjacent

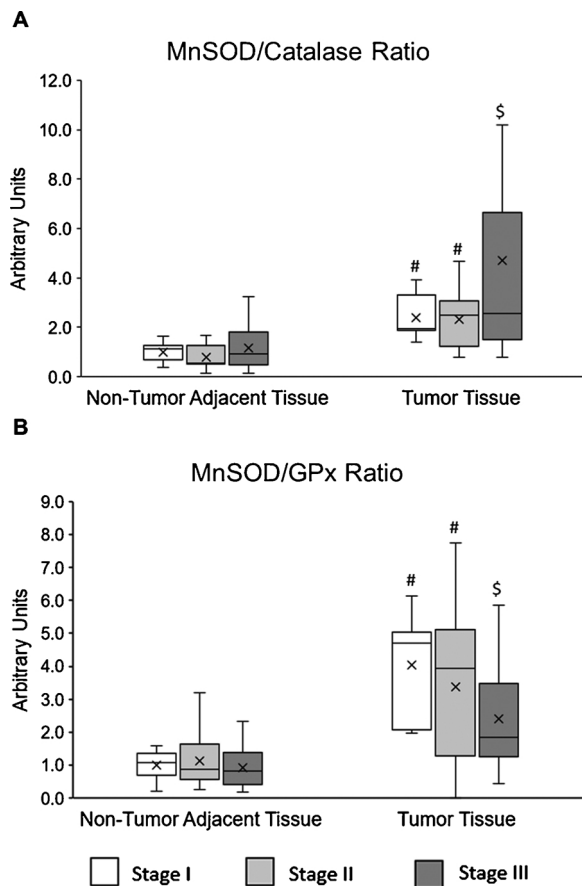


Fig. 4. Boxplot of protein ratios. (A) MnSOD/Catalase ratio. (B) MnSOD/GPx ratio. Stage I non-tumour adjacent tissue is taken as control. ANOVA ($p < 0.05$): 1 indicates that is different from stage I, 2 indicates that is different from stage II and 3 indicates that is different from stage III, in both tissues. t -test (*) Means that there are differences between both tissues. (*) $p < 0.05$; (\$) $p < 0.01$; (#) $p < 0.001$. All experimental groups are relativized to Stage I non-tumour adjacent tissue.

tissue has also an aberrant expression of its transcriptome (Sanz-Pamplona et al., 2014). Other studies have determined that cancer cells can change the behavior of normal cells of their environment and, this way, these cells are able to begin a malignant process nearby to the tumour tissue or to prepare to be invaded by angiogenesis (Guo et al., 2017; Melo et al., 2014).

5. Conclusions

Our results show that the role of antioxidant enzymes can not only take part in the advanced stages of CRC, but also, in the very early phases of the progression of cancer. Furthermore, non-tumour adjacent tissue also showed important changes in antioxidant proteins, suggesting an influence of the tumour tissue on it. For this reason, it may be important to analyse the expression of the antioxidant enzymes not only in tumours, but also in non-tumour adjacent tissue, with especial attention to MnSOD protein levels, which could become a non-metastatic CRC biomarker due to its representative expression in the tumour tissue. These results could set up the base of following studies to determine whether these proteins could be potential biomarkers for early diagnosis of colorectal cancer.

CRedit authorship contribution statement

Auba Gaya-Bover: Conceptualization, Methodology, Data curation, Writing - original draft. **Reyniel Hernández-López:** Conceptualization, Methodology. **Marina Alorda-Clara:** Conceptualization, Methodology. **Javier M. Ibarra de la Rosa:** Resources. **Esther Falcó:** Resources. **Teresa Fernández:** Resources. **Maria Margarita Company:** Resources. **Margalida Torrens-Mas:** Writing - review & editing. **Pilar Roca:** Data curation, Writing - original draft, Writing - review & editing. **Jordi Oliver:** Writing - review & editing. **Jorge Sastre-Serra:** Conceptualization, Methodology, Writing - review & editing, Supervision. **Daniel Gabriel Pons:** Conceptualization, Methodology, Writing - review & editing, Supervision.

Declaration of Competing Interest

None declared.

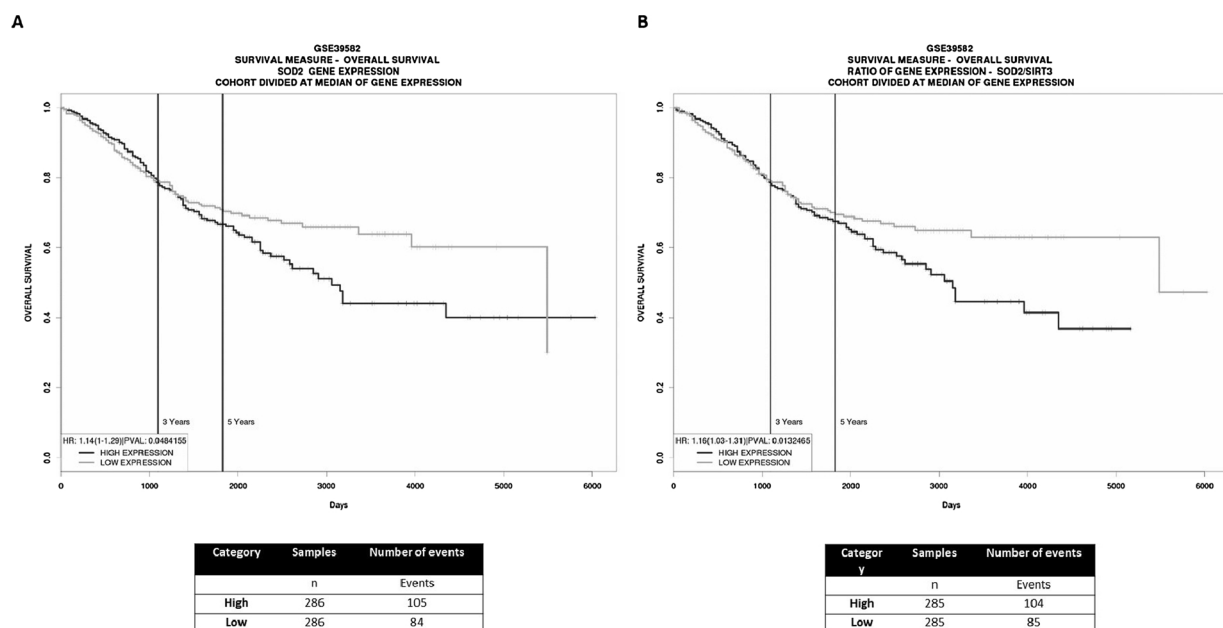


Fig. 5. Kaplan-Meier representation of overall survival of CRC patients. (A) According to SOD2 levels. (B) According to SOD2/SIRT3 ratio. The grey line indicates low value of each parameter and the black line indicates high value of each parameter. High and low expression patients were split up according to median.

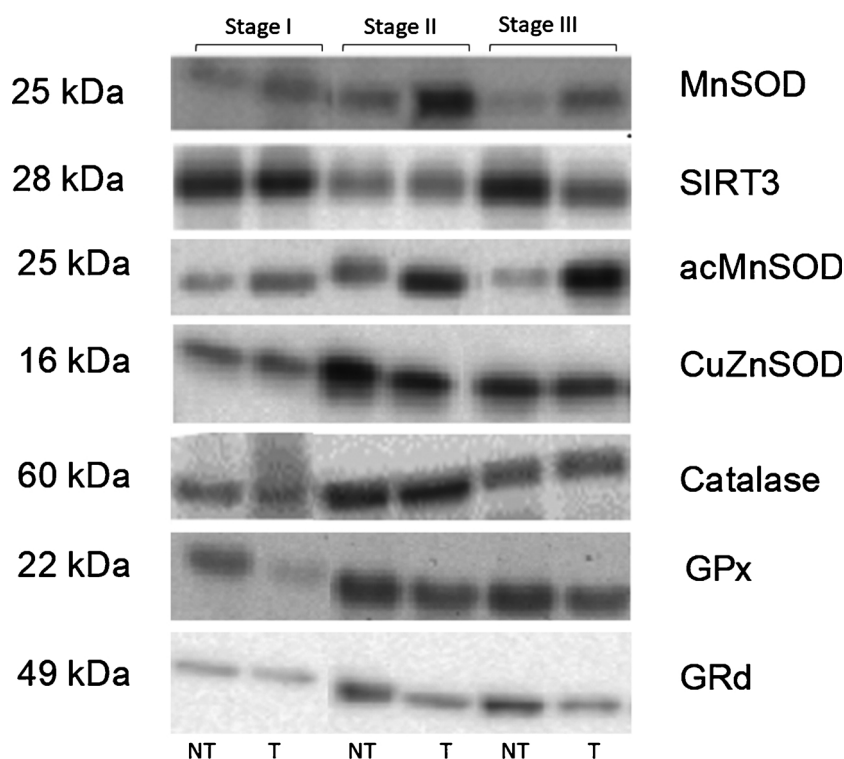


Fig. 6. Western blot representative bands of analysed proteins, from top to bottom: Manganese Superoxide Dismutase (MnSOD), Sirtuin 3 (SIRT3), acetylated Manganese Superoxide Dismutase (acMnSOD), Copper Zinc Superoxide Dismutase (CuZnSOD), Catalase, Glutathione Peroxidase (GPx) and Glutathione Reductase (GRd). At the right side of the bands, protein name is indicated, and at the left side, their molecular weights. NT: non tumour-adjacent tissue, T: tumoral tissue.

Acknowledgments

This work was supported by grants from Fondo de Investigaciones Sanitarias of Instituto de Salud Carlos III [PI14/01434] of the Spanish Government cofinanced by FEDER-Unión Europea (“Una manera de hacer Europa”). M. Torrens-Mas received an FPU grant [FPU14/07042] from Ministerio de Educación, Cultura y Deporte of Spanish Government.

Appendix A. Supplementary data

Supplementary material related to this article can be found, in the online version, at doi:<https://doi.org/10.1016/j.biocel.2020.105698>.

References

- Ahn, B.-H., Kim, H.-S., Song, S., Lee, I.H., Liu, J., Vassilopoulos, A., Deng, C.-X., Finkel, T., 2008. A role for the mitochondrial deacetylase Sirt3 in regulating energy homeostasis. *Proc. Natl. Acad. Sci. U. S. A.* 105, 14447–14452. <https://doi.org/10.1073/pnas.0803790105>.
- Alhazzazi, T.Y., Kamarajan, P., Verdin, E., Kapila, Y.L., 2013. Sirtuin-3 (SIRT3) and the hallmarks of cancer. *Genes Cancer* 4, 164–171. <https://doi.org/10.1177/1947601913486351>.
- Barja de Quiroga, C., 1999. Mitochondrial oxygen radical generation and leak: sites of production in states 4 and 3, organ specificity and relation to aging and longevity. *J. Bioenerg. Biomembr.* 31, 347–366.
- Bradford, M.M., 1976. A rapid and sensitive method for the quantitation of microgram quantities of protein utilizing the principle of protein-dye binding. *Anal. Biochem.* 72, 248–254. [https://doi.org/10.1016/0003-2697\(76\)90527-3](https://doi.org/10.1016/0003-2697(76)90527-3).
- Bray, F., Ferlay, J., Soerjomataram, I., Siegel, R., Torre, L., Jemal, A., 2018. Global cancer statistics 2018: GLOBOCAN estimates of incidence and mortality worldwide for 36 cancers in 185 countries. *CA Cancer J. Clin.* 68, 394–424. <https://doi.org/10.3322/caac.21492>.
- Cancer, L., Ho, J.C., Zheng, S., Comhair, S.A.A., Farver, C., Erzurum, S.C., 2001. Differential Expression of Manganese Superoxide Dismutase and Catalase in. pp. 8578–8585.
- Candas, D., Li, J.J., 2014. MnSOD in oxidative stress response-potential regulation via mitochondrial protein influx. *Antioxid. Redox Signal.* 20, 1599–1617.
- Colorectal Cancer Stages [WWW Document], n.d. URL <https://www.cancer.org/cancer/colon-rectal-cancer/detection-diagnosis-staging/staged.html>. (Accessed 19 May 2018).
- D’Alessio, A., Proietti, G., Sica, G., Scicchitano, B.M., 2019. Pathological and molecular features of glioblastoma and its peritumoral tissue. *Cancers (Basel)*. <https://doi.org/10.3390/cancers11040469>.

- Egeblad, M., Nakasone, E.S., Werb, Z., 2010. Tumors as organs: complex tissues that interface with the entire organism. *Dev. Cell* 18, 884–901. <https://doi.org/10.1016/j.devcel.2010.05.012>.
- Galadari, S., Rahman, A., Pallichankandy, S., Thayyullathil, F., 2017. Reactive oxygen species and cancer paradox: to promote or to suppress? *Free Radic. Biol. Med.* 104, 144–164. <https://doi.org/10.1016/j.freeradbiomed.2017.01.004>.
- Ganci, F., Sacconi, A., Manciooco, V., Covello, R., Benevolo, M., Rollo, F., Strano, S., Valsoni, S., Biciato, S., Spriano, G., Muti, P., Fontemaggi, G., Blandino, G., 2017. Altered peritumoral microRNA expression predicts head and neck cancer patients with a high risk of recurrence. *Mod. Pathol.* 30, 1387–1401. <https://doi.org/10.1038/modpathol.2017.62>.
- Gopčević, K.R., Rovčanin, B.R., Tatić, S.B., Krivokapić, Z.V., Gajić, M.M., Dragutinović, V.V., 2013. Activity of superoxide dismutase, catalase, glutathione peroxidase, and glutathione reductase in different stages of colorectal carcinoma. *Dig. Dis. Sci.* 58, 2646–2652. <https://doi.org/10.1007/s10620-013-2681-2>.
- Goswami, C.P., Nakhatri, H., 2014. PROGgeneV2: enhancements on the existing database. *BMC Cancer* 14, 970. <https://doi.org/10.1186/1471-2407-14-970>.
- Guo, W., Gao, Y., Li, N., Shao, F., Wang, C., Wang, P., Yang, Z., Li, R., He, J., 2017. Exosomes: new players in cancer. *Oncol. Rep.* 38, 665–675. <https://doi.org/10.3892/or.2017.5714>.
- Guzy, R.D., Schumacker, P.T., 2006. Oxygen sensing by mitochondria at complex III: the paradox of increased reactive oxygen species during hypoxia. *Exp. Physiol.* 91, 807–819. <https://doi.org/10.1113/expphysiol.2006.033506>.
- Huang, C., Liu, H., Gong, X., Wen, B., Chen, D., Liu, J., Hu, F., 2016. Analysis of different components in the peritumoral tissue microenvironment of colorectal cancer: a potential prospect in tumorigenesis. *Mol. Med. Rep.* 14, 2555–2565. <https://doi.org/10.3892/mmr.2016.5584>.
- Kacacki, A., Aslan, I., Toplan, S., Oysu, C., Aslan, O., Aydemir, B., 2009. Significance of the counteracting oxidative and antioxidative systems in the pathogenesis of laryngeal carcinoma. *J. Otolaryngol. Head Neck Surg.* 38, 172–177. <https://doi.org/10.2310/7070.2009.OA0165>.
- Kincaid, B., Bossy-Wetzell, E., 2013. Forever young: SIRT3 a shield against mitochondrial meltdown, aging, and neurodegeneration. *Front. Aging Neurosci.* 5, 48. <https://doi.org/10.3389/fnagi.2013.00048>.
- LaGory, E.L., Wu, C., Taniguchi, C.M., Ding, C.K.C., Chi, J.T., von Eyben, R., Scott, D.A., Richardson, A.D., Giaccia, A.J., 2015. Suppression of PGC-1 α is critical for reprogramming oxidative metabolism in renal cell carcinoma. *Cell Rep.* 12, 116–127. <https://doi.org/10.1016/j.celrep.2015.06.006>.
- Lambeth, J.D., 2004. NOX enzymes and the biology of reactive oxygen. *Nat. Rev. Immunol.* 4, 181–189. <https://doi.org/10.1038/nri1312>.
- Lee, P.Y., Chin, S.-F., Low, T.Y., Jamal, R., 2018. Probing the colorectal cancer proteome for biomarkers: current status and perspectives. *J. Proteomics* 187, 93–105. <https://doi.org/10.1016/j.jprot.2018.06.014>.
- Marisa, L., de Reyniès, A., Duval, A., Selves, J., Gaub, M.P., Vescovo, L., Etienne-Grimaldi, M.-C., Schiappa, R., Guenot, D., Ayadi, M., Kirzin, S., Chazal, M., Fléjou, J.-F., Benchimol, D., Berger, A., Lagarde, A., Pencreach, E., Piard, F., Elias, D., Parc, Y., Olschwang, S., Milano, G., Laurent-Puig, P., Boige, V., 2013. Gene expression







- classification of colon cancer into molecular subtypes: characterization, validation, and prognostic value. *PLoS Med.* 10, e1001453. <https://doi.org/10.1371/journal.pmed.1001453>.
- Mayo, J.C., Álvarez-Artime, A., Cepas, V., Hevia, D., Quirós-González, I., Sáinz, R.M., 2018. Overexpression of SOD2/MnSOD promotes tumor growth and poor prognosis in TRAMP mice. *Free Radic. Biol. Med.* 120, S67. <https://doi.org/10.1016/j.freeradbiomed.2018.04.222>.
- Melo, S.A., Sugimoto, H., O'Connell, J.T., Kato, N., Villanueva, A., Vidal, A., Qiu, L., Vitkin, E., Perelman, L.T., Melo, C.A., Lucchi, A., Ivan, C., Calin, G.A., Kalluri, R., 2014. Cancer exosomes perform cell-independent MicroRNA biogenesis and promote tumorigenesis. *Cancer Cell* 26, 707–721. <https://doi.org/10.1016/j.ccr.2014.09.005>.
- Miar, A., Hevia, D., Muñoz-Cimadevilla, H., Astudillo, A., Velasco, J., Sainz, R.M., Mayo, J.C., 2015. Manganese superoxide dismutase (SOD2/MnSOD)/catalase and SOD2/GPx1 ratios as biomarkers for tumor progression and metastasis in prostate, colon, and lung cancer. *Free Radic. Biol. Med.* 85, 45–55. <https://doi.org/10.1016/j.freeradbiomed.2015.04.001>.
- Nishihara, R., Wu, K., Lochhead, P., Morikawa, T., Liao, X., Qian, Z.R., Inamura, K., Kim, S.A., Kuchiba, A., Yamauchi, M., Imamura, Y., Willett, W.C., Rosner, B.A., Fuchs, C.S., Giovannucci, E., Ogino, S., Chan, A.T., 2013. Long-term colorectal-cancer incidence and mortality after lower endoscopy. *N. Engl. J. Med.* 369, 1095–1105. <https://doi.org/10.1056/NEJMoa1301969>.
- Ozden, O., Park, S.-H., Kim, H.-S., Jiang, H., Coleman, M.C., Spitz, D.R., Gius, D., 2011. Acetylation of MnSOD directs enzymatic activity responding to cellular nutrient status or oxidative stress. *Aging (Albany, NY)* 3, 102–107. <https://doi.org/10.18632/aging.100291>.
- Piecuch, A., Brzozowa-Zasada, M., Dziewit, B., Segiet, O., Kurek, J., Kowalczyk-Ziomek, G., Wojnicz, R., Helewski, K., 2016. Immunohistochemical assessment of mitochondrial superoxide dismutase (MnSOD) in colorectal premalignant and malignant lesions. *Prz. Gastroenterol.* 11, 239–246. <https://doi.org/10.5114/pg.2016.57943>.
- Redza-Dutordoir, M., Averill-Bates, D.A., 2016. Activation of apoptosis signalling pathways by reactive oxygen species. *Biochim. Biophys. Acta - Mol. Cell Res.* 1863, 2977–2992. <https://doi.org/10.1016/j.bbamcr.2016.09.012>.
- Ricci, C., Pastukh, V., Leonard, J., Turrens, J., Wilson, G., Schaffer, D., Schaffer, S.W., 2008. Mitochondrial DNA damage triggers mitochondrial-superoxide generation and apoptosis. *Am. J. Physiol. Physiol.* 294, C413–C422. <https://doi.org/10.1152/ajpcell.00362.2007>.
- Sainz, R.M., Lombo, F., Mayo, J.C., 2012. Radical decisions in cancer: redox control of cell growth and death. *Cancers (Basel)* 4, 442–474. <https://doi.org/10.3390/cancers4020442>.
- Santandreu, F.M., Brell, M., Gene, A.H., Oliver, J., Couce, M.E., Roca, P., 2008. Differences in mitochondrial function and anti-oxidant systems between regions of human glioma. *Cell. Physiol. Biochem.* 22, 757–768. <https://doi.org/10.1159/000185559>.
- Sanz-Pamplona, R., Berenguer, A., Cordero, D., Molleví, D.G., Crous-Bou, M., Sole, X., Paré-Brunet, L., Guino, E., Salazar, R., Santos, C., de Oca, J., Sanjuan, X., Rodríguez-Moranta, F., Moreno, V., 2014. Aberrant gene expression in mucosa adjacent to tumor reveals a molecular crosstalk in colon cancer. *Mol. Cancer* 13, 46. <https://doi.org/10.1186/1476-4598-13-46>.
- Simone, R., Gupta, S., Chaturvedi, M., Aggarwal, B.B., 2011. Oxidative stress, inflammation, and cancer: how are they. *Free Radic. Biol. Med.* 46, 1882–1891. <https://doi.org/10.1016/j.ejca.2010.02.004>. *Resveratrol*.
- Solaini, G., Baracca, A., Lenaz, G., Sgarbi, G., 2010. Hypoxia and mitochondrial oxidative metabolism. *Biochim. Biophys. Acta - Bioenerg.* 1797, 1171–1177. <https://doi.org/10.1016/j.bbabi.2010.02.011>.
- Strzelczyk, J.K., Wielkoszynski, T., Krakowczyk, L., Adamek, B., Zalewska-Ziob, M., Gawron, K., Kasperczyk, J., Wiczowski, A., 2012. The activity of antioxidant enzymes in colorectal adenocarcinoma and corresponding normal mucosa. *Acta Biochim. Pol.* 59, 549–556.
- Tao, R., Coleman, M.C., Pennington, J.D., Ozden, O., Park, S.-H., Jiang, H., Kim, H.-S., Flynn, C.R., Hill, S., Hayes McDonald, W., Olivier, A.K., Spitz, D.R., Gius, D., 2010. Sirt3-mediated deacetylation of evolutionarily conserved lysine 122 regulates MnSOD activity in response to stress. *Mol. Cell* 40, 893–904. <https://doi.org/10.1016/j.molcel.2010.12.013>.
- Toh, Y., Kuninaka, S., Oshiro, T., Ikeda, Y., Nakashima, H., Baba, H., Kohnoe, S., Okamura, T., Mori, M., Sugimachi, K., 2000. Overexpression of manganese superoxide dismutase mRNA may correlate with aggressiveness in gastric and colorectal adenocarcinomas. *Int. J. Oncol.* <https://doi.org/10.3892/ijo.17.1.107>.
- Torrens-Mas, M., Hernández-López, R., Oliver, J., Roca, P., Sastre-Serra, J., 2018. Sirtuin 3 silencing improves oxaliplatin efficacy through acetylation of MnSOD in colon cancer. *J. Cell. Physiol.* 233, 6067–6076. <https://doi.org/10.1002/jcp.26443>.
- Tseng, A.H.H., Shieh, S.S., Wang, D.L., 2013. SIRT3 deacetylates FOXO3 to protect mitochondria against oxidative damage. *Free Radic. Biol. Med.* 63, 222–234. <https://doi.org/10.1016/j.freeradbiomed.2013.05.002>.
- Ushijima, T., 2005. Detection and interpretation of altered methylation patterns in cancer cells. *Nat. Rev. Cancer* 5, 223–231. <https://doi.org/10.1038/nrc1571>.
- Winterbourn, C.C., 2013. The biological chemistry of hydrogen peroxide. *Meth. Enzymol.* 3–25. <https://doi.org/10.1016/B978-0-12-405881-1.00001-X>.
- Wu, Q., Ni, X., 2015. ROS-mediated DNA methylation pattern alterations in carcinogenesis. *Curr. Drug Targets* 16, 13–19.

Inflammation-and Metastasis-Related Proteins Expression Changes in Early Stages in Tumor and Non-Tumor Adjacent Tissues of Colorectal Cancer Samples.

Alorda-Clara, M., Torrens-Mas, M., Hernández-López, R., Ibarra de la Rosa, J. M., Falcó, E., Fernández, T., Company, M. M., Sastre-Serra, J., Oliver, J., Pons, D. G., & Roca, P. (2022). *Cancers*, 14(18), 4487.

Article

Inflammation- and Metastasis-Related Proteins Expression Changes in Early Stages in Tumor and Non-Tumor Adjacent Tissues of Colorectal Cancer Samples

Marina Alorda-Clara ^{1,2} , Margalida Torrens-Mas ^{1,2,3} , Reyniel Hernández-López ^{1,2},
 Javier M. Ibarra de la Rosa ^{1,4}, Esther Falcó ^{1,2}, Teresa Fernández ^{1,5}, Maria Margarita Company ^{1,6},
 Jorge Sastre-Serra ^{1,2,7} , Jordi Oliver ^{1,2,7} , Daniel Gabriel Pons ^{1,2,*}  and Pilar Roca ^{1,2,7} 

- ¹ Grupo Multidisciplinar de Oncología Traslacional, Institut Universitari d'Investigació en Ciències de la Salut (IUNICS), Universitat de les Illes Balears, 07122 Palma de Mallorca, Spain
 - ² Instituto de Investigación Sanitaria Illes Balears (IdISBa), Hospital Universitario Son Espases, Edificio S, 07120 Palma de Mallorca, Spain
 - ³ Translational Research in Aging and Longevity (TRIAL) Group, Instituto de Investigación Sanitaria Illes Balears (IdISBa), 07120 Palma de Mallorca, Spain
 - ⁴ Pathological Anatomy, Hospital Universitari Son Llàtzer, 07198 Palma de Mallorca, Spain
 - ⁵ Medical Oncology Service, Hospital Universitari Son Llàtzer, 07198 Palma de Mallorca, Spain
 - ⁶ Pathological Anatomy, Clinica Rotger, 07012 Palma de Mallorca, Spain
 - ⁷ Ciber Fisiopatología Obesidad y Nutrición (CB06/03), Instituto Salud Carlos III, 28029 Madrid, Spain
- * Correspondence: d.pons@uib.es



Citation: Alorda-Clara, M.; Torrens-Mas, M.; Hernández-López, R.; Ibarra de la Rosa, J.M.; Falcó, E.; Fernández, T.; Company, M.M.; Sastre-Serra, J.; Oliver, J.; Pons, D.G.; et al. Inflammation- and Metastasis-Related Proteins Expression Changes in Early Stages in Tumor and Non-Tumor Adjacent Tissues of Colorectal Cancer Samples. *Cancers* **2022**, *14*, 4487. <https://doi.org/10.3390/cancers14184487>

Academic Editors: Ulrike Stein and Wolfgang Walther

Received: 4 August 2022

Accepted: 14 September 2022

Published: 16 September 2022

Publisher's Note: MDPI stays neutral with regard to jurisdictional claims in published maps and institutional affiliations.



Copyright: © 2022 by the authors. Licensee MDPI, Basel, Switzerland. This article is an open access article distributed under the terms and conditions of the Creative Commons Attribution (CC BY) license (<https://creativecommons.org/licenses/by/4.0/>).

Simple Summary: Non-tumor adjacent tissue plays a key role in colorectal cancer development, as well as chronic inflammation, but their role has not yet been elucidated. In addition, inflammation is a process which is related to epithelial-mesenchymal transition and metastasis, but their changes across the different colorectal cancer stages are not fully studied. Understanding how these processes participate in all colorectal cancer phases can be key to a better understanding of the disease.

Abstract: Chronic inflammation can induce malignant cell transformation, having an important role in all colorectal cancer (CRC) phases. Non-tumor adjacent tissue plays an important role in tumor progression, but its implication in CRC has not yet been fully elucidated. The aim was to analyze the expression of inflammatory, epithelial-mesenchymal transition (EMT), and metastasis-related proteins in both tumor and non-tumor adjacent tissues from CRC patients by western blot. Tumor tissue presented an increase in metastasis and EMT-related proteins compared to non-tumor adjacent tissue, especially in stage II. Tumor tissue stage II also presented an increase in inflammatory-related proteins compared to other stages, which was also seen in non-tumor adjacent tissue stage II. Additionally, the relapse-free survival study of Vimentin and VEGF-B expression levels in stage II patients showed that the higher the expression levels of each protein, the lower 10-year relapse-free survival. These could suggest that some metastasis-related signalling pathways may be activated in stage II in tumor tissue, accompanied by an increase in inflammation. Furthermore, non-tumor adjacent tissue presented an increase of the inflammatory status that could be the basis for future tumor progression. In conclusion, these proteins could be useful as biomarkers of diagnosis for CRC at early stages.

Keywords: inflammation; metastasis; epithelial-mesenchymal transition; tumor tissue; non-tumor adjacent tissue; colorectal cancer

1. Introduction

Colorectal cancer (CRC) is the third most common cancer worldwide, being the second cause of cancer death [1]. The American Cancer Society has established the 5-year survival rates for each CRC stage: the 5-year survival rate for localized tumors is 91%; 72% for cancer that has spread to surrounding tissues or lymph nodes; and finally, 14% for cancer

that has spread to distant parts of the body [2]. These data highlight the importance of early detection of this disease. CRC can be classified attending to the TNM staging system and, depending on the tumor extension, can be divided into four stages, numbered from I to IV, with stages I to III being non-metastatic stages, and stage IV the metastatic stage. In stage I, the tumor grows through the mucosa to the muscular layer without dissemination to lymphatic nodes. In stage II, the tumor grows through the muscular layer to nearby structures without dissemination to lymphatic nodes. In stage III, the tumor spreads to nearby organs and the lymphatic nodes, and finally, in stage IV, the tumor spreads to other parts of the body through lymphatic nodes and blood vessels [3].

Despite inflammation being a physiological process, when it is upregulated and becomes chronic, it can induce malignant cell transformation in the surrounding tissue [4]. Inflammation, one of the cancer hallmarks [5], participates in all CRC phases since cytokines are released in response to tissue damage, so innate immune system cells are recruited and release more cytokines [6]. This positive feedback leads to cell survival, immunosuppression, tumor growth, proliferation, differentiation, angiogenesis, epithelial-mesenchymal transition (EMT), and metastasis [4,7–9]. EMT is a biological process where epithelial cells acquire a mesenchymal phenotype and the capability to migrate, invade and metastasize [10]. With the contribution of cytokines, extracellular matrix degradation, invasion, tumor cell evasion, and dissemination, can be possible and lead to metastasis [6].

Non-tumor adjacent tissue plays an important role in tumor progression [8,11]. Oxidative stress-related proteins were analyzed in tumor and non-tumor adjacent tissue from advanced stages (III and IV), and the non-tumor adjacent tissue presented the highest differences [8]. Furthermore, when this family of proteins was analyzed in non-metastatic stages (I, II, and III), the non-tumor adjacent tissue showed higher levels of antioxidant enzymes, although the tumor tissue presented higher levels of manganese superoxide dismutase (SOD2) and acetylated SOD2. On the other hand, the major differences were found between stages I and II in both tissues [11]. These results indicate that antioxidant enzymes play a crucial role in both tumor and non-tumor adjacent tissues in CRC [8,11].

The aim of this study was to analyze the expression of inflammatory, EMT, and metastasis-related proteins in both tumor and non-tumor adjacent tissues in all stages (I, II, III, IV) from CRC patients' samples, to gain a better understanding of the relationship between those biological processes.

2. Materials and Methods

2.1. Reagents

Routine reagents were purchased in Panreac (Barcelona), Sigma-Aldrich (St. Louis, MO, USA), and Bio-Rad Laboratories (Hercules, CA, USA).

2.2. Patients and Tissue Samples

To carry out the study, a total of 38 patients were included. Patients of both sexes without comorbidity were included. Furthermore, patients did not receive chemotherapy or radiotherapy before surgery and had signed an informed consent according to "World Medical Association Declaration of Helsinki" when medical research involves humans.

Tumor tissues and non-tumor adjacent tissues were recollected from *Biobanc de Son Llàtzer*, for 5 years (2005–2010), and maintained at -80°C until their processing to carry out the study. Patient samples were divided into stages (I, II, III, and IV) and into tissue types (tumor tissue and non-tumor adjacent tissue). A total of 8 samples were included in stage I (5 males and 3 females), 10 samples were included in stage II (5 males and 5 females), 8 samples were included in stage III (2 males and 6 females), and 12 samples were included in stage IV (9 males and 3 females). The age average was 70.8 years and SD was 11.9 (male age average was 72.1 ± 11.6 and range 51–95; female age average was 69.1 ± 12.5 and range 50–88). Clinicopathological features of patient samples included in the study are shown in Table S1. Both tissues were histologically examined by a pathologist and classified by TNM staging system.

2.3. Tissue Homogenization and Protein Quantification

Frozen tumor and non-tumor adjacent tissues were homogenized in a proportion 1:10 (*w/v*) in homogenization buffer (Tris 20 mM pH 7.4, Saccharose 250 mM, EGTA 2 mM and KCl 40 mM) with polytron (T10 basic, IKA-Werke 6 mbH, Staufen, Germany). After that, homogenates were sonicated with Vibra Cell Ultrasonic Processor 75185 on ice in two cycles of 25 W for 5 s with an interval of 85 s between pulses and 40% of amplitude. Finally, homogenates were centrifugated at 600 xg for 10 min at 4 °C and supernatant was recovered. Protease and phosphatase inhibitors (PMSF 1 mM, NaF 1 mM, Pepstatin 10 µM, Leupeptin 10 µM and Na₃VO₄ 1 mM) were added to the supernatant. Protein levels were quantified by Bradford method [12].

2.4. Western Blotting

For all SDS-PAGE carried out, 25 µg of total protein was loaded. Electrophoresis for protein separation was conducted on 8%, 10%, and 12% acrylamide/bisacrylamide (30/1) gels. A semi-dry electrotransfer was performed to transfer proteins into a 0.2 µm nitrocellulose membrane (Bio-Rad Laboratories, Hercules, CA, USA) using a trans-blot turbo transfer system (Bio-Rad Laboratories, Hercules, CA, USA). After electrotransfer, membranes were incubated with Ponceau staining for equal sample loading validation. Then, membranes were blocked with 5% bovine serum albumin (BSA) or non-fat powdered milk (for phosphorylated and non-phosphorylated proteins, respectively) in Tris Buffer Saline 0.05% Tween 20 pH 7.6 (TBS-Tween) for 1 h at room temperature and agitation. After TBS-Tween washes, membranes were incubated with primary antibody (5% free fatty acids BSA and 0.05% sodium azide in TBS-Tween) over night at 4 °C and agitation. Primary antibodies used and their respective dilutions were: inhibitor of kappa B phosphorylated (pIκB) 1:1000 (Cell Signaling, cs2859), inhibitor of kappa B (IκB) 1:1000 (Cell Signaling, cs4814), interferon gamma (IFNγ) 1:1000 (Abcam, 9657), peroxisome proliferator activated receptor gamma (PPARγ) 1:200 (Santa Cruz Biotechnology, sc-7196), interleukin 4 receptor (IL-4R) 1:1000 (Santa Cruz Biotechnology, sc-28361), cyclooxygenase 2 (COX2) 1:1000 (Boster Biological, PA1211), heparanase 1:500 (Abcam, 232817), matrix metalloproteinase 9 (MMP9) 1:1000 (Cell Signaling, cs13667), vimentin 1:500 (Santa Cruz Biotechnology, sc-373717), E-cadherin 1:200 (Santa Cruz Biotechnology, sc-8426), N-cadherin 1:100 (Santa Cruz Biotechnology, sc-393933) and vascular endothelial growth factor B (VEGF-B) 1:500 (Cell Signaling, cs2463). After that, TBS-Tween washes were made. Finally, membranes were incubated with horseradish peroxidase-conjugated secondary antibody (2% BSA or non-fat powdered milk in TBS-Tween) for 1 h at room temperature and agitated. Secondary antibodies used and their respective dilutions were: anti-rabbit 1:10,000 (Sigma, A9169) and anti-mouse 1:10,000 (Sigma, A9044). After incubation, membranes were washed and Inmun-Star© Western Chemiluminescence kit Western blotting detection systems (Bio-Rad Laboratories, Hercules, CA, USA) was used to detect the immunoreactivity. Chemidoc XRS densitometer (Bio-Rad Laboratories, Hercules, CA, USA) was used to acquire chemiluminescent signal for pIκB, IκB, IFNγ, PPARγ, IL-4R, COX2, heparinase and MMP9, and, finally, the Quantity One Software (Bio-Rad Laboratories, Hercules, CA, USA) was used to analyze the results. For vimentin, VEGF-B, E-cadherin, and N-cadherin chemiluminescent signal was detected with the ImageQuant LAS 4000 mini Biomolecular Imager (GE Healthcare, Spain). A sample consisting of a mixture of stages I-IV tumor and non-tumor adjacent tissues was loaded as a control to allow comparison between gels, as previously published [8,11,13].

2.5. Kaplan–Meier Survival Curves

Relapse-free survival was assessed for 585 colon cancer patients from GSE39582 dataset [14,15]. The Statistical Program for the Social Sciences software for windows (SPSS, version 24.0; SPSS Inc., Chicago, IL, USA) was used to perform survival curves using Kaplan–Meier curves survival analysis and the Log Rank test for statistical significance,

which was set at $p < 0.05$. Patients were divided into stages (I, II, III, and IV) and low or high Vimentin or VEGF-B expression levels.

2.6. Statistical Analysis

SPSS was used to perform all statistical analyses. Two-way ANOVA was used to analyze differences between tissues and stages. Student's *t*-test was used to analyze differences between stages or tissues in proteins with an interactive effect found by the two-way ANOVA, with minimal statistical significance at $p < 0.05$. All results are presented as box-plot graphs and relativized to the mean of non-tumor adjacent tissue stage I samples, which was set as 100%.

3. Results

3.1. Epithelium-Mesenchymal Transition Proteins Expression Levels

Heparanase, MMP9, vimentin, and VEGF-B protein levels, were studied in both tumor and non-tumor adjacent tissues of all stages from CRC patients (see Figure 1 and Figure 4).

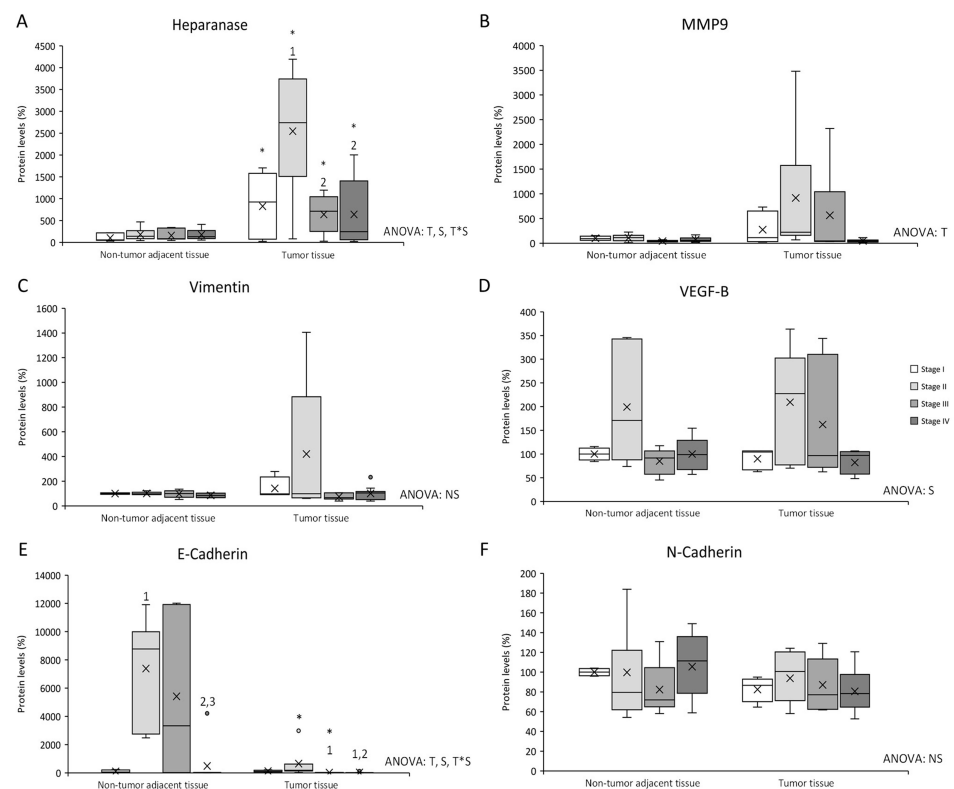


Figure 1. Changes in metastasis-related protein expression levels determined by Western blot: (A) Heparanase; (B) MMP9; (C) Vimentin; (D) VEGF-B; (E) E-cadherin; and (F) N-cadherin. Results are presented as box-plot graphs and relativized to the mean of non-tumor adjacent tissue stage I samples, which was set as 100%; the x in the box represents the mean. **NS:** non-significant differences, **T:** Significant differences between tissue types, **S:** significant differences between stages in the same tissue, **T*S:** interactive effect (ANOVA; $p < 0.05$). * Significant differences between non-tumor adjacent tissue and tumor tissue at the same stage, **1:** significant differences compared to stage I at the same tissue, **2:** significant differences compared to stage II at the same tissue, **3:** significant differences compared to stage III at the same tissue (Student's *t*-test; $p < 0.05$). Original blots are presented in Supplementary Information File S1.

Heparanase levels (Figure 1A) presented differences between non-tumor adjacent tissue and tumor tissue, differences between stages in the same tissue, and an interactive effect between tissue and stage. Tumor tissue showed an increase in heparanase levels

compared to non-tumor adjacent tissue, in all four stages. Furthermore, tumor tissue stage II heparanase levels were higher than tumor tissue stages I, III, and IV.

MMP9 levels (Figure 1B) exhibited differences between non-tumor adjacent tissue and tumor tissue, with tumor tissue MMP9 levels higher than in non-tumor adjacent tissue.

Vimentin levels (Figure 1C) showed no statistically significant differences between tissues or stages.

VEGF-B levels (Figure 1D) presented differences between stages, with stage II VEGF-B levels higher than the other three stages.

E-cadherin levels (Figure 1E) presented differences between non-tumor adjacent tissue and tumor tissue, differences between stages in the same tissue, and an interactive effect between tissue and stage. Tumor tissue stages II and III showed a decrease in E-cadherin levels compared to non-tumor adjacent tissue. Furthermore, non-tumor adjacent tissue stage II E-cadherin levels were higher than non-tumor tissue stage I. In addition, stage IV E-cadherin levels were lower than stages II and III. Tumor tissue stages III and IV E-cadherin levels were lower than stage I, in addition to a decrease of stage IV when it was compared to stage II.

N-cadherin levels (Figure 1F) showed no statistically significant differences between tissues or stages.

3.2. Inflammatory-Related Proteins Expression Levels

pI κ B, I κ B, pI κ B/I κ B ratio, COX2, PPAR γ , IL-4R and IFN γ protein levels were studied in both tumor and non-tumor adjacent tissues in all stages from CRC patients (see Figures 2–4).

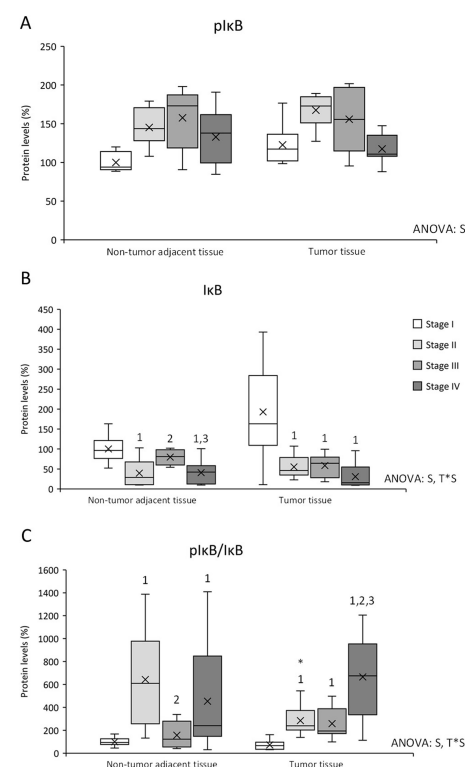


Figure 2. Changes in inflammation-related protein expression levels determined by Western blot: (A) pI κ B; (B) I κ B; and (C) pI κ B/I κ B ratio. Results are presented as box-plot graphs and relativized to the mean of non-tumor adjacent tissue stage I samples, which was set as 100%; the x in the box represents the mean. **NS**: non-significant differences, **T**: significant differences between tissue types, **S**: significant differences between stages in the same tissue, **T*S**: interactive effect (ANOVA; $p < 0.05$). * Significant differences between non-tumor adjacent tissue and tumor tissue at the same stage, **1**: significant differences compared to stage I at the same tissue, **2**: significant differences compared to stage II at the same tissue, **3**: significant differences compared to stage III at the same tissue (Student's *t*-test; $p < 0.05$). Original blots are presented in Supplementary Information File S1.

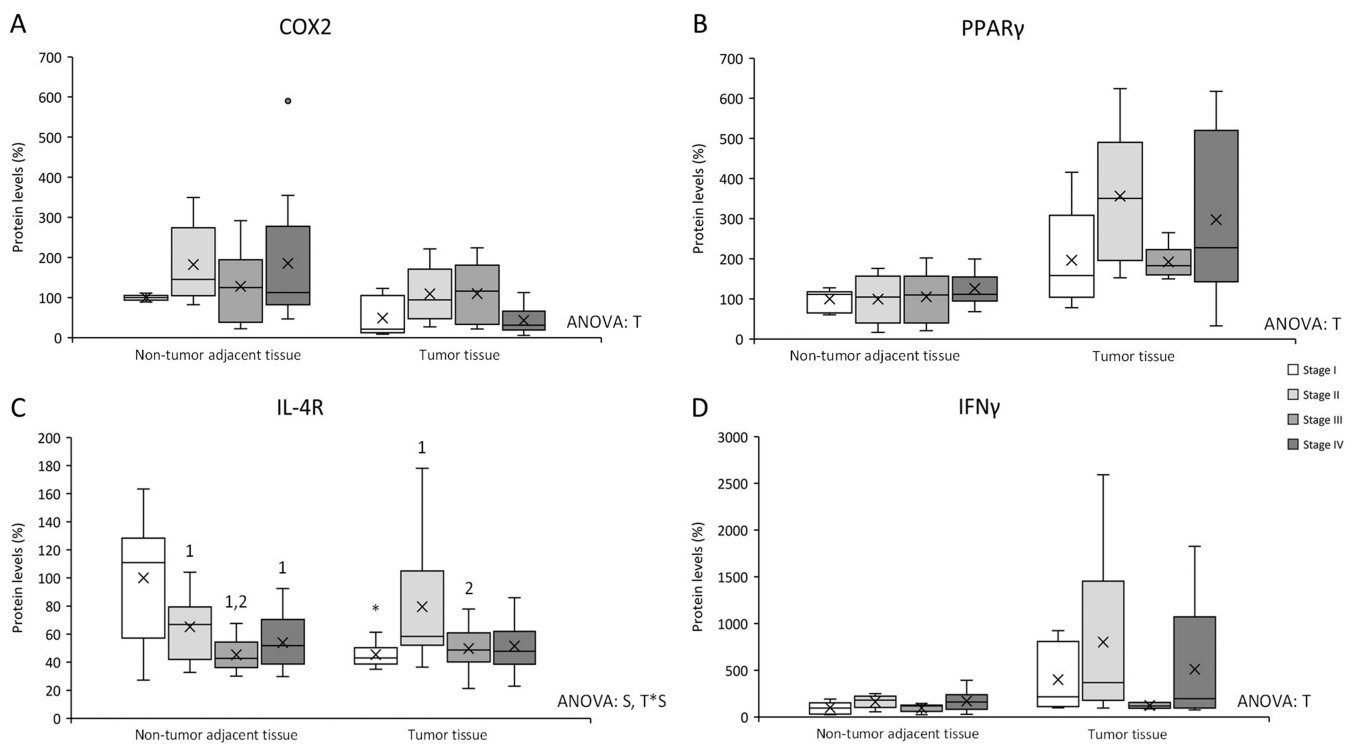


Figure 3. Changes in inflammation-related protein expression levels determined by Western blot: (A) COX2; (B) PPAR γ ; (C) IL-4R; and (D) IFN γ . Results are presented as box-plot graphs and relativized to the mean of non-tumor adjacent tissue stage I samples, which was set as 100%; the x in the box represents the mean. NS: non-significant differences, T: significant differences between tissue types, S: significant differences between stages in the same tissue, T*S: interactive effect (ANOVA; $p < 0.05$). * Significant difference between non-tumor adjacent tissue and tumor tissue at the same stage, 1: significant differences compared to stage I at the same tissue, 2: significant differences compared to stage II at the same tissue, 3: significant differences compared to stage III at the same tissue (Student's t -test; $p < 0.05$). Original blots are presented in Supplementary Information File S1.

pI κ B levels (Figure 2A) presented differences between stages, being stage I pI κ B levels lower than stages II and III in both tissues and lower than stage IV in non-tumor adjacent tissue. I κ B levels (Figure 2B) also showed differences between stages, and an interactive effect between tissue and stage. Stage I I κ B levels were higher in both tissues, and non-tumor adjacent tissue stage III presented higher I κ B levels than stages II and IV from the same tissue. Furthermore, pI κ B/I κ B ratio was also studied to estimate the I κ B degradation and the NF κ B released to the nucleus. pI κ B/I κ B ratio (Figure 2C) presented differences between stages and an interactive effect between tissue and stage. Non-tumor adjacent tissue stage II showed an increase in the ratio compared to tumor tissue stage II. Moreover, this tissue presented higher levels than non-tumor adjacent tissue stages I and III. In addition, non-tumor adjacent tissue stage IV presented an increase in the ratio compared to stage I. Finally, tumor tissue stages II, III, and IV presented an increase in the ratio levels comparing to stage I, being stage IV levels the highest.

COX2 levels (Figure 3A) presented differences between non-tumor adjacent tissue and tumor tissue, being non-tumor adjacent tissue COX2 levels higher than tumor tissue.

PPAR γ levels (Figure 3B) showed differences between non-tumor adjacent tissue and tumor tissue, being tumor tissue PPAR γ levels higher than non-tumor adjacent tissue.

IL-4R levels (Figure 3C) presented differences between stages in the same tissue and an interactive effect between tissue and stage. Non-tumor adjacent tissue stages II, III, and IV, showed a decrease in IL-4R levels when compared to stage I. Additionally, stage III also presented lower levels than stage II. Furthermore, tumor tissue stage II showed an

increase in IL-4R levels compared to tumor tissue stages I and III. Finally, tumor tissue stage I presented lower IL-4R levels than non-tumor adjacent tissue stage I.

IFN γ levels (Figure 3D) presented a tissue effect, being tumor tissue IFN γ levels higher than non-tumor adjacent tissue.

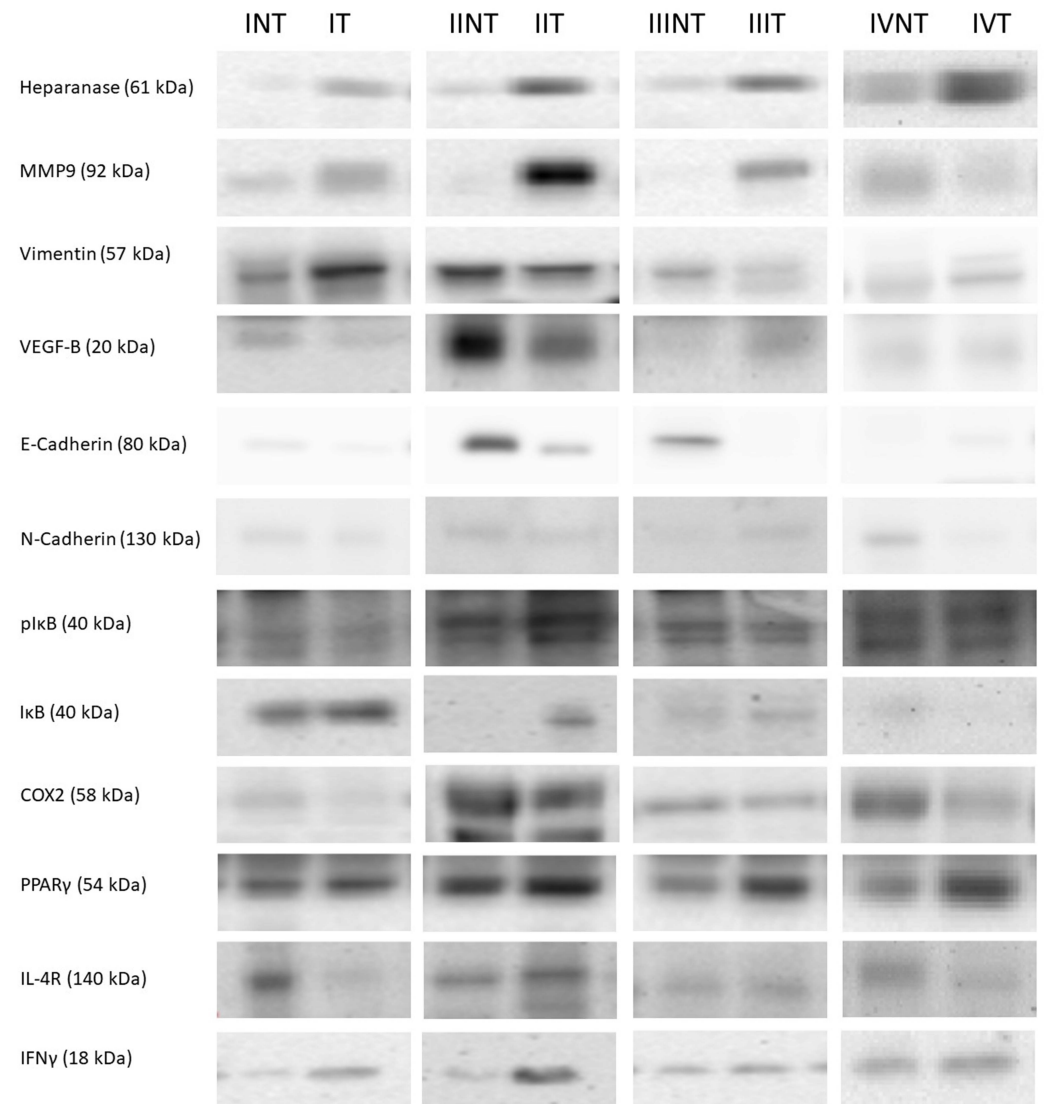


Figure 4. Western blot representative bands and their molecular weight. NT: non-tumor adjacent tissue, T: tumor tissue, I: stage I, II: stage II, III: stage III, IV: stage IV. The whole Western blots were shown in File S1.

3.3. Vimentin and VEGF-B Expression Levels Are Related to Relapse-Free Survival of Colorectal Cancer Patients in Stage II

Vimentin and VEGF-B expression levels were studied according to the tumor stage (I, II, III, and IV) to link them to relapse-free survival of CRC patients (Figure 5). For stage II patients, the higher the expression levels of both vimentin (Figure 5A) and VEGF-B (Figure 5B), the lower 10-year relapse-free survival. No statistically significant results were found in CRC patients in stages I, III, and IV.

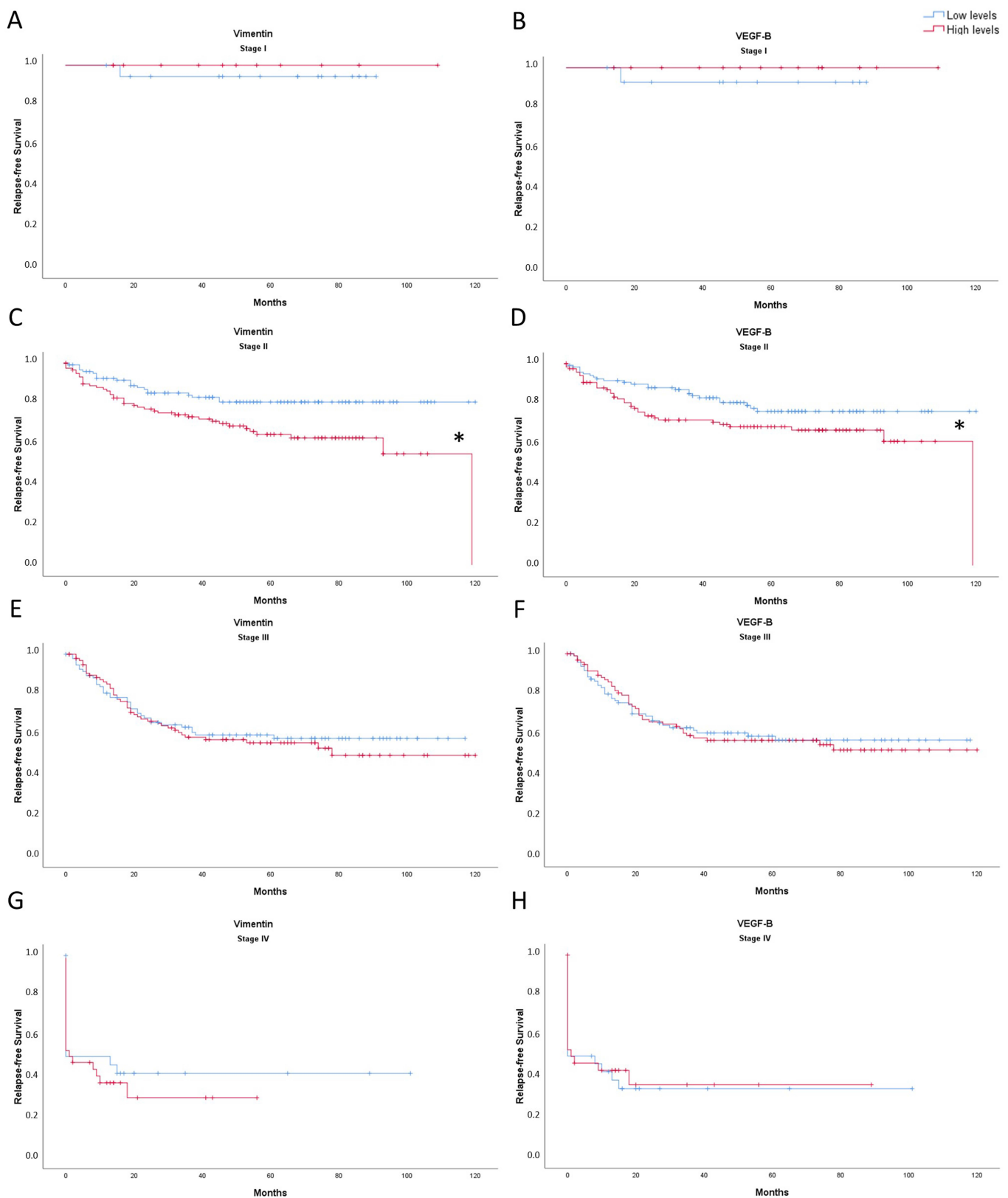


Figure 5. Kaplan-Meier representation of relapse-free survival of Vimentin: ((A): stage I; (C): stage II; (E): stage III; (G): stage IV); and VEGF-B ((B): stage I; (D): stage II; (F): stage III; (H): stage IV) expression levels of CRC patients for 10 years. The blue line indicates low expression levels and red line indicates high expression levels. * Significant differences between low expression levels and high expression levels (Log Rank; $p < 0.05$).

4. Discussion

Changes in proteins related to metastasis and inflammation were studied through all stages (stages I, II, III, and IV) in tumor tissue and non-tumor adjacent tissue from colorectal cancer patient's biopsies. In summary, stage II tumor tissue presented an increase in heparanase and IL-4R, while stage II non-tumor adjacent tissue presented an increase in VEGF-B and the $pI\kappa B/I\kappa B$ ratio. In addition, tumor tissue showed an increase in heparanase, MMP9, PPAR γ , and IFN γ , while non-tumor adjacent tissue showed an increase in E-cadherin and COX2 and a decrease in IL-4R. Finally, high expression of vimentin and VEGF-B in stage II are associated with a lower 10-year relapse-free survival. Briefly, the results obtained could indicate an increase in metastatic indicators in early stages, concretely stage II. As expected, this was observed only in tumoral tissue, but non-tumor adjacent tissue showed an increase in inflammatory markers, also in early stages (Figure 6).

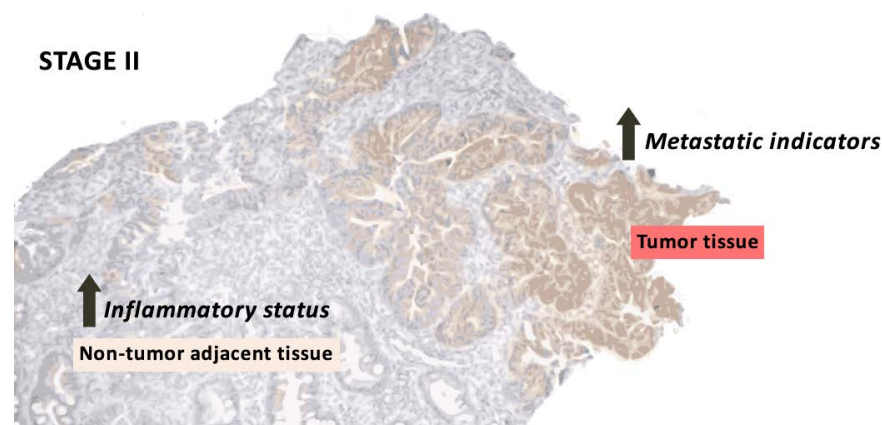


Figure 6. Summary of the most relevant results of stage II in tumor and non-tumor adjacent tissue.

The results obtained in tumor tissue could indicate that metastasis-signaling pathways could be initially stimulated in stage II, since our results showed a huge increase in heparanase levels in tumor tissue compared to non-tumor adjacent tissue, especially in stage II. This is in line with Friedmann et al. results, who demonstrated that heparanase was expressed at early stages of neoplasia, but was non-detectable in normal mucosa [16]. Heparanase's main function is to degrade heparan sulfate chains in the extracellular membrane. Thus, heparanase facilitates several processes including extracellular membrane dissociation, tissular remodeling, cellular migration and dissemination, angiogenesis, metastasis, and inflammation, releasing growth factors and cytokines. Heparanase also regulates inflammation-related genes transcription and inflammatory cell extravasation, and accelerates primary tumor growth [17,18]. Furthermore, our results show that heparanase can be found elevated in non-tumor adjacent tissue in a stage-dependent manner. This could indicate that heparanase is exerting a proinflammatory role [17], which could mean that non-tumor adjacent tissue also presented an increase in its inflammatory status that could be the basis for future tumor initiation.

It has been shown that heparanase can also regulate MMP9 transcription [18]. The main function of this metalloproteinase is to degrade collagen IV from the basement membrane, and it is related to tumoral invasion, metastasis, and angiogenesis induction [19]. MMP9 results showed a similar pattern to non-metastatic stages (I, II, and III) in tumor tissue heparanase levels, as MMP9 presented a huge increase in tumor tissue compared to non-tumor adjacent tissue, especially in stage II. Other authors have also shown overexpression of MMP9 in tumor tissue [20,21]. Following the pattern observed in heparanase and MMP9 levels, vimentin showed a tendency to decrease in stage III when compared to stage II in tumor tissue. Vimentin gene expression has been found to decrease in high-grade CRC tumors [22], while Zhao et al. demonstrated in hepatocellular carcinoma that there were no differences between tumor and non-tumor tissue [23]. Vimentin is considered an EMT-biomarker [23] that participates in the regulation of different physiological functions,

such as maintaining cell shape and cytoplasm integrity, attachment, migration, and cellular signalling [22]. The results obtained from datasets, which indicate that an increase of vimentin expression levels promotes a lower relapse-free survival in stage II, could also support our results indicating that vimentin at stage II could be important for the establishment of metastasis. Considering the results of heparanase, MMP9, and vimentin together, the first signs of EMT could occur in stage II.

In addition, E-cadherin and N-cadherin are two proteins involved in EMT, being E-cadherin an epithelial biomarker of EMT and N-cadherin a mesenchymal biomarker of EMT [24]. Downregulation of E-cadherin increases low differentiation, distant metastasis, vascular invasion, lymph node metastasis, lymphatic invasion, and infiltration [25], while the overexpression of N-cadherin is implicated in tumor differentiation, size and lymph node infiltration, and metastasis [24]. Our results showed an increase in E-cadherin in non-tumor adjacent tissue and in tumor tissue stage II, accompanied by no changes in N-cadherin, which has always opposite expression levels. This suggests that the high expression of E-cadherin could be maintaining cells in the epithelial phenotype and the drop of its expression in stage IV could trigger the mesenchymal phenotype transformation and the metastatic process.

As seen for the other proteins, VEGF-B levels were also increased in stage II in tumor tissue. The main function of VEGF-B is to participate in angiogenesis, stimulating the proliferation of endothelial cells and vessel growth. In addition, VEGF-B is also involved in the maintenance of blood vessels, avoiding cell death and initiating tumorigenesis [26–28]. For these reasons, the increase observed in tumor tissue stage II could suggest that VEGF-B would be participating in the preservation of blood vessels and avoiding cell death to sustain tumor growth. Considering that VEGF-B levels also presented an increase in stage II non-tumor adjacent tissue, VEGF-B could additionally be related to future tumor initiation [28], in line with our observations of the first signs of metastasis in this stage. In addition, the results obtained from datasets, which indicate that an increase of VEGF-B expression levels promotes a lower relapse-free survival in stage II, could also support that metastasis signalling could be starting in stage II. No difference between tumor and non-tumor adjacent tissue was observed, similar to what was reported for gastro-oesophageal cancer and colon adenocarcinoma [26,29].

Accompanying the increase in stage II in tumor tissue of EMT and metastasis-related proteins, there was also an increase in the inflammatory status in both tumor tissue and non-tumor adjacent tissue, caused by the increase in pro-inflammatory-related proteins and the decrease in anti-inflammatory-related proteins. The increase in metastasis-related proteins in stage II on tumor tissue could be achieved by an increase in inflammation status, since inflammation participates in each colon cancer phase [4]. On the other hand, the increase in inflammatory status in non-tumor adjacent tissue could be the basis for future tumor initiation since inflammation in the tumoral microenvironment is associated with tumoral growth, angiogenesis, EMT, and metastasis [4].

In addition to heparanase and VEGF-B results previously explained in non-tumor adjacent tissue, the I κ B ratio presented the higher levels at stage II in non-tumor adjacent tissue. This increase can be translated into an increase in inflammation, as I κ B is a protein that inhibits nuclear factor kappa B (NF- κ B) and, when I κ B is phosphorylated by I κ B kinase (IKK), I κ B is degraded by proteasome and NF- κ B is released [30]. NF- κ B is a transcription factor that, when heterodimerizes, can be translocated into the nucleus, where it induces the transcription of genes related to inflammation, cell growth, and the immune response [30]. This increase in inflammation could mean that non-tumor adjacent tissue in stage II patients is initiating and promoting an inflammatory status that can support tumoral growth. Furthermore, the I κ B ratio presented an increase in stages II, III, and IV in tumor tissue regarding stage I, which means that there was an increase in inflammatory status [30].

Accordingly to the I κ B ratio levels, COX2 levels, which can be regulated by NF- κ B [30], were higher in non-tumor adjacent tissue. This could contribute to perpetuating the inflammatory status in this tissue, as well as increasing cell proliferation, since COX2 converts

free arachidonic acid into prostaglandins to stimulate inflammation, angiogenesis, and tumoral growth [31,32]. Furthermore, it has been seen that COX2 can increase proliferation and invasiveness in epithelial human colon cancer cells [32]. In addition, COX2 levels in non-metastatic stages in tumor tissue also followed the same pattern as the I κ B ratio levels, which could also indicate an increase in inflammation at these stages in addition to an increase in angiogenesis, tumoral growth, proliferation, and invasiveness [31,32]. Moreover, heparanase levels also increased in stage II in tumor tissue contributing to the perpetuation of the inflammatory status besides its role in metastasis [17,18].

Furthermore, IFN γ also presented an increase in tumor tissue that was more pronounced in stage II. IFN γ reduces the number of endothelial cells and induces blood vessel destruction and tumor necrosis [33]. Thus, it is possible that IFN γ is elevated in order to palliate the VEGF-B effects by reducing the number of endothelial cells and blood vessels and producing necrosis. In this regard, in stage III, IFN γ could be reduced to avoid necrosis and continue with metastasis.

On the other hand, our results suggest that the anti-inflammatory proteins cannot palliate the inflammatory status increase. IL-4R presented a decrease in all three stages II, III, and IV in non-tumor adjacent tissue regarding stage I. This decrease could mean that IL-4 cannot alleviate the promotion of inflammation started in non-tumor adjacent tissue because IL-4 has an anti-inflammatory role, as it downregulates NF- κ B transactivation induced by proinflammatory cytokines, decreasing I κ B proteasome degradation [34]. In tumor tissue, IL-4R presented a decrease in tumor tissue, which could mean that IL-4 cannot palliate the inflammatory status present in tumor tissue, thus perpetuating it. Finally, PPAR γ has anti-inflammatory properties since it inhibits inflammation-related genes [35] and can inhibit NF- κ B in different ways [34,36,37]. PPAR γ levels presented an increase in tumor tissue, which was also seen by DuBois et al. [38], that can be interpreted as an insufficient attempt of PPAR γ to avoid I κ B phosphorylation for maintaining NF- κ B at the cytoplasm and decrease the inflammatory status.

Further studies are necessary for a better understanding of metastasis initiation and the associated inflammation. An interesting approach could be the development of 3D models in vitro from a primary explant of CRC tissues to understand in a better way the EMT and metastasis processes. Several approaches can be used to mimic the in vivo cancer environment, including the use of biomaterials [39] or even the use of 3D printed tissue constructs [40], and 3D bone-on-a-chip systems that can allow the study of the bone metastasis [41]. Unfortunately, there are no animal models for the different CRC stages (I, II, III, IV) since there are only animal models for early or late CRC. This situation makes it difficult to investigate the different markers in vivo and across the different stages, despite the existence of some advanced studies about the use of zebrafish xenografts and *Drosophila melanogaster* [42,43].

5. Conclusions

In conclusion, these results could suggest that some metastasis-related signalling pathways may be activated in stage II in tumor tissue due to an increase in inflammation at this stage. Furthermore, non-tumor adjacent tissue presented an increase of the inflammatory status that could be the basis for future tumor progression. Although further analyses are necessary to better understand the metastasis initiation in colorectal cancer and the inflammation associated with the metastatic process, this study indicates the convenience of determining the possibility of using the proteins measured as biomarkers of diagnosis and evolution in the early stages of colon cancer.

Supplementary Materials: The following supporting information can be downloaded at: <https://www.mdpi.com/article/10.3390/cancers14184487/s1>, Table S1: clinicopathological features of patient's samples included in the study, File S1: The whole Western blots.

Author Contributions: conceptualization, M.A.-C., M.T.-M., R.H.-L., J.M.I.d.I.R., E.F., T.F., M.M.C., J.S.-S., J.O., P.R. and D.G.P.; methodology, M.A.-C., M.T.-M., R.H.-L., J.O. and D.G.P.; validation, M.A.-C., M.T.-M., R.H.-L., J.M.I.d.I.R., E.F., T.F., M.M.C., J.S.-S., J.O., P.R. and D.G.P.; formal analysis, M.A.-C., M.T.-M., R.H.-L., J.M.I.d.I.R., E.F., T.F., M.M.C., J.S.-S., J.O., P.R. and D.G.P.; investigation, J.O. and D.G.P.; data curation, M.A.-C., M.T.-M., R.H.-L., J.M.I.d.I.R., E.F., T.F., M.M.C., J.S.-S., J.O., P.R. and D.G.P.; writing—original draft preparation, M.A.-C., J.O. and D.G.P.; writing—review and editing, M.T.-M., P.R. and J.S.-S.; supervision, J.O. and D.G.P.; project administration, J.O. and D.G.P.; funding acquisition, J.O. and D.G.P. All authors have read and agreed to the published version of the manuscript.

Funding: This work was supported by grants from Fondo de Investigaciones Sanitarias of Instituto de Salud Carlos III (PI14/01434) of the Spanish Government cofinanced by FEDER-Unión Europea (“Una manera de hacer Europa”) and from PRIMUS program from the Balearic Islands Health Research Institute (IdISBa), grant number “PRI20/15”. Margalida Torrens-Mas was supported by a grant from Programa postdoctoral Margalida Comas–Comunidad Autónoma de las Islas Baleares (PD/050/2020).

Institutional Review Board Statement: The study was conducted according to the guidelines of the Declaration of Helsinki and approved by the Comité d’ètica de la Investigació de les Illes Balears (IB 2431/14 PI, 26/11/2014).

Informed Consent Statement: Informed consent was obtained from all subjects involved in the study. Written informed consent has been obtained from the patient(s) to publish this paper.

Data Availability Statement: The data presented in this study are available in this article and supplementary material.

Acknowledgments: The authors thank Hospital Universitari Son Llàtzer for sample acquisition.

Conflicts of Interest: The authors declare no conflict of interest. The funders had no role in the design of the study; in the collection, analyses, or interpretation of data; in the writing of the manuscript; or in the decision to publish the results.

References

1. Ferlay, J.; Ervik, M.; Lam, F.; Colombet, M.; Mery, L.; Piñeros, M.; Znaor, A.; Soerjomataram, I.B.F. Global Cancer Observatory: Cancer Today. Available online: <https://gco.iarc.fr/today> (accessed on 1 December 2021).
2. Society, A.C. Survival rates for Colorectal Cancer. Available online: <https://www.cancer.org/cancer/colon-rectal-cancer/detection-diagnosis-staging/survival-rates.html> (accessed on 2 September 2022).
3. AJCC. *AJCC Cancer Staging Manual*, 8th ed.; Springer International Publishing: Chicago, IL, USA, 2017.
4. Landskron, G.; De Fuente, M.; Thuwajit, P.; Thuwajit, C.; Hermoso, M.A. Chronic Inflammation and Cytokines in the Tumor Microenvironment. *J. Immunol. Res.* **2014**, *2014*, 149185. [[CrossRef](#)] [[PubMed](#)]
5. Hanahan, D.; Weinberg, R.A. Hallmarks of cancer: The next generation. *Cell* **2011**, *144*, 646–674. [[CrossRef](#)] [[PubMed](#)]
6. Suarez-Carmona, M.; Lesage, J.; Cataldo, D.; Gilles, C. EMT and inflammation: Inseparable actors of cancer progression. *Mol. Oncol.* **2017**, *11*, 805–823. [[CrossRef](#)] [[PubMed](#)]
7. Terzić, J.; Grivennikov, S.; Karin, E.; Karin, M. Inflammation and Colon Cancer. *Gastroenterology* **2010**, *138*, 2101–2114. [[CrossRef](#)] [[PubMed](#)]
8. Hernández-López, R.; Torrens-mas, M.; Pons, D.G.; Company, M.M.; Falcó, E.; Fernández, T.; Ibarra de la Rosa, J.M.; Sastre-Serra, J.; Oliver, J.; Roca, P. Non-tumor adjacent tissue of advanced stage from CRC shows activated antioxidant response. *Free Radic. Biol. Med.* **2018**, *126*, 249–258. [[CrossRef](#)] [[PubMed](#)]
9. Balkwill, F.; Mantovani, A. Inflammation and cancer: Back to Virchow? *Lancet* **2001**, *357*, 539–545. [[CrossRef](#)]
10. Ieda, T.; Tazawa, H.; Okabayashi, H.; Yano, S.; Shigeyasu, K. Visualization of epithelial-mesenchymal transition in an inflammatory microenvironment—Colorectal cancer network. *Sci. Rep.* **2019**, *9*, 16378. [[CrossRef](#)]
11. Gaya-Bover, A.; Hernández-López, R.; Alorda-Clara, M.; Ibarra de la Rosa, J.M.; Falcó, E.; Fernández, T.; Margarita, M.; Torrens-mas, M.; Roca, P.; Oliver, J.; et al. Antioxidant enzymes change in different non-metastatic stages in tumoral and peritumoral tissues of colorectal cancer. *Int. J. Biochem. Cell Biol.* **2020**, *120*, 105698. [[CrossRef](#)]
12. Bradford, M.M. A rapid and sensitive method for the quantitation of microgram quantities of protein utilizing the principle of protein-dye binding. *Anal. Biochem.* **1976**, *72*, 248–254. [[CrossRef](#)]
13. Hernández-López, R.; Torrens-Mas, M.; Pons, D.G.; Company, M.M.; Falcó, E.; Fernández, T.; Ibarra de la Rosa, J.M.; Roca, P.; Oliver, J.; Sastre-Serra, J. Mitochondrial Function Differences between Tumor Tissue of Human Metastatic and Premetastatic CRC. *Biology* **2022**, *11*, 293. [[CrossRef](#)]

14. Marisa, L.; de Reyniès, A.; Duval, A.; Selves, J.; Gaub, M.P.; Vescovo, L.; Etienne-Grimaldi, M.-C.; Schiappa, R.; Guenot, D.; Ayadi, M.; et al. Gene expression classification of colon cancer into molecular subtypes: Characterization, validation, and prognostic value. *PLoS Med.* **2013**, *10*, e1001453. [[CrossRef](#)] [[PubMed](#)]
15. Provenzani, A.; Fronza, R.; Loreni, F.; Pascale, A.; Amadio, M.; Quattrone, A. Global alterations in mRNA polysomal recruitment in a cell model of colorectal cancer progression to metastasis. *Carcinogenesis* **2006**, *27*, 1323–1333. [[CrossRef](#)] [[PubMed](#)]
16. Friedmann, Y.; Vlodaysky, I.; Aingorn, H.; Aviv, A.; Peretz, T.; Pecker, I.; Pappo, O. Expression of heparanase in normal, dysplastic, and neoplastic human colonic mucosa and stroma: Evidence for its role in colonic tumorigenesis. *Am. J. Pathol.* **2000**, *157*, 1167–1175. [[CrossRef](#)]
17. Vlodaysky, I.; Beckhove, P.; Lerner, I.; Pisano, C.; Meirovitz, A.; Ilan, N.; Elkin, M. Significance of heparanase in cancer and inflammation. *Cancer Microenviron.* **2012**, *5*, 115–132. [[CrossRef](#)] [[PubMed](#)]
18. Masola, V.; Zaza, G.; Gambaro, G.; Franchi, M.; Onisto, M. Role of heparanase in tumor progression: Molecular aspects and therapeutic options. *Semin. Cancer Biol.* **2020**, *62*, 86–98. [[CrossRef](#)]
19. Mylona, E.; Nomikos, A.; Magkou, C.; Kamberou, M.; Papassideri, I.; Keramopoulos, A.; Nakopoulou, L. The clinicopathological and prognostic significance of membrane type 1 matrix metalloproteinase (MT1-MMP) and MMP-9 according to their localization in invasive breast carcinoma. *Histopathology* **2007**, *50*, 338–347. [[CrossRef](#)]
20. Zhang, Y.; Guan, X.Y.; Dong, B.; Zhao, M.; Wu, J.H.; Tian, X.Y.; Hao, C.Y. Expression of MMP-9 and WAVE3 in colorectal cancer and its relationship to clinicopathological features. *J. Cancer Res. Clin. Oncol.* **2012**, *138*, 2035–2044. [[CrossRef](#)]
21. Zheng, C.G.; Chen, R.; Xie, J.B.; Liu, C.B.; Jin, Z.; Jin, C. Immunohistochemical expression of Notch1, Jagged1, NF- κ B and MMP-9 in colorectal cancer patients and the relationship to clinicopathological parameters. *Cancer Biomark.* **2015**, *15*, 889–897. [[CrossRef](#)]
22. Niknami, Z.; Eslamifar, A.; Emamirazavi, A.; Ebrahimi, A.; Shirkoobi, R. The association of vimentin and fibronectin gene expression with epithelial-mesenchymal transition and tumor malignancy in colorectal carcinoma. *EXCLI J.* **2017**, *16*, 1009–1017.
23. Zhao, Q.; Zhou, H.; Qifei, L.; Ye, C.; Gang, W.; Anla, H.; Liang, R.; Sufang, W.; Qingli, B.; Wenjun, C.; et al. Prognostic value of the expression of cancer stem cell-related markers CD133 and CD44 in hepatocellular carcinoma: From patients to patient-derived tumor xenograft modelst. *Oncotarget* **2016**, *7*, 47431–47443. [[CrossRef](#)]
24. Yan, X.; Yan, L.; Liu, S.; Shan, Z.; Tian, Y.; Jin, Z. N-cadherin, a novel prognostic biomarker, drives malignant progression of colorectal cancer. *Mol. Med. Rep.* **2015**, *12*, 2999–3006. [[CrossRef](#)] [[PubMed](#)]
25. Chang, K.; Jiang, L.; Sun, Y.; Li, H. Effect of E-cadherin on Prognosis of Colorectal Cancer: A Meta-Analysis Update. *Mol. Diagn. Ther.* **2022**, *26*, 397–409. [[CrossRef](#)] [[PubMed](#)]
26. Angelescu, C.; Burada, F.; Ioana, M.; Angelescu, R.; Moraru, E.; Riza, A.; Marchian, S.; Mixich, F.; Cruce, M.; Săftoiu, A. VEGF-A and VEGF-B mRNA expression in gastro-oesophageal cancers. *Clin. Transl. Oncol.* **2013**, *15*, 313–320. [[CrossRef](#)] [[PubMed](#)]
27. Li, X.; Kumar, A.; Zhang, F.; Lee, C.; Tang, Z. Complicated life, complicated VEGF-B. *Trends Mol. Med.* **2012**, *18*, 119–127. [[CrossRef](#)]
28. Eppenberger, M.; Zlobec, I.; Baumhoer, D.; Terracciano, L.; Lugli, A. Role of the VEGF ligand to receptor ratio in the progression of mismatch repair-proficient colorectal cancer. *BMC Cancer* **2010**, *10*, 93. [[CrossRef](#)]
29. André, T.; Kotelevets, L.; Vaillant, J.C.; Coudray, A.M.; Weber, L.; Prévot, S.; Parc, R.; Gespach, C.; Chastre, E. VEGF, VEGF-B, VEGF-C, and their receptors KDR, FLT-1 and FLT-4 during the neoplastic progression of human colonic mucosa. *Int. J. Cancer* **2000**, *86*, 174–181. [[CrossRef](#)]
30. Wang, S.; Liu, Z.; Wang, L.; Zhang, X. NF-kappaB signaling pathway, inflammation and colorectal cancer. *Cell. Mol. Immunol.* **2009**, *6*, 327–334. [[CrossRef](#)]
31. Desai, S.J.; Prickril, B.; Avraham, R. Mechanisms of phytonutrient modulation of Cyclooxygenase-2 (COX-2) and inflammation related to cancer. *Nutr. Cancer* **2018**, *70*, 350–375. [[CrossRef](#)]
32. Sheng, J.; Sun, H.; Yu, F.B.; Li, B.; Zhang, Y.; Zhu, Y.T. The role of cyclooxygenase-2 in colorectal cancer. *Int. J. Med. Sci.* **2020**, *17*, 1095–1101. [[CrossRef](#)]
33. Jorgovanovic, D.; Song, M.; Wang, L.; Zhang, Y. Roles of IFN- γ in tumor progression and regression: A review. *Biomark. Res.* **2020**, *8*, 1–16. [[CrossRef](#)]
34. Paintlia, A.S.; Paintlia, M.K.; Singh, I.; Singh, A.K. IL-4-Induced Peroxisome Proliferator-Activated Receptor γ Activation Inhibits NF- κ B Trans Activation in Central Nervous System (CNS) Glial Cells and Protects Oligodendrocyte Progenitors under Neuroinflammatory Disease Conditions: Implication for CNS-Demy. *J. Immunol.* **2006**, *176*, 4385–4398. [[CrossRef](#)] [[PubMed](#)]
35. Hong, C.; Tontonoz, P. Coordination of inflammation and metabolism by PPAR and LXR nuclear receptors. *Curr. Opin. Genet. Dev.* **2008**, *18*, 461–467. [[CrossRef](#)] [[PubMed](#)]
36. Wahli, W. A gut feeling of the PXR, PPAR and NF- κ B connection. *J. Intern. Med.* **2008**, *263*, 613–619. [[CrossRef](#)] [[PubMed](#)]
37. Carter, A.B.; Misyak, S.A.; Hontecillas, R.; Bassaganya-Riera, J. Dietary modulation of inflammation-induced colorectal cancer through PPAR γ . *PPAR Res.* **2009**, *2009*, 498352. [[CrossRef](#)] [[PubMed](#)]
38. DuBois, R.N.; Gupta, R.; Brockman, J.; Reddy, B.S.; Krakow, S.L.; Lazar, M.A. The nuclear eicosanoid receptor, PPAR γ , is aberrantly expressed in colonic cancers. *Carcinogenesis* **1998**, *19*, 49–53. [[CrossRef](#)]
39. Nii, T.; Makino, K.; Tabata, Y. Three-Dimensional Culture System of Cancer Cells Combined with Biomaterials for Drug Screening. *Cancers* **2020**, *12*, 2754. [[CrossRef](#)]
40. Cui, H.; Esworthy, T.; Zhou, X.; Hann, S.Y.; Glazer, R.I.; Li, R.; Shang, L.G. Engineering a novel 3D printed vascularized tissue model for investigating breast cancer metastasis to bone. *Adv. Healthc. Mater.* **2020**, *9*, e1900924. [[CrossRef](#)]

41. Hao, S.; Ha, L.; Cheng, G.; Wan, Y.; Xia, Y.; Sosnoski, D.M.; Mastro, A.M.; Zheng, S. A Spontaneous 3D Bone-On-a-Chip for Bone Metastasis Study of Breast Cancer Cells. *Small* **2018**, *14*, 1702787. [[CrossRef](#)]
42. Póvoa, V.; De Almeida, C.R.; Maia-Gil, M.; Sobral, D.; Domingues, M.; Martinez-lopez, M.; Fuzeta, M.D.A.; Silva, C.; Grosso, A.R.; Fior, R. Innate immune evasion revealed in a colorectal zebrafish xenograft model. *Nat. Commun.* **2021**, *12*, 1156. [[CrossRef](#)]
43. Zipper, L.; Batchu, S.; Kaya, N.H.; Antonello, Z.A. The MicroRNA miR-277 Controls Physiology and Pathology of the Adult *Drosophila* Midgut by Regulating the Expression of Fatty Acid β -Oxidation-Related Genes in Intestinal Stem Cells. *Metabolites* **2022**, *12*, 315. [[CrossRef](#)]

Isolation and Characterization of Extracellular Vesicles in Human Bowel Lavage Fluid.

Alorda-Clara, M., Reyes, J., Trelles-Guzman, M. G., Florido, M., Roca, P., Pons, D. G., & Oliver, J. (2023).
International Journal of Molecular Sciences, 24(8), 7391.



Article

Isolation and Characterization of Extracellular Vesicles in Human Bowel Lavage Fluid

Marina Alorda-Clara ^{1,2} , Jose Reyes ^{1,2,3}, Marita Grimanese Trelles-Guzman ^{1,2,3}, Monica Florido ³, Pilar Roca ^{1,2,4} , Daniel Gabriel Pons ^{1,2,*} and Jordi Oliver ^{1,2,4}

- ¹ Grupo Multidisciplinar de Oncología Traslacional, Institut Universitari d'Investigació en Ciències de la Salut (IUNICS), Universitat de les Illes Balears, E-07122 Palma, Spain; marina.alorda@uib.es (M.A.-C.); jose.reyes@hcin.es (J.R.); marita.trelles@hcin.es (M.G.T.-G.); pilar.roca@uib.es (P.R.); jordi.oliver@uib.es (J.O.)
- ² Instituto de Investigación Sanitaria Illes Balears (IdISBa), Hospital Universitario Son Espases, Edificio S, E-07120 Palma, Spain
- ³ Servicio Aparato Digestivo, Hospital Comarcal de Inca, E-07300 Inca, Spain; monica.florido@hcin.es
- ⁴ Ciber Fisiopatología Obesidad y Nutrición (CB06/03), Instituto Salud Carlos III, E-28029 Madrid, Spain
- * Correspondence: d.pons@uib.es; Tel.: +34-971-173-149

Abstract: Colorectal cancer (CRC) is the third most common cancer worldwide and is detected in late stages because of a lack of early and specific biomarkers. Tumors can release extracellular vesicles (EVs), which participate in different functions, such as carrying nucleic acids to target cells; promoting angiogenesis, invasion, and metastasis; and preparing an adequate tumor microenvironment. Finally, bowel lavage fluid (BLF) is a rarely used sample that is obtained during colonoscopy. It presents low variability and protein degradation, is easy to handle, and is representative of EVs from tumor cells due to proximity of the sample collection. This sample has potential as a research tool and possible biomarker source for CRC prognosis and monitoring. In this study, EVs were isolated from human BLF by ultracentrifugation, then characterized by transmission electron microscopy and atomic force microscopy. EV concentration was determined by nanoparticle tracking analysis, and tetraspanins were determined by Western blot, confirming correct EV isolation. RNA, DNA, and proteins were isolated from these EVs; RNA was used in real-time PCR, and proteins were used in an immunoblotting analysis, indicating that EV cargo is optimal for use and study. These results indicate that EVs from BLF can be a useful tool for CRC study and could be a source of biomarkers for the diagnosis and monitoring of CRC.

Keywords: bowel lavage fluid; extracellular vesicles; colorectal cancer; ultracentrifugation



Citation: Alorda-Clara, M.; Reyes, J.; Trelles-Guzman, M.G.; Florido, M.; Roca, P.; Pons, D.G.; Oliver, J.

Isolation and Characterization of Extracellular Vesicles in Human Bowel Lavage Fluid. *Int. J. Mol. Sci.* **2023**, *24*, 7391. <https://doi.org/10.3390/ijms24087391>

Academic Editor: Carlos CABAÑAS

Received: 9 March 2023

Revised: 3 April 2023

Accepted: 14 April 2023

Published: 17 April 2023



Copyright: © 2023 by the authors. Licensee MDPI, Basel, Switzerland. This article is an open access article distributed under the terms and conditions of the Creative Commons Attribution (CC BY) license (<https://creativecommons.org/licenses/by/4.0/>).

1. Introduction

Colorectal cancer (CRC) is the third most common cancer worldwide and the second leading cause of cancer death [1]. It is known that an early diagnosis of CRC improves patient survival, decreasing mortality; however, at present, CRC is usually detected in late stages because of the lack of early biomarkers and detection techniques [2]. Even so, there are different diagnostic techniques that are used in the clinical setting, the most commonly used of which are diagnostic imaging techniques, such as colonoscopies, positron emission tomography, computed tomography, and nuclear magnetic resonance; however, all these techniques are invasive for the patients [3,4]. There are some less invasive techniques; however, these are non-specific for CRC because of their presence in other pathologies, in addition to their presence in late stages of CRC, such as carcinoembryonic antigen (CEA) detection in plasma, as well as the detection of carbohydrate antigen 19-9 (CA19-9), tumor-associated glycoprotein 72 (TAG-72), and tissue polypeptide-specific antigen (TPS) in serum [4]. Finally, stool is also used for CRC diagnosis; the most used diagnosis techniques are fecal occult blood testing, which presents high sensitivity and specificity but also a

high number of false positives [5,6]; the detection of fecal calprotectin, which presents low sensitivity [7]; and the detection of changes in DNA, which is stable in stool [4].

Minimal information of studies of extracellular vesicles (MISEV) describes the extracellular vesicles (EVs) as “particles naturally released from the cell that are delimited by a lipid bilayer and cannot replicate” [8]. EVs can participate in several diseases, such as cancer, diabetes mellitus, cardiovascular diseases, neurodegenerative diseases, and autoimmune diseases [9]. It is known that CRC cells release EVs starting in the early stages; for this reason, EVs can be used as a possible source of prognostic and monitoring biomarkers for this cancer type [2]. EVs present some advantages over other diagnostic techniques; for example, they are easy to obtain in high concentrations, have a long half-life, can be collected non-invasively, are stabilized and protected by the lipid bilayer, and their cargo can reflect tumor status [3,10,11] because it is based on the genome, transcriptome, and secretome of origin tumoral cells [10,12]. EVs can participate in different functions: debris removal, carrying DNA, RNA and protein targeting of cells, tumor microenvironment formation, tumor formation and progression, angiogenesis, invasion, metastasis, chemoresistance, drug resistance, recrudescence, tissue repair, tumoral therapy, and vaccination [2,9,10,12–15].

Bowel lavage fluid (BLF) is obtained during colonoscopies by direct application of saline serum to the injury area in the colon, enriching it with injury-area cells [16]. Few studies have been conducted using this sample type for CRC research, with most studies focusing on the presence of genomic biomarkers such as an increase in p53 and K-ras mutations, an increase in mutations of the TGF β type II receptor and APC [17,18], the presence of aberrant methylation in CpG islands in a gene panel (miR-124-3p, LOC86758, and SFRP1) [19], and the presence of syndecan-2 methylation [20]. BLF presents some advantages over other samples types such as stool because it is subject to less bacterial and food interference, is easier to handle, presents less variability because of water quantity and time in the bowel, and is less subject to protein degradation [16]. Nowadays, BLF is rarely used, but this type of sample has a great potential as a CRC research tool and could be studied as possible biomarker source for CRC [16].

The aim of this study was to evaluate BLF as a research tool for the study of CRC through EV isolation in this sample type.

2. Results

2.1. Extracellular Vesicles Can Be Isolated from Bowel Lavage Fluid

After EVs isolation from BLF samples by ultracentrifugation method, EVs were characterized by observation under AFM and TEM microscopes (Figures 1 and 2). Furthermore, two different tetraspanins (CD9 and CD63) determined by Western blot were present in EVs from BLF (Figure 3). Finally, the size determination and EVs concentration determined by NTA (Figure 4 and Table 1) indicated no significant differences between groups.

Table 1. Extracellular vesicle concentration (particles/mL) in healthy, low-risk, high-risk, and cancer samples determined by nanoparticle tracking analysis. Values are represented as mean \pm SD. NS: non-significant differences (p 0.690), (ANOVA; p < 0.05). n = 48; for each sample type n = 12 divided into 3 pools of 4 samples each.

	Healthy	Low-Risk	High-Risk	Cancer	ANOVA
Particles/mL	$1.80 \times 10^{10} \pm 7.80 \times 10^9$	$1.36 \times 10^{10} \pm 5.57 \times 10^8$	$1.51 \times 10^{10} \pm 3.59 \times 10^9$	$1.59 \times 10^{10} \pm 2.12 \times 10^9$	NS (p 0.690)

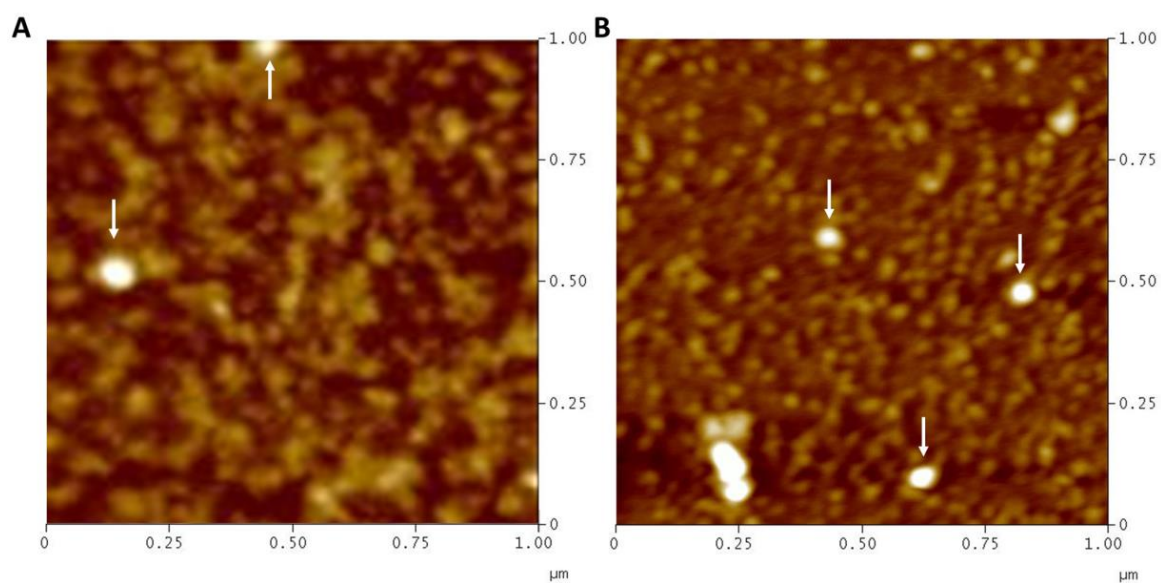


Figure 1. Extracellular vesicle visualization in healthy (A) and cancer (B) samples by atomic force microscopy. White arrows point to extracellular vesicles.

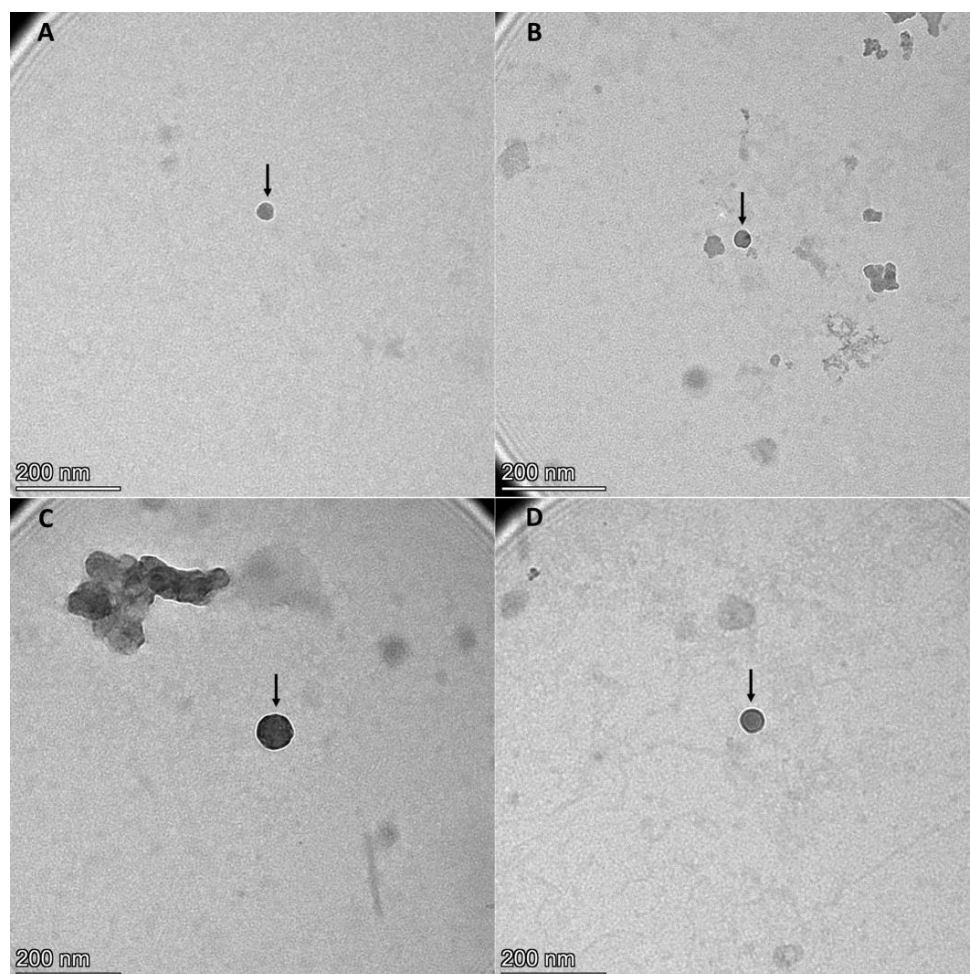


Figure 2. Extracellular vesicle structural and morphological visualization in healthy (A), low-risk (B), high-risk (C), and cancer (D) samples by transmission electron microscopy. Black arrows point to extracellular vesicles. $n = 16$, divided into 4 pools of 4 samples each; 1 pool per sample type.

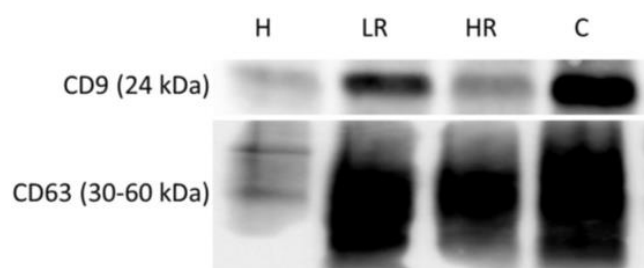


Figure 3. Extracellular vesicle characterization in healthy, low-risk, high-risk, and cancer samples. Tetraspanins (CD9 and CD63) representative bands and their molecular weights determined by Western blot. **H:** healthy samples; **LR:** low-risk samples; **HR:** high-risk samples; **C:** cancer samples.

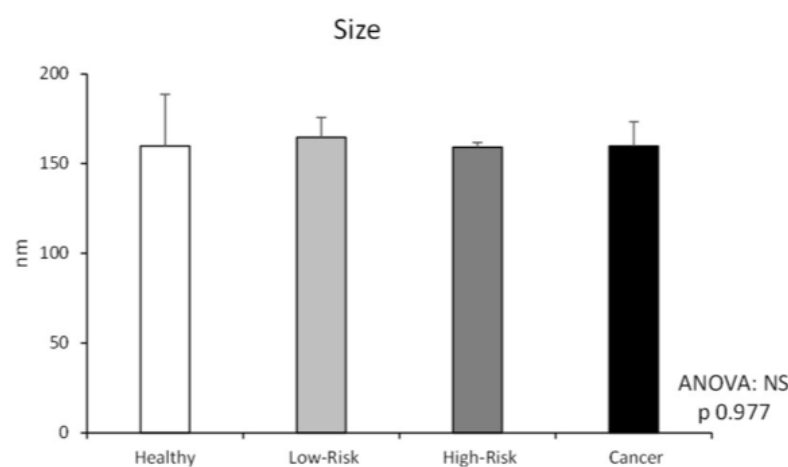


Figure 4. Extracellular vesicle characterization in healthy, low-risk, high-risk, and cancer samples. Extracellular vesicle size (nm) was determined by nanoparticle tracking analysis, and values are represented as mean \pm SD. **NS:** non-significant differences (p 0.977), (ANOVA; $p < 0.05$). $n = 48$; for each sample type, $n = 12$ divided into 3 pools of 4 samples each.

2.2. RNA Can Be Isolated from Extracellular Vesicles from Bowel Lavage Fluid and Can Be Used for Real-Time PCR

RNA can be isolated from EVs from BLF using TRI reagent LS (Table 2). Healthy samples presented an RNA concentration of 17.2–3311 ng/mL, low-risk samples presented a concentration of 46.7–460 ng/mL, high-risk samples presented a concentration of 9.5–2343 ng/mL, and cancer samples presented a concentration of 39.5–8242 ng/mL. The results show non-significant differences between groups.

Table 2. Concentration of extracellular vesicle RNA (ng/mL BLF), extracellular vesicle DNA (ng/mL BLF), extracellular vesicle protein (μ g/mL BLF), and direct protein from bowel lavage fluid (BLF protein; μ g/mL BLF) in healthy, low-risk, high-risk, and cancer samples. $n \geq 17$; values are represented as mean \pm SD. **S:** significant differences (p 0.000 for EV DNA; p 0.003 for BLF protein); **NS:** non-significant differences (p 0.431 for EV RNA; p 0.149 for EV protein), (Kruskal–Wallis; $p < 0.05$).

	Healthy	Low-Risk	High-Risk	Cancer	Kuskal–Wallis
ng/mL BLF of EV RNA	707 \pm 844	225 \pm 187	434 \pm 585	1791 \pm 2744	NS (p 0.431)
ng/mL BLF of EV DNA	1055 \pm 786	800 \pm 482	756 \pm 420	477 \pm 547	S (p 0.000)
μ g/mL BLF of EV Protein	21.7 \pm 17.1	14.0 \pm 9.12	18.0 \pm 12.1	15.5 \pm 12.2	NS (p 0.149)
μ g/mL BLF of BLF Protein	392 \pm 253	387 \pm 249	407 \pm 322	1487 \pm 2179	S (p 0.003)

This RNA can be used for gene expression determination by real-time PCR. The study of B2M expression levels (Table 3) presented non-significant differences between groups.

Table 3. B2M Ct and Tm values in healthy, low-risk, high-risk, and cancer samples determined by real-time PCR. Values are represented as mean \pm SD. **NS:** non-significant differences (p 0.108 for Ct values; p 0.522 for Tm values) (Ct values ANOVA, p < 0.05; Tm values Kruskal–Wallis, p < 0.05).

	Healthy	Low-Risk	High-Risk	Cancer	Statistics
Ct values	32.9 \pm 1.87	28.4 \pm 1.09	32.0 \pm 1.74	31.2 \pm 0.98	ANOVA: NS (p 0.108)
Tm values	81.5 \pm 0.09	81.4 \pm 0.04	81.5 \pm 0.01	81.5 \pm 0.02	Kruskal-Wallis: NS (p 0.522)

2.3. DNA Can Be Isolated from Extracellular Vesicles from Bowel Lavage Fluid

DNA can be isolated from EVs from BLF using TRI reagent LS (Table 2). Healthy samples presented a DNA concentration of 40.3–3213 ng/mL, low-risk samples presented a concentration of 332–2285 ng/mL, high-risk samples presented a concentration of 13.1–1852 ng/mL, and cancer samples presented a concentration of 67.6–2332 ng/mL. The results show significant differences between groups, with a lower DNA concentration in cancer than the other samples.

2.4. Western Blot Analyses of Proteins Isolated from Extracellular Vesicles from Bowel Lavage Fluid and Directly from Bowel Lavage Fluid

Proteins can be isolated from EVs from BLF using TRI reagent LS (Table 2). Healthy samples presented a protein concentration of 1.75–74.4 μ g/mL, low-risk samples presented a protein concentration of 5.10–31.3 μ g/mL, high-risk samples presented a protein concentration of 5.33–58.8 μ g/mL, and cancer samples presented a protein concentration of 1.60–41.6 μ g/mL. The results show non-significant differences between groups. In addition, proteins can be directly determined from BLF (Table 2). Healthy samples presented a protein concentration of 84.0–1184 μ g/mL, low-risk samples presented a protein concentration of 34.9–1302 μ g/mL, high-risk samples presented a protein concentration of 54.1–1395 μ g/mL, and cancer samples presented a protein concentration of 19.0–9994 μ g/mL. The results show significant differences between groups, with a higher BLF protein concentration in cancer samples than the other samples. Finally, these proteins can be studied by Western blot (Figure 5).

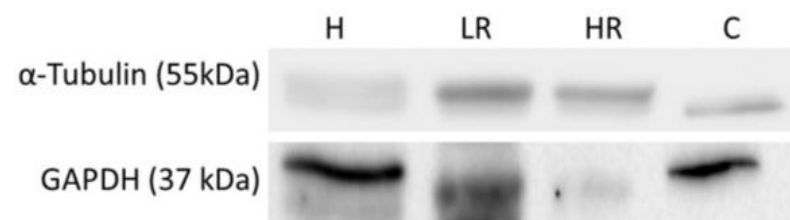


Figure 5. Representative bands and molecular weights of α -Tubulin and GAPDH expression levels directly determined in bowel lavage fluid by Western blot in healthy, low-risk, high-risk, and cancer samples. **H:** healthy samples; **LR:** low-risk samples; **HR:** high-risk samples; **C:** cancer samples.

3. Discussion

BLF has been demonstrated to have great potential as a research tool [16], since it has been used in various diseases, such as for enzyme research on colorectal polyps [21], for endoscopic screening for food allergies [22], CRC diagnosis [19], and molecular screening of inflammatory bowel diseases [23]. However, BLF is a rarely used sample with type with considerable potential for research [24] due to its proximity to the injured area and because this sample type does not cause extra discomfort to patients undergoing colonoscopy, since bowel preparation is the same as that required for a colonoscopy [16]. Nowadays, the use of EVs in liquid samples, such as saliva, amniotic fluid, breast milk, seminal liquid,

nasal secretion, cerebrospinal fluid, lymph node secretion, urine, plasma, serum, placenta, bronchoalveolar fluid, synovial liquid, bile fluid, and ascites [9,25,26], is widespread, but there are no studies on EVs from BLF.

Despite this lack of studies, our results show that EVs can be isolated from BLF, as demonstrated by AFM and TEM results. Moreover, the NTA results demonstrate that these EVs presented a regular size, considering that exosomes have a diameter of 30–100 nm and microvesicles have a diameter of $100 \text{ nm}^{-1} \mu\text{m}$ [27]. The size difference between TEM and NTA results can be attributed to the dehydrating conditions to which EVs are subjected during fixation for TEM analysis [8], in addition to the presence of a sufficient concentration of EVs in BLF, taking into account that in urine, the EV concentration determined by NTA is 1.00×10^{10} [28], whereas in CRC patient blood, the EV concentration is $1.29 \times 10^9 \pm 9.92 \times 10^8$ [29]. Finally, CD9 and CD63 expression, which are two tetraspanins considered EV biomarkers [8], has been found in EVs isolated from BLF. Altogether, these results suggest that EVs can be isolated from BLF.

EV cargo can be determined and studied, since RNA can be used to study gene expression levels [30], DNA mutations can be determined [31], and protein expression levels can be analyzed by Western blot and liquid chromatography–tandem mass spectrometry [29,32–34]. However, given the nature of our sample, it was necessary to confirm the content of these EVs from BLF as a feasible tool for CRC study. The RNA concentration results presented no differences between groups and demonstrated that the RNA concentration and quality are sufficient to determine gene expression levels, as can be seen in the *B2M* expression levels, which is an often used housekeeping gene due to its high and constant expression [35]. In addition, the protein concentration results in EVs did not present differences between groups, indicating an adequate concentration and quality for use for determination of protein expression levels, as can be seen in the CD9 and CD63 expression levels. However, the DNA concentration was lower in cancer samples. In contrast to our results, Bryzgunova and collaborators demonstrated that EVs of urine samples from patients with prostate cancer presented higher DNA concentrations than healthy samples [36], although these variances could be attributed to the different type of sample and cancer from which EVs were isolated. Despite this, DNA from EVs can be studied [31], and our results indicate a sufficient concentration of DNA for use, as shown in studies by Thakur and collaborators, who found that DNA concentration in serum EVs was $10.59 \pm 13.19 \text{ ng/mL}$ [37], or in studies by Choi et al., who determined that the amount of DNA in plasma EVs ranged from 0.1 to 2.48 ng [38]. Finally, protein expression levels can be directly determined in BLF samples, as shown in studies by Kayazawa and collaborators, in which lactoferrin, polymorphonuclear neutrophil elastase, myeloperoxidase, and lysozyme concentrations were determined in BLF samples by ELISA [39]. BLF protein concentrations in cancer samples; however Al-Muhtaseb and Bel'skaya demonstrated that in saliva from breast cancer patients, the total protein concentration was lower than that in control patients [40,41]; however these differences can be attributed to the distinct sample and cancer types. Nevertheless, BLF protein presented an optimal concentration for use to determine protein expression levels, as shown by the α -Tubulin and GAPDH expression levels results, which are often-used proteins for Western blot analysis due to their high expression [42–44], demonstrating that this protein from BLF is suitable for Western blot determinations.

4. Materials and Methods

4.1. Patients and Sample Acquisition

A total of 170 patients (83 females with an average age 63.6 ± 11.4 and 87 males with an average age 63.8 ± 11.1) were included to carry out the study. Patients of both sexes received the a patient's information sheet about the research project, and they signed an informed consent according to the "World Medical Association Declaration of Helsinki" for medical research involving humans. The study was approved by the *Comité d'Ètica de la Investigació de les Illes Balears* (IB 3833/19 PI).

Days prior to colonoscopy, patients received the information about colonoscopy and an information sheet about the research project. Then, 48 h before colonoscopy, patients were required to reduce fiber, fat, and gas intake, and 8 h before colonoscopy, patients drank 3 L of a polyethylene glycol solution to clean the bowel lumen. Colonoscopies were performed in the endoscopy unit at the *Hospital Comarcal d'Inca* with anesthetic sedation. BLF samples were recollected with saline solution (0.9% NaCl) applied directly to the injury area in the mucosa through an endoscopic flushing channel, then aspirated and retained in the polyp-trapping basket of the endoscope in order to avoid mixture with fluids from non-affected zones. The samples were stored at $-80\text{ }^{\circ}\text{C}$ and divided according to pathology: without pathology (healthy samples; $n = 43$), with polyps (divided into low- and high-risk of suffering from neoproliferative processes; $n = 58$ and $n = 29$, respectively), and cancer samples ($n = 40$). Low-risk samples correspond to 1 or 2 tubular adenomatous lesions with low-grade dysplasia and serrated lesions without dysplasia—all less than 10 mm; high-risk samples correspond to 3 or more tubular adenomatous lesions with low-grade dysplasia less than 10 mm, at least one adenomatous lesion with a villous component, high-grade dysplasia of more than 10 mm, and at least one serrated lesion with dysplasia or more than 10 mm [45].

4.2. Extracellular Vesicles Isolation by Ultracentrifugation

BLF samples were centrifuged for 15 min at $2000\times g$ and $4\text{ }^{\circ}\text{C}$ to eliminate debris and cellular components. Then, 4 mL of supernatant was separated, and 8 mL of sterile PBS $1\times$ (500 mM NaCl, 167 mM $\text{NaH}_2\text{PO}_4\cdot 2\text{H}_2\text{O}$, 333 mM Na_2HPO_4) pH 7.5 was added. Next, this mix was centrifuged at $2000\times g$ for 10 min and $4\text{ }^{\circ}\text{C}$ in order to remove the remaining debris. Finally, supernatants were centrifuged at $2000\times g$ for 10 min at $4\text{ }^{\circ}\text{C}$ to eliminate large particles. Subsequently, supernatants were centrifuged for 1 h at $4\text{ }^{\circ}\text{C}$ and $100,000\times g$ in order to precipitate EVs. The resulting pellets containing EVs were resuspended in 100 μL of sterile PBS $1\times$ pH 7.5.

4.3. Atomic Force Microscopy (AFM)

First 50 μL of EV resuspension from healthy and cancer samples was added to a freshly cleaved muscovite mica surface (NanoAndMore GmbH, Wetzlar, Germany) for 10 min, washed with 2.5 mL of deionized water, and dried with nitrogen. Then, EVs were observed under an atomic force microscope (Veeco, Oyster Bay, NY, USA) in tapping mode with aluminum-coated silicon probe tips (HQ:NSC35/Al BS, Mikromasch, Lady's Island, SC, USA). The height and amplitude of the samples were recorded at $512\text{ pixels}\times 512\text{ pixels}$ at a scanning rate of 1 Hz and processed with NanoScope Image Software (v5.10, Veeco, Metrology, NY, USA).

4.4. Transmission Electron Microscopy (TEM)

EV resuspensions were observed by TEM following the protocol of Forteza-Genestra et al. [46]. Briefly, EV resuspensions were mixed 1:1 with 4% formaldehyde (F8775, Sigma-Aldrich, Darmstadt, Germany), and 10 μL of this mix was fixed on copper formvar-carbon-coated grids (Iesmat, Madrid, Spain) for 20 min. Then, grids were washed with PBS three times and incubated with 1% glutaraldehyde (G-7526, Sigma-Aldrich, Darmstadt, Germany) for 5 min. Finally, grids were washed with deionized water eight times. To visualize samples, grids were stained with 2% phosphotungstic acid for 1 min, then washed with deionized water for 1 min, and finally, air-dried. Images were taken with a Talos F200i transmission electron microscope (ThermoFisher, Madrid, Spain) at 20 kV and 50 kV.

4.5. Nanoparticle Tracking Analysis (NTA)

EV size distribution and particle concentration were analyzed using a Nanosight NS3000 (Malvern Instruments, Malvern, PA, USA). Samples were diluted 1:1000 in a final volume of 1 mL before analysis. Then, samples were passed through the chamber in vivo

and recorded three times for 1 min each with a laser at a wavelength of 532 nm and an sCMOS camera. Finally, data were analyzed with NTA 3.2 Dev Build 3.2.16 software.

4.6. RNA Isolation, Reverse Transcription, and Real-Time PCR

Total RNA from EVs was isolated using TRI reagent LS[®] (T3934, Sigma-Aldrich) following the manufacturer's protocol. Briefly, TRI reagent was added to EV samples and left for 5 min at room temperature. Then, chloroform was added and incubated for 15 min at room temperature, followed by centrifugation at 12,000× *g* for 15 min at 4 °C. After centrifugation, three phases were differentiated. Isopropanol was added to the aqueous phase and incubated overnight at −20 °C for better RNA precipitation. After the incubation, samples were centrifuged at 12,000× *g* for 8 min at 4 °C, and the resulting pellets were washed with frozen 75% ethanol and centrifuged at 7500× *g* for 5 min at 4 °C. The supernatants were discarded, and the pellets were dried under vacuum. Finally, RNA was resuspended in 20 µL of RNase-free water and quantified using a BIO-TEK PowerWave XS spectrophotometer at wavelength of 260 nm. The RNA quality was checked by a 260/280 ratio.

The obtained RNA was mixed to create two or three RNA pools for each sample type to better represent each sample type, avoiding the particular patient characteristics. Then, 300 ng of the total RNA was reverse-transcribed to cDNA. First, a denaturalization at 90 °C for 1 min was applied to RNA samples. Next, the reverse transcription reagents were added to the sample (50 µM random hexamers (10609275, Fisher Scientific, Madrid, Spain), 2.5 mM dNTPs mix (100 mM dGTP solution 10218-014, 100 mM dTTP solution 10219-012, 100 mM dATP solution 10216-018, and 100 mM dCTP solution 10217-016; Fisher Scientific), 20 U/µL RNase Out (10615995, Fisher Scientific), 0.1 M DTT, buffer 5×, and 200 U/µL M-MLV (10338842, Fisher Scientific)) and incubated at 25 °C for 10 min, then at 37 °C for 50 min, 70 °C for 15 min, and finally, at 4 °C. cDNA aliquots were frozen at −20 °C after 1/10 dilution in RNase-free water.

A LightCycler 480 System II rapid thermal cycler (Roche Diagnostics, Basel, Switzerland) with SYBR Green technology was used to carry out the real-time PCR, following the manufacturer's protocol. The expression of beta-2-microglobulin (*B2M*) was analyzed (forward primer: 5'-TTT CAT CCA TCC gAC ATT GA-3'; reverse primer: 5'-Cgg CAg gCA TAC TCA TCT TT-3'; accession number: NM_004048). The first step in the amplification program was preincubation for cDNA denaturation at 95 °C for 5 min, followed by 50 cycles of denaturation at 95 °C for 10 s, annealing at 54 °C for 10 s, and elongation at 72 °C for 12 s. Finally, melting was applied at 95 °C for 5 s, followed by 65 °C for 1 min, and 97 °C continuously until cooling at 40 °C.

4.7. DNA Isolation and Quantification

DNA from EVs was isolated using TRI reagent LS[®] (T3934, Sigma-Aldrich) following the manufacturer's protocol. Briefly, after the formation of three phases, 100% ethanol was added to the interphase and organic phase, mixed, and incubated for 3 min at room temperature. Next, samples were centrifuged at 2000× *g* for 5 min at 4 °C, and the supernatants were saved in a new tube for protein isolation. The pellets were mixed with 0.1 M trisodium citrate in 10% ethanol and incubated for 30 min at room temperature, followed by centrifugation at 2000× *g* for 5 min at 4 °C; this step was repeated twice. Then, pellets were washed with 75% ethanol and incubated for 20 min at room temperature, followed by centrifugation at 2000× *g* for 5 min at 4 °C. The resulting pellets were dried at room temperature for 15 min and resuspended in 100 µL of 8 mM NaOH. Finally, centrifugation was performed at 12,000× *g* for 10 at 4 °C, and supernatants were saved. Finally, DNA was quantified using a BIO-TEK PowerWave XS spectrophotometer at a wavelength of 260 nm. The DNA quality was checked by a 260/280 ratio.

4.8. Protein Isolation and Quantification

Protein from EVs was isolated using TRI reagent LS[®] (T3934, Sigma-Aldrich) following the manufacturer's protocol. Briefly, the supernatants saved during DNA isolation were incubated with isopropanol at room temperature for 10 min and centrifuged at 12,000× *g* for 10 min at 4 °C. The supernatants were discarded, and precipitates were washed three times with 0.3 M guanidine hydrochloride in 95% ethanol, incubated at room temperature for 20 min, and centrifuged at 7500× *g* for 5 min at 4 °C. After three washes, 100% ethanol was added to the precipitates and incubated at room temperature for 20 min, followed by centrifugation at 7500× *g* for 5 min at 4 °C. Next, protein pellets were air-dried for 15 min, dissolved in 100 µL of 1% SDS, and incubated overnight at −20 °C. Then, samples were centrifuged at 10,000× *g* for 10 min at 4 °C, and the supernatant was transferred to a new tube. Finally, protein was quantified by a Pierce[®] BCA protein assay kit (10741395, Fisher Scientific) following the manufacturer's protocol.

Protein from BLF samples was directly quantified by the Bradford method [47].

4.9. Western Blot

For all SDS-PAGE assays carried out for EV-protein, 5 µg of total protein was loaded; for all SDS-PAGE assays carried out for BLF-protein, 10 µg of total protein was loaded. First, loading buffer (0.25 M Tris-HCl (pH 6.8), 10% SDS, 40% glycerol, and 0.1% bromophenol blue; for BLF protein, 10% fresh β-mercaptoethanol was added) was added to each sample. Then, samples were boiled for 5 min. Protein was separated by electrophoresis on 12% acrylamide/bisacrylamide (30/1) gels. Next, proteins were electrotransferred onto a 0.2 µm nitrocellulose membrane (Bio-Rad Laboratories, Hercules, CA, USA) using a trans-blot turbo transfer system (Bio-Rad Laboratories, CA, USA). After electrotransfer, membranes were incubated with Ponceau staining for equal sample loading validation. Then, membranes were blocked with 5% non-fat powdered milk in Tris-buffered saline 0.05%–Tween 20 pH 7.6 (TBS-Tween) for 1 h at room temperature under agitation. After blocking, membranes were washed with TBS-Tween and incubated with primary antibody (5% BSA and 0.05% sodium azide in TBS-Tween) overnight at 4 °C under agitation. The following primary antibodies used and dilutions were used: 1:500 α-tubulin (sc-5286, Santa Cruz Biotechnology, Dallas, TX, USA), 1:1000 GAPDH (sc-365062, Santa Cruz Biotechnology, Dallas, TX, USA), 1:1000 CD9 (Ts9, 10626D, ThermoFisher, Spain), and 1:5000 CD63 (Ts63, ab59479, Abcam, Boston, MA, USA). After primary incubation, membranes were washed with TBS-Tween and incubated with horseradish-peroxidase-conjugated secondary antibody and 1:10,000 anti-mouse antibody (A9044, Sigma-Aldrich, Darmstadt, Germany) in 2% non-fat powdered milk in TBS-Tween for 1 h at room temperature under agitation. Then, membranes were washed with TBS-Tween, and TBS and immunoreactivity was detected by an Inmun-Star[®] Western chemiluminescence kit and Western blotting detection system (Bio-Rad Laboratories, Hercules, CA, USA). Chemidoc Imaging System (Bio-Rad Laboratories, Hercules, CA, USA) was used to acquire the chemiluminescent signal.

4.10. Statistical Analysis

Statistical Program for the Social Sciences software for Windows (SPSS, version 25.0; SPSS Inc., Chicago, IL, USA) was used to perform all statistical analyses. First, a boxplot was used to discard the outliers. Then, a normality study was performed using the Shapiro-Wilk test; for parametric results (EV size, EV concentration, and *B2M* Ct values) a one-way ANOVA was used to analyze differences between groups; for non-parametric results (RNA, DNA, EV and BLF protein concentrations, and *B2M* Tm values), the Kruskal–Wallis test was used to analyze differences between groups. All determinations were made with minimal statistical significance at $p < 0.05$, and all results are presented as mean ± SD.

5. Conclusions

In conclusion, bowel lavage fluid is a sample that must be taken into account in the study of colorectal cancer due to its proximity to the tumor. In addition, the extracellular

vesicles isolated from this sample type can be useful as a source of colorectal cancer biomarkers, considering that EV content can be determined and studied by different molecular biology techniques. The possibility of studying the content of extracellular vesicles isolated from bowel lavage fluid could improve knowledge of colorectal cancer, in addition to identifying new biomarkers (for diagnosis, prognosis, and monitoring of the disease), which could be extrapolated to non-invasive samples, such as stool samples. Nevertheless, further investigation of bowel lavage fluid and, specifically the extracellular vesicles from such samples, is necessary to better understand the mechanism whereby EVs are released from cancer cells and the role that their content plays in cancer initiation, progression, and metastasis.

Author Contributions: Conceptualization, M.A.-C., J.R., P.R., D.G.P. and J.O.; methodology, M.A.-C., J.R., M.G.T.-G., M.F., P.R., D.G.P. and J.O.; validation, M.A.-C., P.R., D.G.P. and J.O.; formal analysis, M.A.-C., P.R., D.G.P. and J.O.; investigation, J.R., D.G.P. and J.O.; resources, J.R. and P.R.; data curation, M.A.-C., P.R., D.G.P. and J.O.; writing—original draft preparation, M.A.-C.; writing—review and editing, P.R., D.G.P. and J.O.; supervision, D.G.P. and J.O.; project administration, P.R. and D.G.P.; funding acquisition, J.R. and P.R. All authors have read and agreed to the published version of the manuscript.

Funding: This research was funded by a fundraising from *Fundació Universitat Empresa de les Illes Balears* (FUEIB), *Proyecto del Hospital Comarcal de Inca y la Universidad de las Islas Baleares* (CINUIB).

Institutional Review Board Statement: This study was conducted in accordance with the Declaration of Helsinki and approved by the *Comité d'ètica de la Investigació de les Illes Balears* (IB 3833/19 PI, 21 March 2019).

Informed Consent Statement: Informed consent was obtained from all subjects involved in the study. Written informed consent was obtained from the patient(s) to publish this paper.

Data Availability Statement: The data presented in this study are available in this article.

Acknowledgments: The authors thank Eduardo Iyo and Silvia Patricia Ortega from the *Servicio de Aparato Digestivo del Hospital Comarcal de Inca* for the acquisition of the bowel lavage fluid samples; Joan Cifre from the *Serveis Científicotècnics de la Universitat de les Illes Balears* for assistance and the acquisition of the atomic force microscopy images; Antonio Busquets Bisbal from the *Serveis Científicotècnics de la Universitat de les Illes Balears (Fons Europeu de Desenvolupament Regional, Una manera de fer Europa)* for assistance and the acquisition of the transmission electronic microscopy images; the Cell Therapy and Tissue Engineering (TERCIT) group from *Institut Universitari d'Investigació en Ciències de la Salut (IUNICS—Universitat de les Illes Balears)*, especially Maria Antònia Forteza Genestra, for their help with the isolation and characterization of the extracellular vesicles.

Conflicts of Interest: The authors declare no conflict of interest. The funders had no role in the design of the study; in the collection, analyses, or interpretation of data; in the writing of the manuscript; or in the decision to publish the results.

References

1. Ferlay, J.; Ervik, M.; Lam, F.; Colombet, M.; Mery, L.; Piñeros, M.; Znaor, A.; I Soerjomataram, B.F. Global Cancer Observatory: Cancer Today. Available online: <https://gco.iarc.fr/today> (accessed on 1 December 2021).
2. Cheshomi, H.; Matin, M.M. Exosomes and their importance in metastasis, diagnosis, and therapy of colorectal cancer. *J. Cell. Biochem.* **2019**, *120*, 2671–2686. [CrossRef] [PubMed]
3. Mammes, A.; Pasquier, J.; Mammes, O.; Conti, M.; Douard, R.; Loric, S. Extracellular vesicles: General features and usefulness in diagnosis and therapeutic management of colorectal cancer. *World J. Gastrointest. Oncol.* **2021**, *13*, 1561–1599. [CrossRef] [PubMed]
4. Świdarska, M.; Choromańska, B.; Dąbrowska, E.; Konarzewska-Duchnowska, E.; Choromanska, K.; Szczurko, G.; Mysliwiec, P.; Dada, J.; Ladny, J.R.; Zwierz, K. The diagnostics of colorectal cancer. *Contemp Oncol.* **2014**, *18*, 1–6. [CrossRef]
5. Trelles Guzman, M.G.; Novella Duran, M.T.; Heredia Centeno, M.L.; Florido Garcia, M.; Sanchez-Contador Escudero, M.d.C.; Iyo Miyashiro, E.Y.; Ortega Moya, S.P.; Miro Viamonte, E.; Artigues Vives, G.; Gelabert Zorxona, J.; et al. Result of the first two rounds of the colorectal cancer screening program in the Balearic Islands (Spain). *Gastroenterol. Hepatol.* **2022**, *45*, 55–57. [PubMed]
6. Trelles, M.; Roca, P.; Sastre-Serra, J.; Florido, M.; Iyo, E.; Patricia Ortega, S.; Crespi, M.A.; Sanchez-Contador, C.; Miró, E.; Artigues, G.; et al. Búsqueda de un patrón clínico para la predicción de colonoscopia patológica en los pacientes participantes de las 2 primeras rondas del Programa de Detección precoz de Cáncer Colorrectal del Hospital Comarcal de Inca. *Acad. J. Health Sci.* **2023**, *38*, 76–83. [CrossRef]

7. Vega, P.; Valentín, F.; Cubiella, J. Colorectal cancer diagnosis: Pitfalls and opportunities. *World J. Gastrointest. Oncol.* **2015**, *7*, 422–433. [[CrossRef](#)] [[PubMed](#)]
8. Théry, C.; Witwer, K.W.; Aikawa, E.; Alcaraz, M.J.; Anderson, J.D.; Andriantsitohaina, R.; Antoniou, A.; Arab, T.; Archer, F.; Atkin-smith, G.K.; et al. Minimal information for studies of extracellular vesicles 2018 (MISEV2018): A position statement of the International Society for Extracellular Vesicles and update of the MISEV2014 guidelines. *J. Extracell. Vesicles* **2018**, *7*, 1535750. [[CrossRef](#)]
9. Hooten, N.N.; Byappanahalli, A.M.; Vannoy, M.; Omoniyi, V.; Evans, M.K. Influences of age, race, and sex on extracellular vesicle characteristics. *Theranostics* **2022**, *12*, 4459–4476. [[CrossRef](#)]
10. Ruiz-López, L.; Blancas, I.; Garrido, J.M.; Mut-Salud, N.; Moya-Jódar, M.; Osuna, A.; Rodríguez-Serrano, F. The role of exosomes on colorectal cancer: A review. *J. Gastroenterol. Hepatol.* **2018**, *33*, 792–799. [[CrossRef](#)]
11. Bracci, L.; Lozupone, F.; Parolini, I. The role of exosomes in colorectal cancer disease progression and response to therapy. *Cytokine Growth Factor Rev.* **2020**, *51*, 84–91. [[CrossRef](#)]
12. Zhou, J.; Li, X.L.; Chen, Z.R.; Chng, W.J. Tumor-derived exosomes in colorectal cancer progression and their clinical applications. *Oncotarget* **2017**, *8*, 100781–100790. [[CrossRef](#)] [[PubMed](#)]
13. Xiao, Y.; Zhong, J.; Zhong, B.; Huang, J.; Jiang, L.; Jiang, Y.; Yuan, J.; Sun, J.; Dai, L.; Yang, C.; et al. Exosomes as potential sources of biomarkers in colorectal cancer. *Cancer Lett.* **2020**, *476*, 13–22. [[CrossRef](#)] [[PubMed](#)]
14. Siveen, K.S.; Raza, A.; Ahmed, E.I.; Khan, A.Q.; Prabhu, K.S.; Kuttikrishnan, S.; Mateo, J.M.; Zayed, H.; Rasul, K.; Azizi, F.; et al. The Role of Extracellular Vesicles as Modulators of the Tumor Microenvironment, Metastasis and Drug Resistance in Colorectal Cancer. *Cancers* **2019**, *11*, 746. [[CrossRef](#)] [[PubMed](#)]
15. Pap, E. The Role of Microvesicles in Malignancies. *Adv. Exp. Med. Biol.* **2011**, *714*, 183–199. [[CrossRef](#)] [[PubMed](#)]
16. Rocker, J.M.; DiPalma, J.A.; Pannell, L.K. Rectal Effluent as a Research Tool. *Dig. Dis. Sci.* **2015**, *60*, 24–31. [[CrossRef](#)] [[PubMed](#)]
17. Heinzlmann, M.; Neynaber, S.; Heldwein, W.; Folwaczny, C. K-ras and p53 mutations in colonic lavage fluid of patients with colorectal neoplasias. *Digestion* **2001**, *63*, 229–233. [[CrossRef](#)]
18. Potter, M.A.; Morris, R.G.; Ferguson, A.; Wyllie, A.H. Detection of Mutations Associated with Colorectal Cancer in DNA From Whole-Gut Lavage Fluid. *J. Natl. Cancer Inst.* **1998**, *90*, 623–626. [[CrossRef](#)]
19. Harada, T.; Yamamoto, E.; Yamano, H.O.; Nojima, M.; Maruyama, R.; Kumegawa, K.; Ashida, M.; Yoshikawa, K.; Kimura, T.; Harada, E.; et al. Analysis of DNA methylation in bowel lavage fluid for detection of colorectal cancer. *Cancer Prev. Res.* **2014**, *7*, 1002–1010. [[CrossRef](#)]
20. Park, Y.S.; Kim, D.S.; Cho, S.W.; Park, J.W.; Jeon, S.J.; Moon, T.J.; Kim, S.H.; Son, B.K.; Oh, T.J.; An, S.; et al. Analysis of syndecan-2 methylation in bowel lavage fluid for the detection of colorectal neoplasm. *Gut Liver* **2018**, *12*, 508–515. [[CrossRef](#)]
21. Uno, Y.; Saitoh, H.; Ying, H.; Tamai, Y.; Ono, F.; Yoshiike, M.; Munakata, A.; Yoshida, Y. Enzymes in Intestinal Juice from Patients with Liver Diseases and Colon Polyps: Measurement of Bilirubin, Alkaline Phosphatase, Aspartate Aminotransferase and Lactate Dehydrogenase. *J. Exp. Med.* **1996**, *178*, 163–168. [[CrossRef](#)]
22. Schwab, D.; Raithel, M.; Klein, P.; Winterkamp, S.; Weidenhiller, M.; Radespiel-Troeger, M.; Hochberger, J.; Hahn, E.G. Immunoglobulin E and Eosinophilic Cationic Protein in Segmental Lavage Fluid of the Small and Large Bowel Identify Patients with Food Allergy. *Am. J. Gastroenterol.* **2001**, *96*, 508–514. [[CrossRef](#)] [[PubMed](#)]
23. Heinzlmann, M.; Lang, S.M.; Neynaber, S.; Reinshagen, M.; Emmrich, J.; Stratakis, D.F.; Heldwein, W.; Wiebecke, B.; Loeschke, K. Screening for p53 and K-ras mutations in whole-gut lavage in chronic inflammatory bowel disease. *Eur. J. Gastroenterol. Hepatol.* **2002**, *14*, 1061–1066. [[CrossRef](#)] [[PubMed](#)]
24. Alorda-Clara, M.; Torrens-Mas, M.; Morla-Barcelo, P.M.; Martinez-Bernabe, T.; Sastre-Serra, J.; Roca, P.; Pons, D.G.; Oliver, J.; Reyes, J. Use of Omics Technologies for the Detection of Colorectal Cancer Biomarkers. *Cancers* **2022**, *14*, 817. [[CrossRef](#)] [[PubMed](#)]
25. Andreu, Z.; Yáñez-mó, M. Tetraspanins in extracellular vesicle formation and function. *Front. Immunol.* **2014**, *5*, 1–12. [[CrossRef](#)]
26. Dilsiz, N. Role of exosomes and exosomal microRNAs in cancer. *Futur. Sci.* **2020**, *6*, FSO465. [[CrossRef](#)]
27. György, B.; Szabó, T.G.; Pásztói, M.; Pál, Z.; Misják, P.; Aradi, B.; László, V.; Pállinger, É.; Pap, E.; Kittel, Á.; et al. Membrane vesicles, current state-of-the-art: Emerging role of extracellular vesicles. *Cell. Mol. Life Sci.* **2011**, *68*, 2667–2688. [[CrossRef](#)]
28. Van der Pol, E.; Coumans, F.A.Q.; Grootemaat, A.E.; Gardiner, C.; Sargent, I.L.; Harrison, P.; Sturk, A.; Van Leeuwen, T.G.; Nieuwland, R. Particle size distribution of exosomes and microvesicles determined by transmission electron microscopy, flow cytometry, nanoparticle tracking analysis, and resistive pulse sensing. *J. Thromb. Haemost.* **2014**, *12*, 1182–1192. [[CrossRef](#)]
29. Bar-Sela, G.; Cohen, I.; Avisar, A.; Loven, D.; Aharon, A. Circulating blood extracellular vesicles as a tool to assess endothelial injury and chemotherapy toxicity in adjuvant cancer patients. *PLoS ONE* **2020**, *15*, e0240994. [[CrossRef](#)]
30. Cha, B.S.; Park, K.S.; Park, J.S. Signature mRNA markers in extracellular vesicles for the accurate diagnosis of colorectal cancer. *J. Biol. Eng.* **2020**, *14*, 1–9. [[CrossRef](#)]
31. Li, X.; Wang, Q.; Wang, R. Roles of Exosome Genomic DNA in Colorectal Cancer. *Front. Pharmacol.* **2022**, *13*, 923232. [[CrossRef](#)]
32. Kowal, E.J.K.; Ter-ovanesyan, D.; Regev, A.; Church, G.M. Extracellular Vesicle Isolation and Analysis by Western Blotting. *Methods Mol. Biol.* **2017**, *1660*, 143–152. [[CrossRef](#)]
33. Lee, C.; Im, E.; Moon, P.; Baek, M. Discovery of a diagnostic biomarker for colon cancer through proteomic profiling of small extracellular vesicles. *BMC Cancer* **2018**, *18*, 1058. [[CrossRef](#)] [[PubMed](#)]

34. Yunusova, N.V.; Zambalova, E.A.; Patysheva, M.R.; Elena, S.; Afanas, S.G.; Cheremisina, O.V.; Grigor, A.E.; Tamkovich, S.N.; Kondakova, I. V Exosomal Protease Cargo as Prognostic Biomarker in Colorectal Cancer. *Asian Pac. J. Cancer Prev.* **2021**, *22*, 861–869. [[CrossRef](#)] [[PubMed](#)]
35. Singh, A.i.; Patnam, S.; Koyyada, R.; Samal, R.; Alvi, S.B.; Satyanaryana, G.; Andrews, R.; Panigrahi, A.K.; Rengan, A.K.; Mudigonda, S.S.; et al. Identifying stable reference genes in polyethylene glycol precipitated urinary extracellular vesicles for RT-qPCR-based gene expression studies in renal graft dysfunction patients. *Transpl. Immunol.* **2022**, *75*, 101715. [[CrossRef](#)] [[PubMed](#)]
36. Bryzgunova, O.E.; Zaripov, M.M.; Skvortsova, T.E.; Lekchnov, E.A.; Grigor'eva, A.E.; Zaporozhchenko, I.A.; Morozkin, E.S.; Ryabchikova, E.I.; Yurchenko, Y.B.; Voitsitskiy, V.E.; et al. Comparative study of extracellular vesicles from the urine of healthy individuals and prostate cancer patients. *PLoS ONE* **2016**, *11*, e0157566. [[CrossRef](#)]
37. Thakur, K.; Singh, M.S.; Feldstein-davydova, S.; Hannes, V.; Hershkovitz, D.; Tsurriel, S. Extracellular Vesicle-Derived DNA vs. CfDNA as a Biomarker for the Detection of Colon Cancer. *Genes* **2021**, *12*, 1171. [[CrossRef](#)]
38. Choi, J.; Cho, H.Y.; Jeon, J.; Kim, H.-A.; Han, Y.D.; Ahn, J.B.; Wortzel, I.; Lyden, D.; Kim, H.S. Detection of circulating KRAS mutant DNA in extracellular vesicles using droplet digital PCR in patients with colon cancer. *Front. Oncol.* **2022**, *12*, 1067210. [[CrossRef](#)]
39. Kayazawa, M.; Saitoh, O.; Kojima, K.; Nakagawa, K.; Tanaka, S.; Tabata, K.; Matsuse, R.; Uchida, K.; Hoshimoto, M.; Hirata, I.; et al. Lactoferrin in Whole Gut Lavage Fluid as a Marker for Disease Activity in Inflammatory Bowel Disease: Comparison with Other Neutrophil-Derived Proteins. *Am. J. Gastroenterol.* **2002**, *97*, 360–369. [[CrossRef](#)]
40. Al-Muhtaseb, S.I. Serum and saliva protein levels in females with breast cancer. *Oncol. Lett.* **2014**, *8*, 2752–2756. [[CrossRef](#)]
41. Bel'Skaya, L.V.; Sarf, E.A.; Solomatina, D.V.; Kosenok, V.K. Metabolic Features of Saliva in Breast Cancer Patients. *Metabolites* **2022**, *12*, 166. [[CrossRef](#)]
42. Weldon, S.; Ambroz, K.; Schutz-geschwender, A.; Olive, D.M. Near-infrared fluorescence detection permits accurate imaging of loading controls for Western blot analysis. *Anal. Biochem.* **2008**, *375*, 156–158. [[CrossRef](#)] [[PubMed](#)]
43. Lee, H.; Jo, J.; Hong, H.; Kim, K.K.; Park, J.; Cho, S.; Park, C. State-of-the-art housekeeping proteins for quantitative western blotting: Revisiting the first draft of the human proteome. *Proteomics* **2016**, *16*, 1863–1867. [[CrossRef](#)] [[PubMed](#)]
44. Tobias, I.S.; Lazauskas, K.K.; Arevalo, J.A.; Bagley, J.R.; Brown, L.E.; Galpin, A.J. Fiber type-specific analysis of AMPK isoforms in human skeletal muscle: Advancement in methods via capillary nanoimmunoassay. *J. Appl. Physiol.* **2018**, *124*, 840–849. [[CrossRef](#)]
45. Mangas-sanjuan, C.; Jover, R.; Cubiella, J.; Marzo-Castillejo, M.; Balaguer, F.; Bessa, X.; Bujanda, L.; Bustamante, M.; Castells, A.; Diaz-Tasende, J.; et al. Vigilancia tras resección de pólipos de colon y de cáncer colorrectal. Actualización 2018. *Gastroenterol. Hepatol.* **2019**, *42*, 188–201. [[CrossRef](#)]
46. Forteza-Genestra, M.A.; Antich-Rosselló, M.; Calvo, J.; Gayà, A.; Monjo, M.; Ramis, J.M. Purity Determines the Effect of Extracellular Vesicles Derived from Mesenchymal Stromal Cells. *Cells* **2020**, *9*, 422. [[CrossRef](#)] [[PubMed](#)]
47. Bradford, M.M. A rapid and sensitive method for the quantitation of microgram quantities of protein utilizing the principle of protein-dye binding. *Anal. Biochem.* **1976**, *72*, 248–254. [[CrossRef](#)]

Disclaimer/Publisher's Note: The statements, opinions and data contained in all publications are solely those of the individual author(s) and contributor(s) and not of MDPI and/or the editor(s). MDPI and/or the editor(s) disclaim responsibility for any injury to people or property resulting from any ideas, methods, instructions or products referred to in the content.

Manuscript 4

Analysis of miRNAs and mRNAs expression in extracellular vesicles from bowel lavage fluid in colorectal cancer patients.

Manuscript.

**High Concentrations of Genistein Decrease Cell Viability Depending on Oxidative Stress and Inflammation in
Colon Cancer Cell Lines.**

Alorda-Clara, M., Torrens-Mas, M., Morla-Barcelo, P. M., Roca, P., Sastre-Serra, J., Pons, D. G., & Oliver, J. (2022).
International Journal of Molecular Sciences, 23(14), 7526.



Article

High Concentrations of Genistein Decrease Cell Viability Depending on Oxidative Stress and Inflammation in Colon Cancer Cell Lines

Marina Alorda-Clara ^{1,2}, Margalida Torrens-Mas ^{1,2,3}, Pere Miquel Morla-Barcelo ¹, Pilar Roca ^{1,2,4}, Jorge Sastre-Serra ^{1,2,4}, Daniel Gabriel Pons ^{1,2,*} and Jordi Oliver ^{1,2,4}

- ¹ Grupo Multidisciplinar de Oncología Traslacional, Institut Universitari d'Investigació en Ciències de la Salut (IUNICS), Universitat de les Illes Balears, E-07122 Palma de Mallorca, Illes Balears, Spain; marina.alorda@uib.es (M.A.-C.); margalida.torrens@ssib.es (M.T.-M.); pere.morla@uib.es (P.M.M.-B.); pilar.roca@uib.es (P.R.); jorge.sastre@uib.es (J.S.-S.); jordi.oliver@uib.es (J.O.)
- ² Instituto de Investigación Sanitaria Illes Balears (IdISBa), Hospital Universitario Son Espases, Edificio S, E-07120 Palma de Mallorca, Illes Balears, Spain
- ³ Translational Research in Aging and Longevity (TRIAL) Group, Instituto de Investigación Sanitaria Illes Balears (IdISBa), E-07120 Palma de Mallorca, Illes Balears, Spain
- ⁴ Ciber Fisiopatología Obesidad y Nutrición (CB06/03), Instituto Salud Carlos III, E-28029 Madrid, Madrid, Spain
- * Correspondence: d.pons@uib.es; Tel.: +34-971173149

Abstract: Genistein could play a crucial role in modulating three closely linked physiological processes altered during cancer: oxidative stress, mitochondrial biogenesis, and inflammation. However, genistein's role in colorectal cancer remains unclear. We aimed to determine genistein's effects in two colon cancer cells: HT29 and SW620, primary and metastatic cancer cells, respectively. After genistein treatment for 48 h, cell viability and hydrogen peroxide (H₂O₂) production were studied. The cell cycle was studied by flow cytometry, mRNA and protein levels were analyzed by RT-qPCR and Western blot, respectively, and finally, cytoskeleton remodeling and NF-κB translocation were determined by confocal microscopy. Genistein 100 μM decreased cell viability and produced G₂/M arrest, increased H₂O₂, and produced filopodia in SW620 cells. In HT29 cells, genistein produced an increase of cell death, H₂O₂ production, and in the number of stress fibers. In HT29 cells, mitochondrial biogenesis was increased, however, in SW620 cells, it was decreased. Finally, the expression of inflammation-related genes increased in both cell lines, being greater in SW620 cells, where NF-κB translocation to the nucleus was higher. These results indicate that high concentrations of genistein could increase oxidative stress and inflammation in colon cancer cells and, ultimately, decrease cell viability.

Keywords: colorectal cancer; genistein; cell viability; hydrogen peroxide production; mitochondrial biogenesis; inflammation



Citation: Alorda-Clara, M.; Torrens-Mas, M.; Morla-Barcelo, P.M.; Roca, P.; Sastre-Serra, J.; Pons, D.G.; Oliver, J. High Concentrations of Genistein Decrease Cell Viability Depending on Oxidative Stress and Inflammation in Colon Cancer Cell Lines. *Int. J. Mol. Sci.* **2022**, *23*, 7526. <https://doi.org/10.3390/ijms23147526>

Academic Editor: Seok-Geun Lee

Received: 7 June 2022

Accepted: 6 July 2022

Published: 7 July 2022

Publisher's Note: MDPI stays neutral with regard to jurisdictional claims in published maps and institutional affiliations.



Copyright: © 2022 by the authors. Licensee MDPI, Basel, Switzerland. This article is an open access article distributed under the terms and conditions of the Creative Commons Attribution (CC BY) license (<https://creativecommons.org/licenses/by/4.0/>).

1. Introduction

Genistein (GEN) is a phytoestrogen that belongs to the isoflavones class and is found in soybeans [1]. Asian countries have a higher intake of this isoflavone than European countries because of the level of their soy-derived products consumption [2]. It is known that tumors can be affected by GEN, but the goodness of the effect is still unknown [3]. Colorectal cancer (CRC) is the third-most common cancer and the second-most common cause of cancer death worldwide [4]. Until now, Asia had the lowest CRC incidence, but nowadays it has increased [5]. This increment in the number of CRC cases in Asia can be due to changes in diet, which now is more westernized [6]. CRC is one of the most affected cancers by GEN, as GEN promotes apoptosis, cell cycle arrest, and a decrease in

cell proliferation and metastasis in this cancer, but the mechanism by how GEN affects CRC remains unclear [1,3,7].

The chemopreventive activity of GEN can modulate different physiological processes during cancer, such as oxidative stress [1], cancer cells bioenergetics [8], and inflammation [9], which are important in different phases of CRC [10–12].

GEN has a dual effect in front of oxidative stress. It is well known that GEN acts as an antioxidant during oxidative stress, increasing antioxidant enzymes' expression [1], but GEN can also act as a pro-oxidant when it is present at high concentrations [13–15]. Oxidative stress is the result of a disbalance between reactive oxygen species (ROS) production and antioxidant defenses [16]. Mitochondria are the major producers of ROS in cells during an electronic transport chain [17,18] and form free radicals by the reduction of molecular oxygen, forming superoxide and hydroxyl radicals [17], which are detoxified by the antioxidant enzymes (superoxide dismutases, peroxidases, and catalase) [17,18]. Oxidative stress is involved in the initiation and progression of cancer due to the capacity of ROS to increase DNA mutations, oxidative damage to macromolecules, genomic instability, and cellular proliferation [10]. Furthermore, moderate levels of ROS can decrease apoptosis, interrupt cell–cell communication, and modify second messenger systems [10]. Finally, ROS can activate tumor suppressors in a reversible form [16].

ROS production is closely related to mitochondrial biogenesis, which is a complex process where the nuclear and mitochondrial genome must be highly regulated, since the nuclear genome codifies proteins which control the transcription and replication of mtDNA that, in turn, codifies some mitochondrial proteins such as electron transport chain proteins [19]. This process involves both the replication and transcription of mtDNA [19], and it is a highly regulated pathway [20]. Mitochondrial biogenesis and functionality have always been believed to be compromised in cancer development [11]. The role of mitochondria in metastatic CRC has not been well established yet, but some studies suggested that cells from more advanced stages have a higher oxidative phenotype compared to cells from earlier stages [21]. Finally, GEN could be playing a role in cancer cells' bioenergetics. However, the role of GEN on mitochondrial biogenesis is not well established [8].

In the same way, colorectal tumors suffer an increase of proinflammatory cytokines' expression and a constitutive activation of transcription factors related to inflammatory pathways [22]. These changes in inflammation can be done, at least in part, by mitochondria, since ROS can directly activate inflammatory pathways [23] and inflammasomes [24], which is a multiprotein complex that releases proinflammatory cytokines [25]. Furthermore, when mitochondrial damage is present, mitochondrial DNA is released into the cytosol, where it can activate the inflammasomes [25]. The established cytokine network allows for survival, growth, proliferation, differentiation, immune cells' activation, and tumoral and stromal cells' migration [12]. Inflammation is achieved with the release of cytokines, chemokines, and the activation of pathways related to inflammation participates in all phases of CRC, as it allows tumoral growth and it is associated to angiogenesis, the epithelial–mesenchymal transition, and metastasis [12].

Our aim was to investigate the effects of genistein treatment in oxidative stress, mitochondrial biogenesis, and inflammatory parameters in two colon cancer cell lines: HT29, a primary and moderately differentiated cell line, and SW620, a metastatic and poorly differentiated cell line. For this goal, cell viability, ROS production, the cellular cycle, gene and/or protein expression levels of antioxidant enzymes, mitochondrial biogenesis regulators and inflammation-related genes, the nuclear translocation of nuclear factor kappa B (NF- κ B), and actin cytoskeleton remodeling were studied.

2. Results

2.1. High Concentrations of Genistein Decreased Cell Viability

Cell survival is key in cancer progression; consequently, the effect of GEN in cell viability was studied. Figure 1 shows the cell viability analysis after 48 h of treatment with increasing concentrations of GEN (1, 5, 50, and 100 μ M). Only the highest concentrations

of GEN (50 and 100 μM) caused a statistically significant reduction in cell viability. This decrease was more pronounced in SW620 cells (-63% and -65% , respectively) than in HT29 cells (-6% and -10% , respectively).

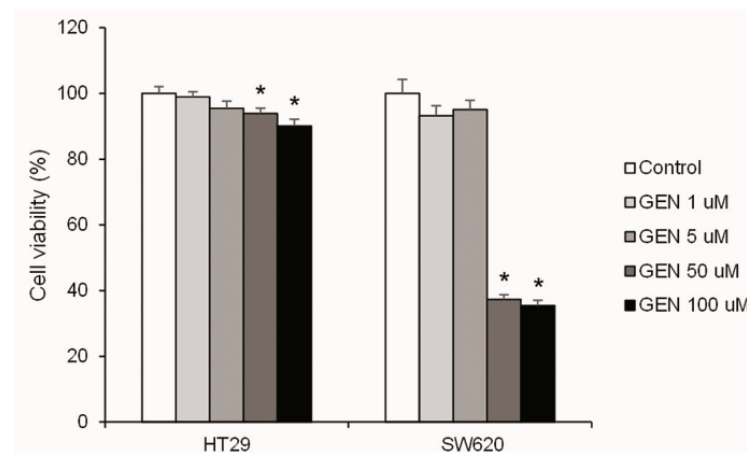


Figure 1. Effects of different concentrations of genistein on cell viability in HT29 and SW620 cells, determined with Hoechst 33342 assay. The value of control cells (DMSO-treated cells) was set at 100%. The coordinate values represent cell viability (%) and the measurements were made with genistein 1, 5, 50, and 100 μM or 0.1% DMSO (control cells) treatment for 48 h. GEN, genistein. * Significant difference between control cells and genistein-treated cells (Student's *t*-test; $p < 0.05$, $n = 6$).

2.2. GEN Produced Cell Cycle Arrest and Apoptosis

The cell cycle (Figure 2) was studied with flow cytometry after 48 h of GEN 100 μM treatment. HT29 cells (Figure 2A) suffered a decrease in the G_0/G_1 phase (-52%), but suffered an increase in the Sub G_0/G_1 , S and G_2/M phases ($+288\%$, $+46\%$, and $+33\%$, respectively). SW620 cells (Figure 2B) presented a decrease in the G_0/G_1 and S phases (-97% and -68% , respectively) and an increase in the Sub G_0/G_1 and G_2/M phases ($+199\%$ and $+504\%$, respectively).

2.3. High Concentrations of Genistein Increased H_2O_2 Production

To know the origin of cell death, the oxidative stress status was studied. The H_2O_2 production was analyzed after 48 h of GEN treatment (Figure 3). HT29 cells presented a weak increase of the H_2O_2 production in a dose-dependent manner, reaching $+18\%$ with the highest concentration. However, in SW620, the results showed an accentuated increase in H_2O_2 production when GEN concentrations were higher ($+120\%$ approximately at 50 and 100 μM), without significant changes with the lower concentrations.

2.4. GEN Modulated the Expression of Different Antioxidant Enzymes

To understand the changes in H_2O_2 production, the mRNA expression levels of different antioxidant enzymes were studied after 48 h of GEN 100 μM treatment. HT29 cells (Figure 4A) suffered a statistically significant increase in *SOD2* ($+40\%$) and *SOD1* ($+36\%$) mRNA expression levels after GEN treatment. Moreover, in SW620 cells (Figure 4B), GEN treatment caused a statistically significant increase in the expression levels of *SOD2* ($+96\%$) and *GPX1* ($+17\%$), in addition to a statistically significant decreased expression level of *CAT* (-28%). Furthermore, the changes in the *SOD2/CAT* (Figure 4C) and *SOD2/GPX1* (Figure 4D) ratios were evaluated, since *SOD2* is the mitochondrial dismutase. HT29 cells showed a statistically significant increase in both ratios ($+56\%$ in both ratios), as well as SW620 cells ($+178\%$ and $+66\%$, respectively).

SW620 cell line gene expression changes were more pronounced than in HT29 cells. In consequence, the protein expression levels of the same antioxidant enzymes were studied in both cell lines after 48 h of GEN 100 μM treatment. HT29 cells (Figure 5A) showed no changes in their protein expression levels of antioxidant enzymes after GEN treatment.

SW620 cells (Figure 5C) showed a statistically significant increase in MnSOD (+64%) protein expression levels, as well as a statistically significant decrease in Catalase (−21%) and GPx (−29%) protein expression levels. Furthermore, the changes in the MnSOD/Catalase (Figure 5E) and MnSOD/GPx (Figure 5F) ratios were evaluated, and SW620 showed a statistically significant increase in both ratios (+106% and +122%, respectively). Figure 5B,D show representative bands in HT29 and SW620, respectively, of the GEN effects on MnSOD, CuZnSOD, Catalase, GPx, and GAPDH expression levels.

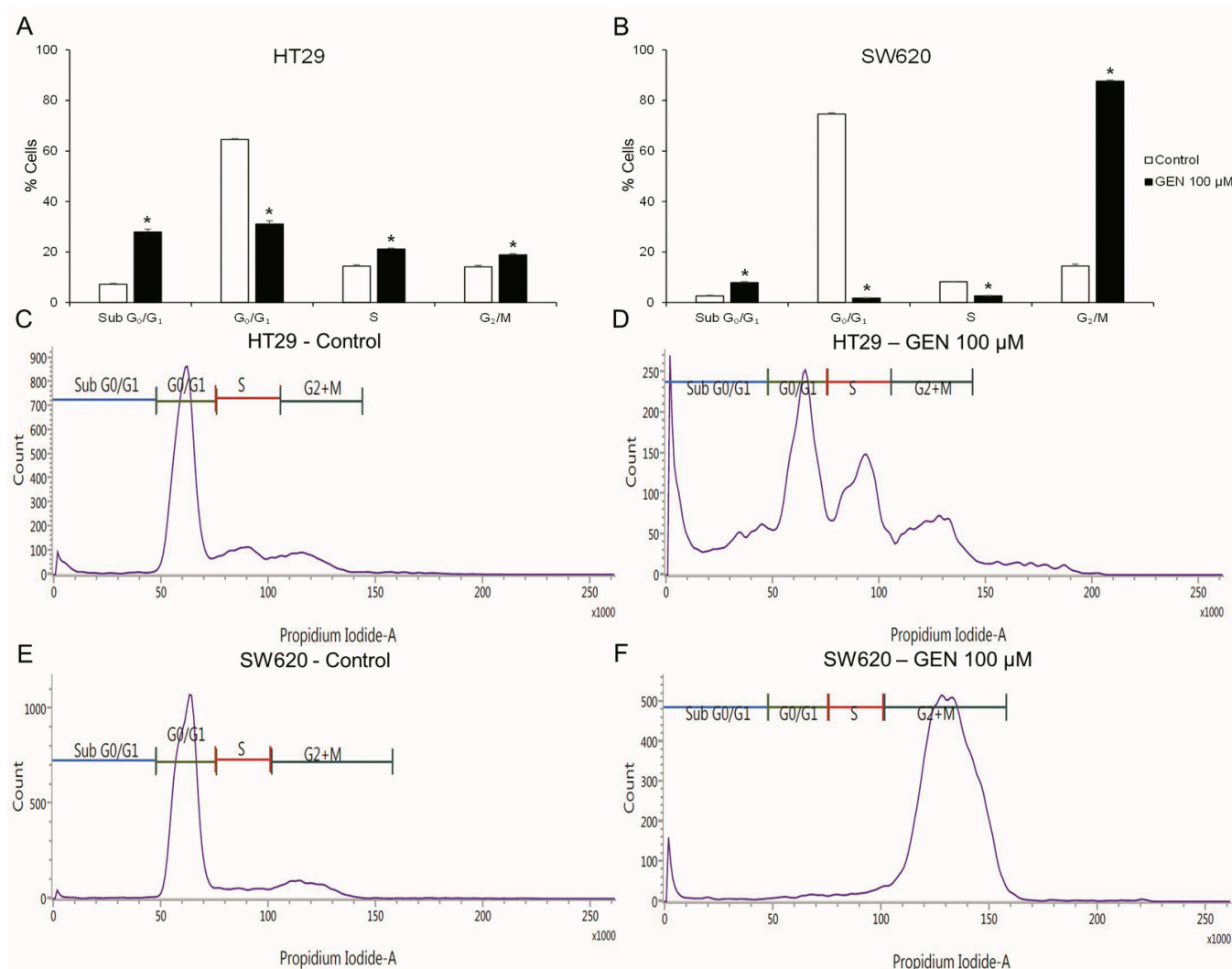


Figure 2. Effects of genistein on cell cycle in (A) HT29 cells and (B) SW620 cells, determined by flow cytometry. Representative event count and propidium iodide fluorescence in HT29 cells (C,E) and SW620 cells (D,F). The measurements were made with 0.1% DMSO (control cells, (C,D)) or genistein 100 μM (E,F) treatment for 48 h. Values are expressed as mean ± SEM. GEN, genistein. * Significant difference between control cells and genistein-treated cells (Student's *t*-test; $p < 0.05$, $n = 6$).

2.5. GEN Affected Actin Cytoskeleton

Actin cytoskeleton remodeling was studied with phalloidin staining after 48 h of GEN 100 μM treatment. Figure 6 shows confocal microscopy images taken after phalloidin and DAPI (for the nucleus staining) incubation, where an increase in the number of stress fibers in the HT29 cell line (Figure 6B) and an increase in the number of filopodia in SW620 cells (Figure 6D) after GEN treatment can be observed.

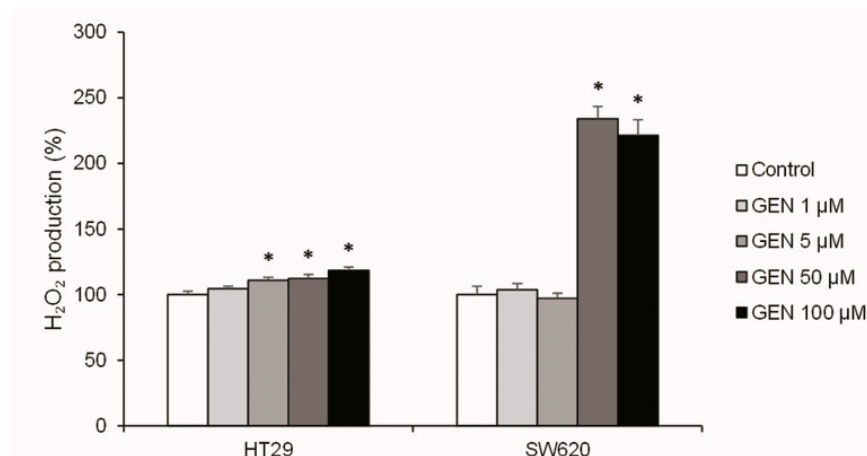


Figure 3. Effects of different concentrations of genistein on H₂O₂ production determined with Amplex[®] Red Hydrogen Peroxide/Peroxidase Assay in HT29 and SW620 cells. The coordinate values represent H₂O₂ production (%) and values are expressed as mean ± SEM and are normalized as percentage of control values (DMSO-treated cells). The measurements were made with genistein 1, 5, 50, and 100 μM or 0.1% DMSO (control cells) treatment for 48 h. GEN, genistein. * Significant difference between control cells and genistein-treated cells (Student's *t*-test; *p* < 0.05, *n* = 6).

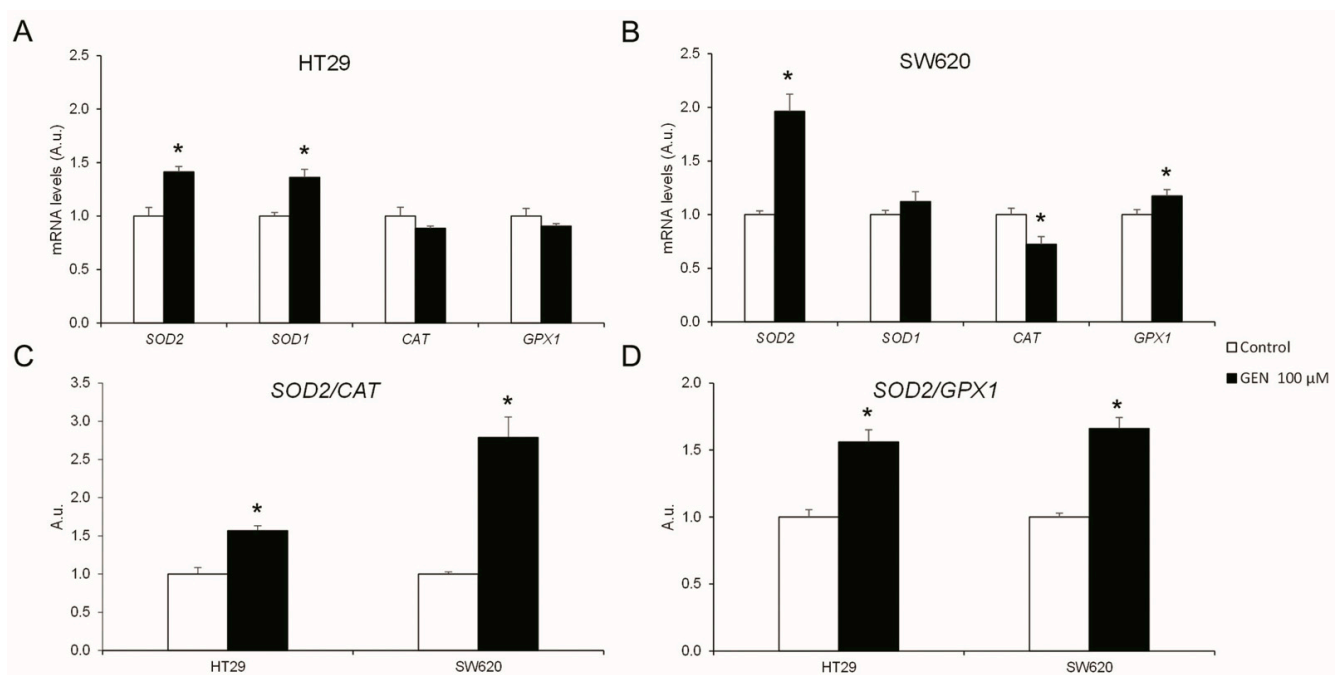


Figure 4. Effects of genistein on antioxidant enzymes' mRNA expression levels (*SOD2*, *SOD1*, *CAT*, and *GPX1*) in (A) HT29 cells and (B) SW620 cells determined by real-time PCR. Effects of genistein on mRNA expression levels ratios of (C) *SOD2/CAT* and (D) *SOD2/GPX1* genes determined by real-time PCR. The measurements were made with genistein 100 μM or 0.1% DMSO (control cells) treatment for 48 h. The coordinate values represent mRNA levels (arbitrary units). Values are expressed as mean ± SEM and control values were set at 1.00. GEN, genistein; A.u., arbitrary units. * Significant difference between control cells and genistein-treated cells (Student's *t*-test; *p* < 0.05, *n* = 6).

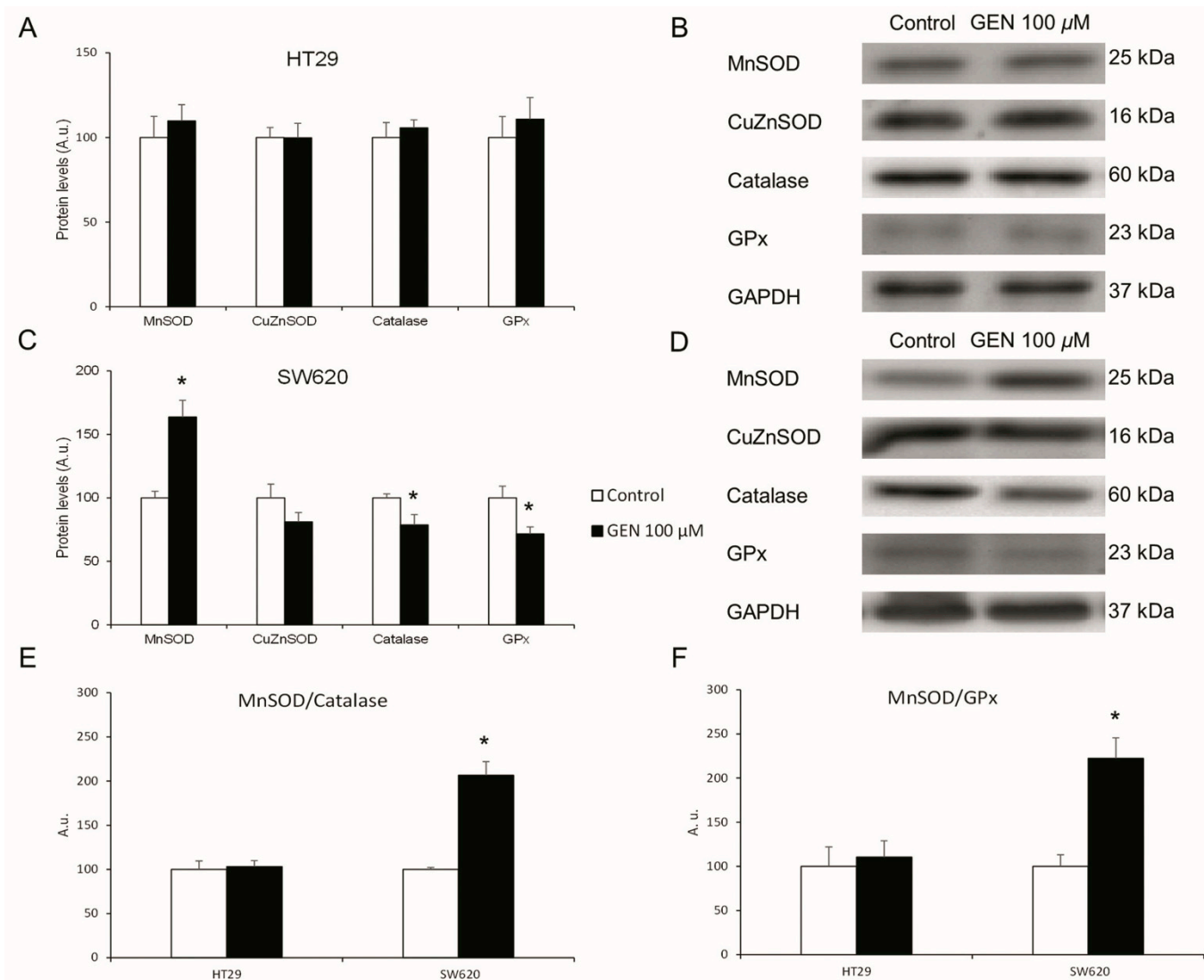


Figure 5. Effects of genistein on protein expression levels. Antioxidant enzymes (MnSOD, CuZnSOD, Catalase, GPx) in (A) HT29 cells and (C) SW620 cells determined by Western blot. Western blot representative bands in (B) HT29 cells and (D) SW620 cells. Effects of genistein on protein expression level ratios of (E) MnSOD/Catalase and (F) MnSOD/GPx determined by Western blot. The measurements were made with genistein 100 μ M or 0.1% DMSO (control cells) treatment for 48 h. Values are expressed as mean \pm SEM and control values (DMSO-treated cells) were set at 100. GEN, genistein; A.u., arbitrary units. * Significant difference between control cells and genistein-treated cells (Student's *t*-test; $p < 0.05$, $n = 6$).

2.6. GEN Modified the Expression of Different Mitochondrial Biogenesis Genes

To understand the changes in the mitochondrial biogenesis regulations, mRNA expression levels of different mitochondrial regulatory genes were studied after 48 h of GEN 100 μ M treatment. HT29 cells (Figure 7A) suffered a statistically significant decrease in *PPARGC1 α* and *ESRRA* (−35% and −23%, respectively) after GEN treatment, while *TFAM* and *SSBP1* suffered a statistically significant increase (+25% and +66%, respectively). In contrast, SW620 cells (Figure 7B) did not suffer changes in *PPARGC1 α* , but *ESRRA*, *TFAM*, and *SSBP1* suffered a statistically significant decrease (−25%, −37%, and −23%, respectively). Furthermore, mitochondrial DNA expression levels (Figure 7C) were also studied after 48 h of GEN 100 μ M treatment, presenting a decrease (−53%) in SW620 cells after GEN treatment.

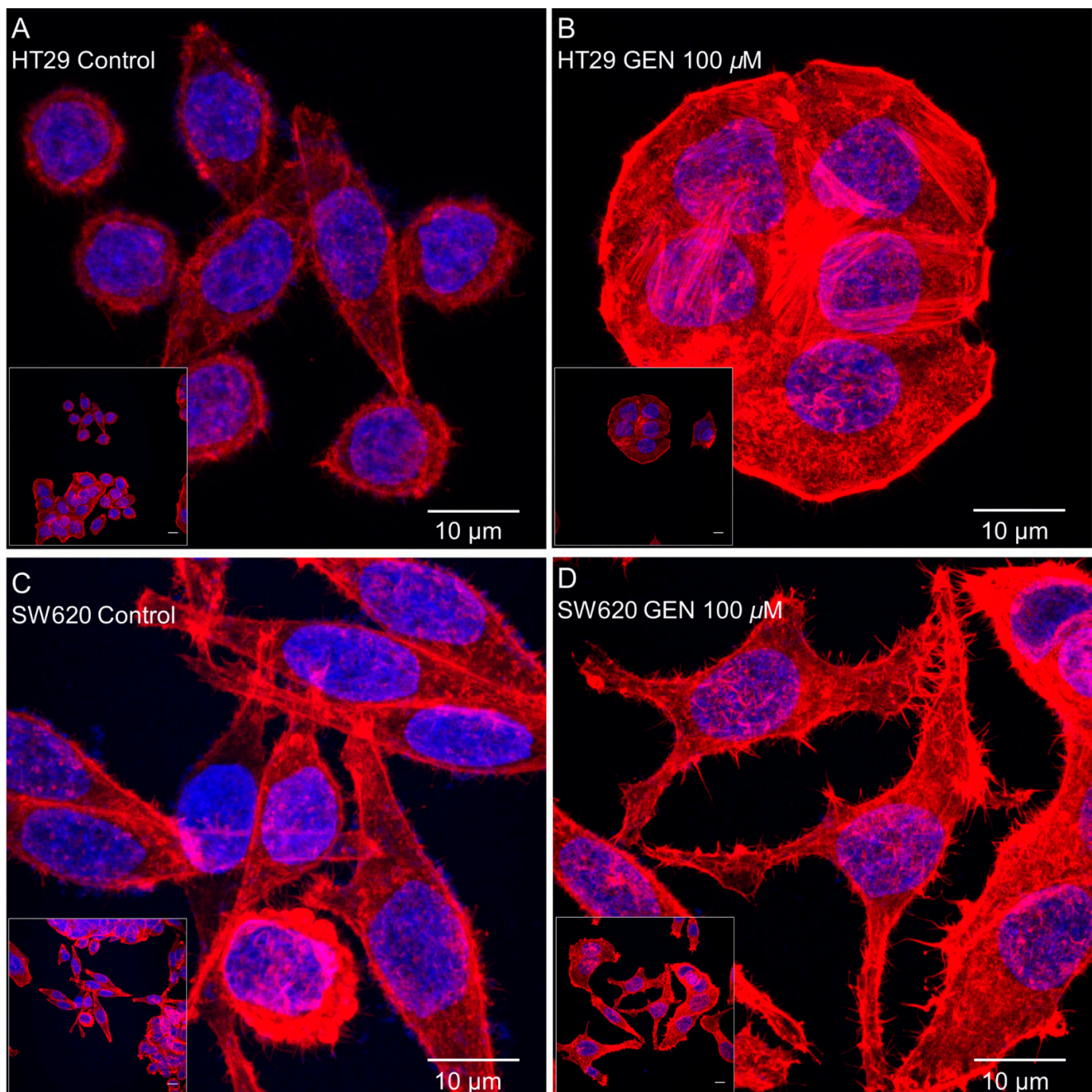


Figure 6. Effects of genistein on actin cytoskeleton in (A,B) HT29 cells and (C,D) SW620 cells, determined by Phalloidin staining. The measurements were made with 0.1% DMSO (control cells, (A,C)) or genistein 100 μM (B,D) treatment for 48 h. The fluorescence was monitored with a Leica TCS-SPE Confocal Microscope, using 63 \times immersion oil (147 N.A.) objective lens. Scale bar 10 μm . White square in the bottom left corner shows the whole field without zoom and the image in the center shows a zoom from the white square image. Nucleus and actin cytoskeleton are represented in the picture in blue and red, respectively.

2.7. GEN Increased the Inflammatory Status

To understand the changes in inflammation, the mRNA expression levels of different interleukins and their receptors, as well as key genes of different inflammation-related pathways, were studied after 48 h of GEN 100 μM treatment. The HT29 cell line (Figure 8A) presented a statistically significant increase in *TNF*, *IL1B*, *CXCR2*, *HPSE*, and *IL10* (+594%, +97%, +135%, +115%, and +21%, respectively) and a statistically significant decrease in

CXCL8 (−19%) mRNA expression after GEN treatment. On the other hand, SW620 cells (Figure 8B) suffered a statistically significant increase in *TNF*, *CXCL8*, *CXCR2*, and *HPSE* (+814%, +174%, +2539%, and +676%, respectively) and a statistically significant decrease in *PPARG* (−70%) mRNA expression after GEN treatment. *IL1B* in SW620 cells also suffered an increase since the control cells showed a 40.6 ± 3.1 crossing point and GEN-treated cells showed a 31.9 ± 0.2 crossing point (data not shown).

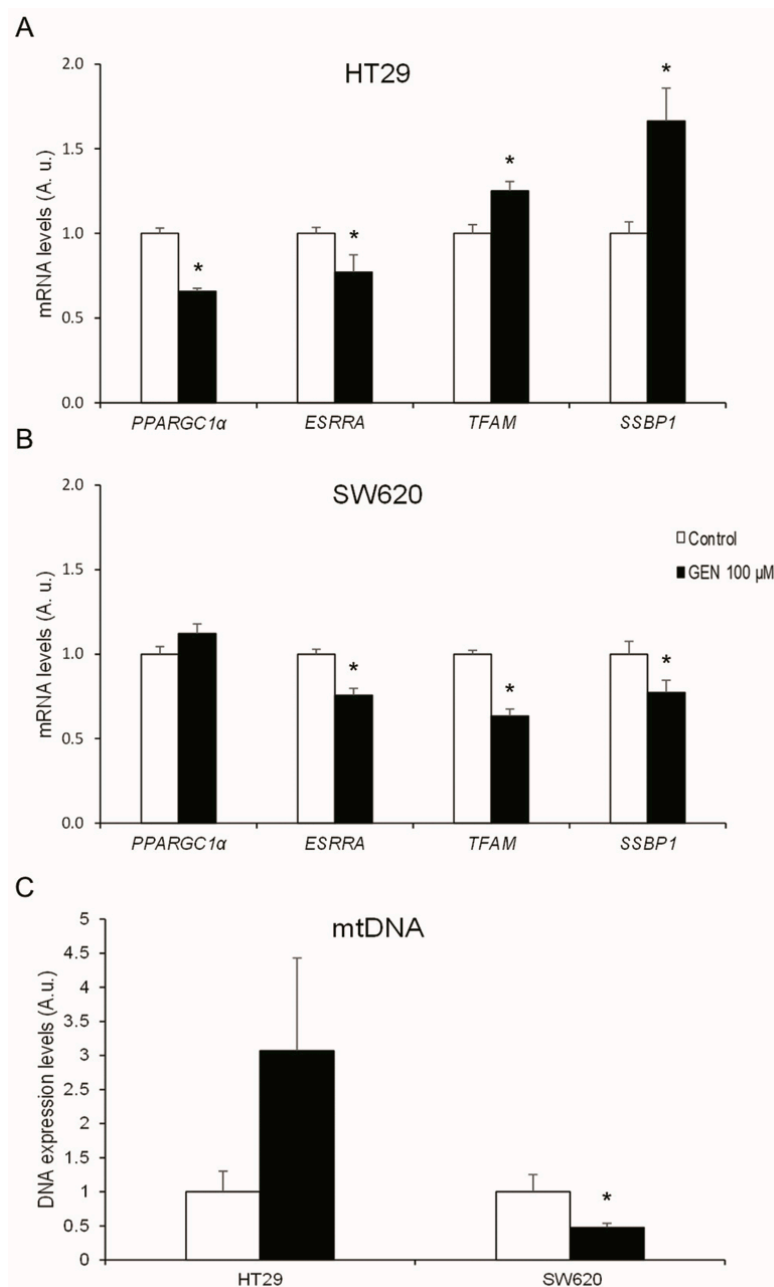


Figure 7. Effects of genistein on mRNA expression levels of mitochondrial biogenesis-related genes (*PPARGC1 α* , *ESRRA*, *TFAM*, and *SSBP1*) in (A) HT29 cells and (B) SW620 cells, determined by real-time PCR. Effects of genistein on DNA expression levels of mitochondrial DNA in (C) HT29 and SW620 cells determined by real-time PCR. The measurements were made with genistein 100 μ M or 0.1% DMSO (control cells) treatment for 48 h. The coordinate values represent mRNA levels (arbitrary units). Values are expressed as mean \pm SEM and control values (DMSO-treated cells) were set at 1.00. GEN, genistein; A.u., arbitrary units. * Significant difference between control cells and genistein-treated cells (Student's *t*-test; $p < 0.05$, $n = 6$).

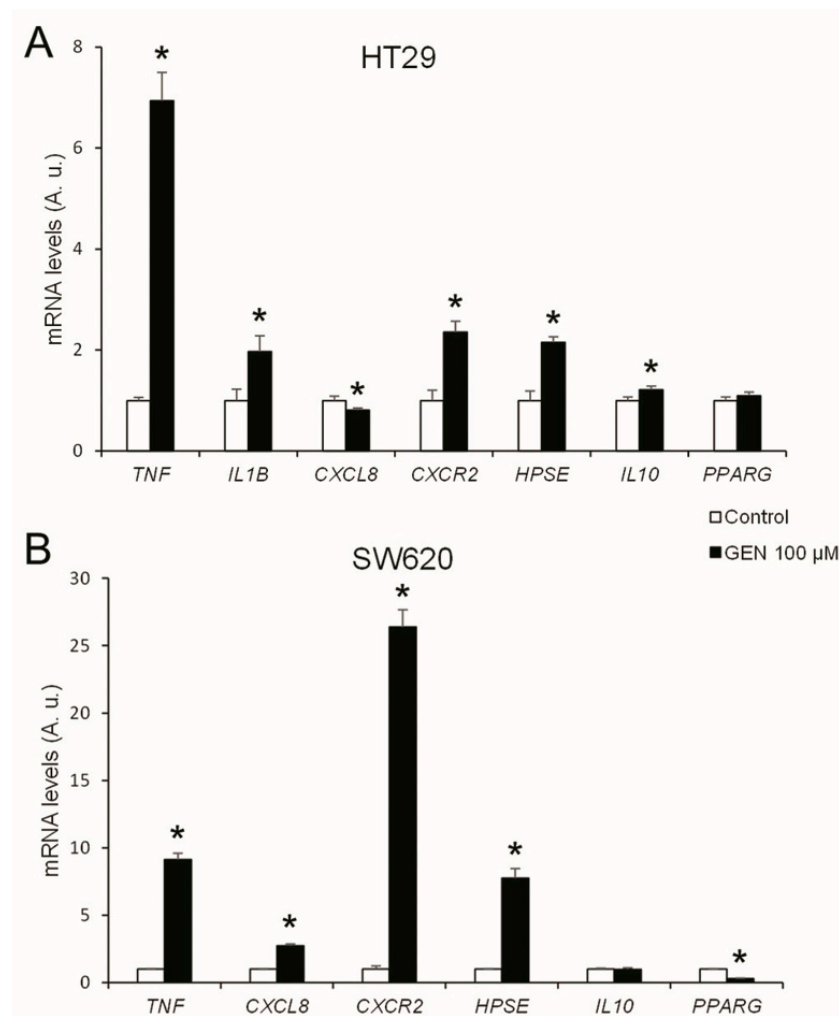


Figure 8. Effects of genistein on mRNA expression levels of inflammation-related genes (*TNF*, *IL1B*, *CXCL8*, *CXCR2*, *HPSE*, *IL10*, and *PPARG*) in (A) HT29 cells and (B) SW620 cells determined by real-time PCR. The measurements were made with genistein 100 μ M or 0.1% DMSO (control cells) treatment for 48 h. Values are expressed as mean \pm SEM and control values (DMSO-treated cells) were set at 1.00. The coordinate values represent mRNA levels (arbitrary units). GEN, genistein; A.u., arbitrary units. * Significant difference between control cells and genistein-treated cells (Student's *t*-test; $p < 0.05$, $n = 6$).

2.8. GEN Affected NF- κ B Translocation into the Nucleus

Inflammatory-related gene changes were more pronounced in the SW620 cell line than in the HT29 cell line, thus, in order to have a more functional parameter related to inflammation, NF- κ B translocation to the nucleus was studied after 48 h of GEN 100 μ M treatment. Figure 9 displays confocal microscopy pictures taken after anti-NF- κ B primary antibody and Hoechst 33342 (for the nucleus staining) incubation, where an increase of NF- κ B translocation into the nucleus after GEN treatment in both cell lines can be observed, but it is more pronounced in the SW620 cells (Figure 9D), which is represented as the merge (pink) of the nucleus (blue) and NF- κ B proteins (red). Furthermore, an increase of the SW620 cells' size can be seen in Figure 9D due to an increase in swelling.

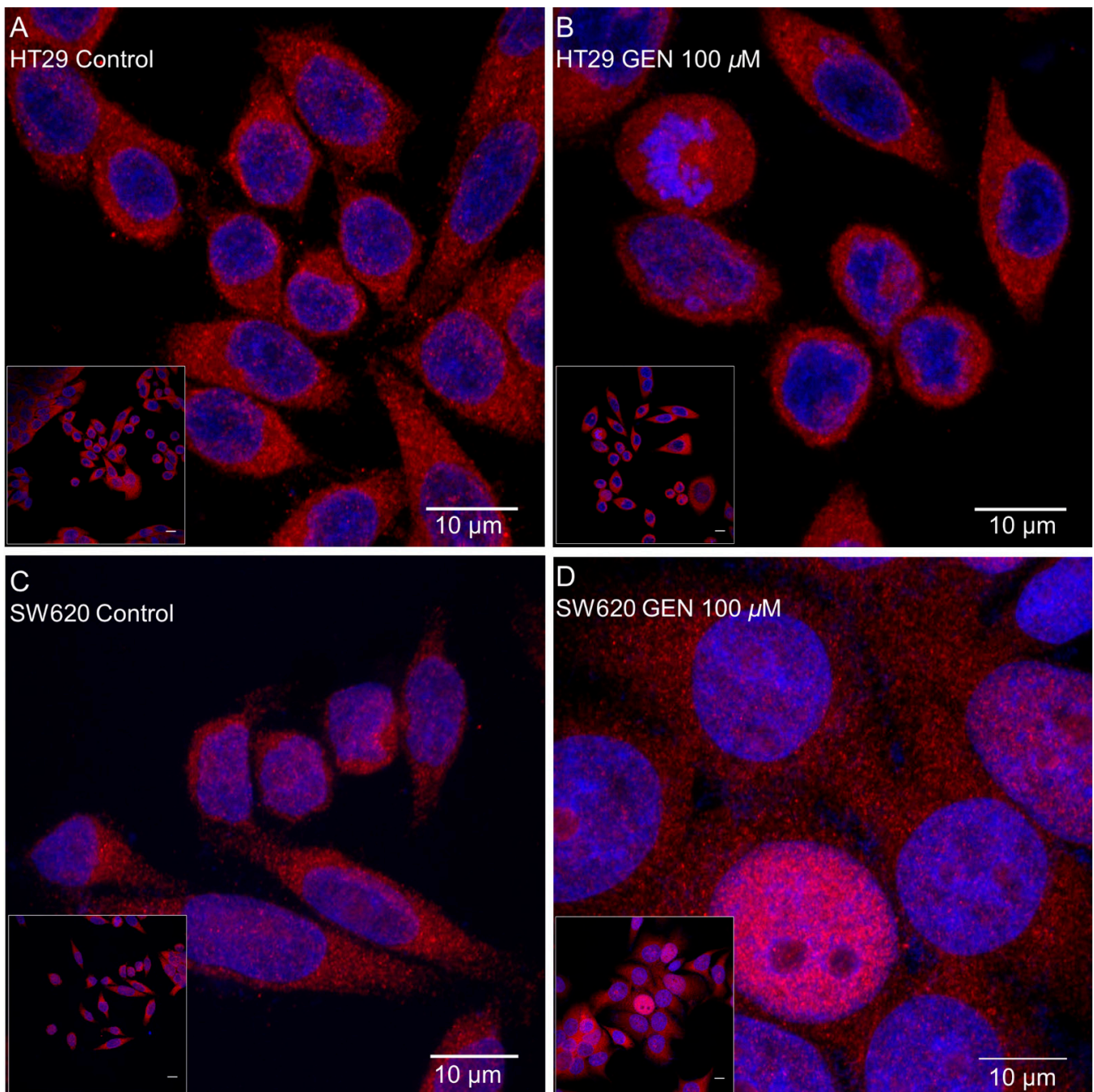


Figure 9. Effects of genistein on NF- κ B nuclear translocation in (A,B) HT29 cells and (C,D) SW620 cells determined by immunocytochemistry. The measurements were made with 0.1% DMSO (control cells, (A,C)) or genistein 100 μ M (B,D) treatment for 48 h. The fluorescence was monitored with a Leica TCS-SPE Confocal Microscope, using 63 \times immersion oil (147 N.A.) objective lens. Scale bar 10 μ m. White square in the bottom left corner shows the whole field without zoom and the image in the center shows a zoom from the white square image. Nucleus and NF- κ B proteins are represented in the picture in blue and red, respectively. The merge between both (pink) indicates that NF- κ B had translocated into the nucleus.

3. Discussion

The effects of high concentrations of the phytoestrogen GEN (100 μ M) in colon cancer cells were analyzed to see the action of this phytoestrogen in cell viability, oxidative stress, mitochondrial biogenesis, and inflammation in colorectal cancer.

Some studies about GEN metabolization and digestion suggest that it could be accumulated in various colon areas, where GEN may exert its effects [26]. For this reason, a high intake of GEN-rich food can cause high doses of GEN to be, physiologically, in some colon areas and, therefore, it could be an interesting point to be studied. The decrease in cell viability with high GEN concentrations we found, which was more pronounced in SW620 cells, was also seen by Lepri et al., who observed an inhibition of cell viability in HT29 colon cancer cells treated with GEN 50 μM and 100 μM [27]. Furthermore, Xiao and collaborators observed an inhibition of cell growth in HT29 and SW620 cells after GEN treatment in a dose- and time-dependent manner [28].

This diminution in cell viability could be related to changes in cell cycle regulation. In HT29 cells, the decrease in cell viability could be promoted by the increase in cell death observed in the cell cycle analysis. The increase in the sub G_0/G_1 phase was previously seen by Salti and collaborators in the HT29 cells with a treatment with GEN 100 μM for 72 h [29]. In contrast, SW620 cells presented a G_2/M cell cycle arrest of more than 85% of the cells, which could explain the decrease in cell viability due to the inability of SW620 cells to divide, causing a cytostatic effect of GEN on this cell line [30].

The results obtained in the cell viability and cell cycle analysis could be linked to an increase in H_2O_2 production [31]. HT29 and SW620 showed an increase in both *SOD2/CAT* and *SOD2/GPX1* mRNA expression ratios. Moreover, SW620 cells showed an increase in both the MnSOD/Catalase and MnSOD/GPx protein expression ratios, which results in a more pronounced increase in H_2O_2 accumulation in this cell line [17,18]. In fact, the accentuated rise in H_2O_2 production in SW620 cells and, consequently, in oxidative stress, results in the pronounced decrease in cell viability at higher GEN concentrations. This increase in oxidative stress was also reported by other authors after GEN 50 μM and 100 μM treatment in breast and colon cancer cells [32,33].

The different effects of GEN in the cell cycle according to the cell line, being more cytotoxic on HT29 cells and more cytostatic on SW620 cells, could be responsible for the difference in cell viability and ROS levels. The HT29 cells suffered cell death, and for this reason, the increase in the ROS levels is lower than in the SW620 cell line. In the SW620 cells, the increase in the ROS levels could be responsible for the cell cycle arrest [34,35] and the subsequent decrease in cell viability.

Stress fibers, the most relevant contractile structures in cells, participate in cellular-cellular and cellular-matrix union formations, cytokinesis, and migration [36]. In addition, filopodia are important for slow migration and can act as sensors and guide organelles [37]. Different studies showed that an increase of H_2O_2 production reorganizes the actin filaments producing stress fibers, filopodia, and lamellipodia in different cell lines, such as HAEC cells (human aortic endothelial cells) [38], SVEC4-10 cells (mouse endothelial cells) [39], and Rat2 fibroblasts [40]. The increase in the number of stress fibers in HT29 cells and filopodia in SW620 cells could be related to the increase in H_2O_2 production and the inflammatory status. In addition to this, the increase in stress fibers and filopodia in HT29 and SW620 cells could be related to the increase in the inflammatory state, since Costanzo and collaborators observed an increase in the number of stress fibers in CaCo2 and HT29 cell lines after $\text{TNF}\alpha$ and $\text{IFN}\gamma$ treatment [41]. Finally, Cui and collaborators demonstrated that RAW 264.7 cells (a murine macrophage cell line), after GEN 50–100 μM treatment for 24 or 48 h, developed long pseudopodia-like protrusions [42].

In the HT29 cell line, mitochondrial biogenesis would be increased after GEN treatment, since after 48 h of treatment, *PPARGC1 α* mRNA levels were lower and *TFAM* and *SSBP1* mRNA levels were higher. *PGC1 α* , the most upstream mitochondrial biogenesis regulator with the highest activation in the short term [43] implicated in mtDNA transcription [44], promotes *TFAM* transcription [43] which, in turn, promotes mtDNA transcription [45], and *mtSSB* participates in mtDNA replication [46]. The new mitochondria could smooth the increase in H_2O_2 caused by GEN 100 μM treatment, leading to a slight accumulation of H_2O_2 . Conversely, SW620 cells had a decrease in the mRNA expression levels of *ESRRA*, *TFAM*, and *SSBP1*, in addition to a decrease in mtDNA expression levels,

which could imply a decrease in mitochondrial biogenesis. Furthermore, a recent study has demonstrated that silencing TFAM increases the H₂O₂ intracellular levels in SW620 cells and compromises SW620 viability due to its high energy demand [47]. All the data suggest that the decrease in the mRNA expression levels of mitochondrial biogenesis-related genes in SW620 cells could lead to a lack of mitochondrial renewal, so a great number of non-functional mitochondria could be accumulated, leading to a strong accumulation of H₂O₂ and, subsequently, a decrease in cell viability and cell cycle arrest.

The SW620 cell line showed an increase in inflammation, which can be seen by the increase in the pro-inflammatory genes' expression and the decrease in the anti-inflammatory genes' expression. Moreover, the increase in the NF-κB translocation to the nucleus demonstrated that this protein is more activated [48]. This cell line also presented swelling (Figure 9D) after GEN treatment, that could corroborate the G₂/M arrest. The increase in inflammation is caused by the accumulation of H₂O₂, which activates NF-κB, allowing its translocation to the nucleus, where it can act as a transcription factor, modulating proinflammatory-related genes' expression [23]. The decrease of *PPARG* also allows the translocation of NF-κB to the nucleus, since PPARγ inactivates NF-κB by avoiding the nuclear factor kappa B inhibitor (IκB) phosphorylation and retaining NF-κB in the cytoplasm [49]. Inside the nucleus, NF-κB permits the transcription of several cytokines (IL-1β, IL-8) and TNFα [23,49], increasing the inflammatory status of the cell. The increase in *TNF* produces an increase in *HPSE*, the main function of heparanase is the degradation of the extracellular matrix, releasing proinflammatory cytokines that are inside the matrix [50], and the transcription of TNFα and IL-1β [51]. Altogether, positive feedback is created and allows the perpetuation of the inflammatory status in SW620 cells. This inflammatory status, initially caused by the increase of H₂O₂, which cannot be palliated neither by the antioxidant enzymes nor mitochondrial biogenesis, could lead SW620 cells to G₂/M cycle arrest and, consequently, a decrease in cell viability. In the HT29 cell line, there was an increase in the inflammatory status that, in comparison, is less pronounced than in the SW620 cell line. HT29 cells suffered a less pronounced increase in proinflammatory genes than SW620 cells, which could be due to the minor accumulation of H₂O₂ in these cells, and furthermore, an increase in the anti-inflammatory gene *IL10*'s expression, which can be increased in order to palliate and produce lower levels of inflammation [52]. Moreover, despite the lower levels of H₂O₂ production compared to SW620 cells, NF-κB translocation to the nucleus was observed, but this translocation was less pronounced than in the SW620 cell line. Previous studies demonstrate that high concentrations of GEN in HT29 cells inhibit NF-κB translocation to the nucleus [53,54], since GEN has antioxidant and anti-inflammatory properties, but our results demonstrate that a high concentration of GEN treatment has pro-oxidant and pro-inflammatory properties. In this cell line, increased apoptosis produced a lower inflammatory status, caused by the lower levels of H₂O₂ and the increase of *IL10*.

4. Materials and Methods

4.1. Reagents

Dulbecco's Modified Eagle's Medium (DMEM) high glucose was purchased from GIBCO (Paisley, UK). Fetal bovine serum and penicillin–streptomycin solution were purchased from Biological Industries (Kibbutz Beit Haemek, Israel). GEN was obtained from Sigma-Aldrich (St-Louis, MO, USA). Routine chemicals were supplied by Panreac (Barcelona, Spain), Sigma-Aldrich (St Louis, MO, USA), Bio-Rad Laboratories (Hercules, CA, USA), and Roche (Barcelona, Spain).

4.2. Cell Culture

Human colon cancer cell lines HT29 and SW620 were obtained from American Type Culture Collection (ATCC; HT-29 (ATCC HTB-38) and SW-620 [SW-620] (ATCC CCL-227); Manassas, VA, USA), and cultured in DMEM supplemented with 10% heat-inactivated fetal bovine serum (FBS) (*v/v*) and 1% penicillin and streptomycin (*v/v*) at 37 °C with 5% CO₂.

Cells were seeded at similar passages and treated, the following day, at 70% of confluency with increasing concentrations (1, 5, 50, and 100 μM) of GEN with 0.1% dimethyl sulfoxide (DMSO) as the vehicle, and the control vehicle-cells were treated with 0.1% DMSO for 48 h for cell viability and hydrogen peroxide (H_2O_2) production determinations. For further experiments, both cell lines were treated only with 100 μM of GEN for 48 h, and control vehicle-treated cells were treated with 0.1% DMSO.

4.3. Cell Viability Determination

Total of 5×10^4 HT29 cells and 4×10^4 SW620 cells were seeded in each well in a 96-well plate and treated with increasing concentrations of GEN for 48 h. Cell viability was determined with Hoechst 33342 (Sigma-Aldrich, St Louis, MO, USA), which emits blue fluorescence when it is bound to double strand DNA. After GEN treatment, the culture medium was removed, and 5 $\mu\text{g}/\text{mL}$ of Hoechst was incubated for 5 min at 37 $^\circ\text{C}$. Finally, FLx800 microplate fluorescence reader (BIO-TEK, Winooski, VT, USA) was used to measure the fluorescence, set at excitation wavelength of 350 nm and emission wavelength of 455 nm.

4.4. Fluorimetric Determination of H_2O_2 Production

H_2O_2 production was determined using an Amplex[®] Red Hydrogen Peroxide/Peroxidase Assay Kit (A22188, Fisher Scientific, Madrid, Spain), according to the method described by Pons et al. [55]. Total of 5×10^4 HT29 cells and 4×10^4 SW620 cells were seeded in each well in a 96-well plate and treated with increasing concentrations of GEN for 48 h. FLx800 microplate fluorescence reader (BIO-TEK, Winooski, VT, USA) was used to measure fluorescence, set at excitation wavelength of 570 nm and emission wavelength of 585 nm. The maximum slope of the increase in the fluorescence was detected within 30 min of exposure to kit reagents. The number of viable cells determined by Hoechst 33342, as previously described, was used to normalize the obtained values.

4.5. RNA Isolation, RT-PCR, and Real-Time PCR

Total of 1.5×10^6 HT29 cells and 2.1×10^6 SW620 cells were seeded in each well in 6-well plates and treated with GEN 100 μM for 48 h. Then, total RNA was isolated by using Tri Reagent[®] (Catalog no. T9424, Sigma-Aldrich) following the manufacturer's protocol. A BioSpec-nano spectrophotometer (Shimadzu Biotech, Kyoto, Japan) was used to quantify the total RNA amount, set at wavelength of 260 nm. The RNA quality was checked by 260/280 and 260/230 ratios.

Then, 1 μg of the total RNA was reverse transcribed to cDNA, according to Pons et al., [55]. cDNA aliquots were frozen after 1/10 dilution in free-RNAase water (-20°C).

A LightCycler 480 System II rapid thermal cycler (Roche Diagnostics, Basel, Switzerland) with SYBR Green technology was used to carry out the real-time PCR. The expression of copper-zinc superoxide dismutase (*SOD1*), manganese superoxide dismutase (*SOD2*), glutathione peroxidase (*GPX1*), catalase (*CAT*), peroxisome proliferator-activated receptor gamma coactivator 1-alpha (*PPARGC1 α*), estrogen-related receptor alpha (*ESRRA*), transcription factor A (*TFAM*), single-stranded mitochondrial binding protein 1 (*SSBP1*), tumor necrosis factor alpha (*TNF*), interleukin-1 beta (*IL1B*), interleukin-8 (*CXCL8*), interleukin-8 receptor (*CXCR2*), heparanase (*HPSE*), interleukin-10 (*IL10*), and peroxisome proliferator-activated receptor gamma (*PPARG*) genes were analyzed, using the expression of beta-2-microglobulin (*B2M*) as housekeeping gene. Genes, primers, and annealing temperatures used are shown in Table 1.

The total reaction volume was processed according to Pons et al. [55], with SYBR green TB Green Premix ExTaq (TAKARA, RR420A). The first step in the amplification program was a preincubation to achieve the denaturation of the template cDNA (5 min, 95 $^\circ\text{C}$), then 40 cycles of denaturation (10 s, 95 $^\circ\text{C}$), followed by annealing (10 s, primer-specific temperature, shown in Table 1) and elongation (12 s, 72 $^\circ\text{C}$). For each gene, a negative control without cDNA was loaded in the real-time PCR.

Table 1. Primers sequences and their respective annealing temperatures and accession number.

Gene	Forward Primer (5'-3') Reverse Primer (5'-3')	Annealing Temperature (°C)	Accession Number
<i>B2M</i>	5'-TTT CAT CCA TCC gAC ATT GA-3' 5'-Cgg CAg gCA TAC TCA TCT TT-3'	54	NM_004048
<i>SOD2</i>	5'-CgT gCT CCC ACA CAT CAA TC-3' 5'-TgA ACg TCA CCg Agg AgA Ag-3'	64	BT006967
<i>SOD1</i>	5'-TCA ggA gAC CAT TgC ATC ATT-3' 5'-CgC TTT CCT gTC TTT gTA CTT TCT TC-3'	64	NM_000454
<i>CAT</i>	5'-CAT CgC CAC ATg AAT ggA TA-3' 5'-CCA ACT ggg ATg AgA ggg TA-3'	61	NM_001752
<i>GPX1</i>	5'-gCg gCg gCC Cag TCg gTg TA-3' 5'-gAg CTT ggg gTC ggT CAT AA-3'	61	M21304
<i>PPARGC1A</i>	5'-TCA gTC CTC ACT ggT ggA CA-3' 5'-TgC TTC gTC gTC AAA AAC Ag-3'	60	AF106698
<i>ESRRA</i>	5'-TCg CTC CTC CTC TCA TCA TT-3' 5'-Tgg CCA AAC CCA AAA ATA AA-3'	52	NM_004451
<i>TFAM</i>	5'-gTg gTT TTC ATC TgT CTT ggC-3' 5'-ACT CCg CCC TAT AAg CAT CTT-3'	60	BT019658
<i>SSBP1</i>	5'-TgT gAA AAA ggg gTC TCg AA-3' 5'-Tgg CCA AAg AAg AAT CAT CC-3'	60	AF277319
<i>TNF</i>	5'-AAg CCT gTA gCC CAT gTT gT-3' 5'-ggA CCT ggg AgT AgA TgA ggT-3'	58	NM_000594
<i>IL1B</i>	5'-TCg CCA gTg AAA TgA Tgg CT-3' 5'-ggT Cgg AgA TTC gTA gCT gg-3'	58	BT007213
<i>CXCL8</i>	5'-ggC ACA AAC TTT CAg AgA CAg CAg-3' 5'-gTT TCT TCC Tgg CTC TTg TCC TAG-3'	66	AK311874
<i>CXCR2</i>	5'-AgT TCT Tgg CAC gTC ATC gT-3' 5'-CCC CTg AAg ACA CCA gTT CC-3'	57	M68932
<i>HPSE</i>	5'-gCA AAC TgC TCA ggA CTg gA-3' 5'-gCT gAC CAA CAT CAg gAC CA-3'	60	AF084467
<i>IL10</i>	5'-ACA TCA Agg CgC ATg TgA AC-3' 5'-CAC ggC CTT gCT CTT gTT TTC-3'	60	M57627
<i>PPARG</i>	5'-gAg CCC AAg TTT gAg TTT gC-3' 5'-CTg TgA ggA CTC Agg gTg gT-3'	61	BT007281
<i>mtDNA</i>	5'-CgT gAC TCC TAC CCC TCA CA-3' 5'-ATC ggg TgA TAg CCA Ag-3'	60	NM_025230.5
<i>18S</i>	5'-ggA CAC ggA CAg gAT TgA CA-3' 5'-ACC CAC ggA ATC gAg AAAGA	60	NR_146119.1

To analyze the Cp values of the real-time PCR, GenEx Standard Software (Multi-DAnalyses, Göteborg, Sweden) was used considering the efficiency of the reaction for each pair of primers and normalizing with the *B2M* housekeeping gene.

4.6. DNA Isolation and Real-Time PCR

Total of 1.5×10^6 HT29 cells and 2.1×10^6 SW620 cells were seeded in 6-well plates and treated with GEN 100 μ M for 48 h. Then, DNA was isolated by using Tri Reagent[®] (Catalog no. T9424, Sigma-Aldrich), following the manufacturer's protocol. A BIO-TEK PowerWave XS spectrophotometer was used to quantify the DNA amount, set at wavelength of 260 nm. The DNA quality was checked by 260/280 ratio. A total amount of 5 ng of DNA was carried out into a real-time PCR, as previously described, and the expression of mitochondrial

DNA (mtDNA) was analyzed, using the expression of *18S* as housekeeping gene. Genes, primers, and annealing temperatures used are shown in Table 1.

4.7. Western Blot Analysis

Total of 8×10^5 HT29 cells and 8×10^5 SW620 cells were seeded in each well in 6-well plates and treated with GEN 100 μ M for 48 h. Cells were harvested in PBS (137 mM NaCl, 2.7 mM KCl, 10 mM Na_2HPO_4 , 2 mM KH_2PO_4 , pH 7.4) with a scraper, and centrifugated at 600 g for 5 min. The pellet was dissolved in RIPA buffer (50 mM Tris-HCl, pH 7.5, 150 mM NaCl, 0.1% SDS, 0.5% deoxycholate, 1% Triton X-100, 1 mM EDTA) with protease inhibitors (Halt protease and phosphatase inhibitor single-use cocktail, EDTA-free 100X, Thermo Scientific 78443) in a proportion of 100:1. Then, cells were sonicated with Vibra Cell Ultrasonic Processor 75185 on ice in three cycles of 25W for 10 s with an interval of 5 s between each pulse and 40% of amplitude. After that, cells were centrifugated at 600 g for 5 min. The supernatant was recovered and the protein amount was quantified by the BCA method (Thermo Scientific™ 23227), following the manufacturer's protocol.

For all SDS-PAGE carried out, 20 μ g of total protein were loaded in each well. Glyceraldehyde-3-phosphate dehydrogenase (GAPDH) was used as loading control. Proteins were separated by electrophoresis on 12% acrylamide/bisacrylamide (30/1) gel, after that, proteins were electrotransferred, by semi-dry electrotransfer, on a 0.2 μ m nitrocellulose membrane (Bio-Rad Laboratories, Hercules, CA, USA) using the Trans-blot Turbo transfer system (Bio-Rad Laboratories, CA, USA). Then, membranes were blocked with 5% non-fat powdered milk in TBS-Tween (Tris Buffer Saline Tween, pH 7.6 containing 0.05% Tween-20) for 1 h at room temperature and agitation. After that, membranes were incubated over night at 4 °C in agitation with primary antibody (5% bovine serum albumin and 0.05% sodium azide in TBS-Tween). The primary antibodies used and their respective dilutions were: copper–zinc superoxide dismutase (CuZnSOD) 1:1000 (Calbiochem, 574597), manganese superoxide dismutase (MnSOD) 1:500 (Santa Cruz, 30080), glutathione peroxidase (GPx) 1:500 (Santa Cruz, 133160), catalase 1:1000 (Calbiochem, 219010), and GAPDH 1:1000 (Santa Cruz, 365062). Finally, membranes were incubated with horseradish peroxidase-conjugated secondary antibody (2% non-fat powdered milk in TBS-Tween) for 1 h at room temperature and agitation. The secondary antibodies used, and their respective dilutions, were: anti-rabbit 1:10,000 (Sigma, A9169), anti-mouse 1:10,000 and 1:2000 for GPx (Sigma, A9044), and anti-sheep 1:10,000 (Sigma, A3415). To detect the immunoreactivity, Immun-Star© Western Chemiluminescence kit Western blotting detection systems (Bio-Rad Laboratories, Hercules, CA, USA) were used. Chemiluminescent signal was acquired with Chemidoc XRS densitometer (Bio-Rad Laboratories, Hercules, CA, USA), and the results were analyzed with Quantity One Software (Bio-Rad Laboratories, Hercules, CA, USA).

4.8. Cell Cycle Analysis

Cell cycle analysis was done by flow cytometry. Total of 9×10^5 HT29 cells and 8×10^5 SW620 cells were seeded in each well in 6-well plates and treated with GEN 100 μ M for 48 h. After that, cells were harvested with trypsin-EDTA and fixed in cold 100% methanol. Fixed cells were incubated at -20 °C overnight and centrifugated for 5 min at $600 \times g$. Before the analysis for DNA staining, cells were incubated at room temperature in the dark for 30 min with an RNAase and propidium iodide mix. Flow cytometry experiments were performed using a Beckton-Dickinson FACSVerse flow cytometer, and the results were analyzed with FACSuite v1.0.6 software.

4.9. Immunocytofluorescence with Confocal Microscopy

Total of 5×10^5 HT29 cells and 5×10^5 SW620 cells were seeded on a glass coverslip inside 6-well plates and treated with GEN 100 μ M for 48 h. Cells were washed with PBS-T (0.1% Tween 20) and then were fixed with 4% paraformaldehyde (Panreac, 141451.1210) in PBS (pH 7.4) for 10 min at room temperature. After that, cells were washed with cold PBS. Permeabilization was carried out with 0.25% Triton X-100 (Sigma, X-100) in PBS for

10 min at room temperature, and then cells were washed with PBS. Then, cells were blocked with 1% BSA (Sigma, A4503-50G) with 22.52 mg/mL glycine (Panreac, A1067) in PBS-T for 30 min at room temperature. After blocking, cells were incubated with NF- κ B primary antibody 1:50 (Santa Cruz, sc-372) with 1% BSA in PBS-T during 1 h in a humidified chamber at room temperature. After incubation, cells were washed with PBS and incubated with anti-rabbit secondary antibody 1:100 (Alexa fluor 555, A-21429, Invitrogen) with 1% BSA in PBS-T for 1 h in a humidified chamber at room temperature in the dark. Before the DNA staining, cells were washed with PBS. For the DNA staining, cells were incubated with 1 μ g/mL Hoechst 33342 (Sigma, B2261) in PBS for 1 min at room temperature in the dark and then washed with PBS. Finally, coverslip was mounted with a drop of DAKO Fluorescent Mounting Medium (DAKO, S3023) and incubated O/N at room temperature in the dark.

The fluorescence was monitored with a Leica TCS-SPE Confocal Microscope, using 63 \times immersion oil (147 N.A.) objective lens. Fluorescence emission was 555 nm.

4.10. Actin Cytoskeleton Remodeling Determination with Confocal Microscopy

Total of 5×10^5 HT29 cells and 5×10^5 SW620 cells were seeded on a glass coverslip inside 6-well plates and treated with GEN 100 μ M for 48 h. Cells were washed with PBS and then were fixed with 4% paraformaldehyde in PBS (pH 7.4) for 10 min at room temperature. After that, cells were washed with PBS and were stained with 0.1 mg/mL Phalloidin-Tetramethylrhodamine B isothiocyanate (1:1000, Sigma, P1951) for 1 h at 37 $^{\circ}$ C. After staining, cells were washed with PBS and, for the DNA staining, cells were incubated with 10 mg/mL DAPI (1:1000, Sigma, D9542) for 10 min at room temperature, and then washed with PBS. Finally, coverslip was mounted with a drop of DAKO Fluorescent Mounting Medium and incubated O/N at room temperature in the dark.

The fluorescence was monitored with a Leica TCS-SPE Confocal Microscope, using 63 \times immersion oil (147 N.A.) objective lens. Fluorescence emission wavelength was 570 nm and fluorescence excitation wavelength was 532 nm.

4.11. Statistical Analysis

Statistical Program for the Social Sciences software for Windows (SPSS, version 24.0; SPSS Inc., Chicago, IL, USA) was used to perform all the statistical analyses. Student's t-test was used to analyze the differences between control and treated cells, with minimal statistical significance at $p < 0.05$. All results are presented as mean values ($n = 6$) \pm standard error of the mean (SEM).

5. Conclusions

High concentrations of genistein induced a decrease in cell viability in colon cancer cells that could be promoted by changes in cell cycle regulation. In colon primary cancer HT29 cells, the increase in cell death promotes a slight raise of oxidative stress that can be mitigated by the increase in mitochondrial biogenesis; the increase in ROS production increments the inflammatory status, and finally, results in a moderate decrease in cell viability. On the other hand, in colon metastatic cancer SW620 cells, the significant increase in ROS production, that cannot be palliated by antioxidant enzymes nor mitochondrial biogenesis, produces a great rise in inflammatory levels, that all together results in a G₂/M cell cycle arrest and a decrease in cell viability. Although further studies are necessary to better understand the role of genistein during anticancer therapy, this work provides new insights into the effects of high doses of this phytoestrogen on the physiology of colon cancer cells.

Author Contributions: Conceptualization: M.A.-C., P.R., J.O., D.G.P. and J.S.-S.; Methodology: M.A.-C., M.T.-M. and P.M.M.-B.; Validation: M.A.-C., M.T.-M., P.M.M.-B., P.R., J.S.-S., J.O. and D.G.P.; Formal analysis: P.R., J.S.-S., D.G.P. and J.O.; Investigation: J.O.; Data curation: M.A.-C., M.T.-M. and P.M.M.-B.; Writing—Original draft preparation: M.A.-C.; Writing—Review and editing: M.A.-C., M.T.-M., P.M.M.-B., P.R., J.O., D.G.P. and J.S.-S.; Supervision: P.R., J.S.-S., J.O. and D.G.P.; Project administration: J.O.; Funding acquisition: J.O. and D.G.P. All authors have read and agreed to the published version of the manuscript.

Funding: This work was supported by grants from Fondo de Investigaciones Sanitarias of Instituto de Salud Carlos III (PI14/01434) of the Spanish Government, co-financed by the FEDER-Unión Europea (“Una manera de hacer Europa”). Margalida Torrens-Mas was supported by a grant from Programa postdoctoral Margalida Comas—Comunidad Autónoma de las Islas Baleares (PD/050/2020).

Institutional Review Board Statement: Not applicable.

Informed Consent Statement: Not applicable.

Data Availability Statement: Not applicable.

Acknowledgments: The authors thank Guillem Ramis from the coelomic unit (IUNICS—UIB) for assistance and the acquisition of the confocal microscopy images, and Catalina Crespi from the cytometry and cell culture unit (IdISBa) for assistance in the flow cytometry.

Conflicts of Interest: The authors declare no conflict of interest.

References

- Ganai, A.A.; Farooqi, H. Bioactivity of genistein: A review of in vitro and in vivo studies. *Biomed. Pharmacother.* **2015**, *76*, 30–38. [[CrossRef](#)] [[PubMed](#)]
- Zamora-Ros, R.; Knaze, V.; Lujan-Barroso, L.; Kuhnle, G.; Mulligan, A.A.; Touillaud, M.; Slimani, N.; Romieu, I.; Powell, N.; Tumino, R.; et al. Dietary intakes and food sources of phytoestrogens in the European Prospective Investigation into Cancer and Nutrition (EPIC) 24-hour dietary recall cohort. *Eur. J. Clin. Nutr.* **2012**, *66*, 932–941. [[CrossRef](#)] [[PubMed](#)]
- Russo, M.; Russo, G.L.; Daglia, M.; Kasi, P.D.; Ravi, S.; Nabavi, S.F.; Nabavi, S.M. Understanding genistein in cancer: The “good” and the “bad” effects: A review. *Food Chem.* **2016**, *196*, 589–600. [[CrossRef](#)] [[PubMed](#)]
- Ferlay, J.; Ervik, M.; Lam, F.; Colombet, M.; Mery, L.; Piñeros, M.; Znaor, A.; Soerjomataram, I.; Bray, F. Global Cancer Observatory: Cancer Today. Available online: <https://gco.iarc.fr/today> (accessed on 1 December 2021).
- Bray, F.; Ferlay, J.; Soerjomataram, I.; Siegel, R.L.; Torre, L.A.; Jemal, A. Global cancer statistics 2018: GLOBOCAN estimates of incidence and mortality worldwide for 36 cancers in 185 countries. *CA Cancer J. Clin.* **2018**, *68*, 394–424. [[CrossRef](#)]
- Morton, M.S.; Arisaka, O.; Miyake, N.; Morgan, L.; Evans, B.A.J. Phytoestrogen Concentrations in Serum from Japanese Men and Women over Forty Years of Age. *J. Nutr.* **2002**, *132*, 3168–3171. [[CrossRef](#)]
- Shafiee, G.; Saidijam, M.; Tavilani, H.; Ghasemkhani, N.; Khodadadi, I. Genistein Induces Apoptosis and Inhibits Proliferation of HT29 Colon Cancer Cells. *Int. J. Mol. Cell Med.* **2016**, *5*, 178–191.
- de Oliveira, M.R. Evidence for genistein as a mitochondriotropic molecule. *Mitochondrion* **2016**, *29*, 35–44. [[CrossRef](#)]
- Fajardo, A.M.; Piazza, G.A. Chemoprevention in gastrointestinal physiology and disease. Anti-inflammatory approaches for colorectal cancer chemoprevention. *Am. J. Physiol. Gastrointest. Liver Physiol.* **2015**, *309*, G59–G70. [[CrossRef](#)]
- Reuter, S.; Gupta, S.C.; Chaturvedi, M.M.; Aggarwal, B.B. Oxidative stress, inflammation, and cancer: How are they linked? *Free. Radic. Biol. Med.* **2010**, *49*, 1603–1616. [[CrossRef](#)]
- Zong, W.; Rabinowitz, J.D.; White, E. Mitochondria and Cancer. *Mol. Cell* **2016**, *61*, 667–676. [[CrossRef](#)]
- Landskron, G.; De La Fuente, M.; Thuwajit, P.; Thuwajit, C.; HERNANDEZ, M.A. Chronic Inflammation and Cytokines in the Tumor Microenvironment. *J. Immunol. Res.* **2014**, *2014*, 149185. [[CrossRef](#)] [[PubMed](#)]
- Wang, G.; Zhang, D.; Yang, S.; Wang, Y.; Tang, Z.; Fu, X. Co-administration of genistein with doxorubicin-loaded polypeptide nanoparticles weakens the metastasis of malignant prostate cancer by amplifying oxidative damage. *Biomater. Sci.* **2018**, *6*, 827–835. [[CrossRef](#)] [[PubMed](#)]
- Sánchez, Y.; Amrán, D.; de Blas, E.; Aller, P. Regulation of genistein-induced differentiation in human acute myeloid leukaemia cells (HL60, NB4): Protein kinase modulation and reactive oxygen species generation. *Biochem. Pharmacol.* **2009**, *77*, 384–396. [[CrossRef](#)] [[PubMed](#)]
- Sánchez, Y.; Amrán, D.; Fernández, C.; De Blas, E.; Aller, P. Genistein selectively potentiates arsenic trioxide-induced apoptosis in human leukemia cells via reactive oxygen species generation and activation of reactive oxygen species-inducible protein kinases (p38-MAPK, AMPK). *Int. J. Cancer* **2008**, *123*, 1205–1214. [[CrossRef](#)] [[PubMed](#)]
- Gorrini, C.; Harris, I.S.; Mak, T.W. Modulation of oxidative stress as an anticancer strategy. *Nat. Rev. Drug Discov.* **2013**, *12*, 931–947. [[CrossRef](#)] [[PubMed](#)]
- Betteridge, D. What Is Oxidative Stress? *Metabolism* **2000**, *49*, 3–8. [[CrossRef](#)]

18. Valko, M.; Rhodes, C.J.; Moncol, J.; Izakovic, M.; Mazur, M. Free radicals, metals and antioxidants in oxidative stress-induced cancer. *Chem. Biol. Interact.* **2006**, *160*, 1–40. [[CrossRef](#)]
19. Ostronoff, L.K.; Izquierdo, J.M.; Enríquez, J.A.; Montoya, J.; Cuezva, J.M. Transient activation of mitochondrial translation regulates the expression of the mitochondrial genome during mammalian mitochondrial differentiation. *Biochem. J.* **1996**, *316*, 183–191. [[CrossRef](#)]
20. Sanchis-Gomar, F.; Garcia-Gimenez, J.; Gomez-Cabrera, M.C.; Pallardo, F. Mitochondrial Biogenesis in Health and Disease. Molecular and Therapeutic Approaches. *Curr. Pharm. Des.* **2014**, *20*, 5619–5633. [[CrossRef](#)]
21. Gaya-Bover, A.; Hernández-López, R.; Alorda-Clara, M.; de la Rosa, J.M.I.; Falcó, E.; Fernández, T.; Company, M.M.; Torrens-Mas, M.; Roca, P.; Oliver, J.; et al. Antioxidant enzymes change in different non-metastatic stages in tumoral and peritumoral tissues of colorectal cancer. *Int. J. Biochem. Cell Biol.* **2020**, *120*, 105698. [[CrossRef](#)]
22. Terzić, J.; Grivennikov, S.; Karin, E.; Karin, M. Inflammation and Colon Cancer. *Gastroenterology* **2010**, *138*, 2101–2114.e5. [[CrossRef](#)] [[PubMed](#)]
23. Chatterjee, S. Oxidative Stress, Inflammation, and Disease. In *Oxidative Stress and Biomaterials*; Elsevier Inc.: Amsterdam, The Netherlands, 2016; ISBN 9780128032701.
24. Neagu, M.; Constantin, C.; Popescu, I.D.; Zipeto, D.; Tzanakakis, G.; Nikitovic, D.; Fenga, C.; Stratakis, C.A.; Spandidos, D.; Tsatsakis, A. Inflammation and Metabolism in Cancer Cell—Mitochondria Key Player. *Front. Oncol.* **2019**, *9*, 348. [[CrossRef](#)] [[PubMed](#)]
25. Missiroli, S.; Genovese, I.; Perrone, M.; Vezzani, B.; Vitto, V.A.M.; Giorgi, C. The Role of Mitochondria in Inflammation: From Cancer to Neurodegenerative Disorders. *J. Clin. Med.* **2020**, *9*, 740. [[CrossRef](#)] [[PubMed](#)]
26. Ahmad, A.; Hayat, I.; Arif, S.; Masud, T.; Khalid, N.; Ahmed, A. Mechanisms Involved in the Therapeutic Effects of Soybean (*Glycine Max*). *Int. J. Food Prop.* **2014**, *17*, 1332–1354. [[CrossRef](#)]
27. Lepri, S.R.; Zanelatto, L.C.; da Silva, P.B.G.; Sartori, D.; Ribeiro, L.R.; Mantovani, M.S. The effects of genistein and daidzein on cell proliferation kinetics in HT29 colon cancer cells: The expression of CTNNBIP1 (β -catenin), APC (adenomatous polyposis coli) and BIRC5 (survivin). *Hum. Cell* **2014**, *27*, 78–84. [[CrossRef](#)]
28. Xiao, X.; Liu, Z.; Wang, R.; Wang, J.; Zhang, S.; Cai, X.; Wu, K.; Bergan, R.C.; Xu, L.; Fan, D. Genistein suppresses FLT4 and inhibits human colorectal cancer metastasis. *Oncotarget* **2015**, *6*, 3225–3239. [[CrossRef](#)]
29. Salti, G.I.; Grewal, S.; Mehta, R.R.; Das Gupta, T.K.; Boddie, A.W., Jr.; Constantinou, A.I. Genistein induces apoptosis and topoisomerase II-mediated DNA breakage in colon cancer cells. *Eur. J. Cancer* **2000**, *36*, 796–802. [[CrossRef](#)]
30. Ning, R.; Chen, G.; Fang, R.; Zhang, Y.; Zhao, W.; Qian, F. Diosmetin inhibits cell proliferation and promotes apoptosis through STAT3/c-Myc signaling pathway in human osteosarcoma cells. *Biol. Res.* **2021**, *54*, 40. [[CrossRef](#)]
31. Galadari, S.; Rahman, A.; Pallichankandy, S.; Thayyullathil, F. Reactive oxygen species and cancer paradox: To promote or to suppress? *Free Radic. Biol. Med.* **2017**, *104*, 144–164. [[CrossRef](#)]
32. Pool-Zobel, B.L.; Adlercreutz, H.; Gleib, M.; Liegibel, U.M.; Sittlison, J.; Rowland, I.; Wähälä, K.; Rechkemmer, G. Isoflavonoids and lignans have different potentials to modulate oxidative genetic damage in human colon cells. *Carcinogenesis* **2000**, *21*, 1247–1252. [[CrossRef](#)]
33. Ullah, M.F.; Ahmad, A.; Zubair, H.; Khan, H.Y.; Wang, Z.; Sarkar, F.H.; Hadi, S.M. Soy isoflavone genistein induces cell death in breast cancer cells through mobilization of endogenous copper ions and generation of reactive oxygen species. *Mol. Nutr. Food Res.* **2011**, *55*, 553–559. [[CrossRef](#)] [[PubMed](#)]
34. Sweeney, E.A.; Inokuchi, J.-I.; Igarashi, Y. Inhibition of sphingolipid induced apoptosis by caspase inhibitors indicates that sphingosine acts in an earlier part of the apoptotic pathway than ceramide. *FEBS Lett.* **1998**, *425*, 61–65. [[CrossRef](#)]
35. Komarnicka, U.K.; Kozioł, S.; Starosta, R.; Kyzioł, A. Selective Cu(I) complex with phosphine-peptide (SarGly) conjugate contra breast cancer: Synthesis, spectroscopic characterization and insight into cytotoxic action. *J. Inorg. Biochem.* **2018**, *186*, 162–175. [[CrossRef](#)] [[PubMed](#)]
36. Svitkina, T.M. Ultrastructure of the actin cytoskeleton. *Curr. Opin. Cell Biol.* **2018**, *54*, 1–8. [[CrossRef](#)] [[PubMed](#)]
37. Aseervatham, J. Cytoskeletal Remodeling in Cancer. *Biology* **2020**, *9*, 385. [[CrossRef](#)]
38. Wang, J.H.-C.; Goldschmidt-Clermont, P.; Yin, F.C.-P. Contractility Affects Stress Fiber Remodeling and Reorientation of Endothelial Cells Subjected to Cyclic Mechanical Stretching. *Ann. Biomed. Eng.* **2000**, *28*, 1165–1171. [[CrossRef](#)]
39. Qian, Y.; Luo, J.; Leonard, S.S.; Harris, G.K.; Millecchia, L.; Flynn, D.C.; Shi, X. Hydrogen Peroxide Formation and Actin Filament Reorganization by Cdc42 Are Essential for Ethanol-induced in Vitro Angiogenesis. *J. Biol. Chem.* **2003**, *278*, 16189–16197. [[CrossRef](#)]
40. Aghajanian, A.; Wittchen, E.S.; Campbell, S.; Burridge, K. Direct Activation of RhoA by Reactive Oxygen Species Requires a Redox-Sensitive Motif. *PLoS ONE* **2009**, *4*, e8045. [[CrossRef](#)]
41. Costanzo, M.; Cesi, V.; Prete, E.; Negroni, A.; Palone, F.; Cucchiara, S.; Oliva, S.; Leter, B.; Stronati, L. Krill oil reduces intestinal inflammation by improving epithelial integrity and impairing adherent-invasive *Escherichia coli* pathogenicity. *Dig. Liver Dis.* **2016**, *48*, 34–42. [[CrossRef](#)]
42. Cui, S.; Wienhoefer, N.; Bilitewski, U. Genistein induces morphology change and G2/M cell cycle arrest by inducing p38 MAPK activation in macrophages. *Int. Immunopharmacol.* **2014**, *18*, 142–150. [[CrossRef](#)]
43. Suliman, H.B.; Carraway, M.S.; Tatro, L.G.; Piantadosi, C.A. A new activating role for CO in cardiac mitochondrial biogenesis. *J. Cell Sci.* **2007**, *120*, 299–308. [[CrossRef](#)] [[PubMed](#)]

44. Schreiber, S.N.; Emter, R.; Hock, M.B.; Knutti, D.; Cardenas, J.; Podvinec, M.; Oakeley, E.J.; Kralli, A. The estrogen-related receptor α (ERR α) functions in PPAR γ coactivator 1 α (PGC-1 α)-induced mitochondrial biogenesis. *Proc. Natl. Acad. Sci. USA* **2004**, *101*, 6472–6477. [[CrossRef](#)] [[PubMed](#)]
45. Uchiumi, T.; Kang, D. The role of TFAM-associated proteins in mitochondrial RNA metabolism. *Biochim. Biophys. Acta-Gen. Subj.* **2012**, *1820*, 565–570. [[CrossRef](#)] [[PubMed](#)]
46. Ruhanen, H.; Borrie, S.; Szabadkai, G.; Tyynismaa, H.; Jones, A.W.; Kang, D.; Taanman, J.-W.; Yasukawa, T. Mitochondrial single-stranded DNA binding protein is required for maintenance of mitochondrial DNA and 7S DNA but is not required for mitochondrial nucleoid organisation. *Biochim. Biophys. Acta-Mol. Cell Res.* **2010**, *1803*, 931–939. [[CrossRef](#)]
47. Lin, C.-S.; Liu, L.-T.; Ou, L.-H.; Pan, S.-C.; Lin, C.-I.; Wei, Y.-H. Role of mitochondrial function in the invasiveness of human colon cancer cells. *Oncol. Rep.* **2018**, *39*, 316–330. [[CrossRef](#)]
48. Wang, S.; Liu, Z.; Wang, L.; Zhang, X. NF- κ B signaling pathway, inflammation and colorectal cancer. *Cell. Mol. Immunol.* **2009**, *6*, 327–334. [[CrossRef](#)]
49. Carter, A.B.; Misyak, S.A.; Hontecillas, R.; Bassaganya-Riera, J. Dietary modulation of inflammation-induced colorectal cancer through PPAR γ . *PPAR Res.* **2009**, *2009*, 498352. [[CrossRef](#)]
50. Vlodaysky, I.; Beckhove, P.; Lerner, I.; Pisano, C.; Meirovitz, A.; Ilan, N.; Elkin, M. Significance of Heparanase in Cancer and Inflammation. *Cancer Microenviron.* **2012**, *5*, 115–132. [[CrossRef](#)]
51. Masola, V.; Zaza, G.; Gambaro, G.; Franchi, M.; Onisto, M. Role of heparanase in tumor progression: Molecular aspects and therapeutic options. *Semin. Cancer Biol.* **2020**, *62*, 86–98. [[CrossRef](#)]
52. Akdis, M.; Burgler, S.; Cramer, R.; Eiwegger, T.; Fujita, H.; Gomez, E.; Klunker, S.; Meyer, N.; O'Mahony, L.; Palomares, O.; et al. Interleukins, from 1 to 37, and interferon- γ : Receptors, functions, and roles in diseases. *J. Allergy Clin. Immunol.* **2011**, *127*, 701–721.e70. [[CrossRef](#)]
53. Luo, Y.; Wang, S.-X.; Zhou, Z.-Q.; Wang, Z.; Zhang, Y.-G.; Zhang, Y.; Zhao, P. Apoptotic effect of genistein on human colon cancer cells via inhibiting the nuclear factor-kappa B (NF- κ B) pathway. *Tumor Biol.* **2014**, *35*, 11483–11488. [[CrossRef](#)] [[PubMed](#)]
54. Zhou, P.; Wang, C.; Hu, Z.; Chen, W.; Qi, W.; Li, A. Genistein induces apoptosis of colon cancer cells by reversal of epithelial-to-mesenchymal via a Notch1/NF-KB/sluc/E-cadherin pathway. *BMC Cancer* **2017**, *17*, 813. [[CrossRef](#)] [[PubMed](#)]
55. Pons, D.G.; Nadal-Serrano, M.; Torrens-Mas, M.; Oliver, J.; Roca, P. The Phytoestrogen Genistein Affects Breast Cancer Cells Treatment Depending on the ER α /ER β Ratio. *J. Cell. Biochem.* **2016**, *117*, 218–229. [[CrossRef](#)] [[PubMed](#)]

5. Recapitulation

The 5-year survival for colorectal cancer (CRC) patients depends on tumor stage at the moment of diagnostic, being the survival rate in stage I about 90%, for stage II about 70%, for stage III of 60%, and for stage IV less than 10% [60,61], exposing the importance of the need of an early CRC diagnosis. CRC screening is active in the Balearic Islands and the gold standard technique is the fecal occult blood test, but this test presents a high rate of false positive results, so the determination of new early CRC biomarkers could improve the overall survival of CRC patients [63,64,134,135]. Nowadays, the treatment election for CRC patients is based on the stage and entity of tumor [169]. This classification is determined by the TNM system, where primary tumor and invasion extension, the presence or absence of metastasis in the regional lymph nodes and the presence or absence of distant metastasis are taken into account [8]. Then, according to primary tumor extension, CRC can be classified in four stages I-IV [8]. At present, clinical practice does not use the molecular markers that are present in tumors, although next-generation sequencing has recently been used for CRC diagnosis based on CRC-related genomic alterations, but this technique is still feasible only in skilled centers [170]. The results obtained in this thesis could indicate that the presence of molecular biomarkers, like oxidative stress, inflammation, and metastasis related proteins, that participate in late phases of the CRC in the early stages, such as stage II, could indicate the preparation of the primary tumor for malignant progression. Results showed changes not only in tumor tissue but also an increase in inflammatory-related proteins expression at molecular level in non-tumor adjacent tissue in different stages of CRC, suggesting that tumor cells and cells from the tumor microenvironment are communicating with each other [171]. Changes at molecular level in non-tumor adjacent tissue could have a role in cancer progression and growth, in addition to be a possible source of diagnostic and prognostic CRC biomarkers. This communication between both cell types could be through the release of extracellular vesicles (EVs) [126].

EVs are particles naturally released from the cell that are delimited by a lipid bilayer and cannot replicate [121]. This lipid bilayer protects the EVs content from degradation and stabilizes it [127,131], and this content varies according to the cell of origin, because it reflects the origin cell status [122]. Finally, the main function of EVs is to participate in cell-cell communication, among others [126]. The primary tumor of a CRC can be

oriented to the lumen of the large bowel and the cells that forms it can release different molecules, some of them included in EVs [127], into the lumen to affect nearby and distant cells [126]. In order to study these EVs from bowel lumen, the presence of EVs in bowel lavage fluid (BLF) was analyzed. BLF is obtained during colonoscopies by the direct application of saline serum to the injured area of the colon [172], for a better collection of the EVs released directly by the cells from the injury area. Unfortunately, nowadays BLF is a rarely used sample, but it has a lot of potential because of the proximity to the tumor [172]. According to our knowledge, this is the first time that EVs are isolated from BLF, and, moreover, the content of these EVs can be used for new biomarker research with molecular biology techniques. Despite this, the BLF use needs to be confirmed in future studies since this is a rarely used sample type. Additionally, these results could be studied in other non-invasive samples, such as stool, for translating the results into clinical practice.

The thesis results corroborated previous studies, which indicate that EVs content depends on the cell of origin because EVs content forms part of the genome, transcriptome, and secretome of the origin cell [122]. The results demonstrated that EVs isolated from BLF from CRC patients presented a different mRNA and miRNA content when it was compared to healthy individuals. To confirm these differences between experimental groups, a validation of the differential content in a larger population cohort would benefit the translational potential of the study. These changes in the EVs mRNA and miRNA content could hypothesize changes in intercellular communication, which were seen in non-tumor adjacent tissues from CRC patients. The EVs released from tumor cells could be the reason why there are changes in non-tumor adjacent tissue in early stages compared to more advanced and metastatic stages.

Metastatic tumors present some characteristics that differ from the primary tumors, such as the importance of inflammation in metastasis, because inflammation has a more important role in metastasis than in first stages of the disease, despite participates in all stages [173], and the decrease in ROS levels during metastasis to avoid cell death [173]. Diet is a risk factor for CRC [174] which participates in oxidative stress [175] and inflammation [176]. Genistein (GEN), a flavonoid found in soybean [46], affects in a different way cells from primary tumor than metastatic tumor, since GEN produces a

decrease in cell viability through the increase of H₂O₂, which cannot be palliated neither by antioxidant enzymes nor mitochondrial biogenesis in the metastatic cells, leading to changes in cell cycle and increasing inflammatory status, which was more accused in the metastatic cell line, as also was the decrease in cell viability. These processes by which GEN decreases cell viability, participate in CRC development, being important for the disease progression [17,43], despite the mechanisms behind the differential response to GEN between cell lines remain unclear. Indeed, our results showed that the content of EVs isolated from BLF of CRC patients presented an enrichment of mRNAs and miRNAs implicated in inflammation and mitochondria and oxidative stress pathways, in addition to pathways related to cell death, proliferation, migration, hypoxia, metabolism, cell-cell communication, and membranes.

According to the results obtained, early stages of CRC, especially stage II, present some molecular changes that are generally expressed in more advanced stages, such as an increase in metastasis-related proteins, which could indicate the importance of the early stages and their possible use as biomarkers for early diagnostic of CRC. The non-tumor adjacent tissue presented an increase in inflammation across the different stages, which could indicate that non-tumor adjacent tissue is affected by communication between its cells and cells from tumor tissue, probably through the release of EVs from tumor cells. These EVs released by CRC cells can be isolated from BLF and its content can also be used as a biomarker source, because EVs content reflects the status of the origin cell. Moreover, the content of these EVs presents a differential expression of mRNAs and miRNAs in CRC patients that were enriched in pathways related to inflammation, mitochondria and oxidative stress, proliferation, and cell death. These processes can be modified by GEN, as high concentrations of GEN affect colon cancer cells depending on if they are from primary tumor or metastatic tumor.

6. Conclusions

1. Early stages of colorectal cancer, such as stage II, present molecular changes that form part of macroscopic changes specific of advanced stages. These molecular changes could be used as molecular markers for an early diagnostic, thus increasing the overall survival of colorectal cancer patients.
2. Colorectal cancer non-tumor adjacent tissue presents changes in inflammation across all stages (I-IV), probably due to the communication between tumor cells and cells from non-adjacent tissue through extracellular vesicles release.
3. Extracellular vesicles released from colorectal cancer cells can be isolated from bowel lavage fluid, and its content could be used as a biomarker source for the diagnosis and prognosis of the disease.
4. The differential content in mRNAs and miRNAs from extracellular vesicles isolated from bowel lavage fluid between colorectal cancer patients and healthy individuals is enriched in different pathways, among which are cell proliferation, mitochondria and oxidative stress, inflammation, and cell death.
5. Processes such as mitochondrial functionality, inflammation, and oxidative stress, together with cell viability, can be altered by genistein, which provokes different response according to the nature of tumor, that is a primary tumor or a metastatic tumor.

7. References

1. Hanahan, D.; Weinberg, R.A. The Hallmarks of Cancer. *Cell* **2000**, *100*, 57–70.
2. Hanahan, D.; Weinberg, R.A. Hallmarks of cancer: The next generation. *Cell* **2011**, *144*, 646–674.
3. Hanahan, D. Hallmarks of Cancer: New Dimensions. *Cancer Discov.* **2022**, *12*, 31–46.
4. Ferlay J, Ervik M, Lam F, Colombet M, Mery L, Piñeros M, Znaor A, Soerjomataram I, B.F. Global Cancer Observatory: Cancer Today Available online: <https://gco.iarc.fr/today> (accessed on Dec 1, 2021).
5. Kuipers, E.J.; Grady, W.M.; Lieberman, D.; Seufferlein, T.; Sung, J.J.; Boelens, P.G.; Velde, C.J.H. van de; Watanabe, T. Colorectal cancer. *Nat Rev Dis Prim.* **2015**, *1*, 1–51.
6. Mármol, I.; Sánchez-de-Diego, C.; Pradilla Dieste, A.; Cerrada, E.; Rodríguez Yoldi, M.J. Colorectal carcinoma: A general overview and future perspectives in colorectal cancer. *Int. J. Mol. Sci.* **2017**, *18*, 197.
7. Giovannucci, E. Molecular Biologic and Epidemiologic Insights for Preventability of Colorectal Cancer. *J. Natl. Cancer Inst.* **2022**, *114*, 645–650.
8. Brierley, J.D.; Gospodarowicz, M.K.; Wittekind, C. *TNM Classification of Malignant Tumors*; Brierley, J.D., Gospodarowicz, M.K., Wittekind, C., Eds.; Eighth Edi.; Wiley-Blackwell, 2017; ISBN 9780323661270.
9. American Cancer Society Available online: <https://www.cancer.org/es/cancer/cancer-de-colon-o-recto/deteccion-diagnostico-clasificacion-por-etapas/clasificacion-de-la-etapa.html> (accessed on Apr 16, 2023).
10. Virginia Oncology Associates Available online: <https://es.virginiacancer.com/colon-rectal/staging/> (accessed on Apr 16, 2023).
11. Bhome, R.; Mellone, M.; Emo, K.; Thomas, G.J.; Sayan, A.E.; Mirnezami, A.H. The Colorectal Cancer Microenvironment: Strategies for Studying the Role of Cancer-Associated Fibroblasts. In *Colorectal Cancer: Methods and Protocols*; 2018; Vol. 1765, pp. 87–98 ISBN 9781493977659.
12. Pin, A.L.; Houle, F.; Huot, J. Recent advances in colorectal cancer research: The microenvironment impact. *Cancer Microenviron.* **2011**, *4*, 127–131.
13. Peddareddigari, V.G.; Wang, D.; Dubois, R.N. The tumor microenvironment in colorectal carcinogenesis. *Cancer Microenviron.* **2010**, *3*, 149–166.
14. Chandra, R.; Karalis, J.D.; Liu, C.; Murimwa, G.Z.; Park, J.V.; Heid, C.A.; Reznik, S.I.; Huang, E.; Minna, J.D.; Brekken, R.A. The colorectal cancer tumor microenvironment and its impact on liver and lung metastasis. *Cancers (Basel)*. **2021**, *13*, 6206.
15. Itatani, Y.; Kawada, K.; Sakai, Y. Transforming growth factor- β signaling pathway in colorectal cancer and its tumor microenvironment. *Int. J. Mol. Sci.* **2019**, *20*, 5822.

16. Zafari, N.; Khosravi, F.; Rezaee, Z.; Esfandyari, S.; Bahiraei, M.; Bahramy, A.; Ferns, G.A.; Avan, A. The role of the tumor microenvironment in colorectal cancer and the potential therapeutic approaches. *J. Clin. Lab. Anal.* **2022**, *36*, e24585.
17. Landskron, G.; Fuente, M. De; Thuwajit, P.; Thuwajit, C.; Hermoso, M.A. Chronic Inflammation and Cytokines in the Tumor Microenvironment. *J Immunol Res* **2014**, *2014*, 1–19.
18. Suarez-carmona, M.; Lesage, J.; Cataldo, D.; Gilles, C. EMT and inflammation : inseparable actors of cancer progression. *Mol. Oncol.* **2017**, *11*, 805–823.
19. Wang, S.; Liu, Z.; Wang, L.; Zhang, X. NF-kappaB signaling pathway, inflammation and colorectal cancer. *Cell. Mol. Immunol.* **2009**, *6*, 327–34.
20. Carter, A.B.; Misyak, S.A.; Hontecillas, R.; Bassaganya-Riera, J. Dietary modulation of inflammation-induced colorectal cancer through PPAR γ . *PPAR Res.* **2009**, *2009*, 1–9.
21. Hong, C.; Tontonoz, P. Coordination of inflammation and metabolism by PPAR and LXR nuclear receptors. *Curr. Opin. Genet. Dev.* **2008**, *18*, 461–467.
22. Paintlia, A.S.; Paintlia, M.K.; Singh, I.; Singh, A.K. IL-4-Induced Peroxisome Proliferator-Activated Receptor γ Activation Inhibits NF- κ B Trans Activation in Central Nervous System (CNS) Glial Cells and Protects Oligodendrocyte Progenitors under Neuroinflammatory Disease Conditions: Implication for CNS-Demyelination. *J. Immunol.* **2006**, *176*, 4385–4398.
23. Akdis, M.; Burgler, S.; Cramer, R.; Eiwegger, T.; Fujita, H.; Gomez, E.; Klunker, S.; Meyer, N.; O'Mahony, L.; Palomares, O.; et al. Interleukins, from 1 to 37, and interferon- γ : Receptors, functions, and roles in diseases. *J. Allergy Clin. Immunol.* **2011**, *127*, 701–721.e70.
24. Balkwill, F.; Mantovani, A. Inflammation and cancer: Back to Virchow? *Lancet* **2001**, *357*, 539–545.
25. Vlodaysky, I.; Beckhove, P.; Lerner, I.; Pisano, C.; Meirovitz, A.; Ilan, N.; Elkin, M. Significance of heparanase in cancer and inflammation. *Cancer Microenviron.* **2012**, *5*, 115–132.
26. Desai, S.J.; Prickril, B.; Avraham, R. Mechanisms of phytonutrient modulation of Cyclooxygenase-2 (COX-2) and inflammation related to cancer. *Nutr. Cancer* **2018**, *70*, 350–375.
27. Sheng, J.; Sun, H.; Yu, F.B.; Li, B.; Zhang, Y.; Zhu, Y.T. The role of cyclooxygenase-2 in colorectal cancer. *Int. J. Med. Sci.* **2020**, *17*, 1095–1101.
28. Eppenberger, M.; Zlobec, I.; Baumhoer, D.; Terracciano, L.; Lugli, A. Role of the VEGF ligand to receptor ratio in the progression of mismatch repair-proficient colorectal cancer. *BMC Cancer* **2010**, *10*, 1–10.
29. Li, X.; Kumar, A.; Zhang, F.; Lee, C.; Tang, Z. Complicated life, complicated VEGF-B. *Trends Mol. Med.* **2012**, *18*, 119–127.

30. Angelescu, C.; Burada, F.; Ioana, M.; Angelescu, R.; Moraru, E.; Riza, A.; Marchian, S.; Mixich, F.; Cruce, M.; Săftoiu, A. VEGF-A and VEGF-B mRNA expression in gastro-oesophageal cancers. *Clin. Transl. Oncol.* **2013**, *15*, 313–320.
31. Mylona, E.; Nomikos, A.; Magkou, C.; Kamberou, M.; Papassideri, I.; Keramopoulos, A.; Nakopoulou, L. The clinicopathological and prognostic significance of membrane type 1 matrix metalloproteinase (MT1-MMP) and MMP-9 according to their localization in invasive breast carcinoma. *Histopathology* **2007**, *50*, 338–347.
32. Zhu, Q.; Gao, R.; Wu, W.; Qin, H. Epithelial-mesenchymal Transition and Its Role in the Pathogenesis of Colorectal Cancer. *Asian Pacific J. Cancer Prev.* **2013**, *14*, 2689–2698.
33. Chattopadhyay, I.; Ambati, R.; Gundamaraju, R. Exploring the Crosstalk between Inflammation and Epithelial-Mesenchymal Transition in Cancer. *Mediators Inflamm.* **2021**, *2021*, 1–13.
34. Huang, Y.; Hong, W.; Wei, X. The molecular mechanisms and therapeutic strategies of EMT in tumor progression and metastasis. *J. Hematol. Oncol.* **2022**, *15*, 1–27.
35. Terzić, J.; Grivennikov, S.; Karin, E.; Karin, M. Inflammation and Colon Cancer. *Gastroenterology* **2010**, *138*, 2101–2114.
36. Zong, W.; Rabinowitz, J.D.; White, E. Mitochondria and Cancer. *Mol. Cell* **2016**, *61*, 667–676.
37. Grasso, D.; Zampieri, L.X.; Capelôa, T.; Van De Velde, J.A.; Sonveaux, P. Mitochondria in cancer. *Cell Stress* **2020**, *4*, 114–146.
38. Lebelo, M.T.; Joubert, A.M.; Visagie, M.H. Warburg effect and its role in tumourigenesis. *Arch. Pharm. Res.* **2019**, *42*, 833–847.
39. Wang, G.; Wang, Q.; Huang, Q.; Chen, Y.; Sun, X.; He, L.; Zhan, L.; Guo, X.; Yin, C.; Fang, Y.; et al. Upregulation of mtSSB by interleukin-6 promotes cell growth through mitochondrial biogenesis-mediated telomerase activation in colorectal cancer. *Int. J. Cancer* **2019**, *144*, 2516–2528.
40. Vasileiou, P.V.S.; Evangelou, K.; Vlasis, K.; Fildisis, G.; Panayiotidis, M.I.; Chronopoulos, E.; Passias, P.G.; Kouloukoussa, M.; Gorgoulis, V.G.; Havaki, S. Mitochondrial homeostasis and cellular senescence. *Cells* **2019**, *8*, 1–25.
41. Popov, L.D. Mitochondrial biogenesis: An update. *J. Cell. Mol. Med.* **2020**, *24*, 4892–4899.
42. Alonso-Molero, J.; González-Donquiles, C.; Fernández-Villa, T.; de Souza-Teixeira, F.; Vilorio-Marqués, L.; Molina, A.J.; Martín, V. Alterations in PGC1 α expression levels are involved in colorectal cancer risk: A qualitative systematic review. *BMC Cancer* **2017**, *17*, 731.
43. Reuter, S.; Gupta, S.C.; Chaturvedi, M.M.; Aggarwal, B.B. Oxidative stress,

- inflammation, and cancer: How are they linked? *Free Radic. Biol. Med.* **2010**, *49*, 1603–1616.
44. Sainz, R.M.; Lombo, F.; Mayo, J.C. Radical decisions in cancer: redox control of cell growth and death. *Cancers (Basel)*. **2012**, *4*, 442–474.
 45. Galadari, S.; Rahman, A.; Pallichankandy, S.; Thayyullathil, F. Reactive oxygen species and cancer paradox: To promote or to suppress? *Free Radic. Biol. Med.* **2017**, *104*, 144–164.
 46. Barone, M.; Tanzi, S.; Lofano, K.; Scavo, M.P.; Guido, R.; Demarinis, L.; Principi, M.B.; Bucci, A.; Di Leo, A. Estrogens, phytoestrogens and colorectal neoproliferative lesions. *Genes Nutr.* **2008**, *3*, 7–13.
 47. Jin, H.; Leng, Q.; Li, C. Dietary flavonoid for preventing colorectal neoplasms. *Cochrane Database Syst. Rev.* **2012**.
 48. Zamora-Ros, R.; Knaze, V.; Luján-Barroso, L.; Kuhnle, G.G.C.; Mulligan, A.A.; Touillaud, M.; Slimani, N.; Romieu, I.; Powell, N.; Tumino, R.; et al. Dietary intakes and food sources of phytoestrogens in the European Prospective Investigation into Cancer and Nutrition (EPIC) 24-hour dietary recall cohort. *Eur. J. Clin. Nutr.* **2012**, *66*, 932–941.
 49. Viggiani, M.T.; Polimeno, L.; Di Leo, A.; Barone, M. Phytoestrogens: Dietary Intake, Bioavailability, and Protective Mechanisms against Colorectal Neoproliferative Lesions. *Nutrients* **2019**, *11*, 1709.
 50. Pampaloni, B.; Palmi, G.; Mavilia, C.; Zonefrati, R.; Tanini, A.; Luisa Brandi, M. In vitro effects of polyphenols on colorectal cancer cells. *World J. Gastrointest. Oncol.* **2014**, *6*, 289–300.
 51. Luo, Y.; Wang, S. xiang; Zhou, Z. quan; Wang, Z.; Zhang, Y. gao; Zhang, Y.; Zhao, P. Apoptotic effect of genistein on human colon cancer cells via inhibiting the nuclear factor-kappa B (NF-κB) pathway. *Tumor Biol.* **2014**, *35*, 11483–11488.
 52. Ganai, A.A.; Farooqi, H. Bioactivity of genistein: A review of in vitro and in vivo studies. *Biomed. Pharmacother.* **2015**, *76*, 30–38.
 53. Fajardo, A.M.; Piazza, G.A. Chemoprevention in gastrointestinal physiology and disease. Anti-inflammatory approaches for colorectal cancer chemoprevention. *Am. J. Physiol. - Gastrointest. Liver Physiol.* **2015**, *309*, G59–G70.
 54. de Oliveira, M.R. Evidence for genistein as a mitochondriotropic molecule. *Mitochondrion* **2016**, *29*, 35–44.
 55. Sánchez, Y.; Amrán, D.; Fernández, C.; De Blas, E.; Aller, P. Genistein selectively potentiates arsenic trioxide-induced apoptosis in human leukemia cells via reactive oxygen species generation and activation of reactive oxygen species-inducible protein kinases (p38-MAPK, AMPK). *Int. J. Cancer* **2008**, *123*, 1205–1214.
 56. Rasheed, S.; Rehman, K.; Shahid, M.; Suhail, S.; Akash, M.S.H. Therapeutic potentials of genistein: New insights and perspectives. *J. Food Biochem.* **2022**,

- 46, e14228.
57. Rendón, J.P.; Cañas, A.I.; Correa, E.; Bedoya-Betancur, V.; Osorio, M.; Castro, C.; Naranjo, T.W. Evaluation of the Effects of Genistein In Vitro as a Chemopreventive Agent for Colorectal Cancer—Strategy to Improve Its Efficiency When Administered Orally. *Molecules* **2022**, *27*, 7042.
 58. Russo, M.; Russo, G.L.; Daglia, M.; Kasi, P.D.; Ravi, S.; Nabavi, S.F.; Nabavi, S.M. Understanding genistein in cancer: The “good” and the “bad” effects: A review. *Food Chem.* **2016**, *196*, 589–600.
 59. Zhou, P.; Wang, C.; Hu, Z.; Chen, W.; Qi, W.; Li, A. Genistein induces apoptosis of colon cancer cells by reversal of epithelial-to-mesenchymal via a Notch1/NF-KB/slug/E-cadherin pathway. *BMC Cancer* **2017**, *17*, 813.
 60. Martins, P.; Martins, S. Assessment of prognosis in patients with stage II colon cancer. *J. Coloproctology* **2015**, *35*, 203–211.
 61. Liu, J.; Huang, X.; Yang, W.; Li, C.; Li, Z.; Zhang, C.; Chen, S.; Wu, G.; Xie, W.; Wei, C.; et al. Nomogram for predicting overall survival in stage II-III colorectal cancer. *Cancer Med.* **2020**, *9*, 2363–2371.
 62. Vega, P.; Valentín, F.; Cubiella, J. Colorectal cancer diagnosis : Pitfalls and opportunities. *World J. Gastrointest. Oncol.* **2015**, *7*, 422–433.
 63. Mammes, A.; Pasquier, J.; Mammes, O.; Conti, M.; Douard, R.; Loric, S. Extracellular vesicles: General features and usefulness in diagnosis and therapeutic management of colorectal cancer. *World J. Gastrointest. Oncol.* **2021**, *13*, 1561–1599.
 64. Świdarska, M.; Choromańska, B.; Dąbrowska, E.; Konarzewska-Duchnowska, E.; Choromanska, K.; Szczurko, G.; Mysliwiec, P.; Dada, J.; Ladny, J.R.; Zwierz, K. The diagnostics of colorectal cancer. *Contemp Oncol (Pozn)* **2014**, *18*, 1–6.
 65. De Vietro, N.; Aresta, A.; Rotelli, M.T.; Zambonin, C.; Lippolis, C.; Picciariello, A.; Altomare, D.F. Relationship between cancer tissue derived and exhaled volatile organic compound from colorectal cancer patients. Preliminary results. *J. Pharm. Biomed. Anal.* **2020**, *180*, 113055.
 66. Mohibul Kabir, K.M.; Donald, W.A. Cancer breath testing: a patent review. *Expert Opin. Ther. Pat.* **2018**, *28*, 227–239.
 67. Haick, H.; Hakim, M. Volatile organic compounds as diagnostic markers for various types of cancer, patent 2011.
 68. Chung, J.; Akter, S.; Han, S.; Shin, Y.; Choi, T.G.; Kang, I.; Kim, S.S. Diagnosis by Volatile Organic Compounds in Exhaled Breath from Patients with Gastric and Colorectal Cancers. *Int. J. Mol. Sci.* **2023**, *24*, 129.
 69. Ohta, R.; Yamada, T.; Sonoda, H.; Matsuda, A.; Shinji, S.; Takahashi, G.; Iwai, T.; Takeda, K.; Ueda, K.; Kuriyama, S.; et al. Detection of KRAS mutations in circulating tumour DNA from plasma and urine of patients with colorectal cancer. *Eur. J. Surg. Oncol.* **2021**.

70. Mallafré-muro, C.; Llambrich, M.; Cumeras, R.; Pardo, A.; Brezmes, J.; Marco, S.; Gumà, J. Comprehensive volatilome and metabolome signatures of colorectal cancer in urine: A systematic review and meta-analysis. *Cancers (Basel)*. **2021**, *13*.
71. Udo, R.; Katsumata, K.; Kuwabara, H.; Enomoto, M.; Ishizaki, T.; Sunamura, M.; Nagakawa, Y.; Soya, R.; Sugimoto, M.; Tsuchida, A. Urinary charged metabolite profiling of colorectal cancer using capillary electrophoresis-mass spectrometry. *Sci. Rep.* **2020**, *10*, 1–10.
72. Ning, W.; Qiao, N.; Zhang, X.; Pei, D.; Wang, W. Metabolic profiling analysis for clinical urine of colorectal cancer. *Asia. Pac. J. Clin. Oncol.* **2021**, *17*, 403–413.
73. Ma, L.; Yu, H.; Zhu, Y.; Xu, K.; Zhao, A.; Ding, L.; Gao, H.; Zhang, M. Isolation and proteomic profiling of urinary exosomes from patients with colorectal cancer. *Proteome Sci.* **2023**, *21*, 1–9.
74. Liu, X.; Wen, J.; Li, C.; Wang, H.; Wang, J.; Zou, H. High-Yield Methylation Markers for Stool-Based Detection of Colorectal Cancer. *Dig. Dis. Sci.* **2019**, *65*, 1710–1719.
75. Vega-Benedetti, A.F.; Loi, E.; Moi, L.; Orrù, S.; Ziranu, P.; Pretta, A.; Lai, E.; Puzzone, M.; Ciccone, L.; Casadei-Gardini, A.; et al. Colorectal Cancer Early Detection in Stool Samples Tracing CpG Islands Methylation Alterations Affecting Gene Expression. *Int. J. Mol. Sci.* **2020**, *21*, 1–16.
76. Jin, S.; Ye, Q.; Hong, Y.; Dai, W.; Zhang, C.; Liu, W.; Guo, Y.; Zhu, D.; Zhang, Z.; Chen, S.; et al. A systematic evaluation of stool DNA preparation protocols for colorectal cancer screening via analysis of DNA methylation biomarkers. *Clin. Chem. Lab. Med.* **2020**, *59*, 91–99.
77. Cheng, Y.C.; Wu, P.H.; Chen, Y.J.; Yang, C.H.; Huang, J.L.; Chou, Y.C.; Chang, P.K.; Wen, C.C.; Jao, S.W.; Huang, H.H.; et al. Using Comorbidity Pattern Analysis to Detect Reliable Methylated Genes in Colorectal Cancer Verified by Stool DNA Test. *Genes (Basel)*. **2021**, *12*.
78. Moradi, K.; Babaei, E.; Feizi, M.A.H.; Safaralizadeh, R.; Rezvani, N. Quantitative detection of SRY-Box 21 (SOX21) gene promoter methylation as a stool-based noninvasive biomarker for early diagnosis of colorectal cancer by MethyLight method. *Indian J. Cancer* **2021**, *58*, 217–224.
79. Ahmed, F.E.; Ahmed, N.C.; Gouda, M.M.; Vos, P.W.; Bonnerup, C. RT-qPCR for Fecal Mature MicroRNA Quantification and Validation. *Methods Mol. Biol.* **2018**, *1765*, 203–215.
80. Gharib, E.; Nazemalhosseini-Mojarad, E.; Baghdar, K.; Nayeri, Z.; Sadeghi, H.; Rezasoltani, S.; Jamshidi-Fard, A.; Larki, P.; Sadeghi, A.; Hashemi, M.; et al. Identification of a stool long non-coding RNAs panel as a potential biomarker for early detection of colorectal cancer. *J. Clin. Lab. Anal.* **2021**, *35*.
81. Komor, M.A.; Bosch, L.J.; Mh Coupé, V.; Rausch, C.; Pham, T. V; Piersma, S.R.; Mongera, S.; Mulder, C.J.; Dekker, E.; Kuipers, E.J.; et al. Proteins in stool as

- biomarkers for non-invasive detection of colorectal adenomas with high risk of progression. *J. Pathol. J Pathol* **2020**, *250*, 288–298.
82. Yang, Y.; Misra, B.B.; Liang, L.; Bi, D.; Weng, W.; Wu, W.; Cai, S.; Qin, H.; Goel, A.; Li, X.; et al. Integrated microbiome and metabolome analysis reveals a novel interplay between commensal bacteria and metabolites in colorectal cancer. *Theranostics* **2019**, *9*, 14.
 83. Song, E.M.; Byeon, J.S.; Lee, S.M.; Yoo, H.J.; Kim, S.J.; Lee, S.H.; Chang, K.; Hwang, S.W.; Yang, D.H.; Jeong, J.Y. Fecal Fatty Acid Profiling as a Potential New Screening Biomarker in Patients with Colorectal Cancer. *Dig. Dis. Sci.* **2018**, *63*, 1229–1236.
 84. Clos-Garcia, M.; Garcia, K.; Alonso, C.; Iruarrizaga-Lejarreta, M.; D’amato, M.; Crespo, A.; Iglesias, A.; Cubiella, J.; Bujanda, L.; Falcón-Pérez, J.M. Integrative Analysis of Fecal Metagenomics and Metabolomics in Colorectal Cancer. *Cancers* **2020**, *Vol. 12*, Page 1142 **2020**, *12*, 1142.
 85. Lin, Y.; Ma, C.; Bezabeh, T.; Wang, Z.; Liang, J.; Huang, Y.; Zhao, J.; Liu, X.; Ye, W.; Tang, W.; et al. ¹H NMR-based metabolomics reveal overlapping discriminatory metabolites and metabolic pathway disturbances between colorectal tumor tissues and fecal samples. *Int. J. Cancer* **2019**, *145*, 1679–1689.
 86. Ding, Q.; Kong, X.; Zhong, W.; Liu, W. Fecal biomarkers : Non-invasive diagnosis of colorectal cancer. *Front. Oncol.* **2022**, *19*, 971930.
 87. Zhang, Z.; Liu, X.; Yang, X.; Jiang, Y.; Li, A.; Cong, J.; Li, Y.; Xie, Q.; Xu, C.; Liu, D. Identification of faecal extracellular vesicles as novel biomarkers for the non-invasive diagnosis and prognosis of colorectal cancer. *J. Extracell. Vesicles* **2023**, *12*, 12300.
 88. Gallardo-Gómez, M.; De Chiara, L.; Álvarez-Chaver, P.; Cubiella, J. Colorectal cancer screening and diagnosis: omics-based technologies for development of a non-invasive blood-based method. *Expert Rev. Anticancer Ther.* **2021**, *21*, 723–738.
 89. Wang, J.Y.; Hsieh, J.S.; Chang, M.Y.; Huang, T.J.; Chen, F.M.; Cheng, T.L.; Alexandersen, K.; Huang, Y.S.; Tzou, W.S.; Lin, S.R. Molecular detection of APC, K-ras, and p53 mutations in the serum of colorectal cancer patients as circulating biomarkers. *World J. Surg.* **2004**, *28*, 721–726.
 90. Hauptman, N.; Glava, D. Colorectal Cancer Blood-Based Biomarkers. *Gastroenterol. Res. Pract.* **2017**.
 91. Bostanci, O.; Sayin, P.; Kiziltan, R.; Algul, S.; Aydin, M.A.; Kemik, O. B7-H3 : A Useful Emerging Diagnostic Marker for Colon Cancer. *Biomed Res. Int.* **2022**, 1–5.
 92. Giessen, C.; Nagel, D.; Glas, M.; Spelsberg, F.; Lau-Werner, U.; Modest, D.P.; Michl, M.; Heinemann, V.; Stieber, P.; Schulz, C. Evaluation of preoperative serum markers for individual patient prognosis in stage I-III rectal cancer. *Tumor Biol.* **2014**, *35*, 10237–10248.

93. Chen, X.; Sun, J.; Wang, X.; Yuan, Y.; Cai, L.; Xie, Y.; Fan, Z.; Liu, K.; Jiao, X. A Meta-Analysis of Proteomic Blood Markers of Colorectal Cancer. *Curr. Med. Chem.* **2021**, *28*, 1176–1196.
94. Villar-Vázquez, R.; Padilla, G.; Fernández-Aceñero, M.J.; Suárez, A.; Fuente, E.; Pastor, C.; Calero, M.; Barderas, R.; Casal, J.I. Development of a novel multiplex beads-based assay for autoantibody detection for colorectal cancer diagnosis. *Proteomics* **2016**, *16*, 1280–1290.
95. Lech, G.; Słotwiński, R.; Słodkowski, M.; Krasnodębski, I.W. Colorectal cancer tumour markers and biomarkers: Recent therapeutic advances. *World J. Gastroenterol.* **2016**, *22*, 1745–1755.
96. Huang, Z.; Huang, D.; Ni, S.; Peng, Z.; Sheng, W.; Du, X. Plasma microRNAs are promising novel biomarkers for early detection of colorectal cancer. *Int. J. Cancer* **2010**, *127*, 118–126.
97. Durán-Vinet, B.; Araya-Castro, K.; Calderón, J.; Vergara, L.; Weber, H.; Retamales, J.; Araya-Castro, P.; Leal-Rojas, P. CRISPR/Cas13-based platforms for a potential next-generation diagnosis of colorectal cancer through exosomes micro-RNA detection: A review. *Cancers (Basel)*. **2021**, *13*, 4640.
98. Sur, D.; Advani, S.; Braithwaite, D. MicroRNA panels as diagnostic biomarkers for colorectal cancer : A systematic review and meta-analysis. *Front. Med.* **2022**, *9*, 915226.
99. Zhang, F.; Zhang, Y.; Zhao, W.; Deng, K.; Wang, Z.; Yang, C.; Ma, L.; Openkova, M.S.; Hou, Y.; Li, K. Metabolomics for biomarker discovery in the diagnosis, prognosis, survival and recurrence of colorectal cancer: A systematic review. *Oncotarget* **2017**, *8*, 35460–35472.
100. Hata, T.; Takemasa, I.; Takahashi, H.; Haraguchi, N.; Nishimura, J.; Hata, T.; Mizushima, T.; Doki, Y.; Mori, M. Downregulation of serum metabolite GTA-446 as a novel potential marker for early detection of colorectal cancer. *Br. J. Cancer* **2017**, *117*, 227–232.
101. Nishiumi, S.; Kobayashi, T.; Kawana, S.; Unno, Y.; Sakai, T.; Okamoto, K.; Yamada, Y.; Sudo, K.; Yamaji, T.; Saito, Y.; et al. Investigations in the possibility of early detection of colorectal cancer by gas chromatography/triple-quadrupole mass spectrometry. *Oncotarget* **2017**, *8*, 17115–17126.
102. Theodoratou, E.; Thaçi, K.; Agakov, F.; Timofeeva, M.N.; Štambuk, J.; Pučić-baković, M.; Vučković, F.; Orchard, P.; Agakova, A.; Din, Farhat, V.N.; et al. Glycosylation of plasma IgG in colorectal cancer prognosis. *Sci. Rep.* **2016**, *6*, 28098.
103. Doherty, M.; Theodoratou, E.; Walsh, I.; Adamczyk, B.; Agakov, F.; Timofeeva, M.; Trbojević-akmačić, I.; Vučković, F.; Duffy, F.; Mcmanus, C.A.; et al. Plasma N -glycans in colorectal cancer risk. *Sci. Rep.* **2018**, *8*, 8655.
104. Coura, M.D.M.A.; Barbosa, E.A.; Brand, G.D.; Bloch, C.; Sousa, J.B. De Identification of Differential N-Glycan Compositions in the Serum and Tissue of

- Colon Cancer Patients by Mass Spectrometry. *Biology (Basel)*. **2021**, *10*, 343.
105. Potter, M.A.; Morris, R.G.; Ferguson, A.; Wyllie, A.H. Detection of Mutations Associated With Colorectal Cancer in DNA From Whole-Gut Lavage Fluid. *J. Natl. Cancer Inst.* **1998**, *90*, 623–626.
 106. Heinzlmann, M.; Neynaber, S.; Heldwein, W.; Folwaczny, C. K-ras and p53 mutations in colonic lavage fluid of patients with colorectal neoplasias. *Digestion* **2001**, *63*, 229–233.
 107. Harada, T.; Yamamoto, E.; Yamano, H.; Nojima, M.; Maruyama, R.; Kumegawa, K.; Masami, A.; Yoshikawa, K.; Kimura, T.; Harada, E.; et al. Analysis of DNA Methylation in Bowel Lavage Fluid for Detection of Colorectal Cancer. *Cancer Prev. Res.* **2014**, *7*, 1002–1010.
 108. Park, Y.S.; Kim, D.S.; Cho, S.W.; Park, J.W.; Jeon, S.J.; Moon, T.J.; Kim, S.H.; Son, B.K.; Oh, T.J.; An, S.; et al. Analysis of syndecan-2 methylation in bowel lavage fluid for the detection of colorectal neoplasm. *Gut Liver* **2018**, *12*, 508–515.
 109. Namavar, F.; Theunissen, E.B.M.; Verweij-Van Vught, A.M.J.J.; Peerbooms, P.G.H.; Bal, M.; Hoitsma, H.F.W.; Maclaren, D.M. Epidemiology of the *Bacteroides fragilis* group in the colonic flora in 10 patients with colonic cancer. *J. Med. Microbiol.* **1989**, *29*, 171–176.
 110. Shen, W.; Sun, J.; Yao, F.; Lin, K.; Yuan, Y.; Chen, Y.; Han, H.; Li, Z.; Zou, J.; Jiao, X. Microbiome in Intestinal Lavage Fluid May Be A Better Indicator in Evaluating The Risk of Developing Colorectal Cancer Compared with Fecal Samples. *Transl. Oncol.* **2020**, *13*, 100772.
 111. Cheng, L.; Han, T.; Zhang, Z.; Yi, P.; Zhang, C.; Zhang, S.; Peng, W. Identification and validation of six autophagy-related long non-coding rnas as prognostic signature in colorectal cancer. *Int. J. Med. Sci.* **2020**, *18*, 88–98.
 112. Buttacavoli, M.; Albanese, N.N.; Roz, E.; Pucci-Minafra, I.; Feo, S.; Cancemi, P. Proteomic profiling of colon cancer tissues: Discovery of new candidate biomarkers. *Int. J. Mol. Sci.* **2020**, *21*.
 113. Vasaikar, S.; Huang, C.; Wang, X.; Petyuk, V.A.; Savage, S.R.; Wen, B.; Dou, Y.; Zhang, Y.; Shi, Z.; Arshad, O.A.; et al. Proteogenomic Analysis of Human Colon Cancer Reveals New Therapeutic Opportunities. *Cell* **2019**, *177*, 1035-1049.e19.
 114. Joo, E.J.; Weyers, A.; Li, G.; Gasimli, L.; Li, L.; Choi, W.J.; Lee, K.B.; Linhardt, R.J. Carbohydrate-Containing Molecules as Potential Biomarkers in Colon Cancer. *Omi. A J. Integr. Biol.* **2014**, *18*, 231–241.
 115. Marolla, A.P.C.; Waisberg, J.; Saba, G.T.; Waisberg, D.R.; Margeotto, F.B.; da Silva Pinhal, M.A. Glycomics expression analysis of sulfated glycosaminoglycans of human colorectal cancer tissues and non-neoplastic mucosa by electrospray ionization mass spectrometry. *einstein* **2015**, *13*, 510–517.
 116. Sethi, M.K.; Kim, H.; Park, C.K.; Baker, M.S.; Paik, Y.; Packer, N.H.; Hancock, W.S.; Fanayan, S.; Thaysen-andersen, M. In-depth N-glycome profiling of paired colorectal cancer and non-tumorigenic tissues reveals cancer-, stage- and EGFR-

- specific protein N-glycosylation. *Glycobiology* **2015**, *25*, 1064–1078.
117. Sethi, M.K.; Hancock, W.S.; Fanayan, S. Identifying N - Glycan Biomarkers in Colorectal Cancer by Mass Spectrometry. *Acc. Chem. Res.* **2016**, *49*, 2099–2106.
 118. Zhang, D.; Xie, Q.; Wang, Q.; Wang, Y.; Miao, J.; Li, L.; Zhang, T.; Cao, X.; Li, Y. Mass spectrometry analysis reveals aberrant N -glycans in colorectal cancer tissues. *Glycobiology* **2019**, *29*, 372–384.
 119. Boyaval, F.; van Zeijl, R.; Dalebout, H.; Holst, S.; van Pelt, G.; Fariña-Sarasqueta, A.; Mesker, W.; Tollenaar, R.; Morreau, H.; Wuhrer, M.; et al. N -Glycomic Signature of Stage II Colorectal Cancer and Its Association With the Tumor Authors N -Glycomic Signature of Stage II Colorectal Cancer and Its Association With the Tumor Microenvironment. *Mol Cell Proteomics* **2021**, *20*, 100057.
 120. Krishn, S.R.; Kaur, S.; Smith, L.M.; Johansson, S.L.; Jain, M.; Patel, A.; Gautam, S.K.; Hollingsworth, M.A.; Mandel, U.; Clausen, H.; et al. Mucins and associated glycan signatures in colon adenoma- carcinoma sequence: prospective pathological implication(s) for early diagnosis of colon cancer. *Cancer Lett.* **2016**, *374*, 304–314.
 121. Théry, C.; Witwer, K.W.; Aikawa, E.; Alcaraz, M.J.; Anderson, J.D.; Andriantsitohaina, R.; Antoniou, A.; Arab, T.; Archer, F.; Atkin-smith, G.K.; et al. Minimal information for studies of extracellular vesicles 2018 (MISEV2018): a position statement of the International Society for Extracellular Vesicles and update of the MISEV2014 guidelines. *J. Extracell. Vesicles* **2018**, *7*, 1535750.
 122. Pap, E. The Role of Microvesicles in Malignancies. *Adv. Exp. Med. Biol.* **2011**, *714*, 183–199.
 123. Siveen, K.S.; Raza, A.; Ahmed, E.I.; Khan, A.Q.; Prabhu, K.S.; Kuttikrishnan, S.; Mateo, J.M.; Zayed, H.; Rasul, K.; Azizi, F.; et al. The Role of Extracellular Vesicles as Modulators of the Tumor Microenvironment , Metastasis and Drug Resistance in Colorectal Cancer. *Cancers (Basel)*. **2019**, *11*, 746.
 124. Dilsiz, N. Role of exosomes and exosomal microRNAs in cancer. *Futur. Sci.* **2020**, *6*.
 125. Mathivanan, S.; Fonseka, P.; Nedeva, C.; Atukorala, I. *New Frontiers : Extracellular Vesicles*; Harris, R.J., Ed.; 2021; ISBN 9783030671709.
 126. Zhou, J.; Li, X.L.; Chen, Z.R.; Chng, W.J. Tumor-derived exosomes in colorectal cancer progression and their clinical applications. *Oncotarget* **2017**, *8*, 100781–100790.
 127. Cheshomi, H.; Matin, M.M. Exosomes and their importance in metastasis, diagnosis, and therapy of colorectal cancer. *J. Cell. Biochem.* **2019**, *120*, 2671–2686.
 128. Ruiz-López, L.; Blancas, I.; Garrido, J.M.; Mut-Salud, N.; Moya-Jódar, M.; Osuna, A.; Rodríguez-Serrano, F. The role of exosomes on colorectal cancer: A review. *J. Gastroenterol. Hepatol.* **2018**, *33*, 792–799.

129. Xiao, Y.; Li, Y.; Yuan, Y.; Liu, B.; Pan, S.; Liu, Q.; Qi, X.; Zhou, H.; Dong, W.; Jia, L. The potential of exosomes derived from colorectal cancer as a biomarker. *Clin. Chim. Acta* **2019**, *490*, 186–193.
130. Lang, T.; Hochheimer, N. Tetraspanins. *Curr. Biol.* **2020**, *30*, R204–R206.
131. Titu, S.; Gata, V.A.; Decea, R.M.; Mocan, T.; Dina, C.; Irimie, A.; Lisencu, C.I. Exosomes in Colorectal Cancer: From Physiology to Clinical Applications. *Int. J. Mol. Sci.* **2023**, *24*, 4382.
132. Shao, H.; Im, H.; Castro, C.M.; Breakefield, X.; Weissleder, R.; Lee, H. *New Technologies for Analysis of Extracellular Vesicles*; 2018; Vol. 118; ISBN 6177268226.
133. Hooten, N.N.; Byappanahalli, A.M.; Vannoy, M.; Omoniyi, V.; Evans, M.K. Influences of age, race, and sex on extracellular vesicle characteristics. *Theranostics* **2022**, *12*, 4459–4476.
134. Lin, J.S.; Piper, M.A.; Perdue, L.A.; Rutter, C.M.; Webber, E.M.; O'Connor, E.; Smith, N.; Whitlock, E.P. Screening for colorectal cancer: Updated evidence report and systematic review for the US preventive services task force. *JAMA - J. Am. Med. Assoc.* **2016**, *315*, 2576–2594.
135. Niedermaier, T.; Balavarca, Y.; Brenner, H. Stage-Specific Sensitivity of Fecal Immunochemical Tests for Detecting Colorectal Cancer: Systematic Review and Meta-Analysis. *Am. J. Gastroenterol.* **2020**, *115*, 56–69.
136. Hernández-López, R.; Torrens-Mas, M.; Pons, D.G.; Company, M.M.; Falcó, E.; Fernández, T.; Ibarra de la Rosa, J.M.; Sastre-Serra, J.; Oliver, J.; Roca, P. Non-tumor adjacent tissue of advanced stage from CRC shows activated antioxidant response. *Free Radic. Biol. Med.* **2018**, *126*, 249–258.
137. Hernández-López, R.; Torrens-Mas, M.; Pons, D.G.; Company, M.M.; Falcó, E.; Fernández, T.; Ibarra de la Rosa, J.M.; Roca, P.; Oliver, J.; Sastre-Serra, J. Mitochondrial Function Differences between Tumor Tissue of Human Metastatic and Premetastatic CRC. *Biology (Basel)*. **2022**, *11*, 1–14.
138. D'Alessio, A.; Proietti, G.; Sica, G.; Scicchitano, B.M. Pathological and molecular features of glioblastoma and its peritumoral tissue. *Cancers (Basel)*. **2019**, *11*.
139. Huang, C.; Liu, H.; Gong, X.; Wen, B.; Chen, D.; Liu, J.; Hu, F. Analysis of different components in the peritumoral tissue microenvironment of colorectal cancer: A potential prospect in tumorigenesis. *Mol. Med. Rep.* **2016**, *14*, 2555–2565.
140. Sanz-Pamplona, R.; Berenguer, A.; Cordero, D.; Molleví, D.G.; Crous-Bou, M.; Sole, X.; Paré-Brunet, L.; Guino, E.; Salazar, R.; Santos, C.; et al. Aberrant gene expression in mucosa adjacent to tumor reveals a molecular crosstalk in colon cancer. *Mol. Cancer* **2014**, *13*, 1–19.
141. Ieda, T.; Tazawa, H.; Okabayashi, H.; Yano, S.; Shigeyasu, K.; Kuroda, S.; Ohara, T.; Noma, K.; Kishimoto, H.; Nishizaki, M.; et al. Visualization of epithelial-mesenchymal transition in an inflammatory microenvironment – colorectal cancer network. *Sci. Rep.* **2019**, *9*, 1–11.

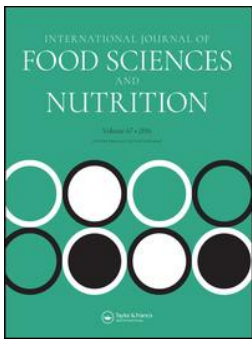
142. Ruiz-López, L.; Blancas, I.; Garrido, J.M.; Mut-Salud, N.; Moya-Jódar, M.; Osuna, A.; Rodríguez-Serrano, F. The role of exosomes on colorectal cancer: A review. *J. Gastroenterol. Hepatol.* **2018**, *33*, 792–799.
143. Bracci, L.; Lozupone, F.; Parolini, I. The role of exosomes in colorectal cancer disease progression and response to therapy. *Cytokine Growth Factor Rev.* **2020**, *51*, 84–91.
144. Xiao, Y.; Zhong, J.; Zhong, B.; Huang, J.; Jiang, L.; Jiang, Y.; Yuan, J.; Sun, J.; Dai, L.; Yang, C.; et al. Exosomes as potential sources of biomarkers in colorectal cancer. *Cancer Lett.* **2020**, *476*, 13–22.
145. Siveen, K.S.; Raza, A.; Ahmed, E.I.; Khan, A.Q.; Prabhu, K.S.; Kuttikrishnan, S.; Mateo, J.M.; Zayed, H.; Rasul, K.; Azizi, F.; et al. The Role of Extracellular Vesicles as Modulators of the Tumor Microenvironment , Metastasis and Drug Resistance in Colorectal Cancer. *Cancers (Basel)*. **2019**, *11*, 746.
146. Rocker, J.M.; DiPalma, J.A.; Pannell, L.K. Rectal Effluent as a Research Tool. *Dig. Dis. Sci.* **2015**, *60*, 24–31.
147. Heinzlmann, M.; Neynaber, S.; Heldwein, W.; Folwaczny, C. K-ras and p53 mutations in colonic lavage fluid of patients with colorectal neoplasias. *Digestion* **2001**, *63*, 229–233.
148. Harada, T.; Yamamoto, E.; Yamano, H.O.; Nojima, M.; Maruyama, R.; Kumegawa, K.; Ashida, M.; Yoshikawa, K.; Kimura, T.; Harada, E.; et al. Analysis of DNA methylation in bowel lavage fluid for detection of colorectal cancer. *Cancer Prev. Res.* **2014**, *7*, 1002–1010.
149. Bray, F.; Ferlay, J.; Soerjomataram, I.; Siegel, R.; Torre, L.; Jemal, A. Global Cancer Statistics 2018: GLOBOCAN Estimates of Incidence and Mortality Worldwide for 36 Cancers in 185 Countries. *CA Cancer J Clin* **2018**, *68*, 394–424.
150. Nadal-Serrano, M.; Pons, D.G.; Sastre-Serra, J.; Blanquer-Rosselló, M. del M.; Roca, P.; Oliver, J. Genistein modulates oxidative stress in breast cancer cell lines according to ER α /ER β ratio: Effects on mitochondrial functionality, sirtuins, uncoupling protein 2 and antioxidant enzymes. *Int. J. Biochem. Cell Biol.* **2013**, *45*, 2045–2051.
151. Pons, D.G.; Nadal-Serrano, M.; Blanquer-Rossello, M.M.; Sastre-Serra, J.; Oliver, J.; Roca, P. Genistein modulates proliferation and mitochondrial functionality in breast cancer cells depending on ER α /ER β ratio. *J. Cell. Biochem.* **2014**, *115*, 949–958.
152. Pons, D.G.; Nadal-Serrano, M.; Torrens-Mas, M.; Oliver, J.; Roca, P. The Phytoestrogen Genistein Affects Breast Cancer Cells Treatment Depending on the ER α /ER β Ratio. *J. Cell. Biochem.* **2016**, *117*, 218–229.
153. Pons, D.G.; Vilanova-Llompart, J.; Gaya-Bover, A.; Alorda-Clara, M.; Oliver, J.; Roca, P.; Sastre-Serra, J. The phytoestrogen genistein affects inflammatory-related genes expression depending on the ER α /ER β ratio in breast cancer cells. *Int. J. Food Sci. Nutr.* **2019**, *0*, 1–9.

154. Santandreu, F.M.; Valle, A.; Oliver, J.; Roca, P. Resveratrol potentiates the cytotoxic oxidative stress induced by chemotherapy in human colon cancer cells. *Cell. Physiol. Biochem.* **2011**, *28*, 219–228.
155. Blanquer-Rosselló, M. del M.; Hernández-López, R.; Roca, P.; Oliver, J.; Valle, A. Resveratrol induces mitochondrial respiration and apoptosis in SW620 colon cancer cells. *Biochim. Biophys. Acta - Gen. Subj.* **2017**, *1861*, 431–440.
156. Sastre-Serra, J.; Ahmiane, Y.; Roca, P.; Oliver, J.; Pons, D.G. Xanthohumol, a hop-derived prenylflavonoid present in beer, impairs mitochondrial functionality of SW620 colon cancer cells. *Int. J. Food Sci. Nutr.* **2019**, *70*, 396–404.
157. Torrens-Mas, M.; Alorda-Clara, M.; Martínez-Vigara, M.; Roca, P.; Sastre-Serra, J.; Oliver, J.; Pons, D.G. Xanthohumol reduces inflammation and cell metabolism in HT29 primary colon cancer cells. *Int. J. Food Sci. Nutr.* **2022**, *73*, 471–479.
158. Wang, G.; Zhang, D.; Yang, S.; Wang, Y.; Tang, Z.; Fu, X. Co-Administration of genistein with doxorubicin-loaded polypeptide nanoparticles weakens the metastasis of malignant prostate cancer by amplifying oxidative damage. *Biomater. Sci.* **2018**, *6*, 827–835.
159. Sánchez, Y.; Amrán, D.; de Blas, E.; Aller, P. Regulation of genistein-induced differentiation in human acute myeloid leukaemia cells (HL60, NB4). Protein kinase modulation and reactive oxygen species generation. *Biochem. Pharmacol.* **2009**, *77*, 384–396.
160. Mangas-sanjuan, C.; Jover, R.; Cubiella, J.; Marzo-Castillejo, M.; Balaguer, F.; Bessa, X.; Bujanda, L.; Bustamante, M.; Castells, A.; Diaz-Tasende, J.; et al. Vigilancia tras resección de pólipos de colon y de cáncer colorrectal. Actualización 2018. *Gastroenterol. Hepatol.* **2019**, *42*, 188–201.
161. Bradford, M.M. A rapid and sensitive method for the quantitation of microgram quantities of protein utilizing the principle of protein-dye binding. *Anal. Biochem.* **1976**, *72*, 248–254.
162. Carvalho, B.S.; Irizarry, R.A. A framework for oligonucleotide microarray preprocessing. *Bioinformatics* **2010**, *26*, 2363–2367.
163. Ru, Y.; Kechris, K.J.; Tabakoff, B.; Hoffman, P.; Radcliffe, R.A.; Bowler, R.; Mahaffey, S.; Rossi, S.; Calin, G.A.; Bemis, L.; et al. The multiMiR R package and database: Integration of microRNA-target interactions along with their disease and drug associations. *Nucleic Acids Res.* **2014**, *42*, e133.
164. Durinck, S.; Spellman, P.T.; Birney, E.; Huber, W. Mapping Identifiers for the Integration of Genomic Datasets with the R/Bioconductor package biomaRt. *Nat. Protoc.* **2009**, *4*, 1184–1191.
165. Bartha, Á.; Györfy, B. TnmpLOT.Com: A web tool for the comparison of gene expression in normal, tumor and metastatic tissues. *Int. J. Mol. Sci.* **2021**, *22*, 1–12.
166. Kern, F.; Fehlmann, T.; Solomon, J.; Schwed, L.; Grammes, N.; Backes, C.; van Keuren-Jensen, K.; Craig, D.W.; Meese, E.; Keller, A. miEAA 2.0: Integrating

- multi-species microRNA enrichment analysis and workflow management systems. *Nucleic Acids Res.* **2020**, *48*, W521–W528.
167. Marisa, L.; de Reyniès, A.; Duval, A.; Selves, J.; Gaub, M.P.; Vescovo, L.; Etienne-Grimaldi, M.-C.; Schiappa, R.; Guenot, D.; Ayadi, M.; et al. Gene expression classification of colon cancer into molecular subtypes: characterization, validation, and prognostic value. *PLoS Med.* **2013**, *10*, e1001453.
168. Provenzani, A.; Fronza, R.; Loreni, F.; Pascale, A.; Amadio, M.; Quattrone, A. Global alterations in mRNA polysomal recruitment in a cell model of colorectal cancer progression to metastasis. *Carcinogenesis* **2006**, *27*, 1323–1333.
169. Glatzer, M.; Panje, C.M.; Sirén, C.; Cihoric, N.; Putora, P.M. Decision Making Criteria in Oncology. *Oncology* **2020**, *98*, 370–378.
170. Abbes, S.; Baldi, S.; Sellami, H.; Amedei, A.; Keskes, L. Molecular methods for colorectal cancer screening: Progress with next-generation sequencing evolution. *World J. Gastrointest. Oncol.* **2023**, *15*, 425–442.
171. Melo, S.A.; Sugimoto, H.; Connell, J.T.O.; Kato, N.; Villanueva, A.; Vidal, A.; Qiu, L.; Vitkin, E.; Perelman, L.T.; Melo, C.A.; et al. Cancer Exosomes Perform Cell-Independent MicroRNA Biogenesis and Promote Tumorigenesis. *Cancer Cell* **2014**, *26*, 707–721.
172. Rocker, J.M.; DiPalma, J.A.; Pannell, L.K. Rectal Effluent as a Research Tool. *Dig. Dis. Sci.* **2015**, *60*, 24–31.
173. Greten, F.R.; Grivennikov, S.I. Inflammation and Cancer: Triggers, Mechanisms and Consequences. *Immunity* **2019**, *51*, 27–41.
174. Baena, R.; Salinas, P. Diet and colorectal cancer. *Maturitas* **2015**, *80*, 258–264.
175. Aleksandrova, K.; Koelman, L.; Rodrigues, C.E. Dietary patterns and biomarkers of oxidative stress and inflammation: A systematic review of observational and intervention studies. *Redox Biol.* **2021**, *42*, 101869.
176. Galland, L. Diet and inflammation. *Nutr. Clin. Pract.* **2010**, *25*, 634–640.

The phytoestrogen genistein affects inflammatory-related genes expression depending on the ER α /ER β ratio in breast cancer cells.

Pons, D. G., Vilanova-Llompart, J., Gaya-Bover, A., Alorda-Clara, M., Oliver, J., Roca, P., & Sastre-Serra, J. (2019). *International Journal of Food Sciences and Nutrition*, 70(8), 941-949.



The phytoestrogen genistein affects inflammatory-related genes expression depending on the ER α /ER β ratio in breast cancer cells

Daniel Gabriel Pons, Joana Vilanova-Llompart, Auba Gaya-Bover, Marina Alorda-Clara, Jordi Oliver, Pilar Roca & Jorge Sastre-Serra

To cite this article: Daniel Gabriel Pons, Joana Vilanova-Llompart, Auba Gaya-Bover, Marina Alorda-Clara, Jordi Oliver, Pilar Roca & Jorge Sastre-Serra (2019): The phytoestrogen genistein affects inflammatory-related genes expression depending on the ER α /ER β ratio in breast cancer cells, International Journal of Food Sciences and Nutrition, DOI: [10.1080/09637486.2019.1597025](https://doi.org/10.1080/09637486.2019.1597025)

To link to this article: <https://doi.org/10.1080/09637486.2019.1597025>



Published online: 04 Apr 2019.



Submit your article to this journal [↗](#)









View Crossmark data [↗](#)

RESEARCH ARTICLE



The phytoestrogen genistein affects inflammatory-related genes expression depending on the ER α /ER β ratio in breast cancer cells

Daniel Gabriel Pons^{a,b} , Joana Vilanova-Llompart^a, Auba Gaya-Bover^{a,b} , Marina Alorda-Clara^{a,b} , Jordi Oliver^{a,b,c} , Pilar Roca^{a,b,c}  and Jorge Sastre-Serra^{a,b,c} 

^aGrupo Multidisciplinar de Oncología Traslacional Institut, Universitari d'Investigació en Ciències de la Salut (IUNICS) Universitat de les Illes Balears, Palma de Mallorca, Spain; ^bInstituto de Investigación Sanitaria de las Islas Baleares (IdISBa), Hospital Universitario Son Espases, edificio S, Palma de Mallorca, Spain; ^cCiber Fisiopatología Obesidad y Nutrición (CB06/03) Instituto Salud Carlos III, Madrid, Spain

ABSTRACT

Breast cancer is the most common malignancy in women of developed countries. The aim of this study was to investigate the effects of the phytoestrogen genistein on the inflammatory profile in three breast cancer cell lines with different oestrogen receptors alpha (ER α) and beta (ER β) ratio. MCF-7 (high ER α /ER β ratio), T47D (low ER α /ER β ratio), and MDA-MB-231 (ER α -negative) cells were treated with 1 μ M of genistein for 48 h (cell proliferation and ROS production) or 4 h (mRNA expression of 18S, ER α , ER β , pS2, Sirtuin1, IL-1 β , NF- κ B, COX-2, TGF β 1, PPAR γ). Genistein caused a significant decrease in cell viability and an increase in ROS production in MCF-7, and the opposite happens in T47D cells. In addition, genistein rise pro-inflammatory and reduced anti-inflammatory genes expression in MCF-7, provoking the opposite effects in T47D cells. In conclusion, the phytoestrogen genistein could modulate the expression of inflammatory-related genes through its interaction with both ERs, and its effects depends on the ER α /ER β ratio.

ARTICLE HISTORY

Received 12 November 2018
Revised 11 March 2019
Accepted 15 March 2019

KEYWORDS

Breast cancer; genistein;
ER α /ER β ratio;
inflammation; sirtuin

Introduction

Breast cancer is one of the most commonly diagnosed malignancies leading to cancer-related deaths in women worldwide (Cronin et al. 2018). The origin of most cases of breast cancer is still unknown, but according to previous studies, the combination of genetic, epigenetic and environmental factors has been identified (Fernández et al. 2018).

Lifestyle has also been closely related to the frequency of breast cancer. The main risk factors identified are diet, alcohol, exposure to radiation and exposure to hormones, specially oestrogens, including physiological variations associated with menarche, pregnancy, menopause, hormonal contraceptive use and/or therapy hormone replacement (Dieterich et al. 2014).

The exposure to circulating oestrogens, which can be done throughout a woman's life, has been considered a risk factor for breast cancer (James et al. 2011). The role of oestrogen in hormonal carcinogenesis has already been investigated in cell cultures, animal models and humans. Numerous studies have linked endogenous and exogenous hormones with breast and ovarian cancer development.

Oestrogen action is mediated through binding to oestrogen receptors (ER), the ER α and ER β , which belong to the nuclear steroid receptors type I superfamily, also known as steroid receptors (Kumar et al. 1987). Previous studies suggest that the oestrogen-stimulated proliferative response is determined by the ER α /ER β ratio. ER α effects are related to proliferative processes, while the ER β is related to antiproliferative and differentiation processes. Both receptors can form a heterodimer, and ER β decreases the sensitivity of E2 for the ER α , acting as a physiological regulator of the proliferative effects of ER α (Helguero et al. 2005; Hartman et al. 2009). Recent studies carried out in our research group demonstrated the influence of ER α /ER β ratio in the oxidative stress, the mitochondrial biogenesis, dynamic and functionality and the response to antitumoral treatments in breast cancer (Nadal-Serrano et al. 2012; Sastre-Serra et al. 2012a, 2012b; Pons et al. 2015).

Phytoestrogens are a class of plant-derived compounds that are characterised by a structure similar to the principal mammalian oestrogen, 17 β -oestradiol (E2), and which have been classically defined as

possible selective modulators of oestrogen receptors. The initial interest of phytoestrogens as potential therapeutic agents in breast cancer was attributed to the low incidence of the disease in Asian countries, where natural products containing soy, a rich source of phytoestrogens, are an important component of the diet. Its beneficial properties for health have been described in different types of cancer, including breast cancer (Kostelac et al. 2003). One of the most studied phytoestrogen is genistein (GEN), because it is the predominant phytoestrogen in soy products and, as stated above, the previous epidemiological studies have shown an inverse correlation between the intake of GEN and the incidence of breast cancer (Adlercreutz 2002; Nadal-Serrano et al. 2013). It has been shown that GEN has anticancer properties such as the induction of apoptosis and differentiation, inhibition of cell cycle progression, angiogenesis and metastasis. Moreover, previous results in our research group and other authors have demonstrated that GEN has antioxidant activity (Ruiz-Larrea et al. 1997; Nadal-Serrano et al. 2013).

GEN is a phytoestrogen which binds to ER β with much more affinity than to ER α , has 30 times more affinity for ER β compared to ER α , and this binding has implications related to the risk of breast cancer in cells with different ER α /ER β ratio (Kuiper et al. 1997). Barros et al. suggest that when ER β is activated by certain ligands, this activated complex inhibits the growth of breast cancer cells as well as the stimulatory effects of ER α (Barros et al. 2006). For this reason, a lot of in vitro and in vivo studies support that GEN it could be a chemopreventive agent for the treatment of different types of cancer (Mukund et al. 2017).

Recently, GEN has been considered to have anti-inflammatory properties (Spagnuolo et al. 2015). Inflammation plays a very important role in carcinogenesis, especially in cancers related to the hormonal environment, such as breast cancer. There are several types of signalling molecules that are involved in inflammation. The function and expression of these molecules can be altered by genetic mutations or by environmental factors (Verdrengh et al. 2003). GEN may play its role as an anti-inflammatory agent by negatively regulating the transduction of cytokine-induced signals in cells of the immune system (Verdrengh et al. 2003). There is a link between cell proliferation, oxidative stress and inflammation, where a sustained oxidative stress can lead to chronic inflammation, and this inflammation could be related to the regulation of cell proliferation-related genes expression (Reuter et al. 2010).

The aim of the present study was to investigate the effects of the treatment with a physiological concentration of the phytoestrogen genistein on the expression of both oestrogen receptors, pS2, inflammatory-related genes and Sirtuin 1; and cell proliferation and ROS production in breast cancer cell lines with different ER α /ER β ratio.

Materials and methods

Materials

Genistein and dimethyl sulfoxide (DMSO) were purchased from Sigma-Aldrich (St. Louis, MO, USA). Primers were purchased from Metabion (Planegg, Germany). Routine chemicals were supplied by Takara Bio Inc. (Kusatsu, Japan), Panreac (Barcelona, Spain), Sigma-Aldrich and Bio-Rad Laboratories (Hercules, CA).

Cell culture and treatment

Human breast cancer cell lines were obtained from ATCC and maintained in Dulbecco's modified Eagle's medium (DMEM) with phenol red supplemented with 10% foetal bovine serum (FBS) and 1% penicillin/streptomycin cocktail in 5% CO₂ atmosphere at 37°C until the experiments were performed. The three breast cancer cell lines are well characterised, especially for the oestrogen receptors supply. Thus, MCF-7 cells have an elevated ER α /ER β ratio, T47D cells show a low ER α /ER β ratio, while MDA-MB-231 cells do not present ER α , and very little amount of ER β , therefore, these cells are often considered as negative for oestrogen receptors (Pons et al. 2014). To evaluate the effect of physiological concentrations of genistein, cells were treated with 1 μ M of this phytoestrogen, which is the serum concentration of genistein in regular consumer of soy-rich products (Morton et al. 2002). Twenty-four hours before the treatment with vehicle or genistein, cells were shifted to phenol red-free DMEM with 10% charcoal stripped-FBS and 1% of antibiotics. Vehicle-treated cells were treated with 0.001% DMSO.

Cell viability assay

Cells were seeded in 96-well plates at 10,000 cells per well. Twenty-four hours before treatment, cells were shifted to phenol red-free DMEM supplemented with charcoal-FBS. Then cells were treated with vehicle or genistein for 48 hours. The number of viable cells was determined by DNA binding Hoechst 33342

fluorescence (Richards et al. 1985). Briefly, after 48 h of vehicle or genistein treatment, DMEM was removed and each well was washed once with PBS. Then, 100 µl of 5 µg/ml Hoechst 33342 solution were added and incubated for 5 min at 37 °C. Fluorescence was measured at 350 nm of excitation length and 455 nm of emission length.

ROS production

Cells were plated in 96-well plates at 10,000 cells per well. Twenty-four hours before treatment, cells were shifted to phenol red-free DMEM supplemented with charcoal-FBS. Then cells were treated with vehicle or genistein for 48 hours. ROS production was determined by the addition of 10 µM 2',7'-dichlorofluorescein diacetate (DCFDA). Plates were then incubated for 90 min at 37 °C. Assay was performed at 37 °C in a 96-well microplate fluorimeter FLx800 (BIO-TEK instruments, Winooski, VT). The production of hydrogen peroxide was measured by the increase in fluorescence (excitation at 485 nm and emission at 530 nm) by measurements of fluorescence every 15 min. The slope obtained was normalised with the cell viability assay to correct the effect of treatment in the number of cells.

RT-PCR

Cells were cultured in six-well plates and 24 hours before treatment, cells were shifted to phenol red-free DMEM supplemented with charcoal-FBS. Then cells were treated with vehicle or genistein for 4 hours. Total RNA was isolated from cells using Tri-Reagent® (Sigma-Aldrich) following the manufacturer's protocol and quantified using a BioSpec-nano spectrophotometer (Shimadzu Biotech, Kyoto, Japan) set at 260 nm. One microgram of total RNA was reverse transcribed to cDNA at 42 °C for 60 min with 25 U of MuLV reverse transcriptase in a 10 µl volume of retrotranscription reaction mixture containing 10 mM Tris-HCl (pH 9.0), 50 mM KCl, 0.1% Triton X-100, 2.5 mM MgCl₂, 2.5 mM random hexamers, 10 U RNAase inhibitor, and 500 mM of each dNTP. Each resulting cDNA was diluted 1/10.

PCR was done for the target genes showed in Table 1 using SYBR green technology on a Light-Cycler 480 rapid thermal cycler (Roche Diagnostics, Basel, Switzerland). Total reaction volume was 10 µl, containing 7.5 µl Lightcycler® 480 aster SYBR Green I (with 0.5 µM sense and antisense specific primers) and 2.5 µl of the cDNA template. The amplification programme

Table 1. Primers and conditions used for RT-PCR.

Gene	Forward primer (5'-3')	T An. (°C)
	Reverse Primer (5'-3')	
<i>18s</i>	ggA CAC ggA Cag gAT TgA CA ACC CAC ggA ATC gAg AAA gA	60
<i>esr1 (ERα)</i>	AAT TCA gAT AAT CgA CgC CAg gTg TTT CAA CAT TCT CCC TCC Tg	60
<i>esr2 (ERβ)</i>	TAg Tgg TCC ATC gCC AgT TAT ggg AgC CAC ACT TCA CCA T	64
<i>ps2</i>	TTg Tgg TTT TCC Tgg TgT ACA gCA gAT CCC TgC AgA AgT gT	60
<i>sirt1</i>	gCA gAT TAg TAg gCg gCT Tg TCT ggC ATg TCC CAC TAT CA	54
<i>il-1β</i>	CAg AAg TAC CTg AgC TcG CC ggT Cgg AgA TTC gTA gCT gg	63
<i>nfixb</i>	CCT ggA TgA CTC TTg ggA AA TCA gCC AgC TgT TTC ATg TC	58
<i>cox-2</i>	CCC TTC TgC CTg ACA CCT TT TTC TgT ACT gCg ggT ggA AC	60
<i>tgfb1</i>	TCC Tgg CgA TAC CTC AgC AA Cgg TAg TgA ACC CgT TgA Tg	60
<i>pparγ</i>	gAg CCC AAg TTT gAg TTT gC CTg TgA ggA CTC Agg gTg gT	61

consisted of a preincubation step for denaturation (10 min 95 °C) followed by 40 cycles consisting of a denaturation step (10 s, 95 °C), an annealing step (10 s, temperature depends on each pair of specific primers), and an extension step (12 s, 72 °C for all). A negative control without cDNA template was run in each assay.

The Ct values of the real-time PCR were analysed, considering the efficiency of the reaction and referring these results to the total DNA amount, using the GenEx Standard Software (MultiDAnalises, Sweden).

Statistical analysis

The statistical analyses were performed with the Statistical Programme for the Social Sciences software for Windows (SPSS, version 21.0; SPSS Inc, Chicago, IL). Data are presented as mean ± standard error of the mean (SEM). The statistical differences between vehicle- and genistein-treated cells were analysed using a Student's *t*-test. Statistical significance was set at $p < 0.05$.

Results

Effects of genistein treatment on cell viability

As shown in Figure 1, GEN exerted different effects in breast cancer cells depending on the ERα/ERβ ratio. In MCF-7 cells, genistein promoted a significant increment on cell proliferation (+12%). However, the GEN treatment in T47D and MDA-MB-231 cells triggered a significant decrease in cell viability by -6% and -5%, respectively.

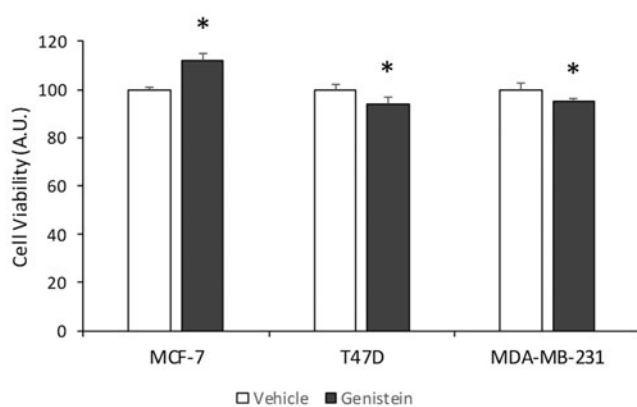


Figure 1. Effects of genistein on MCF-7, T47D, and MDA-MB-231 breast cancer cell lines viability. Cancer cells were incubated for 48 h with vehicle (0.001% DMSO) or 1 μ M of genistein. Cell viability was assessed by DNA staining with Hoechst 33342 and represented as percentage with respect to vehicle-treated cells of each cell line. Data represent means \pm SEM. Statistically significant difference between treated and vehicle-treated cells (Student's *t*-test, * $p < 0.05$, $n = 6$). A.U.: arbitrary units.

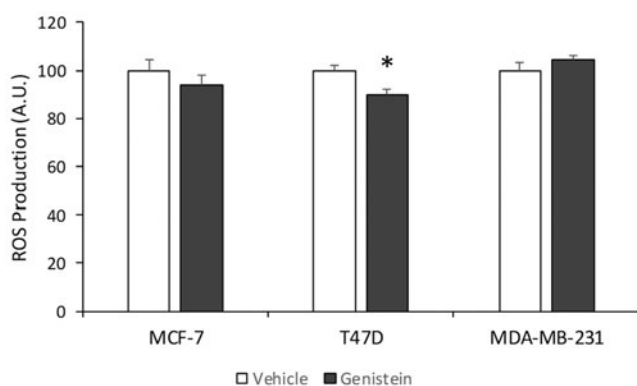


Figure 2. Effects of genistein on MCF-7, T47D, and MDA-MB-231 breast cancer cell lines ROS production. Cancer cells were incubated for 48 h with vehicle (0.001% DMSO) or 1 μ M of genistein. ROS production was assessed by DCF-DA assay. The slope was obtained after 90 min of incubation with DCF-DA and the values obtained were normalised with the cell viability assay to correct the effect of treatment in the number of cells. Data are represented as percentage with respect to vehicle-treated cells of each cell line. Data represent means \pm SEM. Statistically significant difference between treated and vehicle-treated cells (Student's *t*-test, * $p < 0.05$, $n = 6$). A.U.: arbitrary units.

Effects of genistein treatment on ROS production

The Figure 2 shows that GEN treatment caused a significant decrease in ROS production in T47D cells (–10%), while in MCF-7 and MDA-MB-231 cells, the treatment with this phytoestrogen did not yield any significant difference in ROS production regarding the vehicle-treated cells.

Effects of genistein treatment on gene expression

Table 2 shows that GEN treatment significantly affected the expression of both oestrogen receptors (ERs) in MCF-7 and T47D, with no significant changes in MDA-MB-231 cells. In MCF-7 breast cancer cells, GEN treatment decreased the expression of ER α (1.00 vs. 0.47), with the subsequent increment of human oestrogen-responsive gene pS2 expression (1.00 vs. 1.40); moreover, GEN greatly increased the expression of ER β (1.00 vs. 2.61). In T47D breast cancer cells, GEN treatment increased the expression of ER α (1.00 vs. 1.86) and, in a dramatically way, the expression of ER β by four times (1.00 vs. 4.00). It is important to note that the expression of pS2 did not present any significant modification after GEN treatment both in T47D and MDA-MB-231 cells.

As shown in the Table 3, GEN treatment triggered a significant fall in Sirt1 mRNA expression in MCF-7 cells (1.00 vs. 0.76), while in T47D the GEN treatment resulted in a very significant raise of Sirt1 expression (1.00 vs. 1.64). The expression of Sirt1 did not raise any significant change in GEN-treated MDA-MB-231 cells.

Additionally, the Table 3 shows the expression of inflammatory-related genes. In the table it can be observed that GEN treatment significantly increased the expression of COX2 gene (1.00 vs. 1.53) in MCF-7 cells, with no significant changes in IL-1 β and NF κ B mRNA expression levels in these cells. The treatment with the phytoestrogen genistein provoked a statistically significant decrease in IL-1 β expression (1.00 vs. 0.45) in T47D cells, with no significant changes in NF κ B and COX2 mRNA expression levels. In MDA-MB-231 breast cancer cell line, the GEN treatment did not raise any significant changes in the expression of the pro-inflammatory genes.

Finally, in the Table 3 are shown two anti-inflammatory-related genes, TFG β and PPAR γ . As it can be observed in the figure, in MCF-7 cells, GEN treatment caused a significant decrease in the expression of TFG β (1.00 vs. 0.64) and PPAR γ (1.00 vs. 0.67). Moreover, in T47D cells, GEN treatment significantly increased the expression of TFG- β (1.00 vs. 1.49) and PPAR γ (1.00 vs. 1.45). In MDA-MB-231 cells, GEN treatment did not change the expression of any anti-inflammatory-related gene.

Discussion

Chronic inflammation is associated with the development of a variety of epithelial cancers. According to previous studies, the chronic inflammatory

Table 2. Relative expression of oestrogen receptors (ER α and ER β) and p52 in MCF-7, T47D and MDA-MB-231 breast cancer cell lines

Gene	MCF-7		T47D		MDA-MB-231	
	Vehicle	GEN	Vehicle	GEN	Vehicle	GEN
ER α	1.00 \pm 0.17	0.47 \pm 0.06*	1.00 \pm 0.16	1.86 \pm 0.16*	UD	UD
ER β	1.00 \pm 0.22	2.61 \pm 0.62*	1.00 \pm 0.19	4.00 \pm 0.44*	1.00 \pm 0.26	1.34 \pm 0.35
p52	1.00 \pm 0.13	1.40 \pm 0.11*	1.00 \pm 0.15	0.90 \pm 0.04	1.00 \pm 0.07	0.98 \pm 0.16

Cancer cells were incubated for 4 h with vehicle (0.001% DMSO) or 1 μ M of genistein. Data are represented as relative mRNA expression with respect to vehicle-treated cells of each cell line. Data represent means \pm SEM. Statistically significant difference between treated and vehicle-treated cells (Student's *t*-test, **p* < 0.05, *n* = 6).

Table 3. Relative expression of Sirt1 and Inflammation-related genes in MCF-7, T47D and MDA-MB-231 breast cancer cell lines.

Gene	MCF-7		T47D		MDA-MB-231	
	Vehicle	GEN	Vehicle	GEN	Vehicle	GEN
Sirt1	1.00 \pm 0.06	0.76 \pm 0.07*	1.00 \pm 0.15	1.64 \pm 0.04*	1.00 \pm 0.18	1.24 \pm 0.17
IL-1 β	1.00 \pm 0.56	1.15 \pm 0.39	1.00 \pm 0.13	0.45 \pm 0.12*	1.00 \pm 0.14	1.22 \pm 0.22
NF- κ B	1.00 \pm 0.14	0.78 \pm 0.10	1.00 \pm 0.11	1.19 \pm 0.09	1.00 \pm 0.11	1.14 \pm 0.19
COX-2	1.00 \pm 0.19	1.53 \pm 0.16*	1.00 \pm 0.18	1.21 \pm 0.38	1.00 \pm 0.17	1.35 \pm 0.26
TFG β	1.00 \pm 0.16	0.64 \pm 0.05*	1.00 \pm 0.14	1.49 \pm 0.14*	1.00 \pm 0.17	1.13 \pm 0.13
PPAR γ	1.00 \pm 0.12	0.67 \pm 0.10*	1.00 \pm 0.15	1.45 \pm 0.29*	1.00 \pm 0.10	1.03 \pm 0.12

Cancer cells were incubated for 4 h with vehicle (0.001% DMSO) or 1 μ M of genistein. Data are represented as relative mRNA expression with respect to vehicle-treated cells of each cell line. Data represent means \pm SEM. Statistically significant difference between treated and vehicle-treated cells (Student's *t*-test, **p* < 0.05, *n* = 6).

environment causes genomic alterations that eventually lead to the development of the tumour. The essential components in this association are the cytokines produced by the tumour cells themselves, as well as by the innate immune cells activated during the inflammatory process (Mantovani et al. 2008). Inflammatory breast cancer is one of the most aggressive types of breast cancer, suggesting that inflammation may be related to this disease (Key et al. 2001). In this study, we have demonstrated that the phytoestrogen genistein, in the range of concentrations found in plasma of regular Asian women consuming soy-rich products (Morton et al. 2002), could play an important role in the expression of Sirtuin 1 and the inflammation-related genes in breast cancer cells depending on their ER α /ER β ratio. This could be crucial in cell proliferation and ROS production due to their link with the inflammation.

Several pro-inflammatory gene products have been identified that mediate a critical role in the suppression of apoptosis, proliferation, angiogenesis, invasion and metastasis. The expression of all these genes is regulated mainly by the NF- κ B transcription factor. These considerations imply that anti-inflammatory agents that suppress NF- κ B-regulated products must have a potential both in the prevention and in the treatment of cancer (Coussens and Werb 2002).

Previous studies had shown that genistein had anti-inflammatory effects and anticancer properties (Ruiz-Larrea et al. 1997; Spagnuolo et al. 2015). Genistein is

a phytoestrogen that has a structure similar to 17 β -oestradiol, and it has been defined as a possible selective modulator of oestrogen receptors, with 30 times more affinity for ER β than for ER α (Kuiper et al. 1997). In previous experiments carried out in our lab, we observed how GEN exerted its functions through its interaction with ERs, with different concentrations in diverse breast cancer cells with different ER α /ER β ratio (Pons et al. 2014). According to the results obtained in the present study, differences can be observed between the three cell lines with different ER α /ER β ratio, in terms of mRNA expression after treatment with GEN for 4 hours.

To start the study, we confirmed the effects of physiological concentrations of GEN on the oestrogen receptors expression. GEN treatment induces a great increase in ER β gene (*esr2*) expression in MCF-7 and T47D, suggesting an accumulative effect of this phytoestrogen in these cells, as we demonstrated in previous studies at mRNA and protein expression levels (Nadal-Serrano et al. 2013). In addition to this, Kuiper and collaborators found, twenty years ago, that genistein presented both more affinity and transactivation activity for ER β than for ER α (Kuiper et al. 1998). The increase of ER β gene (*esr2*) expression after GEN treatment in MCF-7 cells has been described previously (Nadal-Serrano et al. 2013), however, this increment would be not enough to counteract the effects of the interaction of this phytoestrogen with the ER α (Nadal-Serrano et al. 2013;

Pons et al. 2014). The results obtained of *ps2* gene mRNA expression could indicate that in MCF-7 GEN is acting through its interaction and activation of the ER α , the predominant oestrogen receptor found in this cell line, as *ps2* expression is an ER α -responsive gene, but not ER β -responsive gene (Bièche et al. 2001). In T47D and MDA-MB-231 cells, the expression of *ps2* was not modified after GEN treatment, suggesting that the observed effects of the genistein could be caused mainly by its interaction with the ER β .

Another issue to consider is the possible ER-independent effects of genistein. In this sense, other authors have described that genistein does not cause non-ER-mediated effects up to concentrations higher than 10 μ M (Matsukawa et al. 1993; Koroma and de Juan 1997; Bouker and Hilakivi-Clarke 2000), so the GEN concentration used in this study seems to be related to the ER-mediated effects of genistein.

We were able to demonstrate that GEN influence the cell viability through its interaction with both ERs. Cell viability assay revealed that GEN treatment provokes an increase of cell proliferation in those breast cancer cells with high ER α /ER β ratio, but this treatment reduces cell viability in breast cancer cells with low ER α /ER β ratio. In this sense, we have demonstrated in a previous work that GEN can influence in breast cancer cells proliferation depending on their ER α /ER β ratio (Pons et al. 2014). These results could be due to the modulation of ROS production exerted by both ERs. It is well known that the ER α /ER β ratio modulates the oxidative stress in the presence of their ligands, ER α promoting and ER β inhibiting ROS production, both in breast cancer cell lines and in breast tumours (Nadal-Serrano et al. 2012; Sastre-Serra et al. 2013). The results obtained in MDA-MB-231 cells, where GEN treatment reduces significantly the cell viability, could be due to its non-genomic effects through the activation of the mitogen-activated protein kinase pathway, which could induce apoptosis in this breast cancer cell line (Li et al. 2008).

Sirtuins are a highly conserved family of proteins that can play an important role in a wide variety of diseases, including cancer, because they are key regulators of responses to stress and metabolism (Martinez-Pastor and Mostoslavsky 2012). Sirtuin 1 (SIRT1) is a NAD⁺ dependent histone deacetylase and it is known as an important metabolic regulator, reprogramming epigenetically inflammation by altering histones and transcription factors such as NF- κ B. This evidence supports that the failure on metabolism and bioenergetics reprogramming results in many

chronic and acute inflammatory diseases (Vachharajani et al. 2016). For this reason, is one of the most studied in cancer biology since it may have a role as tumour promoter and/or suppressor, depending on whether it regulates cell death or survival (Nadal-Serrano et al. 2013). In our study, we demonstrate that GEN treatment could increase Sirt1 gene expression and its anti-inflammatory effect, decreasing ROS production, in those breast cancer cell with predominance of ER β . In MCF-7 cell line, which has highest ER α /ER β ratio, we observed that GEN treatment lowered Sirt1 mRNA expression levels while in T47D cells, which has a low ER α /ER β ratio, showed the opposite effect. Our previous results showed a significant positive regulation in SIRT1 protein levels in T47D cells after 48 hours of GEN treatment ameliorating the oxidative stress and improving mitochondrial function (Nadal-Serrano et al. 2012). SIRT1 could be related to the inflammation process as its expression is regulated by inflammation related genes such as TFG- β (Xu et al. 2012), and SIRT1 knockout in mice increase pro-inflammatory cytokines such as IL-1 β (Gillum et al. 2011). In this sense, the synthesis of cytokines such as IL-1 β , as well as the expression of cyclooxygenase-2 (COX-2), is mediated directly by NF- κ B. SIRT1 inhibits NF- κ B signalling directly by deacetylating the p65 subunit of NF- κ B complex. SIRT1 stimulates oxidative energy production via the activation of AMPK, PPAR α and PGC-1 α and simultaneously, these factors inhibit NF- κ B signalling and suppress inflammation (Kauppinen et al. 2013).

Interleukin-1 is one of the main pro-inflammatory cytokines and previous studies has shown to be positively regulated in many types of tumours and has been implicated as a factor in tumour progression through the expression of metastatic and angiogenic genes, and growth factors (Perrier et al. 2009). Kurtzman et al. confirmed the presence of IL-1 α and IL-1 β in tumour cells of breast cancer and demonstrated that they play a fundamental role in the regulation of breast tumour growth and metastasis (Kurtzman et al. 1999). Interestingly, with the support of the results obtained in this study, GEN treatment could act as an anti-inflammatory agent in T47D breast cancer cell line, decreasing IL-1 β expression, suggesting that this phytoestrogen could modulate the expression of the IL-1 β through its interaction with ER β . It has been demonstrated that IL-1 β increase ROS production through mitochondria and NADPH oxidase (Yang et al. 2007), suggesting a role of IL-1 β in ROS-mediated cancer progression. In our results, GEN treatment has no effects in MCF-7 cells (with

high ER α /ER β ratio) through its binding to ER α , however, in 2002 Honma et al. demonstrated that IL-1 β stimulated the proliferation of breast cancer cells in presence of oestrone, a type of oestrogen, in MCF-7 cell lines (Honma et al. 2002), although in our case, the proliferative effects of genistein could be caused by other inflammatory mechanisms.

The presence of IL-1 β induce COX-2 mRNA expression (Bianchi et al. 2005). COX-2 is a key enzyme that allows the body to produce prostaglandins from arachidonic acid, thus regulating inflammation (Agarwal et al. 2009). Inflammatory stimuli initiate the signalling cascades that cause an increase in the nuclear levels of NF- κ B and this in turn leads to the induction of COX-2. The most abundant prostaglandin, PGE₂, increases the transactivation function of NF- κ B, which enhances the expression of NF- κ B-dependent inflammatory genes and contribute to oncogenesis (Poligone and Baldwin 2001; Tak et al. 2001). The increase observed in COX-2 mRNA expression in MCF-7 cells after GEN treatment agree with previous studies which suggest that increased expression of COX-2 may play a role in the progression of primary breast carcinoma (Jana et al. 2014). So, GEN treatment could enhance the proliferation of MCF-7 cells, with a high ER α /ER β ratio, throughout the raise of the expression of COX-2.

Finally, we have studied how GEN treatment affects to transforming growth factor-beta 1 (TGF- β 1) and Peroxisome Proliferator Activated Receptor gamma (PPAR γ) mRNA expression. TGF- β 1 is considered a cell growth inhibitor and anti-inflammatory gene (Bierie et al. 2009). But there is some controversy about the role of TGF- β 1 in breast cancer. Apparently, in early stages of breast cancer, this cytokine inhibits the progression of the epithelial cell cycle and promotes apoptosis, showing tumour suppressive effects. However, in late stages, TGF- β 1 is related to greater tumour progression, increased cell motility, cancer invasion and metastasis (Zarzynska 2014). The signalling pathways of ER α and TGF- β are major regulators during the development, function and tumorigenesis of the mammary gland, but have opposite roles in proliferation and apoptosis. While ER α signalling supports cell proliferation acting as anti-apoptotic, epithelial cells of the mammary gland are very sensitive to cell cycle arrest induced by TGF- β and apoptosis. Our results agree with those obtained by other authors who suggest that ER α blocks the TGF- β pathway by multiple means (Band and Laiho 2011). Here, we demonstrate that GEN treatment decrease TGF- β 1 mRNA expression, through its interaction with ER α ; nevertheless, GEN treatment increases the

expression of TGF- β 1, probably due to its interaction with ER β , suggesting an important relationship between ER β activation and TGF- β 1 expression, in agreement partially with the results obtained by Stope et al., who found that TGF- β 1 signal is modulated by the presence of ER α , but not ER β (Stope et al. 2010). In the same way, GEN treatment produced a decrease in PPAR γ mRNA expression levels in MCF-7 cells, with a high ER α /ER β ratio, and an increase in PPAR γ in T47D, with a low ER α /ER β ratio. GEN treatment could play an anti-inflammatory role since PPAR γ participates in inflammation as an anti-inflammatory protein through the inhibition of NF κ B (Carter et al. 2009), and this anti-inflammatory role of genistein could be related to its interaction with ER α or ER β . These results suggest that GEN had an anti-inflammatory effect in the low ER α /ER β ratio cell line, by increasing the TGF- β 1 and PPAR γ mRNA expression.

Conclusion

To sum up, the treatment with phytoestrogen genistein at physiological concentrations causes an increase of cell proliferation and an increment of the inflammatory status in those breast cancer cells with high ER α /ER β ratio. However, genistein treatment provokes a decrease in cell proliferation and ROS production with a reduction of the inflammatory status. Taking together, these results suggest that genistein could regulate, through the Sirt1 expression modulation, the inflammatory response and, therefore, the cell proliferation and ROS production depending on the ER α /ER β ratio of breast cancer cells.

Disclosure statement

No potential conflict of interest was reported by the authors.

ORCID

Daniel Gabriel Pons  <http://orcid.org/0000-0002-2931-7939>

Auba Gaya-Bover  <http://orcid.org/0000-0003-4274-2531>

Marina Alorda-Clara  <http://orcid.org/0000-0002-3610-7809>

Jordi Oliver  <http://orcid.org/0000-0002-5702-7306>

Pilar Roca  <http://orcid.org/0000-0003-3878-5424>

Jorge Sastre-Serra  <http://orcid.org/0000-0003-3405-0535>

References

- Adlercreutz H. 2002. Phytoestrogens and breast cancer. *J Steroid Biochem Mol Biol.* 83(1-5):113-118.

- Agarwal S, Reddy GV, Reddanna P. 2009. Eicosanoids in inflammation and cancer: the role of COX-2. *Expert Rev Clin Immunol.* 5(2):145–165.
- Band AM, Laiho M. 2011. Crosstalk of TGF- β and estrogen receptor signaling in breast cancer. *J Mammary Gland Biol Neoplasia.* 16(2):109–115.
- Bianchi A, Moulin D, Sebillaud S, Koufany M, Galteau M-M, Netter P, Terlain B, Jouzeau J-Y. 2005. Contrasting effects of peroxisome-proliferator-activated receptor (PPAR) γ agonists on membrane-associated prostaglandin E2 synthase-1 in IL-1 β -stimulated rat chondrocytes: evidence for PPAR γ -independent inhibition by 15-deoxy-Delta12,14-prostaglandin J2. *Arthritis Res Ther.* 7(6):R1325.
- Bièche I, Parfait B, Laurendeau I, Girault I, Vidaud M, Lidereau R. 2001. Quantification of estrogen receptor α and β expression in sporadic breast cancer. *Oncogene.* 20(56):8109–8115.
- Bierie B, Chung CH, Parker JS, Stover DG, Cheng N, Chytil A, Aakre M, Shyr Y, Moses HL. 2009. Abrogation of TGF- β signaling enhances chemokine production and correlates with prognosis in human breast cancer. *J Clin Invest.* 119(6):1571–1582.
- Bouker KB, Hilakivi-Clarke L. 2000. Genistein: does it prevent or promote breast cancer? *Environ Health Perspect.* 108(8):701–708.
- Carter AB, Misyak SA, Hontecillas R, Bassaganya-Riera J. 2009. Dietary modulation of inflammation-induced colorectal cancer through PPAR γ . *PPAR Res.* 2009:1–9.
- Coussens LM, Werb Z. 2002. Inflammation and cancer. *Nature.* 420(6917):860–867.
- Cronin KA, Lake AJ, Scott S, Sherman RL, Noone AM, Howlader N, Henley SJ, Anderson RN, Firth AU, Ma J, et al. 2018. Annual report to the nation on the status of cancer, part I: National cancer statistics. *Cancer.* 124(13):2785–2800.
- Dieterich M, Stubert J, Reimer T, Erickson N, Berling A. 2014. Influence of lifestyle factors on breast cancer risk. *Breast Care.* 9(6):407–414.
- Fernández M, Reina-Pérez I, Astorga J, Rodríguez-Carrillo A, Plaza-Díaz J, Fontana L. 2018. Breast cancer and its relationship with the microbiota. *Int J Environ Res Public Health.* 15(8):1747.
- Gillum MP, Kotas ME, Erion DM, Kursawe R, Chatterjee P, Nead KT, Muise ES, Hsiao JJ, Frederick DW, Yonemitsu S, et al. 2011. Sirt1 regulates adipose tissue inflammation. *Diabetes.* 60(12):3235–3245.
- Hartman J, Ström A, Gustafsson JÅ. 2009. Estrogen receptor beta in breast cancer-diagnostic and therapeutic implications. *Steroids.* 74(8):635–641.
- Helguero LA, Faulds MH, Gustafsson J-Å, Haldosén L-A. 2005. Estrogen receptors alfa (ER α) and beta (ER β) differentially regulate proliferation and apoptosis of the normal murine mammary epithelial cell line HC11. *Oncogene.* 24(44):6605–6616.
- Honma S, Shimodaira K, Shimizu Y, Tsuchiya N, Saito H, Yanaiharu T, Okai T. 2002. The influence of inflammatory cytokines on estrogen production and cell proliferation in human breast cancer cells. *Endocr J.* 49(3):371–377.
- James RE, Lukanova A, Dossus L, Becker S, Rinaldi S, Tjønneland A, Olsen A, Overvad K, Mesrine S, Engel P, et al. 2011. Postmenopausal serum sex steroids and risk of hormone receptor-positive and -negative breast cancer: a nested case-control study. *Cancer Prev Res.* 4(10):1626–1635.
- Jana D, Sarkar DK, Ganguly S, Saha S, Sa G, Manna AK, Banerjee A, Mandal S. 2014. Role of cyclooxygenase 2 (COX-2) in prognosis of breast cancer. *Indian J Surg Oncol.* 5(1):59–65.
- Kauppinen A, Suuronen T, Ojala J, Kaarniranta K, Salminen A. 2013. Antagonistic crosstalk between NF- κ B and SIRT1 in the regulation of inflammation and metabolic disorders. *Cell Signal.* 25(10):1939–1948.
- Key TJ, Verkasalo PK, Banks E. 2001. Epidemiology of breast cancer. *Lancet Oncol.* 2(3):133–140.
- Koroma BM, de Juan E. 1997. Inhibition of protein tyrosine phosphorylation in endothelial cells: relationship to anti-proliferative action of genistein. *Biochem Soc Trans.* 25(1):35–40.
- Kostelac D, Rechkemmer G, Briviba K. 2003. Phytoestrogens modulate binding response of estrogen receptors α and β to the estrogen response element. *J Agric Food Chem.* 51(26):7632–7635.
- Kuiper GG, Carlsson B, Grandien K, Enmark E, Häggblad J, Nilsson S, Gustafsson JA. 1997. Comparison of the ligand binding specificity and transcript tissue distribution of estrogen receptors alpha and beta. *Endocrinology.* 138(3):863–870.
- Kuiper GG, Lemmen JG, Carlsson B, Corton JC, Safe SH, van der Saag PT, van der Burg B, Gustafsson JA. 1998. Interaction of estrogenic chemicals and phytoestrogens with estrogen receptor beta. *Endocrinology.* 139(10):4252–4263.
- Kumar V, Green S, Stack G, Berry M, Jin JR, Chambon P. 1987. Functional domains of the human estrogen receptor. *Cell.* 51(6):941–951.
- Kurtzman SH, Anderson KH, Wang YP, Miller LJ, Renna M, Stankus M, Lindquist RR, Barrows G, Kreutzer DL. 1999. Cytokines in human breast cancer: IL-1 α and IL-1 β expression. *Oncol Rep.* 6(1):65–70.
- Li Z, Li J, Mo B, Hu C, Liu H, Qi H, Wang X, Xu J. 2008. Genistein induces cell apoptosis in MDA-MB-231 breast cancer cells via the mitogen-activated protein kinase pathway. *Toxicol In Vitro.* 22(7):1749–1753.
- Mantovani A, Allavena P, Sica A, Balkwill F. 2008. Cancer-related inflammation. *Nature.* 454(7203):436–444.
- Martinez-Pastor B, Mostoslavsky R. 2012. Sirtuins, metabolism, and cancer. *Front Pharmacol.* 3:22.
- Matsukawa Y, Marui N, Sakai T, Satomi Y, Yoshida M, Matsumoto K, Nishino H, Aoike A. 1993. Genistein arrests cell cycle progression at G2-M. *Cancer Res.* 53(6):1328–1331.
- Morton MS, Arisaka O, Miyake N, Morgan LD, Evans B. 2002. Phytoestrogen concentrations in serum from Japanese men and women over forty years of age. *J Nutr.* 132(10):3168–3171.
- Mukund V, Mukund D, Sharma V, Mannarapu M, Alam A. 2017. Genistein: Its role in metabolic diseases and cancer. *Crit Rev Oncol Hematol.* 119:13–22.
- Nadal-Serrano M, Pons DG, Sastre-Serra J, Blanquer-Rossello MM, Roca P, Oliver J. 2013. Genistein modulates oxidative stress in breast cancer cell lines according to ER α /ER β ratio: effects on mitochondrial



- functionality, sirtuins, uncoupling protein 2 and antioxidant enzymes. *Int J Biochem Cell Biol.* 45(9):2045–2051.
- Nadal-Serrano M, Sastre-Serra J, Pons DG, Miró AM, Oliver J, Roca P. 2012. The ER α /ER β ratio determines oxidative stress in breast cancer cell lines in response to 17 β -estradiol. *J Cell Biochem.* 113(10):3178–3182.
- Perrier S, Caldefie-Chézet F, Vasson MP. 2009. IL-1 family in breast cancer: potential interplay with leptin and other adipocytokines. *FEBS Lett.* 583(2):259–265.
- Poligone B, Baldwin AS. 2001. Positive and negative regulation of NF- κ B by COX-2: roles of different prostaglandins. *J Biol Chem.* 276(42):38658–38664.
- Pons DG, Nadal-Serrano M, Blanquer-Rossello MM, Sastre-Serra J, Oliver J, Roca P. 2014. Genistein modulates proliferation and mitochondrial functionality in breast cancer cells depending on ER α /ER β ratio. *J Cell Biochem.* 115(5):949–958.
- Pons DG, Torrens-Mas M, Nadal-Serrano M, Sastre-Serra J, Roca P, Oliver J. 2015. The presence of estrogen receptor β modulates the response of breast cancer cells to therapeutic agents. *Int J Biochem Cell Biol.* 66:85–94.
- Reuter S, Gupta SC, Chaturvedi MM, Aggarwal BB. 2010. Oxidative stress, inflammation, and cancer: how are they linked? *Free Radic Biol Med.* 49(11):1603–1616.
- Richards WL, Song MK, Krutzsch H, Evarts RP, Marsden E, Thorgeirsson SS. 1985. Measurement of cell proliferation in microculture using Hoechst 33342 for the rapid semiautomated microfluorimetric determination of chromatin DNA. *Exp Cell Res.* 159(1):235–246.
- Ruiz-Larrea MB, Mohan AR, Paganga G, Miller NJ, Bolwell GP, Rice-Evans CA. 1997. Antioxidant activity of phytoestrogenic isoflavones. *Free Radic Res.* 26(1):63–70.
- Sastre-Serra J, Nadal-Serrano M, Pons DG, Roca P, Oliver J. 2012a. Mitochondrial dynamics is affected by 17 β -estradiol in the MCF-7 breast cancer cell line. Effects on fusion and fission related genes. *Int J Biochem Cell B.* 44(11):1901–1905.
- Sastre-Serra J, Nadal-Serrano M, Pons DG, Valle A, Garau I, García-Bonafé M, Oliver J, Roca P. 2013. The oxidative stress in breast tumors of postmenopausal women is ER α /ER β ratio dependent. *Free Radical Bio Med.* 61:11–17.
- Sastre-Serra J, Nadal-Serrano M, Pons DG, Valle A, Oliver J, Roca P. 2012b. The effects of 17 β -estradiol on mitochondrial biogenesis and function in breast cancer cell lines are dependent on the ER α /ER β ratio. *Cell Physiol Biochem.* 29(1–2):261–268.
- Spagnuolo C, Russo GL, Orhan Llkay E, Habtemariam S, Daglia M, Sureda A, Nabavi SF, Devi KP, Loizzo MR, Tundis R, et al. 2015. Genistein and cancer: current status, challenges, and future directions. *Adv Nutr.* 6:408–419.
- Stope MB, Popp SL, Knabbe C, Buck MB. 2010. Estrogen receptor α attenuates transforming growth factor- β signaling in breast cancer cells independent from agonistic and antagonistic ligands. *Breast Cancer Res Treat.* 120(2):357–367.
- Tak PP, Firestein GS, Tak PP, Firestein GS. 2001. NF- κ B: a key role in inflammatory diseases. *J Clin Invest.* 107(1):7–11.
- Vachharajani VT, Liu T, Wang X, Hoth JJ, Yoza BK, McCall CE. 2016. Sirtuins link inflammation and metabolism. *J Immunol Res.* 2016:8167273.
- Verdrengh M, Jonsson IM, Holmdahl R, Tarkowski A. 2003. Genistein as an anti-inflammatory agent. *Inflamm Res.* 52(8):341–346.
- Barros RPA, Machado UF, Warner M, Gustafsson JA. 2006. *Proc Natl Acad Sci USA.* 103(5):1605–1608.
- Xu B, Chen H, Xu W, Zhang W, Buckley S, Zheng SG, Warburton D, Kolb M, Gauldie J, Shi W. 2012. Molecular mechanisms of MMP9 overexpression and its role in emphysema pathogenesis of Smad3-deficient mice. *Am J Physiol Lung Cell Mol Physiol.* 303(2):L89–L96.
- Yang D, Elner SG, Bian ZM, Till GO, Petty HR, Elner VM. 2007. Pro-inflammatory cytokines increase reactive oxygen species through mitochondria and NADPH oxidase in cultured RPE cells. *Exp Eye Res.* 85(4):462–472.
- Zarzynska JM. 2014. Two faces of TGF- β 1 in breast cancer. *Mediat Inflamm.* 2014:141747.

Micronutrients selenomethionine and selenocysteine modulate the redox status of MCF-7 breast cancer cells.

Pons, D. G., Moran, C., Alorda-Clara, M., Oliver, J., Roca, P., & Sastre-Serra, J. (2020). *Nutrients*, 12(3), 865.

Article

Micronutrients Selenomethionine and Selenocysteine Modulate the Redox Status of MCF-7 Breast Cancer Cells

Daniel Gabriel Pons ^{1,2} , Carmen Moran ¹, Marina Alorda-Clara ^{1,2}, Jordi Oliver ^{1,2,3}, Pilar Roca ^{1,2,3,*} and Jorge Sastre-Serra ^{1,2,3} 

¹ Grupo Multidisciplinar de Oncología Traslacional, Institut Universitari d'Investigació en Ciències de la Salut (IUNICS), Universitat de les Illes Balears, E-07122 Palma de Mallorca, Illes Balears, Spain; d.pons@uib.es (D.G.P.); carmen.moran.04@gmail.com (C.M.); marina.alorda@uib.es (M.A.-C.); jordi.oliver@uib.es (J.O.); jorge.sastre@uib.es (J.S.-S.)

² Instituto de Investigación Sanitaria de las Islas Baleares (IdISBa), Hospital Universitario Son Espases, edificio S, E-07120 Palma de Mallorca, Illes Balears, Spain

³ Ciber Fisiopatología Obesidad y Nutrición (CB06/03) Instituto Salud Carlos III, E-28029 Madrid, Spain

* Correspondence: pilar.roca@uib.es; Tel.: +34-971-173172

Received: 26 February 2020; Accepted: 20 March 2020; Published: 24 March 2020



Abstract: Selenium is a micronutrient which is found in many foods, with redox status modulation activity. Our aim was to evaluate the effects of two chemical forms of selenoamino acids, Seleno-L-methionine and Seleno-L-cystine (a diselenide derived from selenocysteine), at different concentrations on cell viability, hydrogen peroxide production, antioxidant enzymes, UCP2 protein expression, as well as lipid and protein oxidative damage in MCF-7 breast cancer cells. Results showed that Seleno-L-methionine did not cause an increase in hydrogen peroxide production at relatively low concentrations, accompanied by a rise in the antioxidant enzymes catalase and MnSOD, and UCP2 protein expression levels. Furthermore, a decrease in protein and lipid oxidative damage was observed at 10 μ M concentration. Otherwise, Seleno-L-cystine increased hydrogen peroxide production from relatively low concentrations (100 nM) to a large increase at high concentrations. Moreover, at 10 μ M, Seleno-L-cystine decreased UCP2 and MnSOD protein expression. In conclusion, the chemical form of selenoamino acid and their incorporation to selenoproteins could affect the regulation of the breast cancer cell redox status. Taken together, the results obtained in this study imply that it is important to control the type of selenium-enriched nutrient consumption, taking into consideration their composition and concentration.

Keywords: selenomethionine; selenocysteine; oxidative stress; antioxidant enzymes; ucp2; oxidative damage

1. Introduction

Selenium is a micronutrient found in cereals, mushrooms, onion, nuts, broccoli, cabbage, garlic, fish, and meats [1]. Selenium has been associated with antioxidant, anti-inflammatory and cytostatic activity [2,3]. For all these properties ascribed to selenium, particular interest has been focused towards its role as a cancer preventive agent [1]. The antioxidant action is associated with the presence of selenium in some antioxidant enzymes that protect cells from oxidative damage [4].

Oxidative stress is a physio-pathological situation caused by an imbalance between antioxidant defenses of the cell and reactive oxygen species (ROS) production [5], and this stress is implicated in cancer development and progression [6–9]. Due to the antioxidant properties of selenium, this micronutrient could be a possible candidate to serve as a chemopreventive agent against cancer, and more

concretely breast cancer [10]. Seafoods and organ meats are the richest food sources of selenium, but selenium is significantly present in breads, grains, poultry, and eggs [11,12]. Soil selenium content and specification is a key factor for the incorporation of selenium in plants and, therefore, concentrations in animals is dependent on their plant intake, and therefore selenium content in plant and animal products can vary depending on the location [11,13]. The chemical form is important to establish the mechanisms by which selenium exerts its activities. Organic forms of selenium (selenomethionine and selenocysteine) are good dietary sources of selenium [14]. Most selenium is in the form of selenomethionine in animal and human tissues (skeletal muscle is the major site of selenium storage), as it can be incorporated non-specifically with the amino acid methionine in body proteins [14]. The human body is able to absorb more than 90% of selenomethionine present in food sources, as well as in multimineral supplements [15]. However, selenocysteine is reduced to generate hydrogen selenide, which is converted to selenophosphate for selenoprotein biosynthesis [16].

In animal models, Selenomethionine exerts, in general, dose-response chemoprevention effects without signs of toxicity [17], although Se-methylselenocysteine has also shown to have mammary chemoprevention [18]. Thus, selenium could have different effects over breast cancer related to initiation, promotion and progression of the disease. These effects include the inhibition of oxidative stress, the inhibition of cell proliferation and induction of apoptosis (modulating cell cycle progression, apoptotic genes and signaling molecules), modulation of immune response, and downregulation of angiogenesis-related genes [10].

Because of all of these precedents, the main objective of this study was to evaluate the effects of two chemical forms of selenoaminoacids: Seleno-L-methionine (SeMet) and Seleno-L-cystine (SeCys). The parameters studied were: cell viability, hydrogen peroxide production, antioxidant enzymes and UCP2 protein expression, and lipid and protein oxidative damage in MCF-7 breast cancer cells.

2. Material and Methods

2.1. Materials and Reagents

Seleno-L-Methionine (Se-Met) and Seleno-L-Cystine (Se-Cys) were obtained from Sigma-Aldrich (St. Louis, MO, USA). Routine chemicals were supplied by Roche (Barcelona, Spain), Panreac (Barcelona, Spain), Sigma-Aldrich and Bio-Rad Laboratories (Hercules, CA, USA). Amplex[®] Red Hydrogen Peroxide/Peroxidase Assay Kit was purchased from Invitrogen—Molecular Probes—Thermo Fisher Scientific (Waltham, MA, USA).

2.2. Cell Culture and Treatments

Human breast cancer cell line MCF-7 was purchased from ATCC and maintained in Dulbecco's modified Eagle's medium (DMEM) with phenol red supplemented with 10% fetal bovine serum (FBS) and 1% penicillin/streptomycin cocktail in a 5% CO₂ atmosphere at a temperature of 37 °C. All treatments were carried out when cells reached 70–80% confluence. For cell viability and ROS production assays, cells were treated with increasing concentrations of Se-Met (from 1 nM to 1 mM) or Se-Cys (from 100 pM to 50 µM). For western blot and oxidative damage analysis, cells were treated with 10 nM or 10 µM of both selenoamino acids. Vehicle-treated cells were treated with 0.001% dimethyl sulfoxide (DMSO).

2.3. Cell Viability Assay

Cells were seeded at 15,000 cells per well in 96-well plates. The day after the seed, cells were treated with vehicle (0.001% DMSO) or increasing concentrations of each selenoamino acid for 48 h. The number of viable cells was determined by fluorescence emitted by the DNA binding dye Hoechst 33342 [19]. Briefly, after a 48 h treatment, DMEM was removed and each well was washed once with PBS. Then, 100 µl of 5 µg/mL Hoechst 33342 solution in PBS were added and incubated for 5 min at 37 °C. Fluorescence was measured at 350 nm of excitation length and 455 nm of emission length.

2.4. Measurement of ROS Production

Cells were seeded at 15,000 cells per well in 96-well plates. The day after the seed, cells were treated with increasing concentrations of both selenoamino acids for 48h. ROS production after the treatment was determined by Amplex[®] Red Hydrogen Peroxide/Peroxidase Assay Kit, following manufacturer's protocol, and described by Sastre-Serra et al. [20]. Briefly, after a 48h treatment, DMEM was removed and cells were washed with Krebs-Ringer phosphate buffer (145 mM NaCl, 4.86 mM KCl, 0.54 mM CaCl₂, 1.22 mM MgSO₄, 5.5 mM glucose, 5.7 mM sodium phosphate, pH 7.4). Then, 50 μM Amplex[®] Red reagent and 0.1 U/mL HRP (horseradish peroxidase) diluted in Krebs-Ringer phosphate buffer was added to each well. The fluorescence measurement was monitored at times 0, 15, 30 and 60 min using a FLx800 microplate fluorescence reader (Bio-Tek, Winooski, VT, USA) adjusted at excitation and emission wavelengths of 570 and 585 nm, respectively, and the slope values were used for the calculations. All measurements were normalized by number of viable cells determined by the Hoechst 33342 method as described above.

2.5. Western Blot

Cells were seeded in 6-well plates at a density of 3.5×10^5 cells/well. Then, cells were treated with vehicle (0.001% DMSO), 10 nM and 10 μM of each selenoamino acid for 48 h. After treatment, cells were harvested by scraping them with 200 μL of lysis buffer (50 mM Tris-Base pH 8.8, 1 mM EDTA-Na, 1% Igepal, 1 mM PMSF, 1 mM leupeptin, 1 mM pepstatin, 1 mM Na₃VO₄) on ice. The total protein content was determined using a BCA[™] Protein Assay Kit (Pierce, Bonn, Germany), following manufacturer's protocol. For Western blot analysis, 30 μg of total protein from cell lysates were solubilized in sample buffer (50% glycerol, 10% SDS, 300 mM Tris-HCl pH 6.8, 0.05% bromophenol blue, 10% of β-mercaptoethanol) and boiled for 5 min. Then, proteins were separated on a 12% SDS-PAGE and electrotransferred on nitrocellulose membranes with Trans-Blot[®] Turbo[™] Transfer System (Bio-Rad). After the electrotransfer, membranes were blocked with 5% non-fat powdered milk in Tris-buffered saline-Tween-20 (20 mM Tris-HCl, 0.13 mM NaCl and 0.05% Tween-20) (TBS-T) for 1h. The membranes were then incubated with primary antibodies (diluted in 5% BSA in TBS-T) to detect the following proteins: uncoupling protein 2 (UCP2) and tubulin as loading control (Santa Cruz Biotechnologies, CA, USA) at 1:200 and 1:1000 dilutions respectively; catalase, CuZn-superoxide dismutase (CuZnSOD) and MnSOD (Calbiochem, San Diego, CA, USA) at 1:1000 dilution. The membranes were then washed with TBS-T and incubated with rabbit or mouse secondary antibodies conjugated with horseradish peroxidase (Santa Cruz Biotechnology, Texas, CA, USA) at 1:10,000 dilution in 2% non-fat powdered milk in TBS-T. After washing membranes with TBS-T, protein bands were visualized by Immuno-Star[®] WesternC[©] Chemiluminescent Kit Western blotting detection systems (Bio-Rad). The chemiluminescence signal was acquired with a Chemidoc XRS densitometer (Bio-Rad Laboratories) and results were analyzed with Quantity One Software (Bio-Rad).

2.6. Measurement of Carbonyl Groups

The presence of carbonyl groups was analyzed using an immunological method with the OxySelect[™] Protein Carbonyl Immunoblot kit (Cell Biolabs, San Diego, CA, USA), following the manufacturer's protocol. Briefly, protein carbonyls of 10 μg of total protein were detected by labelling them with 2,4-dinitrophenylhydrazine (DNPH) for 5 min. Total protein was loaded and separated in a 12% SDS-PAGE and electrotransferred on a nitrocellulose membrane as described above. After de blockage of the membrane for 1 h, it was incubated with the DNP antibody (1:2000) in 5% BSA in TBS-T for 2 h and then incubated with the secondary antibody anti-mouse at 1:2000 dilution in 2% non-fat powdered milk in TBS-T for 1 h. The band detection was performed as described above in the Western blotting section.

2.7. Measurement of 4-Hydroxy-2-Nonenal Adducts

For 4-hydroxy-2-nonenal (4-HNE) adducts analysis, 30 µg of total protein were loaded in a 12% SDS-PAGE and electrotransferred as described above. After the blockage of the membrane, it was incubated with antiserum against 4-HNE (Santa Cruz Biotechnologies, CA, USA) at a dilution of 1:1000 in 5% BSA in TBS-T. Then, the membrane was incubated with the secondary antibody anti-goat at 1:10,000 dilution in 2% non-fat powdered milk in TBS-T for 1 h. The band detection was performed as describe above in the Western blotting section.

2.8. Statistical Analysis

The statistical analysis was performed with the Statistical Program for the Social Sciencies software for Windows (SPSS, version 24.0; SPSS Inc, Chicago, IL, USA). Data are presented as mean ± standard error of the mean (SEM). The statistical differences between vehicle- and selenoamino acids-treated cells were analyzed using a Student's t-test. Statistical significances were set at $p < 0.05$ or at $p < 0.1$.

3. Results

3.1. Effects of Increasing Concentrations of Selenoamino Acids on Cell Viability and H₂O₂ Production

Figure 1A shows that increasing SeMet concentrations up to a concentration of 10 µM of SeMet did not cause any significant changes in cell viability. Nonetheless, above this concentration (10 µM) of SeMet, cell viability gradually decreased until a drop of 33% in the highest SeMet concentration tested, 1 mM. Moreover, H₂O₂ production was not affected under low concentrations of SeMet and this parameter increased slightly in a concentration-dependent manner, until reaching a maximum increase of 47% with the highest SeMet concentration tested, 1 mM.

In Figure 1B, for the SeCys treatment, a decrease in cell viability can be observed at the concentration of 1 nM and this decrease was higher in a concentration-dependent manner, until a drop of 68% was noted in the highest SeCys concentration tested, at 50 µM. At high concentrations of SeCys, there was an increase in H₂O₂ production in a concentration-dependent manner, and this became increasingly more pronounced from 5 µM (+40%) to 50 µM (+264%).

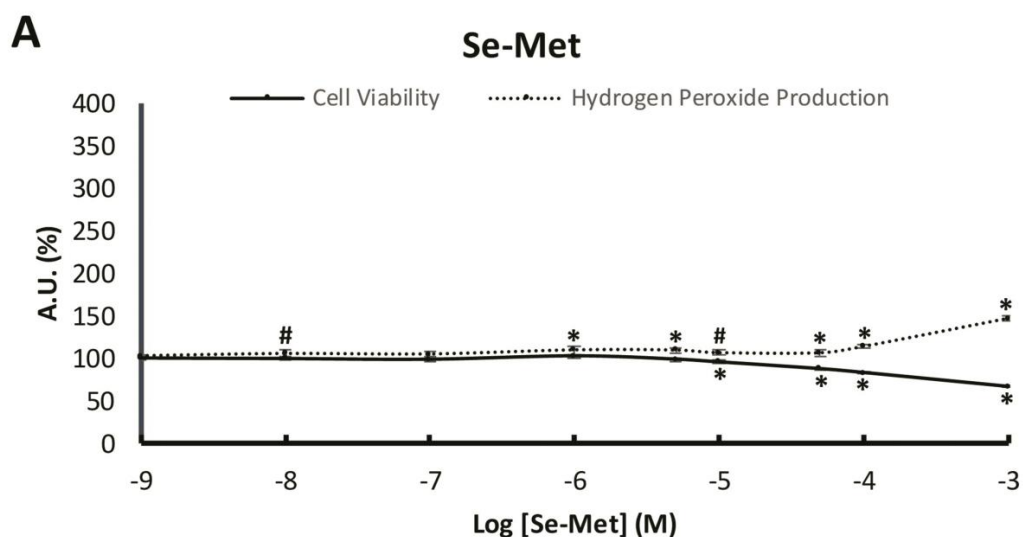


Figure 1. Cont.

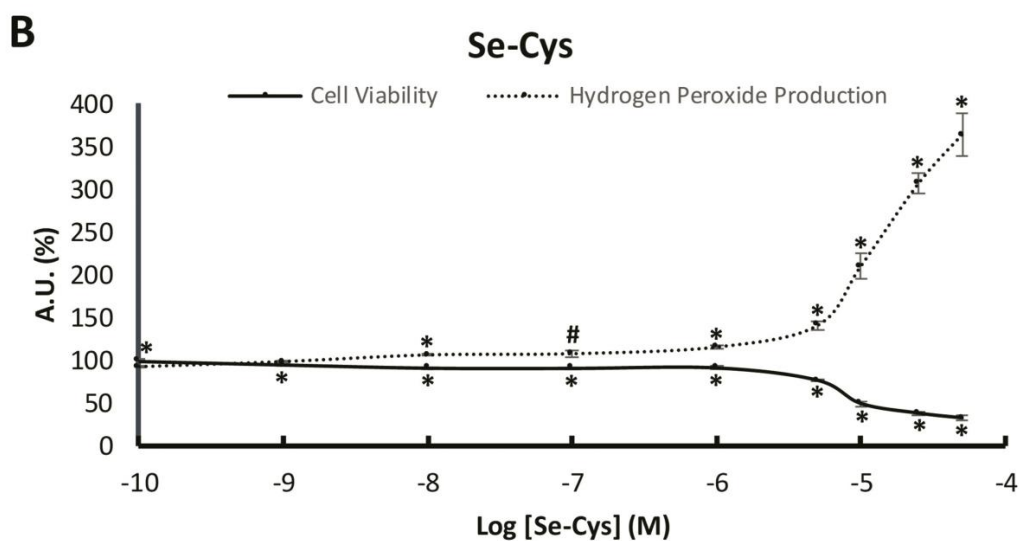


Figure 1. Cell viability and hydrogen peroxide production in MCF-7 breast cancer cells after selenomethionine or selenocystine treatment. (A) The cells were treated with vehicle or with increasing concentrations of selenomethionine (from 1 nM to 1 mM) for 48 h. (B) The cells were treated with vehicle (data not shown) or with increasing concentrations of selenocystine (from 100 pM to 50 μ M) for 48 h. Solid line represents the cell viability and pointed line represents hydrogen peroxide production. Points in lines represent means and error bars represent SEM ($n = 6$). The value of control cells was set at 100% (data not shown) and the rest of values were calculated referenced to the control set at 100%. * Significant differences between selenoamino acid treated and control cells (Student's t-test; $p \leq 0.05$). # Significant differences between selenoamino acid treated and control cells (Student's t-test; $p \leq 0.1$). AU: Arbitrary Units.

3.2. Effects of Selenoamino Acids on Antioxidant Enzymes and UCP2 Protein Levels

For the analysis of the antioxidant enzymes and UCP2 protein levels, we chose two concentrations of each Se-aminoacid, 10 nM and 10 μ M, representative of the results obtained in the cell viability and H₂O₂ production analysis. Figure 2 displays the results obtained in the protein levels of manganese superoxide dismutase (MnSOD), copper-zinc superoxide dismutase (CuZnSOD), catalase and uncoupling protein 2 (UCP2) by western blot analysis.

Figure 2A represents the MnSOD protein expression levels, showing an increase in SeMet-treated cells at both concentrations (+37% 10 nM and +71% 10 μ M) and a decrease in 10 μ M SeCys-treated cells (−34%). In Figure 2B the CuZnSOD protein levels are displayed which did not undergo any significant change for either SeMet or SeCys treatment in MCF-7 cells. In Figure 2C the catalase protein levels are presented, indicating only one, albeit a very noteworthy, statistically significant change in catalase protein level, with a 10 μ M SeMet treatment (+69%). Figure 2D shows a remarkably significant increase in UCP2 protein expression levels when cells were treated with SeMet at both concentrations (+42% for 10 nM and +113% for 10 μ M), in addition to a decrease in UCP2 protein levels when cells were treated with SeCys at 10 μ M (−24%). Western blot cropped representative bands of selenomethionine-treated and selenocystine-treated MCF-7 breast cancer cells can be observed in Figure 3.

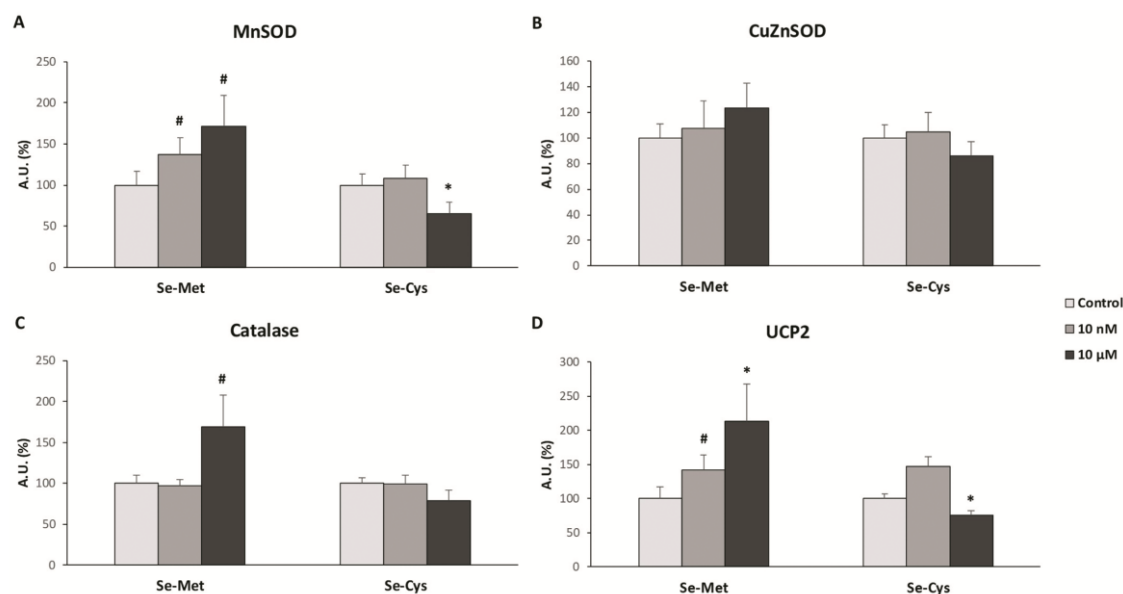


Figure 2. Antioxidant enzymes and UCP2 protein levels in MCF-7 breast cancer cell lines after treatment with selenoamino acids at 10 nM and 10 μ M. The cells were treated with vehicle (clear grey bars), selenoamino acid at 10 nM (dark grey bars) or selenoamino acid at 10 μ M (black bars) for 48 h. (A) Manganese Superoxide Dismutase (MnSOD). (B) Copper-Zinc Superoxide Dismutase (CuZnSOD). (C) Catalase. (D) Uncoupling protein 2 (UCP2). The proteins levels were measured by Western Blot. Bars represent means and error bars represent SEM ($n = 6$). The value of control cells was set at 100% and the rest of values were calculated referenced to the control set at 100%. * Significant differences between selenoamino acid treated and control cells (Student's t-test; $p \leq 0.05$). # Significant differences between selenoamino acid treated and control cells (Student's t-test; $p \leq 0.1$). AU: Arbitrary Units.

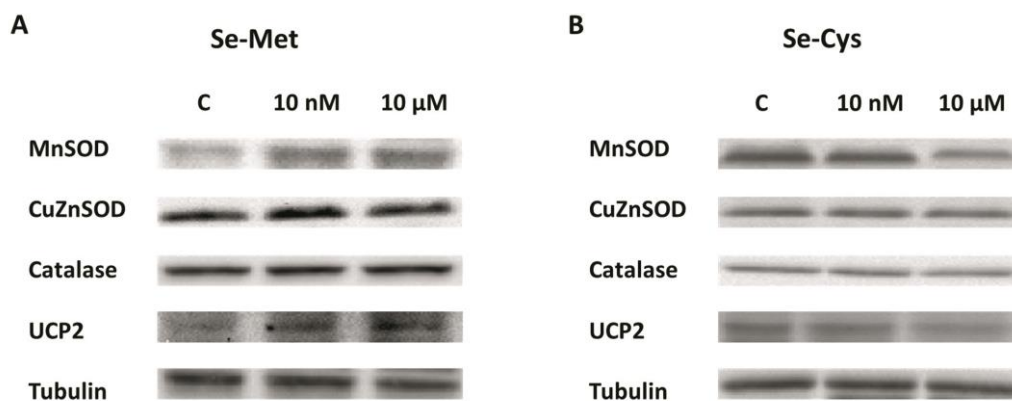


Figure 3. Western blot cropped representative bands of (A) selenomethione-treated and (B) selenocystine-treated MCF-7 breast cancer cell line are shown.

3.3. Effects of Selenoamino Acids Treatment on Protein and Lipid Oxidative Damage

As the protein expression levels change with selenoamino acid treatment, for the analysis of the oxidative damage, we chose the same two concentrations of each selenoamino acid, 10 nM and 10 μ M, in order to obtain comparable results. In Figure 4 the protein and lipid oxidative damage is represented, analyzed with protein carbonyls and 4-HNE formation respectively.

Figure 4A displays the protein carbonyls formation, showing that after SeMet treatment at 10 μ M, MCF-7 cells presented a lower carbonyls formation (−25%), while there were no significant changes after SeCys treatment, for either at the 10 nM or at 10 μ M concentrations. In Figure 4B, the 4-HNE formation are presented, indicating a decrease after treatment with SeMet at 10 μ M (−19%), with no significant differences after SeCys treatment at both concentrations studied.

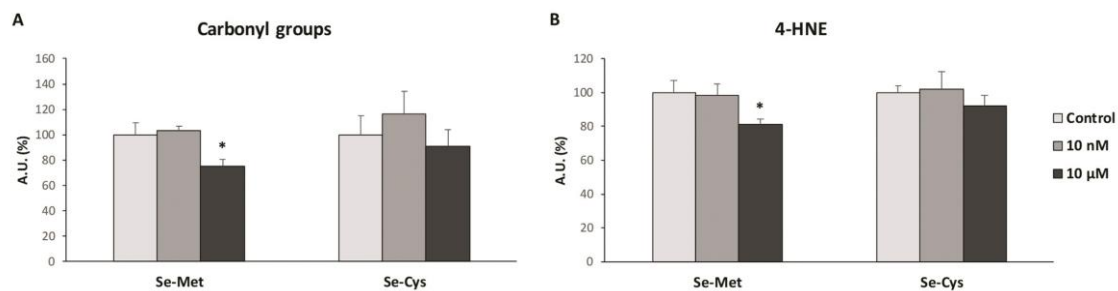


Figure 4. Protein and lipid oxidative damage in MCF-7 breast cancer cell lines after treatment with selenoamino acids at 10 nM and 10 μM. The cells were treated with vehicle (clear grey bars), selenoamino acid at 10 nM (dark grey bars) or selenoamino acid at 10 μM (black bars) for 48h. (A) Protein carbonyl groups formation. (B) 4-Hydroxy-2-Nonenal adducts formation (4-HNE). Bars represent means and error bars represent SEM ($n = 6$). The value of control cells was set at 100% and the rest of values were calculated referenced to the control set at 100%. * Significant differences between selenoamino acid treated and control cells (Student's t-test; $p \leq 0.05$). AU: Arbitrary Units.

4. Discussion

The results obtained in this study have revealed different biological effects of selenium depending on the chemical form of the selenoamino acid. Thus, seleno-L-methionine (SeMet) did not modify the cell viability and hydrogen peroxide production, except at the highest concentrations, in MCF-7 breast cancer cells. Moreover, SeMet treatment at 10 μM produced a decrease in oxidative damage in lipids and proteins, which was accompanied by an increase of the UCP2 and antioxidant enzymes protein expression. However, seleno-L-cystine (SeCys), a diselenide derived from selenocysteine, produced a decrease in cell viability and an increase in hydrogen peroxide production at a concentration of 1 nM and above in a concentration-dependent manner. In this case, SeCys treatment at 10 μM did not produce any statistically significant change in the oxidative damage of both lipids and proteins, although it did decrease the UCP2 and antioxidant enzymes protein expression.

In our study, we found that SeMet did not significantly increase hydrogen peroxide production, except at very high concentrations (>100 μM). The observed effects of SeMet are similar to those found twenty years ago by Stewart et al. [21], who determined that SeMet neither resulted in cell death nor DNA oxidative damage in BALB/c MK-2 cells (mouse keratinocyte cell line), compared to other selenium compounds such as selenite and selenocystamine [21]. This is plausible, as SeMet is a non-catalytic compound and does not generate superoxide anion [22]. Moreover, we found an overexpression of some antioxidant enzymes when MCF-7 cells were treated with SeMet, especially at 10 μM, which suggests that this selenoamino acid could, in some way, improve the redox state of these cells through the overexpression or the extension of the half-life of these antioxidant enzymes. These results are in concordance with a recent study carried out in chicken myocardial tissue that suggests that SeMet reduces hydrogen peroxide production and lipid oxidative damage, in addition to an increase in the enzymatic activity of antioxidant enzymes such as SOD and catalase [23]. Our results demonstrate that, in addition to an increase in the protein levels of antioxidant enzymes and UCP2 with SeMet treatment, concomitant oxidative damage in macromolecules such as proteins and lipids also decrease, which corroborates the antioxidant properties of this molecule observed in older and recent studies [23,24].

Nonetheless, the other selenoamino acid studied, selenocysteine, presented very different effects compared to SeMet. It is important to note that cells reduce selenocysteine to selenocystine through reactions with glutathione and cysteine, so that selenocystine form exerts the main effects over the cells [25]. SeCys treatment caused an increase in hydrogen peroxide production at relatively low concentrations (from 1 μM), which became greatly evident at higher concentrations. Moreover, cell viability was compromised. In a previous study carried out in MCF-7 cell-based breast cancer xenograft model in nude mice, methylselenocysteine led to synergistic inhibition of tumor growth that was

associated with inhibition of cyclin D1 as well as inhibition of cell proliferation and induction of apoptosis [26]. Both results, i.e., the increase in hydrogen peroxide production and the decrease in cell viability after SeCys treatment, suggest that SeCys could diminish cancer cell proliferation through the raise in oxidative stress, although SeCys is known to form part of some antioxidant enzymes [27]. Other studies have proven the effects of SeCys in the rise in ROS production measured with DCFH-DA, a generalist dye detecting ROS levels, in MCF-7 and other cancer cell types [28]. In addition to all these evidences, Chen and Wong found that selenocystine treatment increased MCF-7 breast cancer cells apoptosis by modulation of ERK and Akt phosphorylation or with the involvement of p53 phosphorylation and ROS generation [29,30], supporting the results obtained in this study.

The different effects observed in both selenoamino acids could be due to the capacity of SeCys to form hydrogen selenide and, from this molecule, different prooxidant products can be created, producing reactive oxygen species such as superoxide anion, among others [31]. In contrast, SeMet would be mostly incorporated into antioxidant proteins in a non-specific way, and higher concentrations of this selenium compound would be required to produce ROS since this selenoamino acid would first need to be converted to SeCys, with selenium metabolism being one of the key factors to understand the role of selenoamino acids in human health and cancer chemoprevention [32]. In this context, other authors have demonstrated that sodium selenite at high nanomolar to low micromolar concentrations down-regulate the expression of MnSOD and UCP2 proteins [33]. According to the data obtained, and taking in consideration other previously published studies, selenomethionine could be considered, in the future, as a possible food supplement for the improvement of the redox activity of cells. On the other hand, selenocystine could be considered as an adjuvant treatment against breast tumors through a dramatic increase in ROS production in cancer cells and, therefore, induction of the cell death ways.

The present study has some limitations, as it has been done in *in vitro* conditions. To investigate the real effects of these selenoamino acids, *in vivo* studies are necessary and the research in the expression of some enzymes such as the methionine gamma-lyase, which modifies the chemical structure and therefore the biological function of these selenoamino acids [34]. In fact, a treatment based in the combination of selenomethionine with methionine gamma-lyase inhibited the tumor growth in rodents and prolonged their survival [35]. Moreover, another enzyme found in the liver, cystathione gamma-lyase, could play a crucial role in the effects of these selenoamino acids [36]. This enzyme catalyzes the transformation of the SeMet in SeCys, so its expression could be important in the final effects of both selenoamino acids [36].

5. Conclusions

In conclusion, the micronutrients selenomethionine and selenocysteine could play a crucial role in the regulation of the redox status in breast cancer cells. Selenomethionine increases the antioxidant enzymes and UCP2 protein expression, reducing the oxidative damage in both lipids and proteins, suggesting that this molecule could improve the redox status of cells. On the other hand, selenocystine treatment causes a drastic increase in ROS production followed by a dramatic drop in breast cancer cells viability at relative high concentrations. Moreover, selenocystine decrease the antioxidant enzymes and UCP2 protein expression, suggesting that this selenoamino acid could increase the oxidative stress in cells. Taken together, the results obtained in this study imply that it is important to control the type of selenium-enriched nutrient consumption, taking into consideration their composition and concentration.

Author Contributions: Conceptualization, D.G.P., J.O., P.R. and J.S.-S.; Methodology, C.M., M.A.-C. and P.R.; Validation, D.G.P., C.M., M.A.-C., J.O., P.R. and J.S.-S.; Formal Analysis, D.G.P., J.O., P.R. and J.S.-S.; Investigation, D.G.P., C.M. and P.R.; Data Curation, D.G.P., J.O., P.R. and J.S.-S.; Writing—Original Draft Preparation, D.G.P., C.M. and P.R.; Writing—Review & Editing, D.G.P., J.O., P.R. and J.S.-S.; Supervision, P.R. and J.S.-S.; Project Administration, D.G.P., J.O., P.R. and J.S.-S.; Funding Acquisition, P.R. All authors have read and agreed to the published version of the manuscript.

Funding: This work was supported by the Fundraising Project: Proyecto Investigación en Cáncer de Mama (InCaM), Fundació Universitat Empresa de les Illes Balears (FUEIB)—Oficina de Fundraising. Feim Camí per Viure—Santa Maria del Camí.

Acknowledgments: This work was published thanks to funding from “LIBERI 2020” program from the Balearic Islands Health Research Institute (IdISBa).

Conflicts of Interest: The authors declare no conflict of interest.

References

1. Rayman, M.P. Selenium and human health. *Lancet* **2012**, *379*, 1256–1268. [[CrossRef](#)]
2. Jackson, M.I.; Combs, G.F. Selenium and anticarcinogenesis: Underlying mechanisms. *Curr. Opin. Clin. Nutr. Metab. Care* **2008**, *11*, 718–726. [[CrossRef](#)] [[PubMed](#)]
3. Chen, Y.C.; Sosnoski, D.M.; Gandhi, U.H.; Novinger, L.J.; Prabhu, K.S.; Mastro, A.M. Selenium modifies the osteoblast inflammatory stress response to bone metastatic breast cancer. *Carcinogenesis* **2009**, *30*, 1941–1948. [[CrossRef](#)] [[PubMed](#)]
4. Schrauzer, G.N. Anticarcinogenic effects of selenium. *Cell. Mol. Life Sci.* **2000**, *57*, 1864–1873. [[CrossRef](#)] [[PubMed](#)]
5. Cutler, R.G. Oxidative stress profiling: Part I. Its potential importance in the optimization of human health. *Ann. N. Y. Acad. Sci.* **2005**, *1055*, 93–135. [[CrossRef](#)]
6. Sastre-Serra, J.; Valle, A.; Company, M.M.; Garau, I.; Oliver, J.; Roca, P. Estrogen down-regulates uncoupling proteins and increases oxidative stress in breast cancer. *Free Radic. Biol. Med.* **2010**, *48*, 506–512. [[CrossRef](#)]
7. Miró, A.M.; Sastre-Serra, J.; Pons, D.G.; Valle, A.; Roca, P.; Oliver, J. 17 β -Estradiol regulates oxidative stress in prostate cancer cell lines according to ERalpha/ERbeta ratio. *J. Steroid Biochem. Mol. Biol.* **2011**, *123*, 133–139. [[CrossRef](#)]
8. Nadal-Serrano, M.; Sastre-Serra, J.; Pons, D.G.; Miró, A.M.; Oliver, J.; Roca, P. The ERalpha/ERbeta ratio determines oxidative stress in breast cancer cell lines in response to 17Beta-estradiol. *J. Cell. Biochem.* **2012**, *113*, 3178–3182. [[CrossRef](#)]
9. Pons, D.G.; Nadal-Serrano, M.; Torrens-Mas, M.; Valle, A.; Oliver, J.; Roca, P. UCP2 inhibition sensitizes breast cancer cells to therapeutic agents by increasing oxidative stress. *Free Radic. Biol. Med.* **2015**, *86*, 67–77. [[CrossRef](#)]
10. Fontelles, C.C.; Ong, T.P. Selenium and Breast Cancer Risk: Focus on Cellular and Molecular Mechanisms. *Adv. Cancer Res.* **2017**, *136*, 173–192.
11. Ross, A.C.; Cousins, R.J.; Caballero, B.; Tucker, K.L.; Ziegler, T.R. *Modern Nutrition in Health and Disease*, 11th ed.; Wolters Kluwer Health, Lippincott Williams & Wilkins: Philadelphia, PA, USA, 2014; ISBN 978-1-60-547461-8.
12. Chun, O.K.; Floegel, A.; Chung, S.J.; Chung, C.E.; Song, W.O.; Koo, S.I. Estimation of Antioxidant Intakes from Diet and Supplements in U.S. Adults. *J. Nutr.* **2010**, *140*, 317–324. [[CrossRef](#)]
13. Coates, P.; Betz, J.M.; Blackman, M.R.; Cragg, G.; Levine, M.; Moss, J.; White, J. *Encyclopedia of Dietary Supplements Encyclopedia of Dietary Supplements*, 2nd ed.; Taylor & Francis: Abingdon, UK, 2010; ISBN 9781439819289.
14. Erdman, J.W.; MacDonald, I.; Zeisel, S.H. *Present Knowledge in Nutrition*, 10th ed.; International Life Sciences Institute: Washington, DC, USA, 2012; ISBN 9780470959176.
15. Medicine, I. *Dietary Reference Intakes for Vitamin C, Vitamin E, Selenium, and Carotenoids*; National Academies Press: Washington, DC, USA, 2000; ISBN 978-0-309-06935-9.
16. Davis, C.D. Selenium Supplementation and Cancer Prevention. *Curr. Nutr. Rep.* **2012**, *1*, 16–23. [[CrossRef](#)]
17. Ip, C. Lessons from Basic Research in Selenium and Cancer Prevention. *J. Nutr.* **1998**, *128*, 1845–1854. [[CrossRef](#)]
18. El-Bayoumy, K.; Sinha, R. Mechanisms of mammary cancer chemoprevention by organoselenium compounds. *Mutat. Res. Fundam. Mol. Mech. Mutagen.* **2004**, *551*, 181–197. [[CrossRef](#)]
19. Richards, W.L.; Song, M.K.; Krutzsch, H.; Evarts, R.P.; Marsden, E.; Thorgeirsson, S.S. Measurement of cell proliferation in microculture using Hoechst 33342 for the rapid semiautomated microfluorimetric determination of chromatin DNA. *Exp. Cell Res.* **1985**, *159*, 235–246. [[CrossRef](#)]

20. Sastre-Serra, J.; Ahmiane, Y.; Roca, P.; Oliver, J.; Pons, D.G. Xanthohumol, a hop-derived prenylflavonoid present in beer, impairs mitochondrial functionality of SW620 colon cancer cells. *Int. J. Food Sci. Nutr.* **2019**, *70*, 396–404. [\[CrossRef\]](#)
21. Stewart, M.S.; Spallholz, J.E.; Neldner, K.H.; Pence, B.C. Selenium compounds have disparate abilities to impose oxidative stress and induce apoptosis. *Free Radic. Biol. Med.* **1999**, *26*, 42–48. [\[CrossRef\]](#)
22. Yan, L.; Spallholz, J.E. Generation of reactive oxygen species from the reaction of selenium compounds with thiols and mammary tumor cells. *Biochem. Pharmacol.* **1993**, *45*, 429–437.
23. Liu, J.; Wang, S.; Zhang, Q.; Li, X.; Xu, S. Selenomethionine alleviates LPS-induced chicken myocardial inflammation by regulating the miR-128-3p-p38 MAPK axis and oxidative stress. *Metallomics* **2020**, *12*, 54–64. [\[CrossRef\]](#)
24. Thomson, C.D.; Robinson, M.F.; Butler, J.A.; Whanger, P.D. Long-term supplementation with selenate and selenomethionine: Selenium and glutathione peroxidase (EC 1.11.1.9) in blood components of New Zealand women. *Br. J. Nutr.* **1993**, *69*, 577–588. [\[CrossRef\]](#)
25. Dickson, R.C.; Tappel, A.L. Reduction of Selenocystine by Cysteine or Glutathione. *Arch. Biochem. Biophys.* **1969**, *130*, 547–550. [\[CrossRef\]](#)
26. Li, Z.; Carrier, L.; Belame, A.; Thiyagarajah, A.; Salvo, V.A.; Burow, M.E.; Rowan, B.G. Combination of methylselenocysteine with tamoxifen inhibits MCF-7 breast cancer xenografts in nude mice through elevated apoptosis and reduced angiogenesis. *Breast Cancer Res. Treat.* **2009**, *118*, 33–43. [\[CrossRef\]](#)
27. Kryukov, G.V.; Castellano, S.; Novoselov, S.V.; Lobanov, A.V.; Zehab, O.; Guigó, R.; Gladyshev, V.N. Characterization of mammalian selenoproteomes. *Science* **2003**, *300*, 1439–1443. [\[CrossRef\]](#)
28. Chen, T.; Wong, Y.S. Selenocystine induces reactive oxygen species-mediated apoptosis in human cancer cells. *Biomed. Pharmacother.* **2009**, *63*, 105–113. [\[CrossRef\]](#)
29. Chen, T.; Wong, Y.S. Selenocystine induces S-phase arrest and apoptosis in human breast adenocarcinoma MCF-7 cells by modulating ERK and Akt phosphorylation. *J. Agric. Food Chem.* **2008**, *56*, 10574–10581. [\[CrossRef\]](#)
30. Chen, T.; Wong, Y.S. Selenocystine induces caspase-independent apoptosis in MCF-7 human breast carcinoma cells with involvement of p53 phosphorylation and reactive oxygen species generation. *Int. J. Biochem. Cell Biol.* **2009**, *41*, 666–676. [\[CrossRef\]](#)
31. Jackson, M.I.; Combs, G.F. *Selenium: Its Molecular Biology and Role in Human Health*; Hatfield, D.L., Berry, M.J., Gladyshev, V.N., Eds.; Springer: Berlin/Heidelberg, Germany, 2012; ISBN 9781461410256.
32. Combs, G.F.; Gray, W.P. Chemopreventive agents: Selenium. *Pharmacol. Ther.* **1998**, *79*, 179–192. [\[CrossRef\]](#)
33. Shilo, S.; Aharoni-Simon, M.; Tirosh, O. Selenium Attenuates Expression of MnSOD and Uncoupling Protein 2 in J774.2 Macrophages: Molecular Mechanism for Its Cell-Death and Antiinflammatory Activity. *Antioxid. Redox Signal.* **2005**, *7*, 276–286. [\[CrossRef\]](#)
34. Tanaka, H.; Esaki, N.; Soda, K. A versatile bacterial enzyme: L-methionine γ -lyase. *Enzyme Microb. Technol.* **1985**, *7*, 530–537. [\[CrossRef\]](#)
35. Miki, K.; Xu, M.; Gupta, A.; Ba, Y.; Tan, Y.; Al-Refaie, W.; Bouvet, M.; Makuuchi, M.; Moossa, A.R.; Hoffman, R.M. Methioninase cancer gene therapy with selenomethionine as suicide prodrug substrate. *Cancer Res.* **2001**, *61*, 6805–6810.
36. Okuno, T.; Ueno, H.; Nakamuro, K. Cystathionine γ -Lyase Contributes to Selenomethionine Detoxification and Cytosolic Glutathione Peroxidase Biosynthesis in Mouse Liver. *Biol. Trace Elem. Res.* **2006**, *109*, 155–171. [\[CrossRef\]](#)



© 2020 by the authors. Licensee MDPI, Basel, Switzerland. This article is an open access article distributed under the terms and conditions of the Creative Commons Attribution (CC BY) license (<http://creativecommons.org/licenses/by/4.0/>).

Xanthohumol reduces inflammation and cell metabolism in HT29 primary colon cancer cells.

Torrens-Mas, M., Alorda-Clara, M., Martínez-Vigara, M., Roca, P., Sastre-Serra, J., Oliver, J., & Pons, D. G. (2022).
International Journal of Food Sciences and Nutrition, 73(4), 471-479.



Xanthohumol reduces inflammation and cell metabolism in HT29 primary colon cancer cells

Margalida Torrens-Mas, Marina Alorda-Clara, Maria Martínez-Vigara, Pilar Roca, Jorge Sastre-Serra, Jordi Oliver & Daniel Gabriel Pons

To cite this article: Margalida Torrens-Mas, Marina Alorda-Clara, Maria Martínez-Vigara, Pilar Roca, Jorge Sastre-Serra, Jordi Oliver & Daniel Gabriel Pons (2021): Xanthohumol reduces inflammation and cell metabolism in HT29 primary colon cancer cells, International Journal of Food Sciences and Nutrition, DOI: [10.1080/09637486.2021.2012561](https://doi.org/10.1080/09637486.2021.2012561)

To link to this article: <https://doi.org/10.1080/09637486.2021.2012561>



Published online: 08 Dec 2021.



Submit your article to this journal [↗](#)



Article views: 10



View related articles [↗](#)




View Crossmark data [↗](#)

RESEARCH ARTICLE



Xanthohumol reduces inflammation and cell metabolism in HT29 primary colon cancer cells

Margalida Torrens-Mas^{a,b,c} , Marina Alorda-Clara^{b,c} , Maria Martínez-Vigara^b, Pilar Roca^{b,c,d} , Jorge Sastre-Serra^{b,c,d} , Jordi Oliver^{b,c,d}  and Daniel Gabriel Pons^{b,c} 

^aTranslational Research in Aging and Longevity (TRIAL) Group, Vascular and Metabolic Pathologies Group, Instituto de Investigación Sanitaria de las Islas Baleares (IdISBa), Palma, Spain; ^bGrupo Multidisciplinar de Oncología Traslacional, Institut Universitari d'Investigació en Ciències de la Salut (IUNICS) Universitat de les Illes Balears, Palma, Spain; ^cInstituto de Investigación Sanitaria de las Islas Baleares (IdISBa), Palma de Mallorca, Spain; ^dCiber Fisiopatología Obesidad y Nutrición (CB06/03), Instituto Salud Carlos III, Madrid, Spain

ABSTRACT

Xanthohumol (XN) is a prenylated flavonoid known for its antioxidant and anti-inflammatory effects and has been studied as an anti-cancer agent. In this study, we aimed at analysing the effect of XN on a primary colorectal adenocarcinoma cell line, HT29, on cell viability, inflammatory and antioxidant gene expression, and metabolism. For this purpose, cells were treated with 10 nM and 10 μM XN, and cell viability, H₂O₂ production, lipid peroxidation and gene expression of inflammatory, antioxidant, and mitochondrial-related genes, as well as protein levels of metabolic enzymes, were determined. Results showed no significant effects on cell viability and a general decrease in pro-inflammatory, antioxidant and mitochondrial biogenesis gene expression with the lower concentration of XN. Furthermore, glucose and oxidative metabolism enzymes were also reduced. These results suggest that XN treatment, at low doses, could stop the proliferation and progression of HT29 cells by downregulating inflammatory signals and cell metabolism.

ARTICLE HISTORY

Received 18 September 2021
Revised 8 November 2021
Accepted 26 November 2021

KEYWORDS

Colon cancer; inflammation; xanthohumol; oxidative metabolism



Introduction

Colorectal cancer (CRC) is the third most frequently diagnosed cancer and the second leading cause of death by cancer worldwide (Sung et al. 2021). It is widely accepted that inflammation is a crucial driver of tumour initiation and progression (Zhang et al. 2019). In fact, inflammation is considered an important risk factor for the development of colon cancer, since patients with inflammatory bowel disease have a higher risk of this type of cancer (Landskron et al. 2014; Zhang et al. 2019).

Mitochondria participate in several cellular processes, such as metabolism and energy production, proliferation, reactive oxygen species (ROS) production, and apoptosis, among others (Porporato et al. 2018). These organelles are involved in all the described hallmarks of cancer, including tumour-promoting inflammation (Giampazolias and Tait 2016), and therefore become key players in cancer progression and a potential therapeutic target.

Xanthohumol (XN) is a prenylflavonoid present in hops (*Humulus lupulus L.*, *Cannabaceae*) that has gained a lot of attention due to its anti-inflammatory and antioxidant properties (Torrens-Mas and Roca 2020). XN has been tested as a chemotherapeutic agent in different types of cancers (Jiang et al. 2015; Sun et al. 2018; Wei et al. 2018; Logan et al. 2019; Seitz et al. 2021). Our group has previously reported that high doses of XN can exert a prooxidant effect and reduce cell viability and mitochondrial function in breast cancer (Blanquer-Rossello et al. 2013) and colon cancer metastatic cells (Sastre-Serra et al. 2019).

Although it is known that XN is metabolised by gut microbiota and converted into isoxanthohumol and 8-prenylnaringerin, some pharmacokinetics studies show that XN can be found in blood and in other organs, such as breast tissue, reaching 10⁻⁹ M values. Furthermore, supplementation studies suggest that 10⁻⁶ M concentrations can also be reached, especially in the colon (Bolca et al. 2010; Legette et al. 2014; Harish et al. 2021).

CONTACT Jordi Oliver  jordi.oliver@uib.es  Departamento de Biología Fundamental y Ciencias de la Salud, Universitat de les Illes Balears, Cra de Valldemossa, km 7'5, Palma de Mallorca 07122, España

© 2021 Taylor & Francis Group, LLC

Table 1 Primers sequences, with their respective annealing temperatures, accession number, and primer efficiency.

Gene	Forward primer (5'-3') Reverse primer (5'-3')	Accession number	Annealing T (°C)	Primer efficiency
18S	5'-GGA CAC GGA CAG GAT TGA CA-3' 5'-ACC CAC GGA ATC GAG AAA GA-3'	HQ387008	61	2.00
GAPDH	5'-CTG GTG GTC CAG GGG TCT TA-3' 5'-CCA CTC CTC CAC CTT TGA CG-3'	NM_001357943	60	1.95
PPARG	5'-GAG CCC AAG TTT GAG TTT GC-3' 5'-CTG TGA GGA CTC AGG GTG GT-3'	NM_001354666	61	2.00
NFKB1	5'-CCT GGA TGA CTC TTG GGA AA-3' 5'-TCA GCC AGC TGT TTC ATG TC-3'	NM_001382627	58	1.82
TNF	5'-AAG CCT GTA GCC CAT GTT GT-3' 5'-GGA CCT GGG AGT AGA TGA GGT-3'	NM_000594	58	2.00
IL6R	5'-TGG GAG GTG GAG AAG AGA GA-3' 5'-AGG ACC TCA GGT GAG AAG CA-3'	NM_001382774	60	1.94
TGFB1	5'-TCC TGG CGA TAC CTC AGC AA-3' 5'-CGG TAG TGA ACC CGT TGA TGT-3'	NM_000660	60	1.99
NFE2L2	5'-CTC CGC CAT CTT TTC TC-3' 5'-GGA GGC TCA CGA GGT ACA AG-3'	NM_001313903	60	1.80
CAT	5'-CAT CGC CAC ATG AAT GGA TA-3' 5'-CCA ACT GGG ATG AGA GGG TA-3'	NM_001752	61	2.00
GPX1	5'-GCG GCG GCC CAG TCG GTG TA-3' 5'-GAG CTT GGG GTC GGT CAT AA-3'	NM_001329455	61	2.00
GSR	5'-TCA CGC AGT TAC CAA AAG GAA A-3' 5'-CAC ACC CAA GTC CCC TGC ATA GT-3'	NM_001195102	64	2.00
SOD1	5'-TCA GGA GAC CAT TGC ATC ATT-3' 5'-CGC TTT CCT GTC TTT GTA CTT TCT TC-3'	NM_000454	64	2.00
SOD2	5'-CGT GCT CCC ACA CAT CAA TC-3' 5'-TGA ACG TCA CCG AGG AGA AG-3'	NM_001322819	64	1.99
UCP2	5'-ACA AGA CCA TTG CCC GAG AG -3' 5'-GGC AAG GGA GGT CAT CTG TC-3'	NM_001381944	60	1.94
SLC25A14	5'-CAA GCC GTT GGT CTC CTA AG-3' 5'-CGT TTT CAA TGT CAC CCA TC-3'	NM_001282197	60	1.99
PPARGC1A	5'-CGG TGA CTT ATC CTG TGG TCC-3' 5'-CGG TCG CAC TTG TCA TAC AC-3'	NM_001393947	60	1.94
NRF1	5'-GTA GCC ACA TTG GCT GAT GC-3' 5'-CTC TGA TGC TTG CGT CGT CT-3'	NM_001040110	60	2.00
TFAM	5'-GTG GTT TTC ATC TGT CTT GGC-3' 5'-ACT CCG CCC TAT AAG CAT CTT-3'	NM_001270782	60	2.00
SSBP1	5'-TGT GAA AAA GGG GTC TCG AA-3' 5'-TGG CCA AAG AAG AAT CAT CC-3'	NM_003143	60	1.80
COX4I1	5'-AAC GAG TGG AAG ACG GTT GT-3' 5'-TCA TGT CCA GCA TCC TCT TG-3'	NM_001318786	61	1.82

This study aimed to determine the effects of the flavonoid XN on inflammation, metabolism, and oxidative stress on a primary colorectal adenocarcinoma cell line. For this purpose, we treated the HT29 cell line, with an epithelial morphology, with a high and a low dose of XN and parameters such as cell viability, expression levels of inflammatory, antioxidant, and mitochondrial function-related genes, and H₂O₂ production were analysed.

Materials and methods

Reagents

Dulbecco's Modified Eagle's medium (DMEM) high glucose was purchased from GIBCO (Paisley, UK). Foetal bovine serum and penicillin-streptomycin solution were purchased from Biological Industries (Kibbutz Beit Haemek, Israel). Xanthohumol was obtained from Cayman Chemical Company (Michigan, USA). Routine chemicals were supplied by

Sigma-Aldrich (St. Louis, MO, USA), Roche (Barcelona, Spain), Panreac (Barcelona, Spain) and Bio-Rad Laboratories (Hercules, CA, USA).

Cell culture and treatments

Human colorectal adenocarcinoma cell line HT29 (RRID: CVCL_0320) was purchased from American Type Culture Collection (ATCC; Manassas, VA, USA) and maintained in DMEM supplemented with 10% (v/v) foetal bovine serum (FBS) and 1% (v/v) penicillin and streptomycin at 37 °C and 5% CO₂.

Cells were seeded in 96-well and 6-well plates at a density of 5×10^4 and 1.2×10^6 cells per well, respectively. To determine cell viability, 24 h after seeding cells were treated for 48 h with different concentrations of XN, ranging from 1 nM to 10 μ M, and vehicle-control cells were treated with 0.1% DMSO. For all the other experiments, two concentrations, 10 nM and 10 μ M XN, were used with the same procedure.

Cell viability

After treatment with XN for 48 h, cell viability was assessed with Hoechst 33342. Briefly, cells were washed with PBS and incubated with 1 µg/mL Hoechst 33342 for 5 min at 37 °C and 5% CO₂. Fluorescence was measured in a FLx800 microplate fluorescence reader (BioTek, Winooski, USA) set at excitation and emission wavelengths of 350 and 455 nm, respectively.

RT-pcr

RNA was isolated using TRI Reagent® (Sigma-Aldrich, St. Louis, MO, USA) following the manufacturer's protocol and then quantified using a BioSpec-nano spectrophotometer (Shimadzu Biotech, Kyoto, Japan) set at 260 nm. RNA quality was also assessed by analysing the 260/280 and 260/230 ratios, which indicate protein and phenol contamination, respectively. Both ratios were in the range of 2.0-2.2 for all samples included in this study. For each sample, 1 µg of the total RNA was reverse transcribed to cDNA at 37 °C for 50 min with a reaction mix containing 200 U/µL M-MLV reverse transcriptase, 250 mM Tris-HCl (pH 8.3), 375 mM KCl, 15 mM MgCl₂, 20 µM DTT, 2.5 µM random hexamers, 20 U RNase inhibitor, and 500 µM each dNTP.

PCR was performed using SYBR Green technology on a LightCycler 480 System II rapid thermal cycler (Roche Diagnostics, Basel, Switzerland). The genes, primers and temperatures for the annealing step are specified in Table 1. Total reaction volume was 10 µL, containing 7.5 µL SYBR TB Green® Premix Ex Taq™ (RR420A, Takara), containing 0.5 µM of the sense and antisense specific primers and 2.5 µL of the cDNA template. The amplification program consisted of a preincubation step for denaturation of the template cDNA (5 min, 95 °C), followed by 45 cycles consisting of a denaturation step (10 s, 95 °C), an annealing step (10 s, temperature depending on primers; listed in Table 1), and an elongation step (12 s, 72 °C min). A negative control lacking cDNA template was run in each assay.

The crossing point values obtained were analysed using the GenEx Standard Software (Multi-DAnalyses, Sweden). Each value was corrected by the corresponding primer efficiency (Table 1) and both *18S* and *GAPDH* were used as housekeeping genes. These genes were selected as appropriate housekeeping genes by geNorm and Normfinder algorithms as they were unaffected by treatment.

Western blot analysis

After 48 h of XN treatment, cells were scraped with PBS and then centrifuged at 600xg for 5 min at 4 °C. The resultant pellet was resuspended in RIPA buffer (50 mM Tris-HCl pH 7.5, 150 mM NaCl, 0.1% SDS, 0.5% deoxycholate, 1% Triton X-100, 1 mM EDTA, 0.01 mM leupeptin, 0.01 M pepstatin, 2 mM PMSF, 1 mM NaF and 1 mM Na₃VO₄) and protein content was determined with a bicinchoninic acid (BCA) protein assay kit (Pierce, Bonn, Germany).

For Western Blot, 20 µg of protein were separated on 12% SDS-PAGE gels and electrotransferred to 0.22 µm nitrocellulose membranes using the Trans-blot Turbo transfer system (Bio-Rad). Membranes were blocked with 5% non-fat powdered milk in Tris-buffered saline-Tween (TBS with 0.05% Tween-20) for 1 h. Antisera against GAPDH, PDH-E1α (sc-25778 and sc-377092, respectively, Santa Cruz Biotechnology), 4-HNE (#HNE11-S, Alpha-Diagnostics), LDHA (cs-2012, Cell Signalling Technology), and OXPHOS (AB110411, Abcam) were used as primary antibodies and incubated overnight. Mouse/rabbit/goat secondary antibodies conjugated with horseradish peroxidase were incubated for 1 h and protein bands were visualised by Immun-Star® Western C® Kit reagent (Bio-Rad) Western blotting detection systems. The chemiluminescence signal was captured with a Chemidoc XRS densitometer (Bio-Rad) and results were analysed with Quantity One Software (Bio-Rad).

H₂O₂ production

The Amplex® Red Hydrogen Peroxide/Peroxidase Assay Kit (Molecular Probes, Eugene, Oregon, USA) was used to measure H₂O₂ production following manufacturer's instructions. Briefly, a reaction mixture containing Krebs-Ringer phosphate buffer (145 mM NaCl, 4.86 mM KCl, 0.54 mM CaCl₂, 1.22 mM MgSO₄, 5.5 mM glucose, 5.7 mM sodium phosphate, pH 7.4) with 50 µM Amplex red reagent and 0.1 U/mL horseradish peroxidase was added to cells in a 96-well plate. Fluorescence measurement was recorded at times 0, 15, 30 and 60 minutes in an FLx800 microplate fluorescence reader (Bio-Tek Winooski, Vermont, USA) set at excitation and emission wavelengths of 571 and 585, respectively. Values were normalised per number of viable cells determined by Hoechst 33342 assay.

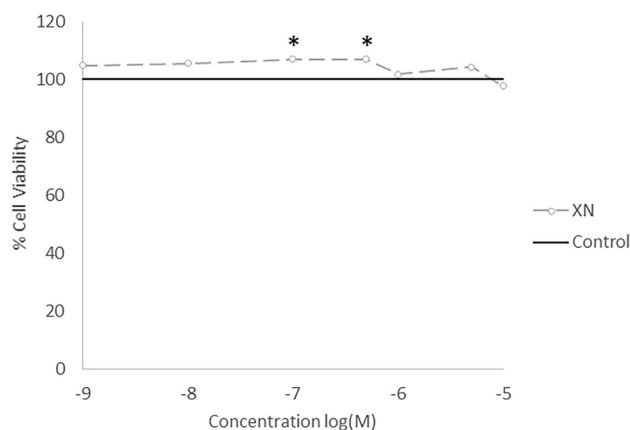


Figure 1. Cell viability after XN treatment at different concentrations. Cells were treated with 1 nM, 10 nM, 100 nM, 500 nM, 1 μ M, 5 μ M, and 10 μ M xanthohumol (XN) for 48 h. Viability of control cells (full line) was set at 100% and values of treated cells (dotted line) were normalised to the control situation. *indicates a significant difference between control XN-treated cells ($p < 0.05$).

Statistical analysis

The Statistical Program for the Social Sciences software for Windows (SPSS, version 27.0; SPSS Inc, Chicago, IL) was used for all statistical analyses. Results are presented as mean values \pm standard error of the mean (SEM) from six independent experiments. The effects of XN treatment were assessed using the Student's t-test and statistical significance was set at $p < 0.05$.

Results

XN treatment does not affect cell viability of primary cancer cells

Different concentrations of XN were tested, including 1 nM, 10 nM, 100 nM, 500 nM, 1 μ M, 5 μ M, and 10 μ M, to determine the effects of this flavonoid on cell viability (Figure 1). Interestingly, only 100 nM and 500 nM XN produced a significant 7% increase in cell viability. However, this difference was minimal, thus XN does not produce a biologically relevant effect on cell viability in the HT29 cell line. After this, cells were only treated with 10 nM and 10 μ M XN in further experiments, to determine whether the effects of XN differ from the higher concentration to a lower one.

A low concentration of XN induces an anti-inflammatory response

Figure 2 shows the mRNA expression levels of different anti- and pro-inflammatory genes. At the lower concentration, XN significantly decreased the levels of peroxisome proliferator-activated receptor gamma (PPARG,

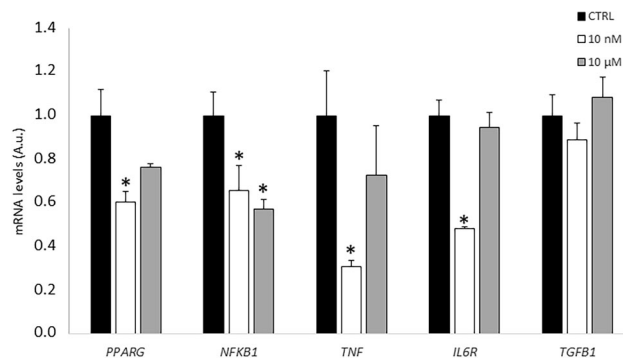


Figure 2. Gene expression of inflammation-related genes after XN treatment. mRNA levels were determined by RT-qPCR after treatment with 10 nM and 10 μ M XN for 48 h. Values are expressed as mean \pm SEM ($n = 6$) and values of control cells were set at 1. *indicates a significant difference between control and XN-treated cells ($p < 0.05$). A.u., arbitrary units; PPARG, peroxisome proliferator-activated receptor gamma; NFKB1 nuclear factor kappa b; TNF, tumour necrosis factor alpha; IL6R, receptor of interleukin; TGFB1, transforming growth factor beta.

–41%), nuclear factor kappa b (NFKB1, –35%), tumour necrosis factor alpha (TNF, –77%) and receptor of interleukin 6 (IL6R, –52%). However, 10 μ M XN only decreased the mRNA expression of NFKB1. Conversely, neither 10 nM nor 10 μ M XN affected the expression level of transforming growth factor beta (TGFB1).

XN treatment at low concentration downregulates antioxidant gene expression

Antioxidant gene expression was evaluated after treatment with both high and low concentrations of XN. As shown in Figure 3, 10 nM XN induced a general decrease in most of the genes analysed. This low concentration of XN especially affected the expression of glutathione reductase (GSR, –76%), superoxide dismutase 1 (SOD1, –62%), and uncoupling protein 5 (SLC25A14, –58%), while catalase (CAT) and glutathione peroxidase (GPX1) suffered a 30% decrease. On the other hand, the high concentration of XN only decreased the levels of SOD1 (–57%), uncoupling protein 2 (UCP2, –31%), and SLC25A14 (–41%).

We also determined the levels of H₂O₂ production (Figure 4(A)) and the levels of 4-HNE adducts (Figure 4(B)), an indicator of lipid peroxidation. Surprisingly, XN treatment did not affect significantly any of these measurements, suggesting that XN does not present an antioxidant effect in this cell line at these concentrations.

XN decreases mitochondrial biogenesis and function

Figure 5 shows the expression levels of genes related to mitochondrial biogenesis and function.

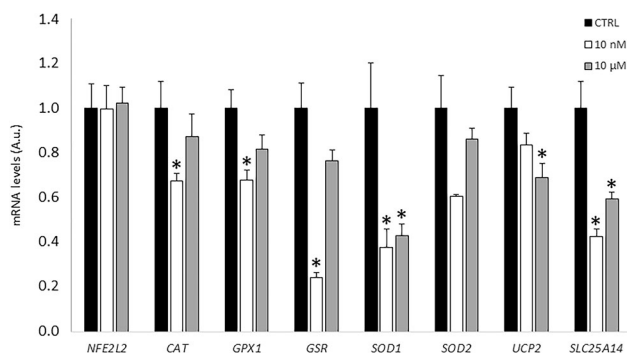


Figure 3. Effect of XN treatment on antioxidant gene expression. mRNA levels were determined by RT-qPCR after treatment with 10 nM and 10 μM XN for 48 h. Values are expressed as mean ± SEM ($n=6$) and values of control cells were set at 1. *indicates a significant difference between control and XN-treated cells ($p < 0.05$). A.u., arbitrary units; *NFE2L2*, nuclear factor erythroid 2-related factor 2; *CAT*, catalase; *GPX1*, glutathione peroxidase; *GSR*, glutathione reductase; *SOD1*, superoxide dismutase 1; *SOD2*, superoxide dismutase 2; *UCP2*, uncoupling protein 2; *SLC25A14*, uncoupling protein 5.

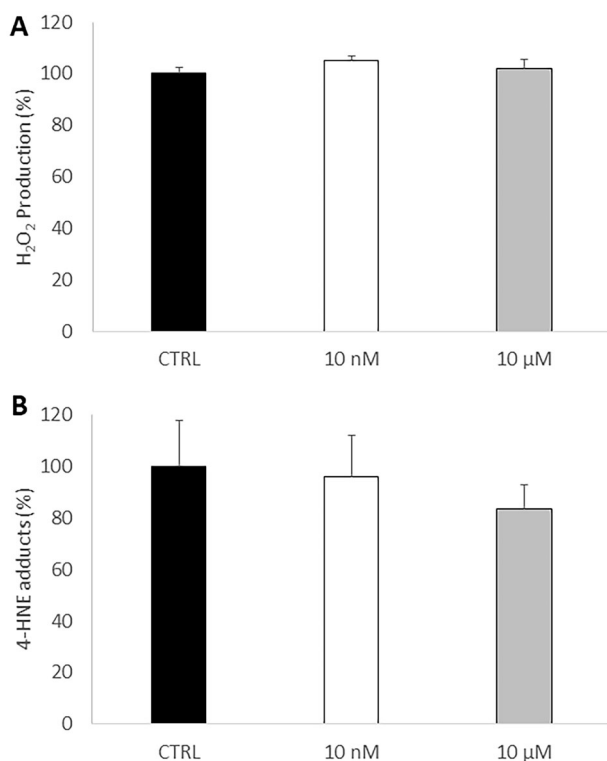


Figure 4. Effects of XN treatment on (A) H₂O₂ production and (B) lipid peroxidation. H₂O₂ production was measured with the Amplex® Red kit and lipid peroxidation was measured by detecting 4-HNE adducts by Western Blot. Values are expressed as mean ± SEM ($n=6$) and normalised to control values, set at 100%. *indicates a significant difference between control and XN-treated cells ($p < 0.05$).

Interestingly, both high and low concentrations of XN significantly decreased the mRNA levels of the nuclear respiratory factor 1 (*NRF1*), single-stranded DNA-

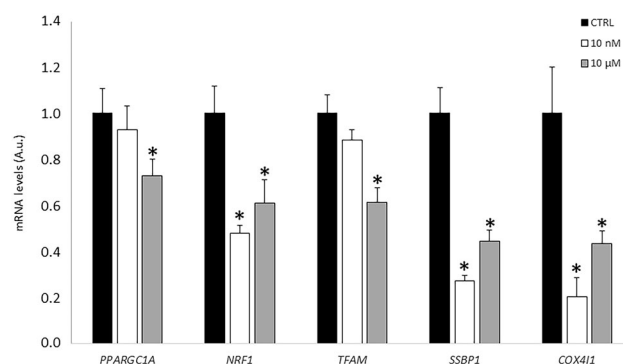


Figure 5. Gene expression of mitochondrial biogenesis- and function-related genes. mRNA levels were determined by RT-qPCR after treatment with 10 nM and 10 μM XN for 48 h. Values are expressed as mean ± SEM ($n=6$) and values of control cells were set at 1. *indicates a significant difference between control and XN-treated cells ($p < 0.05$). A.u., arbitrary units; *PPARGC1A*, peroxisome proliferator-activated receptor gamma coactivator 1-alpha; *NRF1*, nuclear respiratory factor 1; *TFAM*, mitochondrial transcription factor A; *SSBP1*, single-stranded DNA-binding protein; *COX4I1*, cytochrome c oxidase subunit 4I1.

binding protein (*SSBP1*), and cytochrome oxidase IV subunit 4 (*COX4I1*). Furthermore, 10 μM XN also decreased the expression of peroxisome proliferator-activated receptor gamma coactivator 1-alpha (*PPARGC1A*) and mitochondrial transcription factor A (*TFAM*).

Next, we evaluated the protein levels of OXPHOS complexes after treatment with XN (Figure 6(A)). Complex IV was affected by the two concentrations of XN, decreasing its levels by 49% with 10 nM XN and by 30% with 10 μM XN. Complex II also decreased with 10 nM XN, while the other complexes remained unchanged with treatment.

Finally, we determined the levels of lactate dehydrogenase A (LDHA) and the E1 enzyme of the pyruvate dehydrogenase complex (PDH-E1α). As seen in Figure 6(B), only 10 nM XN decreased the levels of both LDH and PDH-E1α, while 10 μM XN did not affect the levels of these two enzymes.

Discussion

In this study, we have shown that XN reduced the expression of inflammatory and antioxidant genes, without significant changes in oxidative stress and cell viability. Furthermore, XN treatment decreased the expression of mitochondrial biogenesis-related genes, and consequently, affected the protein levels of some OXPHOS complexes. Finally, both LDH and PDH protein levels were also reduced by XN treatment.

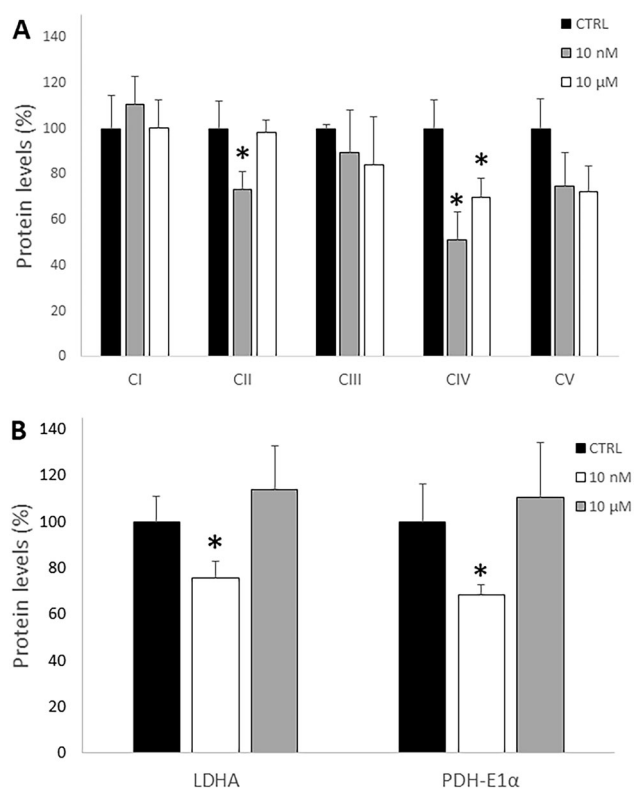


Figure 6. Protein levels of (A) OXPHOS complexes and (B) LDHA and PDH metabolic enzymes after XN treatment. Protein levels were analysed by Western Blot. Values are expressed as mean \pm SEM ($n=6$) and normalised to control values, set at 100%. *indicates a significant difference between control and XN-treated cells ($p < 0.05$). CI, Complex I subunit NDUFB8; CII, Complex II subunit 30 kDa; CIII, Complex III subunit Core 2; CIV, Complex IV subunit II; CV, ATP synthase subunit alpha; LDHA, lactate dehydrogenase A, PDH-E1 α , E1 enzyme of the pyruvate dehydrogenase complex.

XN has been widely studied as an anti-cancer agent as it reduces cell proliferation of different cancer cell lines, including gastric cancer (Guo et al. 2018; Wei et al. 2018), larynx cancer (Sławińska-Brych et al. 2015), melanoma (Seitz et al. 2021), lung cancer (Yong et al. 2015), cholangiocarcinoma (Walden et al. 2017), breast cancer (Blanquer-Rossello et al. 2013), and colon cancer (Sastre-Serra et al. 2019). However, no significant changes in cell viability were observed with the two concentrations of XN tested. Different IC50 values have been reported for HT29 cells, ranging from 10-12 μ M (X. Liu et al. 2019; Scagliarini et al. 2020) to 50 μ M (Logan et al. 2019). In fact, a report by Shikata et al. (2017) classified HT29 cells as XN-insensitive, which is in line with our results of cell viability. Notably, the concentrations of XN used in this study were 10 nM and 10 μ M, as these values are close to the concentration reached in blood without and with prenylflavonoid supplementation, respectively, and the higher concentration could be

expected in the colon (Bolca et al. 2010; Legette et al. 2014; Logan et al. 2019).

XN is a flavonoid known for its anti-inflammatory properties (Gupta et al. 2014). Here, we have shown that XN treatment downregulated the levels of *NFKB1* expression, which has been observed in other types of cancer (Zhao et al. 2016; Saito et al. 2018; Wei et al. 2018; Krajka-Kuźniak et al. 2020). Furthermore, at nanomolar doses, XN decreased the expression of both *TNF* and *IL6R*, which also suggests a decrease in inflammation levels. In fact, IL-6 and TNF- α induce the activation of NF- κ B, STAT1, and STAT3 in CRC cells, increasing their aggressiveness and stem-like properties (Chung et al. 2017). On the other hand, Chang et al. (2016) previously reported that the levels of pro-inflammatory cytokines, including IL-6 and TNF- α , could be used as progression markers for CRC. Thus, we show here that XN treatment could halt tumour progression in the HT29 primary cancer cell line by reducing inflammatory signalling.

Furthermore, we also observed a decrease in mitochondrial function, as seen by the decrease in some mitochondrial biogenesis-related genes and the decrease in some OXPHOS subunits levels. The decrease in OXPHOS levels and activity by XN has been previously described in colon cancer cells (Sastre-Serra et al. 2019) and other types of cancer (Blanquer-Rossello et al. 2013; Zhang et al. 2015). As mitochondria are the main source of ROS, a decrease in their number and/or function could lead to a decrease in ROS levels and in antioxidant enzyme expression (Galadari et al. 2017). In line with this, we observed a general decrease in the expression levels of antioxidant genes. However, H₂O₂ levels and lipid damage did not change with XN treatment. This could be explained by the slight increase in the ratios of *SOD2/CAT* and *SOD2/GPX1*, since the levels of *CAT* and *GPX1*, H₂O₂-detoxifying enzymes, were decreased. Therefore the detoxification capacity of H₂O₂ is reduced and its production remains similar to control cells (Ighodaro and Akinloye 2018).

Finally, XN treatment also produced a decrease in both LDH and PDH levels, which could indicate a slowdown of energy metabolism and glycolysis in HT29 cells. A reduction of the glycolysis rate by XN has been previously reported in colon cancer (W. Liu et al. 2019) and glioblastoma (Yuan et al. 2020). Thus, XN treatment could reduce glucose and oxidative metabolism of HT29 primary cancer cells.

One of the limitations of this study is the lack of a non-transformed cell line to analyse the chemo-preventive effect of XN. However, some studies have

reported the effects of XN on normal cell lines. For instance, Hemachandra et al. (2012) showed that XN at μM concentrations reduced malignant transformation of MCF-10A cells, a human mammary epithelial cell line. Furthermore, XN treatment had no effect on normal breast (Yoshimaru et al. 2015), gastric (Wei et al. 2018), and hepatic (Dorn et al. 2010) cells, suggesting that XN selectively targets cancer cells. On the other hand, Zajc et al. (2012) showed that XN may reduce cell viability in normal astrocytes in vitro at high concentrations, although the effects on cancer cells were significantly more pronounced. Finally, XN treatment did not show any effects on cell proliferation on Caco-2 cells (Machado et al. 2017), which although they are derived from a colon carcinoma, they are commonly used as a model of intestinal drug absorption.

Another important limitation of the present study is that XN is transformed into several active metabolites throughout the digestive tract, with participation of gut microbiota. Although these metabolic transformations have not been considered in this study, there are several strategies under development to improve bioavailability of XN. These include chemical modifications (Stompor et al. 2019) or the inclusion of XN in micellar formulations (Khayyal et al. 2020), which may also enhance the anti-cancer effects of XN.

Conclusion

Taken together, our results show an anti-inflammatory effect of XN in colon cancer, and although no difference in H_2O_2 production or lipid oxidative damage was found, a reduction in antioxidant enzymes expression was observed. Furthermore, HT29 cells also showed signs of reduced mitochondrial function. Thus, XN treatment, especially at nanomolar doses which are achievable in the colon with the diet, could slow down the progression of primary colorectal cancer cells by reducing inflammatory signalling and metabolism.

Disclosure statement

No potential conflict of interest was reported by the author(s).

Funding

This work was supported by the Centro de Información Cerveza y Salud (Madrid, Spain) under grant awarded the Manuel de la Oya: Beer, Health and Nutrition, and MT-M by the Postdoctoral Program Margalida Comas from the

Comunidad Autónoma de las Islas Baleares under grant number PD/050/2020.

ORCID

Margalida Torrens-Mas  <http://orcid.org/0000-0002-2983-1620>

Marina Alorda-Clara  <http://orcid.org/0000-0002-3610-7809>

Pilar Roca  <http://orcid.org/0000-0003-3878-5424>

Jorge Sastre-Serra  <http://orcid.org/0000-0003-3405-0535>

Jordi Oliver  <http://orcid.org/0000-0002-5702-7306>

Daniel Gabriel Pons  <http://orcid.org/0000-0002-2931-7939>

References

- Blanquer-Rossello MM, Oliver J, Valle A, Roca P. 2013. Effect of xanthohumol and 8-prenylnaringenin on MCF-7 breast cancer cells oxidative stress and mitochondrial complexes expression. *J Cell Biochem.* 114(12): 2785–2794.
- Bolca S, Li J, Nikolic D, Roche N, Blondeel P, Possemiers S, De Keukeleire D, Bracke M, Heyerick A, van Breemen RB, Depypere H. 2010. Disposition of hop prenylflavonoids in human breast tissue. *Health Psychol.* 54(02): S284–S294.
- Chang P-H, Pan Y-P, Fan C-W, Tseng W-K, Huang J-S, Wu T-H, Chou W-C, Wang C-H, Yeh K-Y. 2016. Pretreatment serum interleukin-1 β , interleukin-6, and tumor necrosis factor- α levels predict the progression of colorectal cancer. *Cancer Med.* 5(3) :426–433.
- Chung SS, Wu Y, Okobi Q, Adekoya D, Atefi M, Clarke O, Dutta P, Vadgama JV. 2017. Proinflammatory cytokines IL-6 and TNF- α increased telomerase activity through NF- κ B/STAT1/STAT3 activation, and withaferin A inhibited the signaling in colorectal cancer cells. *Mediators Inflammation.* 2017:1–11.
- Dorn C, Weiss TS, Heilmann J, Hellerbrand C. 2010. Xanthohumol, a prenylated chalcone derived from hops, inhibits proliferation, migration and interleukin-8 expression of hepatocellular carcinoma cells. *Int J Oncol.* 36(2): 435–541.
- Galadari S, Rahman A, Pallichankandy S, Thayyullathil F. 2017. Reactive oxygen species and cancer paradox: To promote or to suppress? *Free Radic Biol Med.* 104: 144–164.
- Giampazolias E, Tait SWG. 2016. Mitochondria and the hallmarks of cancer. *Febs J.* 283(5) :803–814.
- Guo D, Zhang B, Liu S, Jin M. 2018. Xanthohumol induces apoptosis via caspase activation, regulation of Bcl-2, and inhibition of PI3K/Akt/mTOR-kinase in human gastric cancer cells. *Biomed Pharmacother.* 106(April): 1300–1306. Elsevier,
- Gupta SC, Tyagi AK, Deshmukh-Taskar P, Hinojosa M, Prasad S, Aggarwal BB. 2014. Downregulation of tumor necrosis factor and other proinflammatory biomarkers by polyphenols. *Arch Biochem Biophys.* 559(June):91–99. Elsevier Inc.,

- Harish V, Haque E, Śmiech M, Taniguchi H, Jamieson S, Tewari D, Bishayee A. 2021. Xanthohumol for human malignancies: chemistry, pharmacokinetics and molecular targets. *IJMS*. 22(9):4478.
- Ighodaro OM, Akinloye OA. 2018. First line defence antioxidants-superoxide dismutase (SOD), catalase (CAT) and glutathione peroxidase (GPX): Their fundamental role in the entire antioxidant defence grid. *Alexandria J Med*. 54(4) :287–293.
- Jiang W, Zhao S, Xu L, Lu Y, Lu Z, Chen C, Ni J, Wan R, Yang L. 2015. The inhibitory effects of xanthohumol, a prenylated chalcone derived from hops, on cell growth and tumorigenesis in human pancreatic cancer. *Biomed Pharmacother*. 73:40–47. Elsevier Masson SAS,
- Khayyal MT, El-Hazek RM, El-Sabbagh WA, Frank J, Behnam D, Abdel-Tawab M. 2020. Micellar solubilization enhances the anti-inflammatory effect of xanthohumol. *Phytomedicine*. 71(April):153233–153239.
- Krajka-Kuźniak V, Cykowiak M, Szafer H, Kleszcz R, Baer-Dubowska W. 2020. Combination of xanthohumol and phenethyl isothiocyanate inhibits NF- κ B and activates Nrf2 in pancreatic cancer cells. *Toxicol in Vitro*. 65(February):104799.
- Landskron G, De la Fuente M, Thuwajit P, Thuwajit C, Hermoso MA. 2014. Chronic inflammation and cytokines in the tumor microenvironment. *J Immunol Res*. 2014: 1–19. Hindawi Publishing Corporation,
- Legette L, Karnpracha C, Reed RL, Choi J, Bobe G, Christensen JM, Rodriguez-Proteau R, Purnell JQ, Stevens JF. 2014. Human pharmacokinetics of xanthohumol, an anti-hyperglycemic flavonoid from hops. *Mol Nutr Food Res*. 58 (2) :248–255.
- Liu W, Li W, Liu H, Yu X. 2019. Xanthohumol inhibits colorectal cancer cells via downregulation of hexokinases ii-mediated glycolysis. *Int J Biol Sci*. 15(11) :2497–2508.
- Liu X, An LJ, Li Y, Wang Y, Zhao L, Lv X, Guo J, Song AL. 2019. Xanthohumol chalcone acts as a powerful inhibitor of carcinogenesis in drug-resistant human colon carcinoma and these effects are mediated via G2/M phase cell cycle arrest, activation of apoptotic pathways, caspase activation and targeting Ras/MEK/ERK pa. *J Buon*. 24(6) :2442–2447.
- Logan I, Miranda C, Lowry M, Maier C, Stevens J, Gombart A. 2019. Antiproliferative and cytotoxic activity of xanthohumol and its non-estrogenic derivatives in colon and hepatocellular carcinoma cell lines. *IJMS*. 20(5):1203.
- Machado JC, Faria MA, Melo A, Ferreira IMPLVO. 2017. Antiproliferative effect of beer and hop compounds against human colorectal adenocarcinoma Caco-2 cells. *J Funct Foods*. 36 :255–261.
- Hemachandra LP, Madhubhani P, Chandrasena R, Esala P, Chen S-N, Main M, Lankin DC, Scism RA, Dietz BM, Pauli GF, et al. 2012. Hops (*Humulus lupulus*) inhibits oxidative estrogen metabolism and estrogen-induced malignant transformation in human mammary epithelial cells (MCF-10A). *Cancer Prev Res*. 5(1) :73–81.
- Porporato PE, Filigheddu N, Pedro JMB-S, Kroemer G, Galluzzi L. 2018. Mitochondrial metabolism and cancer. *Cell Res*. 28(3) :265–280.
- Saito K, Matsuo Y, Imafuji H, Okubo T, Maeda Y, Sato T, Shamoto T, Tsuboi K, Morimoto M, Takahashi H, et al. 2018. Xanthohumol inhibits angiogenesis by suppressing nuclear factor- κ B activation in pancreatic cancer. *Cancer Sci*. 109(1) :132–140.
- Sastre-Serra J, Ahmiane Y, Roca P, Oliver J, Pons DG. 2019. Xanthohumol, a hop-derived prenylflavonoid present in beer, impairs mitochondrial functionality of SW620 colon cancer cells. *Int J Food Sci Nutr*. 70(4) :396–404.
- Scagliarini A, Mathey A, Aires V, Delmas D. 2020. Xanthohumol, a prenylated flavonoid from hops, induces DNA damages in colorectal cancer cells and sensitizes SW480 cells to the SN38 chemotherapeutic agent. *Cells*. 9(4):932.
- Seitz T, Hackl C, Freese K, Dietrich P, Mahli A, Thasler RM, Thasler WE, Lang SA, Bosserhoff AK, Hellerbrand C, et al. 2021. Xanthohumol, a prenylated chalcone derived from hops, inhibits growth and metastasis of melanoma cells. *Cancers*. 13(3):511–512.
- Shikata Y, Yoshimaru T, Komatsu M, Katoh H, Sato R, Kanagaki S, Okazaki Y, Toyokuni S, Tashiro E, Ishikawa S, et al. 2017. Protein kinase A inhibition facilitates the antitumor activity of xanthohumol, a valosin-containing protein inhibitor. *Cancer Sci*. 108(4) :785–794.
- Sławińska-Brych A, Król SK, Dmoszyńska-Graniczka M, Zdzisińska B, Stepulak A, Gagoś M. 2015. Xanthohumol inhibits cell cycle progression and proliferation of larynx cancer cells in vitro. *Chem Biol Interact*. 240:110–118.
- Stompor M, Świtalska M, Wietrzyk J. 2019. The influence of a single and double biotinylation of xanthohumol on its anticancer activity. *Acta Biochim Pol*. 66(4) :559–565.
- Sun Z, Zhou C, Liu F, Zhang W, Chen J, Pan Y, Ma L, Liu Q, Du Y, Yang J, et al. 2018. Inhibition of breast cancer cell survival by Xanthohumol via modulation of the notch signaling pathway in vivo and in vitro. *Oncol Lett*. 15(1) :908–916.
- Sung H, Ferlay J, Siegel RL, Laversanne M, Soerjomataram I, Jemal A, Bray F. 2021. Global cancer statistics 2020: GLOBOCAN estimates of incidence and mortality worldwide for 36 cancers in 185 countries. *CA A Cancer J Clin*. 71(3) :209–249.
- Torrens-Mas M, Roca P. 2020. Phytoestrogens for cancer prevention and treatment. *Biology*. 9(12):427–419.
- Walden D, Kunnimalaiyaan S, Sokolowski K, Clark TG, Kunnimalaiyaan M. 2017. Antiproliferative and apoptotic effects of xanthohumol in cholangiocarcinoma. *Oncotarget*. 8(50) :88069–88078.
- Wei S, Sun T, Du J, Zhang B, Xiang D, Li W. 2018. Xanthohumol, a prenylated flavonoid from Hops, exerts anticancer effects against gastric cancer in vitro. *Oncol Rep*. 40(6) :3213–3222.
- Yong W, Ho Y, Abd Malek S. 2015. Xanthohumol induces apoptosis and S phase cell cycle arrest in A549 non-small cell lung cancer cells. *Phcog Mag*. 11(44) :275.
- Yoshimaru T, Komatsu M, Tashiro E, Imoto M, Osada H, Miyoshi Y, Honda J, Sasa M, Katagiri T. 2015. Xanthohumol suppresses oestrogen-signalling in breast cancer through the inhibition of BIG3-PHB2 interactions. *Sci Rep*. 4(1):1–9.








- Yuan J, Peng G, Xiao G, Yang Z, Huang J, Liu Q, Yang Z, Liu D. 2020. Xanthohumol suppresses glioblastoma via modulation of Hexokinase 2 -mediated glycolysis. *J Cancer*. 11(14):4047–4058.
- Zajc I, Filipič M, Lah T. 2012. Xanthohumol induces different cytotoxicity and apoptotic pathways in malignant and normal astrocytes. *Phytother Res*. 26(11):1709–1713.
- Zhang B, Chu W, Wei P, Liu Y, Wei T. 2015. Xanthohumol induces generation of reactive oxygen species and triggers apoptosis through inhibition of mitochondrial electron transfer chain complex i. *Free Radic Biol Med*. 89: 486–497.
- Zhang S, Cao L, Li Z, Qu D. 2019. Metabolic reprogramming links chronic intestinal inflammation and the oncogenic transformation in colorectal tumorigenesis. *Cancer Lett*. 450(February):123–131.
- Zhao X, Jiang K, Liang B, Huang X. 2016. Anticancer effect of xanthohumol induces growth inhibition and apoptosis of human liver cancer through NF- κ B/p53-apoptosis signaling pathway. *Oncol Rep*. 35(2) :669–675.

Use of Omics Technologies for the Detection of Colorectal Cancer Biomarkers.

Alorda-Clara, M., Torrens-Mas, M., Morla-Barcelo, P. M., Martinez-Bernabe, T., Sastre-Serra, J., Roca, P., Pons, D.G., Oliver, J. & Reyes, J. (2022). *Cancers*, 14(3), 817.

Review

Use of Omics Technologies for the Detection of Colorectal Cancer Biomarkers

Marina Alorda-Clara ^{1,2} , Margalida Torrens-Mas ^{1,2,3} , Pere Miquel Morla-Barcelo ¹,
Toni Martinez-Bernabe ^{1,2} , Jorge Sastre-Serra ^{1,2,4} , Pilar Roca ^{1,2,4} , Daniel Gabriel Pons ^{1,2} ,
Jordi Oliver ^{1,2,4,*}  and Jose Reyes ^{1,2,5,*}

- ¹ Grupo Multidisciplinar de Oncología Traslacional, Institut Universitari d'Investigació en Ciències de la Salut (IUNICS), Universitat de les Illes Balears, E-07122 Palma de Mallorca, Illes Balears, Spain; marina.alorda@uib.es (M.A.-C.); margalida.torrens@ssib.es (M.T.-M.); pere.morla@uib.es (P.M.M.-B.); toni.martinez@uib.es (T.M.-B.); jorge.sastre@uib.es (J.S.-S.); pilar.roca@uib.es (P.R.); d.pons@uib.es (D.G.P.)
- ² Instituto de Investigación Sanitaria Illes Balears (IdISBa), Hospital Universitario Son Espases, Edificio S, E-07120 Palma de Mallorca, Illes Balears, Spain
- ³ Translational Research in Aging and Longevity (TRIAL) Group, Instituto de Investigación Sanitaria Illes Balears (IdISBa), E-07120 Palma de Mallorca, Illes Balears, Spain
- ⁴ Ciber Fisiopatología Obesidad y Nutrición (CB06/03) Instituto Salud Carlos III, E-28029 Madrid, Madrid, Spain
- ⁵ Servicio Aparato Digestivo, Hospital Comarcal de Inca, E-07300 Inca, Illes Balears, Spain
- * Correspondence: authors: jordi.oliver@uib.es (J.O.); jose.reyes@hcin.es (J.R.); Tel.: +34-971-259-643 (J.O.)



Citation: Alorda-Clara, M.; Torrens-Mas, M.; Morla-Barcelo, P.M.; Martinez-Bernabe, T.; Sastre-Serra, J.; Roca, P.; Pons, D.G.; Oliver, J.; Reyes, J. Use of Omics Technologies for the Detection of Colorectal Cancer Biomarkers. *Cancers* **2022**, *14*, 817. <https://doi.org/10.3390/cancers14030817>

Academic Editors: Luis Bujanda, Ajay Goel and Ane Etxart

Received: 31 December 2021

Accepted: 4 February 2022

Published: 6 February 2022

Publisher's Note: MDPI stays neutral with regard to jurisdictional claims in published maps and institutional affiliations.



Copyright: © 2022 by the authors. Licensee MDPI, Basel, Switzerland. This article is an open access article distributed under the terms and conditions of the Creative Commons Attribution (CC BY) license (<https://creativecommons.org/licenses/by/4.0/>).

Simple Summary: Colorectal cancer (CRC) is one of the most frequent cancers worldwide. Early detection of CRC is crucial, as it greatly improves the survival of patients. Currently, the CRC screening programs consist of a stool test to detect the presence of blood in stool and a subsequent colonoscopy to confirm the diagnosis. However, CRC screening can be further improved with the use of new biomarkers. Omics technologies, that is, techniques that generate a vast amount of data, can help to establish these markers. Here, we discuss the use of omics with different types of samples (breath, urine, stool, blood, bowel lavage fluid, and tissue) and highlight some of the most relevant biomarkers that have been recently detected.

Abstract: Colorectal cancer (CRC) is one of the most frequently diagnosed cancers with high mortality rates, especially when detected at later stages. Early detection of CRC can substantially raise the 5-year survival rate of patients, and different efforts are being put into developing enhanced CRC screening programs. Currently, the faecal immunochemical test with a follow-up colonoscopy is being implemented for CRC screening. However, there is still a medical need to describe biomarkers that help with CRC detection and monitor CRC patients. The use of omics techniques holds promise to detect new biomarkers for CRC. In this review, we discuss the use of omics in different types of samples, including breath, urine, stool, blood, bowel lavage fluid, or tumour tissue, and highlight some of the biomarkers that have been recently described with omics data. Finally, we also review the use of extracellular vesicles as an improved and promising instrument for biomarker detection.

Keywords: omics; colorectal cancer; extracellular vesicles; tumour tissue; blood; stool; bowel lavage fluid; urine; breath

1. Introduction

Colorectal cancer (CRC) is one of the most frequently diagnosed cancers, with more than 1.9 million estimated new cases worldwide [1]. In Spain, CRC accounted for around 15,288 deaths in 2018, and has an annual age-standardized mortality rate of 30 per 100,000 inhabitants. This makes CRC the sixth-leading cause of death and the second leading cause of cancer-related mortality [2]. Early diagnosis raises the 5-year survival rate of these patients up to 94% [3]. Given the high burden of CRC on the National Health Service and the

importance of early detection, significant efforts have been directed toward developing CRC screening programs. The main aim of these programs is to remove pre-malignant lesions which could ultimately develop into malignant tumours, as well as to start treatment in early-stage detected cancers. This way, it is expected to reduce CRC incidence and CRC-specific mortality, which has been proven effective [4].

One of the main problems for CRC is the late diagnosis, giving rise to a decrease in survival since there is a lack of early biomarkers [5]. Different tools have been developed for CRC screening, which include colonoscopy, flexible sigmoidoscopy, guaiac faecal occult blood testing (gFOBT), faecal immunochemical testing (FIT), and carcinoembryonic antigen (CEA) in plasma, which has low sensitivity and specificity [6]. Intention-to-treat estimates from meta-analyses of large randomized trials report reductions in CRC mortality of 20–30% for flexible sigmoidoscopy [7,8], 8–16% for gFOBT, and 41% for FIT and follow-up colonoscopy [9]. Currently, the screening program in Spain consists of biennial FIT with colonoscopy follow-up on positive subjects, according to the European guidelines [10]. However, every autonomous region implements this program at a different pace and there are important differences among regions [11,12]. Although this screening program has led to a decrease in mortality, the performance of this test is suboptimal, with a sensitivity and specificity for CRC of 54–89% and 89–97%, respectively [13]. Furthermore, it has been noted that this sensitivity may vary with the tumour stage, being lower with early-stage CRC [14]. This leads to a substantial number of false negative and false positive tests and, consequently, to missed diagnoses or unneeded colonoscopies. Thus, there is an urgent need for more accurate and, ideally, non-invasive tests to implement for CRC screening and monitoring tumour progression and treatment efficacy.

The emergence of omics technologies is a promising strategy for detecting biomarkers of CRC. These methods generate high-throughput data that have the potential to detect significant changes that reflect the tumour initiation and progression. In this review, we discuss the utility of these technologies in different types of samples, such as breath, urine, stool, blood, bowel lavage fluid, and tumour tissue, and highlight some of the most promising results obtained in recent years. Finally, we also consider the isolation of extracellular vesicles (EVs) as an enhanced tool to detect new disease biomarkers.

2. Omics Techniques

2.1. Genomics

The National Cancer Institute defines genomics as the study of the complete set of DNA (including all of its genes) in a person or other organism. The genome contains all the information needed for an individual to develop and grow. Analyzing the genome may help researchers understand how genes interact with each other and the environment and how certain diseases, such as cancer, diabetes, or heart disease develop. This may lead to new ways to diagnose, treat, and prevent disease [15]. Genetic alterations have been identified as major players in tumorigenesis. Therefore, genomics has gained attention as a tool to identify genetic markers that can lead to better diagnosis and prognosis and at the same time, allow researchers to improve the understanding of cancer. Apart from gene mutations and single nucleotide polymorphisms (SNP), the epigenetic signature has also proven useful to establish a more personalised diagnosis [16].

The development of high-throughput methods for genome and gene expression studies has increased the amount of information available. These data are deposited in international public repositories and can be studied by other research groups. NCBI Gene Expression Omnibus (GEO) is the most important database repository of high-throughput gene expression data and hybridization arrays, chips, and microarrays [17]. The Cancer Genome Atlas (TCGA) of the National Cancer Institute (NCI) is another relevant database in oncology. TCGA is a project to classify the genetic mutations that cause cancer, using genome sequencing and integrating bioinformatics tools to analyse this information [18].

Finally, the use of metagenomics, which evaluates the microbiome genes, holds special promise for CRC. Metagenomics has shown the potential to identify differences between

control and CRC-associated microbiomes and eventually describe new CRC biomarkers [19].

2.2. Transcriptomics

Transcriptomics is the study of all RNA molecules in a cell and could give more information about how genes are turned on and off in different cell types and how this can contribute to cancer [20]. Differential gene expression comparison studies have emerged as a prospective approach to detecting promising biomarkers of enormous clinical value. This type of study is fuelled by and analyses the data deposited in the TGCA and GEO databases [21].

2.3. Proteomics

Proteomics is the study of the structure and function of proteins, including how they work and interact with each other [22]. In the search for new CRC biomarkers, proteomics studies are focused on differential protein expression between normal and cancer cells or the detection of different proteomic profiles in corporal fluids. Some of the most useful techniques for the identification of protein biomarkers in cancer are two-dimensional gel electrophoresis coupled with liquid chromatography/mass spectrometry (2-DE-MS), two-dimensional difference gel electrophoresis (2D-DIGE), or liquid chromatography–mass spectrometry (LC-MS) [23]. Multiplexed quantitative proteomic assays are capable of measuring changes in proteins and their interacting partners, isoforms, and post-translational modifications [23].

2.4. Metabolomics

Metabolomics is the study of metabolites in cells and tissues, which can be measured in different body fluids. The presence of a tumour can alter the whole individual's metabolism, and the use of some fuels can be modified to meet the energy demands of the tumour. Furthermore, the tumour metabolism may change as the tumour progresses. Considering that the dysregulation of metabolism is one of the hallmarks of cancer, this omics could open a new way to study cancer [24].

2.5. Glycomics

Glycomics studies the structure and function of glycans, N- and O- linked glycoproteins, glycolipids, and proteoglycans [25,26]. The most common alterations in lipid and protein glycosylation are an increase in the branching of N-glycans, high density of O-glycans, incomplete glycans synthesis, neosynthesis, and sialylation and fucosylation increase [27]. Glycans characterization can be done by a large number of techniques, such as microarrays, flow cytometry, enzyme-linked immunosorbent assay, mass spectrometry, and chromatographic techniques [27].

2.6. Volatolomics

Volatolomics is the study of volatile organic compounds that have high vapor pressure. This is a non-invasive, fast, and potentially inexpensive way of analysing the human body chemistry for monitoring of diseases such as cancer [28]. The volatilome, volatile organic compounds (VOC) profile, is being used in the detection of CRC. Alterations in the metabolism of cancer cells can be reflected in a characteristic profile of VOCs, as these compounds are produced in metabolic processes such as inflammation, cancer metabolic alterations, and necrosis processes [29–33]. Cancer-associated VOCs are directly excreted from the affected organ or tissue to stool or blood. Thus, the VOCs are exhaled in breath, excreted in urine, or released from the skin [34–36]. However, the VOCs interactions with the microbiota may affect the volatilome of stool [29]. The most used techniques in volatolomics are gas chromatography with mass spectrometry (GC-MS), which enables the separation and quantification of individual VOCs; proton transfer reaction—mass spectrometry (PTR-MS), for simultaneous real-time monitoring of VOCs without sample

preparation; and eNose, which allows the analysis of a specific VOC pattern in real-time. The latter is a low cost, easy-to-use equipment that can detect cancer at an early stage and can differentiate between cancer and healthy subjects [29,33,37].

Several studies have demonstrated the potential of the exhaled volatilome for CRC diagnosis and screening due to its sensitivity and specificity. However, further studies and standardization of collection and analysis methods for volatilome detection and its application to CRC diagnosis are needed [31,35–39].

3. Sample Types for the Omics Analyses in Colorectal Cancer

3.1. Breath Samples

Breath is a type of non-invasive sample easily collected that can be used to diagnose CRC.

Volatolomics

The determination of the volatilome in breath could provide new biomarkers for the detection of CRC. De Vietro et al. have shown differences in the release of VOCs between normal and cancerous colonic mucosa, the latter releasing higher amounts of benzaldehyde, benzene ethyl, and indole; these compounds can be detected in the breath of patients [30]. Politi and collaborators analysed the VOCs of different types of cancers, and specifically reported dinitrogen oxide, nitrous acid, acetic acid, and 1,3-butadiene in the breath of CRC patients [32].

Haick and Hakim have patented a colon cancer VOC marker, 1,3,5-cycloheptatriene. This compound is present in the breath of CRC patients and is not found in other types of cancer (breast, prostate, head, and neck cancer) or in healthy subjects. Moreover, other compounds can be found in the breath of these patients, such as 1,1'-(1-butenylidene) bis benzene, 1methyl-3-(1-methylethyl) benzene, 1-iodo nonane, [(1,1-dimethylethyl) thio] acetic acid, 2-amino-5-isopropyl-8-methyl-1-azulenecarbonitrile, 3,3-dimethyl hexane, 1-ethyl-2,4-dimethyl benzene, 1,1'-(3-methyl-1-propone-1,3-diyl)bis benzene, 2-methyl 1,3-butadiene. However, several of these compounds are also found in other types of cancers or healthy subjects [40].

Recent studies using discriminatory models with 14 VOCs (see Table 1) exhaled by patients were able to discriminate between patients with CRC and healthy patients. These models had a statistically significant likelihood of discrimination with an area under the ROC curve of 0.979 [41].

Table 1. Main biomarkers found in breath samples of CRC patients with volatolomics.

Omics	Biomarker	Change	Reference
Volatolomics (GC-MS)	Benzaldehyde, Benzene ethyl, Indole	Upregulated	[30]
Volatolomics (GC-IMR-MS)	1,3-butadiene, N ₂ O	Upregulated	[32]
Volatolomics (GC-IMR-MS)	Acetic acid, HNO ₂	Downregulated	[32]
Volatolomics (GC-MS)	1,3,5-cycloheptatriene	Upregulated	[40]
Volatolomics (GC-MS)	Tetradecane, Ethylbenzene, Methylbenzene, 5,9-Undecadien-2-one, 6,10-dimethyl, Benzaldehyde, Decane, Benzoic acid, 1,3-Bis(1-methylethenyl) benzene, Dodecane, Ethanone, 1[4-(1-methylethenyl)phenyl], acetic acid	Upregulated	[40,41]
Volatolomics (GC-MS)	Decanal, 2-Ethyl-1-hexanol	Downregulated	[40]

3.2. Urine Samples

Urine is a sample that can be easily collected and is a non-invasive method for detecting molecules related to CRC, such as blood and stool.

3.2.1. Genomics

The latest advances in urine genomics focus on the study of mutations in *KRAS*. Ohta et al., evaluated the quantity of ctDNA derived from urine (transrenal ctDNA) and the accuracy of *KRAS* mutation detection in relation to CRC stage [42].

3.2.2. Proteomics

The urine of patient-derived xenograft (PDX) mice with CRC tumours has been evaluated to find protein biomarkers [43]. This approach has helped to improve the clinical efficacy of markers of colorectal liver metastasis, such as CEA [44]. Moreover, the cargo of exosomes as a source for proteomics studies has been recently studied, not only in urological cancers, but also in non-urological cancers such as CRC. Erozenski and collaborators analysed MS-based proteomic data on urinary exosomes from cancer patients and discussed the potential of urinary exosome-derived biomarkers in cancer [45].

3.2.3. Metabolomics

In a systematic review, up to 244 compounds in urine samples from cancer patients were identified [46]. Four upregulated metabolites and seven downregulated compounds were reported in the metabolome and the volatilome, as shown in Table 2 [46].

Interestingly, in one study comparing the metabolic profile of plasma, stool, and urine of advanced colon cancer and healthy subjects, the authors determined that metabolites from the stool samples were negatively correlated with those found in the urine samples [47]. In another study, 154 metabolites were identified, including metabolites of glycolysis, tricarboxylic acid (TCA) cycle, amino acids, urea cycle, and polyamine pathways. The concentration of these metabolites gradually increased with the stage of cancer, with the difference in stage IV being the greatest. Furthermore, the analysis of metabolites allowed for discriminating between polyps and CRC samples [48]. Ning et al. described eleven metabolites that were up-regulated, while four other metabolites were down-regulated in urine samples from CRC patients compared to healthy controls, as shown in Table 2. Analysing the pathways involving these metabolites, they found alterations in the energy metabolism in CRC patients, reflecting an upregulation of glycolysis and amino acid metabolism and a decrease in lipid metabolism [49].

On the other hand, a new metabolomics-based urine test (UMT) can detect adenomatous polyps and CRC. According to the authors, this UMT could be more cost-effective if used in CRC screening programs [50]. Another approach is urine nuclear magnetic resonance (NMR) metabolomics as a diagnostic tool for early detection of CRC [51].

Other studies have also been developed with a focus on the diet, specifically with the presence of metabolites derived from white beans. Concretely, a dietary intervention was carried out for 4 weeks with white beans, and changes in different metabolic pathways which are important for CRC prevention were observed [52]. All biomarkers are summarized in the Table 2.

Table 2. Main biomarkers found in urine samples of CRC patients with metabolomics.

Omics	Biomarker	Change	Reference
Metabolomics	3-hydroxybutyric acid, L-dopa, L-histidinol, and N1, N12-diacetylspermine	Upregulated	[46]
Metabolomics	pyruvic acid, hydroquinone, tartaric acid, hippuric acid, butyraldehyde, ether, and 1,1,6-trimethyl-1,2-dihydronaphthalene	Downregulated	[46]
Metabolomics	Hydroxyproline dipeptide, tyrosine, glucuronic acid, tryptophan, pseudouridine, glucose, glycine, histidine, 5-oxoproline, isocitric acid, threonic acid	Upregulated	[49]
Metabolomics	Citric acid, octadecanoic acid, hexadecanoic acid, propanoic acid-2-methyl-1-(1,1-dimethylethyl)-2-methyl-1,3-propanediyl ester	Downregulated	[49]
Metabolomics	3-(4-hydroxyphenyl)propionate, betaine, pipercolate, S-methylcysteine, choline, eicosapentaenoate (20:5n3), benzoate, S-adenosylhomocysteine, N-delta-acetylmethionine, cysteine, 3-(4-hydroxyphenyl)lactate, gentisate, hippurate, 4-hydroxyhippurate, and salicylate.	Up- and downregulated	[52]

3.3. Stool Samples

The use of stool samples offers several advantages as a source of CRC biomarkers. Sample collection is non-invasive, the test can be performed at home, there is no sample amount limitation, and the stool effectively samples the entire length of the inner bowel wall contents (including tumour) as it passes down the gastrointestinal tract [53]. For this reason, stool samples are increasingly gaining attention in the search for new biomarkers for the early detection of CRC [54,55].

3.3.1. Genomics

In one study analysing the stool microbiome, four gene markers were identified to be enriched in early-stage (I-II) CRC patients, highlighting the potential for using stool metagenomic biomarkers for the early diagnosis of CRC [19]. Among these four genes, butyryl-CoA dehydrogenase from *F. nucleatum* was identified as the best potential CRC biomarker [19]. Another study has shown an increase of gut microbial *baiF* gene copy numbers in CRC patients' stool samples, in addition to *baiF* RNA expression [56]. In another interesting study, the authors compared the gut microbiome between CRC patients and their healthy family members, to avoid lifestyle interferences, by sequencing extracted DNA from stool samples. The best biomarker they obtained was from *Coprobacillus* [57]. In a very recent study with more than 1,000 participants, a metagenomics analysis was carried out and results were validated by targeted quantitative PCR. The authors identified a novel bacterial marker, *m3*, from *Lachnoclostridium* species for adenoma detection [58].

On the other hand, the utility of DNA methylation as a biomarker for CRC has been analysed. One study identified 4 potential methylation markers (*COL4A1*, *COL4A2*, *TLX2*, and *ITGA4*) upregulated in CRC patients' stool, using real-time methylation-specific PCR based on TaqMan probe fluorescence (TaqMan qMSP) technology after a selection of these genes in CRC cell lines and CRC patients' tissue [59]. Another similar report performed a methylation analysis using MethyLight qPCR and droplet digital PCR, reporting elevated CpG islands methylation in two genes: *GRIA4* and *VIPR2* [60]. Two additional DNA methylation markers analysed with multiplex quantitative PCR assay, *SDC2* and *NDRG4*, were found in another study, providing a solid foundation for multi-target DNA biomarker analysis in stool samples for CRC screening [61]. Previously, other authors reported *SDC2* methylation as a good candidate for potential non-invasive diagnostic tool for early detection of CRC [62]. In fact, a clinical trial was conducted in 2020, with more than 1000 participants to assess a stool DNA test of methylated *SDC2* for CRC detection, with promising results [63]. In a study published in September 2021, *SDC2* methylation, as well as *ADHFE1* and *PPP2R5C* methylation, have been revealed as good CRC biomarkers, confirming the accuracy of *SDC2* methylation as a CRC indicator [64]. Another gene promoter methylation, *SOX21*, was demonstrated in a very recent analysis in stool to be a good non-invasive biomarker with a high sensitivity and specificity [65]. All these biomarkers are summarized in Table 3.

3.3.2. Transcriptomics

Almost 15 years ago, the very first studies for the search and standardization of transcriptomic molecular markers in CRC patients' stool were conducted, as the authors assured that RNA-based detection methods were more comprehensive than either DNA-, protein- or methylation-based screening methods [66]. Years later, an analysis of miRNAs in the stool of control and CRC patients was performed [67]. In this study, seven miRNAs were found to be upregulated in CRC (miR-21, miR-106a, miR-96, miR-203, miR-20a, miR-326 and miR-92) and another seven were found to be downregulated (miR-320, miR-126, miR-484-5p, miR-143, miR-145, miR-16 and miR-125b) [67]. Interestingly, the authors correlated miRNAs with their target mRNAs, having a more precise idea of the activated or inhibited molecular pathways [67]. In a more recent study, the same authors revealed 12 miRNAs (miR-7, miR-17, miR-20a, miR-21, miR-92a, miR-96, miR-106a, miR-134, miR-183, miR-196a, miR-199a-3p, and miR-214) overexpressed and 8 miRNAs (miR-9, miR-29b, miR-127-5p, miR-138, miR-143, miR-146a, miR-222, and miR-938) with decreased expression in CRC patients' stool [68]. The novelty of this study is the fact that these changes in expression were more pronounced as the cancer progressed from early to late TNM stages [68]. Another type of RNAs, lncRNAs, were recently used to do a panel of potential biomarkers for early detection of CRC in stool colonocytes, including *CCAT1*, *CCAT2*, *H19*, *HOTAIR*, *HULC*, *MALAT1*, *PCAT1*, *MEG3*, *PTENP1*, and *TUSC7* [69]. All biomarkers are summarized in Table 3.

3.3.3. Proteomics

In recent years, several studies have investigated new methods to mine deeply into the stool proteome to reveal candidate proteins to be potential biomarkers for CRC [53]. A recent publication has reviewed the main biomarkers obtained in stool samples among other corporal fluids and biopsies [70]. Using tandem mass spectrometry (LC-MS/MS), Yang et al. identified seven proteins (*Hp*, *LAMP1*, *SYNE2*, *LRG1*, *RBP4*, *FN1*, and *ANXA6*) alone or in combination, to detect high-risk adenomas and CRCs [71]. All biomarkers are summarized in Table 3.

3.3.4. Metabolomics

In a study carried out in China, GC-MS based metabolomics approach was used to discriminate healthy individuals from CRC patients, associating different metabolites with health status or disease phenotype. In this work, polyamines (cadaverine and putrescine)

were found as potential biomarkers for CRC prediction [72]. Previously, in a clinical trial done in Korea, the same method revealed changes in the fatty acid metabolome of CRC patients, implying that stool fatty acids, concretely increased oleic acid, could be used as a novel screening tool for CRC [73]. Differences in cholesteryl esters and sphingolipids have also been found in the stool of CRC patients using an UHPLC-MS metabolomics approach [74]. Recently, using the proton nuclear magnetic resonance (^1H NMR) technique, downregulation of butyrate and upregulation of alanine, lactate, glutamate and succinate was reported in CRC tissue and stool [75]. Finally, it is important to note the relationship between the metabolomic profile and the microbiota presence in the stool. Some studies have shown changes in the microbiome, such an enrichment of *Proteobacteria*, *Fusobacteria*, *Parvoimonas*, and *Staphylococcus* in CRC and *Firmicutes* in healthy groups as well as an uneven and lesser microbial diversity in CRC [72,74]. All biomarkers are summarized in Table 3.

Table 3. Main biomarkers found in stool samples of CRC patients with different omics technologies.

Omics	Biomarker	Change	Reference
Genomics (metagenomics)	butyryl-CoA dehydrogenase from <i>F. nucleatum</i>	Upregulated	[19]
Genomics and Transcriptomics	<i>baiF</i>	Upregulated	[56]
Genomics (metagenomics)	<i>Coprobacillus</i>	Upregulated	[57]
Genomics (metagenomics)	<i>m3</i> from <i>Lachnoclostridium</i>	Upregulated	[58]
Genomics (methylation)	<i>COL4A1</i> , <i>COL4A2</i> , <i>TLX2</i> , <i>ITGA4</i>	Upregulated	[59]
Genomics (methylation)	<i>GRIA4</i> , <i>VIPR2</i>	Upregulated	[60]
Genomics (methylation)	<i>SDC2</i> , <i>NDRG4</i>	Upregulated	[61]
Genomics (methylation)	<i>SDC2</i>	Upregulated	[62]
Genomics (methylation)	<i>SDC2</i> , <i>ADHFE1</i> , <i>PPP2R5C</i>	Upregulated	[64]
Genomics (methylation)	<i>SOX21</i>	Upregulated	[65]
Transcriptomics (miRNAs)	miR-21, miR-106a, miR-96, miR-203, miR-20a, miR-326, miR-92	Upregulated	[67]
Transcriptomics (miRNAs)	miR-320, miR-126, miR-484-5p, miR143, miR-145, miR-16, miR-125b	Downregulated	[67]
Transcriptomics (miRNAs)	miR-7, miR-17, miR-20a, miR-21, miR-92a, miR-96, miR-106a, miR-134, miR-183, miR-196a, miR-199a-3p, miR-214	Upregulated	[68]
Transcriptomics (miRNAs)	miR-9, miR-29b, miR-127-5p, miR-138, miR-143, miR-146a, miR-222, miR-938	Downregulated	[68]

Table 3. Cont.

Omics	Biomarker	Change	Reference
Transcriptomics (lncRNAs)	CCAT1, CCAT2, H19, HOTAIR, HULC, MALAT1, PCAT1, MEG3, PTENP1, TUSC7	Upregulated	[69]
Proteomics	Hp, LAMP1, SYNE2, LRG1, RBP4, FN1, ANXA6	Upregulated	[71]
Metabolomics	Polyamines (cadaverine and putrescine)	Upregulated	[72]
Metabolomics	Cholesteryl esters, Sphingomyelins	Upregulated	[74]
Metabolomics	Oleic acid	Upregulated	[73]
Metabolomics	Butyrate, Alanine, Lactate, Glutamate, Succinate	Upregulated (except Butyrate downregulated)	[75]

3.4. Blood Samples

In recent years, the low invasiveness and easy accessibility of liquid biopsies have made them the object of many studies, since the biologic materials present in blood samples are potential sources of non-invasive biomarkers that could improve CRC diagnosis and prognosis [76].

Detection of serum or plasma CRC biomarkers from blood samples is challenging due to their low concentration and the presence of material from healthy cells. However, the recent development of separation methods and sample processing has improved the analysis [77]. In blood, we can identify circulating free DNA or RNA (cfDNA and cfrRNA). These cfDNA and cfrRNA can be circulating tumour DNA or RNA (ctDNA and ctRNA), which can come from tumour cells, tumour circulating cells (CTCs), and EVs. Complementarily, different proteins and metabolites released into the blood circulation can be detected [78].

3.4.1. Genomics

Recent studies have focused on cfDNA as a quite important biomarker [79–81]. Quantification of total cfDNA and the DNA integrity index (DII: ratio of long DNA fragments resulting from necrosis and short DNA fragments resulting from apoptosis) have been reported elevated in CRC patients by using ALU and GAPDH sequences [80,81]. Furthermore, cfDNA are highly influenced by tumour stage and chemotherapy treatment; it is possible to also analyse point mutations, hypermethylation of gene promoters, or microsatellite alterations or MSI [76]. In fact, metastatic CRC presents less fragmented cfDNA compared to primary CRC [81]. In addition, KRAS, APC, and TP53 are the most featured genes with mutations after the analysis of the Idylla panel (KRAS, NRAS, and BRAF mutations, and characterization of MSI), the PlasmaSELECT-R panel (sequence alterations and translocations in 63 genes), the Guardant360 panel (point mutations in 70 genes and identification of gene fusions, insertions and deletions), the OncoBEAM panel (CRC-specific mutations), and the MassDetect CRC panel [78,82]. Furthermore, MSI is detected in 15% of CRCs and associated with defects in DNA mismatch repair genes [83], and with a greater resistance to chemotherapy [84]. Despite being a marker that can be detected in 35% of CRC patients, the detection rate varies from 0 to 60% in studies [76].

Finally, it is important to consider the epigenetic signature. The use of different commercial tests, such as Epi proColon 2.0 (Epigenomics) or RealTime ms9 (Abbptt), has identified various hypermethylation sites (BCAT1 and IKZF1) [78] and aberrant methylation in numerous genes (APC, MLH1, FRP2, NGFR) and gene promoters [76,78]. Nonetheless,

the most promising potential epigenetic biomarker is the SEPT9 gene, which has shown 90% of sensitivity and 88% of specificity [76,78]. All biomarkers are summarized in Table 4.

3.4.2. Transcriptomics

The detection of differential gene expression could be influenced by the stages of CRC [76,78,85]. Most of these studies found differential expression of CK19, CK20, and CEA, whose overall sensitivity was up to 72% [85]. Moreover, studies based on expression panels identified *MDM2*, *DUSP6*, *CPEB4*, *MMD*, *EIF2S3*, *ANXA3*, *CLEC4D*, *LMNB1*, *PRRG4*, *TNFAIP6*, *VNN1*, and *IL2RB* as differentially expressed genes [76,78].

On the other hand, some of the most relevant miRNA molecules assessed, such as miR-145, miR-143, miR-135, and miR-17-92, showed a significant diagnostic value for advanced neoplasia [86]. Furthermore, a recent study has used SHERLOCK-based miRNA detection to enhance and facilitate exosome-miRNA detection in blood, showing miR-126, miR-1290, miR-23a, and miR-940 as the best predictive biomarkers for early CRC stages [87]. Other miRNAs have been described as potential biomarkers, such as miR-92a, miR-29a, miR-125b, miR-19a-3p, miR-223-3p, miR-92a-3p and miR-422a, although miR-21 is by far the most studied for CRC [78]. Currently, there are few studies about circulating lncRNA as a potential non-invasive diagnostic biomarker in CRC. In fact, only three transcripts (CRNDE-h, CCAT1 and HOTAIR1) are described as promising biomarkers [76,78]. However, UCA1 and circHIPK3 are lncRNA from serum exosomes which could discriminate against CRC [78]. All biomarkers are summarized in Table 4.

3.4.3. Proteomics

Currently, CEA and Carbohydrate Antigen 19-9 (CA19-9) are the standard biomarkers used for monitoring CRC patients using blood-based tests. Elevated CEA and CA19-9 levels correlate with poor CRC prognosis. However, increased CEA levels are not exclusive to CRC, as its increase can also be associated with other diseases, such as intestinal inflammation, pancreatitis, liver disease and other malignancies. For this reason, although this biomarker is more specific and sensitive than the CA19-9 antigen, there is a need to increase the panel of biomarkers to improve CRC diagnosis [76]. Consequently, Giessen et al. improved the specificity of CEA by combining it with serum amyloid A (SAA) [88].

Chen and collaborators demonstrated that Mammalian STE20-like protein kinase 1/Serine threonine kinase 4 (MST1/STK4), S100 calcium-binding protein A9 (S100A9) and tissue inhibitor of metalloproteinases 1 (TIMP1) can be used as CRC biomarkers [83]. In addition, a high correlation of Cysteine-rich 61 (Cyr61) with advanced CRC stages has been described [89]. In this context, Bhardwaj et al. reported a potential panel based on 12 proteins for the early detection of CRC [90].

Additionally, blood antibodies produced in response to tumour-associated antigens (TAAs) have been studied. The panel proposed by Villar-Vázquez et al. focuses on general transcription factor IIB (GTF2B), EGF-like repeats, discoidin I-like domains 3 (EDIL3), HCK, PIM-1, STK4 and tumour protein P53 [91]. All biomarkers are summarized in Table 4.

3.4.4. Metabolomics

The study of blood-related metabolites as potential non-invasive biomarkers of CRC has increased in the recent years [92]. The comparison between healthy individuals and CRC patients revealed a decrease in serum glucose levels, as well as lower concentration of novel circulating long-chain hydroxy fatty acids, especially GTA-446 [93,94]. On the other hand, the activation of glycolysis and glycine, serine, and threonine metabolism was observed by Gu et al. through CRC serum ¹H-NMR analysis, reflecting the rapid consumption of energy due to the Warburg effect [95]. Furthermore, Nishiumi et al. developed a preliminary but potential panel based on 8 metabolites (pyruvic acid, tryptophan, lysine, glycolic acid, palmitoleic acid, ornithine, fumaric acid, and 3-hydroxyisovaleric acid) for early detection of CRC in plasma [96]. All biomarkers are summarized in Table 4.

3.4.5. Glycomics

The study of plasma IgG glycans presented some alterations that are associated with CRC mortality, such as a decrease in galactosylation and sialylation of fucosylated IgG glycan structures, in addition to an increase in bisecting GlcNAc in IgG glycan structures [97]. Furthermore, Doherty and collaborators found several glycome alterations in plasma associated with CRC: increase of glycans with no galactose residues (agalactosylation), decrease of mono- and di-galactosylated structures, increase of tri- and tetra-galactosylated glycans (galactosylation), decrease of mono-sialylated glycans and increase of tri- and tetra-sialylated structures (sialylation), decrease of galactosylated and sialylated bi-antennary GlcNAc glycans, increase of highly branched glycans (GlcNAc antennae) and decrease of neutral core fucosylated glycans with one or two galactose residues (core fucose) [98].

A positive correlation between CRC progression and multi-antennary and sialylated glycans has been described in serum samples, in addition to a negative correlation between CRC progression and bi-antennary core-fucosylated N-glycans [99]. Finally, a downregulation of 23 N-glycan compositions (mostly galactosylated forms), in addition to an upregulation of mannose-rich HexNAc2Hex7, fucosylated bi-antennary glycan HexNAc4Hex5Fuc1NeuAc2, and tetra-antennary HexNAc6Hex7NeuAc3 was observed in the serum of CRC patients in stages II and III [100]. All biomarkers are summarized in Table 4.

Table 4. Main biomarkers found in blood samples of CRC patients with different omics technologies.

Omics	Biomarker	Change	Reference
Genomics	cfDNA	Increase	[80,81]
Genomics	<i>KRAS, APC, TP53</i>	Mutation	[78,82]
Genomics	cfDNA Microsatellite instability	Increase	[84,101]
Transcriptomics	<i>CK19, CK20, CEA, MDM2, DUSP6, CPEB4, MMD, EIF2S3, ANXA3, CLEC4D, LMNB1, PRRG4, TNEAIP6, VNN1, and IL2RB</i>	Upregulated	[76,78,85]
Transcriptomics	miR-145, miR-143, miR-135, miR-17-92, miR-92a, miR-29a, miR-125b, miR-19a-3p, miR-223-3p, miR-92a-3p and miR-422a, miR-21	Upregulated	[78,86,87]
Epigenomics	<i>SEPT9</i>	Methylation	[76]
Proteomics	CEA, CA19-9 and SAA	Increase	[76,88]
Proteomics	MST1/STK4 and S100A9	Increase	[83]
Proteomics	Cyr61	Increase	[89]
Proteomics	Antibodies against EDIL3, GTF2B, HCK, p53, PIM1 and STK4	Increase	[91]
Metabolomics	Glucose and long-chain hydroxy fatty acids	Decrease	[93,94]
Metabolomics	Pyruvic acid, lysine, glycolic acid, ornithine, fumaric acid	Increase	[96]
Metabolomics	Palmitoleic acid, tryptophan, lysine, 3-hydroxyisovaleric acid	Decrease	[96]
Glycomics	Galactosylation and sialylation of fucosylated IgG glycan structures	Decrease	[97]

Table 4. Cont.

Omics	Biomarker	Change	Reference
Glycomics	Bisecting GlcNAc in IgG glycan structures	Increase	[97]
Glycomics	Glycans with no galactose residues, tri- and tetra-galactosylated glycans, tri- and tetra-sialyted structures, highly branched glycans	Increase	[98]
Glycomics	Mono- and di-galactosylated structures, mono-sialyted glycans, galactosylated and sialylated bi-antennary GlcNAc glycans, neutral core fucosylated glycans with one or two galactose residues	Decrease	[98]
Glycomics	Mannose-rich HexNAc2Hex7, fucosylated bi-antennary glycan HexNAc4Hex5Fuc1NeuAc2, tetra-antennary HexNAc6Hex7NeuAc3	Upregulated	[100]

3.5. Bowel Lavage Fluid Samples

Before a colonoscopy, patients have to intake polyethylene glycol electrolyte lavage solutions to increase bowel visibility during the intervention. Once there, saline solution is applied directly to the area of the lesion to obtain the bowel lavage fluid (BLF), which contains a high concentration of cells in contact with this lesion. BLF presents some advantages in front of stool samples, such as lower bacterial interference and lower food leftovers, easier handling in the laboratory, less variability because of the different times in the bowel and water quantity and, finally, less protein degradation [102]. Nowadays, the use of BLF is not extended, although it is a very useful sample with high potential for new biomarkers that needs to be studied.

3.5.1. Genomics

BLF genomics is based on DNA mutations and methylations, since DNA extraction is easier in BLF than in stool [103]. Twenty years ago, it was discovered that BLF from CRC patients presented an increase of mutated *KRAS* and *P53* [103,104]. Furthermore, BLF from CRC patients also presented mutations in *TGFβ RII* and *APC* genes [104]. The microbiome metagenomics in this type of sample has also been studied in CRC patients. There was an increase in *Proteobacteria* and *Fusobacteria* in BLF from CRC patients, as well as a decrease in *Firmicutes* [105]. In addition, Yuan et al. studied the difference between BLF and tumour tissue from CRC patients, demonstrating that *Proteobacteria*, *Firmicutes* and *Bacteroidetes* were increased in BLF in front of tumour tissue in these patients [106].

Regarding the epigenetics signature, Harada and collaborators analysed 14 targets for aberrant methylation of CpG islands in CRC by MethyLight assays with PCR. They found three possible biomarkers that allow the discrimination between CRC patients and healthy subjects that can be used individually or as a panel: miR-124-3, LOC386758, and SFRP1 [107]. Finally, the hypermethylation of *SDC2*, which has been mentioned before, has also been described in BLF [108]. All biomarkers are summarized in Table 5.

3.5.2. Proteomics

Proteomics displayed the worst results of all BLF biomarkers, since the identified proteins are not CRC-specific. For instance, Adnab-9 was found increased in patients with a high risk of CRC, but was also raised in coeliac patients' stools [102]. Finally,

haemoglobin was increased in BLF from CRC patients, but was also increased in patients with inflammatory bowel disease and diverticulosis [109].

3.5.3. Microbiome Study

The use of selective media for *Bacteroides fragilis* for 3 days in BLF from CRC patients demonstrated that the identification of this species may serve as a CRC biomarker in this sample type [110], as shown in Table 5.

Table 5. Main biomarkers found in bowel lavage fluid samples of CRC patients with different omics technologies.

Omics	Biomarker	Change	Reference
Genomics	<i>KRAS, P53</i>	Mutation	[103,104]
Genomics	<i>TGFβ RII, APC</i>	Mutation	[104]
Genomics	miR-124-3, LOC386758, SFRP1	Methylation	[107]
Genomics	<i>SDC2</i>	Methylation	[108]
Genomics (metagenomics)	<i>Proteobacteria,</i> <i>Fusobacteria</i>	Increase	[105]
Genomics (metagenomics)	<i>Firmicutes</i>	Decrease	[105]
Microbiome study	<i>Bacteroides fragilis</i>	Presence	[110]

3.6. Tumour Tissue Samples

Tumour biopsies allow the direct study of the characteristics of the cancerous tissue. This information is of undoubted and often irreplaceable interest. Together with basic research, this has led to the development of the first general biomarkers for diagnosis, without forgetting, of course, anatomopathological studies. Currently, the diagnostic panel for CRC comprises MSI/mismatch repair (MMR) status, KRAS/NRAS, BRAF, and PIK3CA mutations, and HER2 amplification [111]. Commercial gene expression signatures for CRC have been developed and some are considered in NCCN and ESMO guidelines (reviewed in [112]).

3.6.1. Genomics

Lin et al. established that DNA damage response (DDR)-related ATM or BRCA2 somatic mutations are promising biomarkers for assessing the response of stage III CRC patients to oxaliplatin-based chemotherapy [113]. Very recently, in a bioinformatics analysis, Wills et al. conducted a whole genome-wide association study (GWAS) in a very large cohort of patients and reported an association with overall survival and rs79612564 in the receptor tyrosine kinase ERBB4. Patients with high ERBB4 expression in colon tumours showed worse survival; both the rs79612564 variant and ERBB4 were proposed as predictive biomarkers of survival [114]. Next generation sequencing (NGS), in addition to demonstrating that mutations are common in advanced colon tumours, has proven that tumours located in the right colon have more genetic aberrations than in the left colon. This could be responsible for the different responses of patients depending on the location of the tumour [115].

On the other hand, Van den Berg et al. have defined a methylation marker panel to distinguish between consensus molecular subtype 2 (canonical) and consensus molecular subtype 3 (metabolic) CRC (defined in [116]), which can be used to determine the patient's treatment [117]. Finally, a 10-gene-methylation-based signature for prognosis prediction of CRC has also been established using the TCGA database and bioinformatics tools [118].

3.6.2. Transcriptomics

Using bioinformatics analysis, a prognostic signature based on the expression of REG1B, TGM6, NTF4, PNMA5, and HOXC13 could provide significant prognostic value for CRC [119]. Gu et al. have identified and validated metastasis-associated biomarkers. Concretely, they described that FAS and GSR are downregulated, while CYP1B1 is overexpressed in CRC [120]. Another study showed that the prognosis of CRC was significantly correlated with the expression of the E-selectin gene (SELE) [121].

A prognostic signature comprising six autophagy-related lncRNAs was identified in patients with CRC and could be used for prognosis in these types of patients [122]. This signature includes AC125603.2, LINC00909, AC016876.1, MIR210HG, AC009237.14, and LINC01063 [122]. All biomarkers are summarized in Table 6. In a more complex study, Xi et al. performed a bioinformatic analysis to construct a competing endogenous RNA (ceRNA) network based on the differentially expressed lncRNA and RNAs in two colon cancer gene expression datasets [123]. In summary, they were able to identify two new regulatory pathways as LINC00114/miR-107/PCKS5, UCA1/miR-107/PCKS5, and UCA1/miR-129-5p/SEMA6A. Therefore, two new lncRNAs (LINC00114 and UCA1) were identified by bioinformatics analysis [123]. Furthermore, LINC00114 could be linked to the overall survival of colon cancer patients [123].

3.6.3. Proteomics

In a study by Buttacavoli et al. performing a 2D-DIGE proteomic analysis on a paired tumour and normal adjacent tissues, transgelin (TAGL) was identified as a potential biomarker for CRC [124]. Using a similar design, performing a comparative proteomic and phosphoproteomic analysis of paired tumour and normal adjacent tissues, Vasaiakar et al. identified an association between decreased CD8 T cell infiltration and increased glycolysis in MSI-H tumours, suggesting a shift to glycolysis in immune-resistant MSI-H tumours [125]. All biomarkers are summarized in Table 6.

3.6.4. Glycomics

The study of glycomics in tumour tissue is characterized by the comparative between tumour tissue and non-tumour adjacent tissue. These studies demonstrate that there is a downregulation in the tumour tissue of glypican-3 and syndecan-1 [25], an underrepresentation of complex N-glycans and α 2,3-sialylation [126], a decrease of bisecting GlNAcylation, Lewis-type fucosylation [127], 9 N-glycans (M/Z 973²⁺, 1055²⁺, 1060²⁺, 1075²⁺, 1162²⁺, 1177²⁺, 1264²⁺, 1279²⁺, 1352²⁺) [128], and a decrease of fucosylation levels and highly branched N-glycans in stage II CRC [129]. On the other hand, there is an increase in tumour tissue of glucosylceramide, lactosylceramide, monosialic acid ganglioside, globoside 4 [25], chondroitin sulphate, dermatan sulphate [130], high mannose, hybrid and paucimannosidic type N-glycans [126], α 2,6-sialylation together with an increase in total sialylation in mid- to late tumours, mannose type N-glycan structures [127], glycan-Tn/STn-MUC1 [131], 3 N-glycans (M/Z 1013²⁺, 1116²⁺, 1228²⁺) [128], overrepresentation of oligomannosidic, bi-antennary hypogalactosylated and branched compositions [100], and an increase in stage II CRC of sialylation levels and high-mannose glycans [129]. All biomarkers are summarized in Table 6.

Table 6. Main biomarkers found in tissue samples of CRC patients with different omics technologies.

Omics	Biomarker	Change	Reference
Transcriptomics	CYP1B1	Upregulated	[120]
Transcriptomics	FAS, GSR	Downregulated	[120]
Transcriptomics	AC125603.2, LINC00909, AC0168676.1, MIR210HG, AC009237, LINC01063	Prognosis biomarkers	[122]
Proteomics	Transgelin	Decrease	[124]
Proteomics	CD8 T cell infiltration	Decrease	[125]
Proteomics	Glycolysis in MSI-H tumours	Increase	[125]
Glycomics	Glypican-3, syndecan-1	Downregulated	[25]
Glycomics	Glycosylceramide, lactosylceramide, monosialic acid ganglioside, globoside 4	Upregulated	[25]
Glycomics	Heparan sulphate	Decrease	[130]
Glycomics	Chondroitin sulphate, dermatan sulphate	Increase	[130]
Glycomics	Complex N-glycans, α 2,3-sialylation	Decrease	[126]
Glycomics	High mannose, hybrid and paucimannosidic type N-glycans	Increase	[126]
Glycomics	Bisecting GINAcylation, Lewis-Type fucosylation	Decrease	[127]
Glycomics	α 2,6-sialylation, total sialylation, mannose type N-glycan structures	Increase	[127]
Glycomics	M/Z 973 ²⁺ , 1055 ²⁺ , 1060 ²⁺ , 1075 ²⁺ , 1162 ²⁺ , 1177 ²⁺ , 1264 ²⁺ , 1279 ²⁺ , 1352 ²⁺	Decrease	[128]
Glycomics	M/Z 1013 ²⁺ , 1116 ²⁺ , 1228 ²⁺	Increase	[128]
Glycomics	Fucosylation levels, highly branched N-glycans	Decrease	[129]
Glycomics	Sialylation, high-mannose glycans	Increase	[129]
Glycomics	Glycan-Tn/STn-MUC1	Increase	[131]
Glycomics	Oligomannosidic, bi-antennary hypogalactosylated, branched compositions	Increase	[100]

3.6.5. Multi-Omics

The underlying factors of human disease are complex, and the multi-omics perspective is valuable in identifying the pathogenic factors of diseases [132]. There is a debate regarding the differences between left-sided colon cancer and right-sided colon cancer, which was studied with a multi-omics perspective by Hu et al. [132]. Gene mutation, DNA methylation, gene expression, and miRNA were integrally compared between left-sided and right-sided colon cancer datasets from TCGA [132]. The results suggest that there are more aggressive markers in the right-sided colon cancer with the activation of the

phosphatidylinositol 3-kinase pathway (PI3K) pathway that shows crosstalk with the RAS and P53 pathways [132].

A multi-omics approach using a gene expression dataset, a miRNA-seq dataset, a copy number variation dataset, a DNA methylation dataset, and a transcription factor (TF) dataset was performed by Yang et al. and found that these types of approaches are more effective than the single omics dataset approach [133].

4. Use of Extracellular Vesicles as Colorectal Cancer Biomarkers

CRC cells release EVs since early stages. For this reason, the EVs' cargo could be a possible molecular biomarker of early diagnosis and prognosis [5]. Minimal information for studies of extracellular vesicles (MISEV2018) defines EVs as "particles naturally released from the cell that are delimited by a lipid bilayer and cannot replicate" [134]. EVs present several advantages in front of other kinds of biomarkers. They are easy to get, and the samples of origin are not invasive. Furthermore, the lipid bilayer allows their stabilization in circulation and protects them from ribonucleases and DNases degradation. Finally, EVs are very abundant and possess a long half-life, and the DNA inside the EVs reflects the mutational state of tumours [6,135,136].

The EVs content is based on tumour cell-derived genome, transcriptome, and secretome. Concretely, the cargo are oncoproteins, transcriptional regulators, splicing factors, proteins related to the cytoskeleton, apoptosis, cell cycle, cellular signalling, oxidative stress, focal adhesions, cellular mobility, DNA fragments, RNA (mRNA, miRNAs, non-coding RNA), and suppressor tumoral mutated genes [135,137]. EVs could improve early CRC biomarkers, since they are released by tumoral cells and carry RNA, DNA, and proteins to target cells, participating in tumoral microenvironment, tumour formation, progression, angiogenesis, invasion, metastasis, chemoresistance, drug resistance, and recrudescence [5,135,137–140].

Nowadays, there is no standard technique for EVs isolation, which leads to differences in cargo, in addition to a lack of a standard classification [140]. The gold standard isolation technique is ultracentrifugation, but EVs can also be isolated by gradient centrifugation, microfiltration, polymer-based precipitation, size-exclusion chromatography, immunoaffinity chromatography, microfluidic filtering, commercial kits, or antibody immobilization against membrane proteins [5,135,140,141]. EVs cargo and function, in addition to the protection of the lipidic membrane, make them the future of CRC early diagnosis and prognosis.

5. Conclusions

Omics techniques are a useful tool for new CRC biomarkers research, in both in situ tissue samples and different fluids related to this type of cancer. Great efforts and advances have been made by the scientific community to identify biomarkers through these techniques that could help in the management of CRC patients. The main types of samples and the omics applied to them are described in Figure 1. Despite the number of new biomarkers, there is a lack of standardization, since CRC is only diagnosed by colonoscopy, faecal occult blood testing, and the presence of CEA in plasma, although these techniques present some disadvantages. For these reasons, there is a need to study new sample types, such as bowel lavage fluid, and new biomarker source types, such as extracellular vesicles.

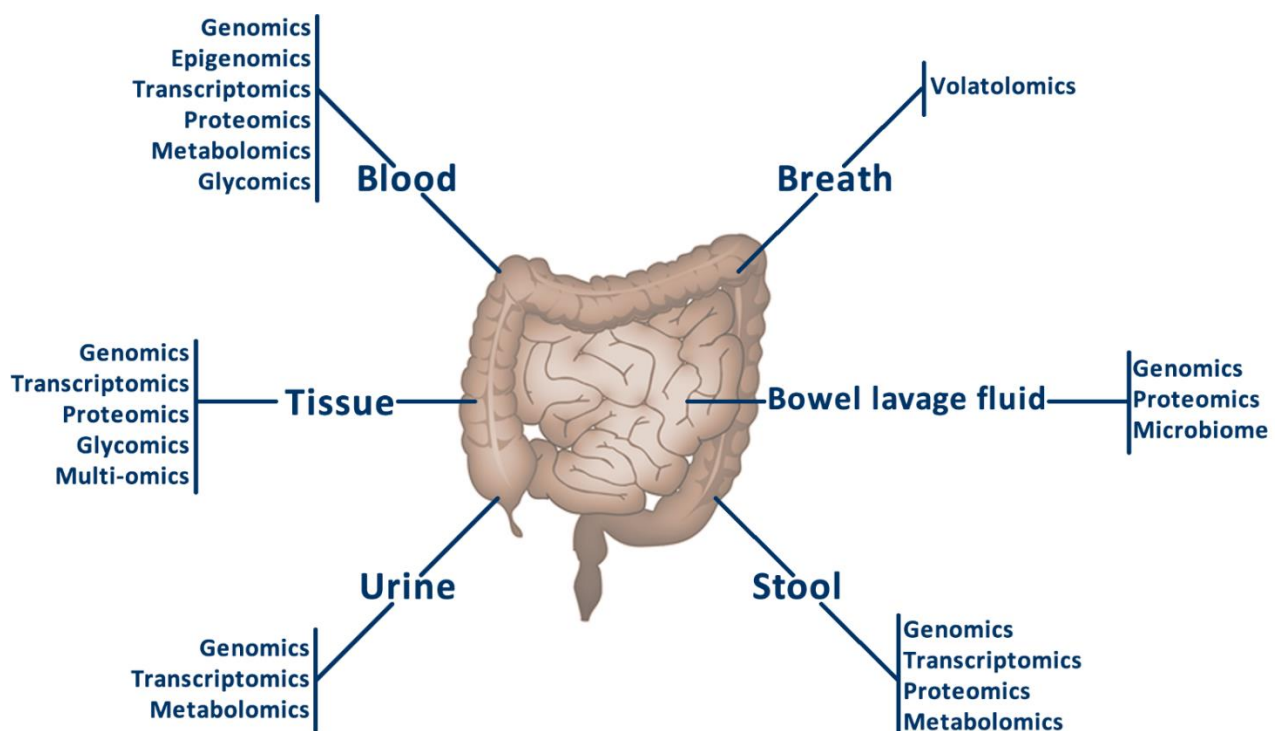


Figure 1. Main types of samples and the omics applied to them.

Author Contributions: Conceptualization, M.A.-C., M.T.-M., P.M.M.-B., T.M.-B., J.S.-S., P.R., D.G.P., J.O. and J.R.; writing—original draft preparation, M.A.-C., M.T.-M., P.M.M.-B., T.M.-B., J.S.-S., P.R., D.G.P., J.O. and J.R.; writing—review and editing, M.A.-C., J.O. and J.R.; supervision, J.O. and J.R. All authors have read and agreed to the published version of the manuscript.

Funding: Margalida Torrens-Mas was supported by a grant from Programa postdoctoral Margalida Comas—Comunidad Autónoma de las Islas Baleares (PD/050/2020). Toni Martínez-Bernabe was funded by “Ayuda Formación Personal Investigador FPI 2020” grant from “Consejería de Educación, Universidad e Investigación del Gobierno de las Illes Balears”.

Acknowledgments: Proyecto del Hospital Comarcal de Inca y la Universidad de las Islas Baleares (CINUIB) from Fundació Universitat Empresa de les Illes Balears (FUEIB).

Conflicts of Interest: The authors declare no conflict of interest.

References

1. Sung, H.; Ferlay, J.; Siegel, R.L.; Laversanne, M.; Soerjomataram, I.; Jemal, A.; Bray, F. Global Cancer Statistics 2020: GLOBOCAN Estimates of Incidence and Mortality Worldwide for 36 Cancers in 185 Countries. *CA Cancer J. Clin.* **2021**, *71*, 209–249. [[CrossRef](#)] [[PubMed](#)]
2. Sociedad Española de Oncología Médica Las Cifras del Cáncer en España 2020. 2020. Available online: <https://seom.org/prensa/el-cancer-en-cifras> (accessed on 24 December 2021).
3. Zamorano-Leon, J.J.; López-De-Andres, A.; Álvarez-González, A.; Maestre-Miquel, C.; Astasio-Arbiza, P.; López-Farré, A.; De-Miguel-Diez, J.; Jiménez-García, R.; Albaladejo-Vicente, R. Trends and Predictors for the Uptake of Colon Cancer Screening Using the Fecal Occult Blood Test in Spain from 2011 to 2017. *Int. J. Environ. Res. Public Health* **2020**, *17*, 6222. [[CrossRef](#)] [[PubMed](#)]
4. Roselló, S.; Simón, S.; Cervantes, A. Programmed colorectal cancer screening decreases incidence and mortality. *Transl. Gastroenterol. Hepatol.* **2019**, *4*, 84. [[CrossRef](#)] [[PubMed](#)]
5. Cheshomi, H.; Matin, M.M. Exosomes and their importance in metastasis, diagnosis, and therapy of colorectal cancer. *J. Cell. Biochem.* **2019**, *120*, 2671–2686. [[CrossRef](#)]
6. Mammes, A.; Pasquier, J.; Mammes, O.; Conti, M.; Douard, R.; Loric, S. Extracellular vesicles: General features and usefulness in diagnosis and therapeutic management of colorectal cancer. *World J. Gastrointest. Oncol.* **2021**, *13*, 1561–1598. [[CrossRef](#)]
7. Brenner, H.; Stock, C.; Hoffmeister, M. Effect of screening sigmoidoscopy and screening colonoscopy on colorectal cancer incidence and mortality: Systematic review and meta-analysis of randomised controlled trials and observational studies. *BMJ* **2014**, *348*, g2467. [[CrossRef](#)]

8. Elmunzer, B.J.; Hayward, R.A.; Schoenfeld, P.S.; Saini, S.D.; Deshpande, A.; Waljee, A.K. Effect of Flexible Sigmoidoscopy-Based Screening on Incidence and Mortality of Colorectal Cancer: A Systematic Review and Meta-Analysis of Randomized Controlled Trials. *PLoS Med.* **2012**, *9*, e1001352. [[CrossRef](#)]
9. Gini, A.; Jansen, E.E.L.; Zielonke, N.; Meester, R.G.S.; Senore, C.; Anttila, A.; Segnan, N.; Mlakar, D.N.; de Koning, H.J.; Lansdorp-Vogelaar, I.; et al. Impact of colorectal cancer screening on cancer-specific mortality in Europe: A systematic review. *Eur. J. Cancer* **2020**, *127*, 224–235. [[CrossRef](#)]
10. Deandrea, S.; Molina-Barceló, A.; Uluturk, A.; Moreno, J.; Neamtii, L.; Peiró-Pérez, R.; Saz-Parkinson, Z.; Lopez-Alcalde, J.; Lerda, D.; Salas, D. Presence, characteristics and equity of access to breast cancer screening programmes in 27 European countries in 2010 and 2014. Results from an international survey. *Prev. Med.* **2016**, *91*, 250–263. [[CrossRef](#)]
11. Borràs, J.M.; Colomer, C.; Soria, P.; López, R. Priorities for cancer control in Spain. *Ann. Oncol.* **2010**, *21*, iii111–iii114. [[CrossRef](#)]
12. Cobo-Cuenca, A.I.; Laredo-Aguilera, J.A.; Rodríguez-Borrego, M.-A.; Santacruz-Salas, E.; Carmona-Torres, J.M. Temporal Trends in Fecal Occult Blood Test: Associated Factors (2009–2017). *Int. J. Environ. Res. Public Heal.* **2019**, *16*, 2120. [[CrossRef](#)] [[PubMed](#)]
13. Lin, J.S.; Piper, M.A.; Perdue, L.A.; Rutter, C.M.; Webber, E.M.; O'Connor, E.; Smith, N.; Whitlock, E.P. Screening for colorectal cancer: Updated evidence report and systematic review for the US preventive services task force. *JAMA J. Am. Med. Assoc.* **2016**, *315*, 2576–2594. [[CrossRef](#)] [[PubMed](#)]
14. Niedermaier, T.; Balavarca, Y.; Brenner, H. Stage-Specific Sensitivity of Fecal Immunochemical Tests for Detecting Colorectal Cancer: Systematic Review and Meta-Analysis. *Am. J. Gastroenterol.* **2020**, *115*, 56–69. [[CrossRef](#)] [[PubMed](#)]
15. Definition of genomics—NCI Dictionary of Cancer Terms—National Cancer Institute. Available online: <https://www.cancer.gov/publications/dictionaries/cancer-terms/def/genomics> (accessed on 27 December 2021).
16. Grady, W.M.; Yu, M.; Markowitz, S.D. Epigenetic Alterations in the Gastrointestinal Tract: Current and Emerging Use for Biomarkers of Cancer. *Gastroenterology* **2021**, *160*, 690–709. [[CrossRef](#)] [[PubMed](#)]
17. Clough, E.; Barrett, T. The Gene Expression Omnibus Database. *Methods Mol. Biol.* **2016**, *1418*, 93–110. [[PubMed](#)]
18. Wang, Z.; Jensen, M.A.; Zenklusen, J.C. A Practical Guide to The Cancer Genome Atlas (TCGA). *Methods Mol. Biol.* **2016**, *1418*, 111–141. [[PubMed](#)]
19. Yu, J.; Feng, Q.; Wong, S.H.; Zhang, D.; Liang, Q.Y.; Qin, Y.; Tang, L.; Zhao, H.; Stenvang, J.; Li, Y.; et al. Metagenomic analysis of faecal microbiome as a tool towards targeted non-invasive biomarkers for colorectal cancer. *Gut* **2017**, *66*, 70–78. [[CrossRef](#)]
20. Definition of transcriptomics—NCI Dictionary of Cancer Terms—National Cancer Institute. Available online: <https://www.cancer.gov/publications/dictionaries/cancer-terms/def/transcriptomics> (accessed on 27 December 2021).
21. Ahluwalia, P.; Kolhe, R.; Gahlay, G.K. The clinical relevance of gene expression based prognostic signatures in colorectal cancer. *Biochim. Biophys. Acta—Rev. Cancer* **2021**, *1875*, 188513. [[CrossRef](#)]
22. Definition of proteomics—NCI Dictionary of Cancer Terms—National Cancer Institute. Available online: <https://www.cancer.gov/publications/dictionaries/cancer-terms/def/proteomics> (accessed on 27 December 2021).
23. Boja, E.S.; Rodriguez, H. Proteogenomic convergence for understanding cancer pathways and networks. *Clin. Proteom.* **2014**, *11*, 22. [[CrossRef](#)]
24. Nannini, G.; Meoni, G.; Amedei, A.; Tenori, L. Metabolomics profile in gastrointestinal cancers: Update and future perspectives. *World J. Gastroenterol.* **2020**, *26*, 2514–2532. [[CrossRef](#)]
25. Joo, E.J.; Weyers, A.; Li, G.; Gasimli, L.; Li, L.; Choi, W.J.; Lee, K.B.; Linhardt, R.J. Carbohydrate-Containing Molecules as Potential Biomarkers in Colon Cancer. *OMICS: A J. Integr. Biol.* **2014**, *18*, 231–241. [[CrossRef](#)] [[PubMed](#)]
26. Drake, R.R. *Glycosylation and Cancer: Moving Glycomics to the Forefront*, 1st ed.; Elsevier Inc.: Amsterdam, The Netherlands, 2015; Volume 126.
27. Holst, S.; Wuhler, M.; Rombouts, Y. *Glycosylation Characteristics of Colorectal Cancer*, 1st ed.; Elsevier Inc.: Amsterdam, The Netherlands, 2015; Volume 126.
28. Hakim, M.; Broza, Y.Y.; Barash, O.; Peled, N.; Phillips, M.; Amann, A.; Haick, H. Volatile organic compounds of lung cancer and possible biochemical pathways. *Chem. Rev.* **2012**, *112*, 5949–5966. [[CrossRef](#)] [[PubMed](#)]
29. Bosch, S.; Berkhout, D.J.; Larbi, B.I.; De Meij, T.G.; De Boer, N.K. Fecal volatile organic compounds for early detection of colorectal cancer: Where are we now? *J. Cancer Res. Clin. Oncol.* **2019**, *145*, 223–234. [[CrossRef](#)] [[PubMed](#)]
30. De Vietro, N.; Aresta, A.; Rotelli, M.T.; Zamboni, C.; Lippolis, C.; Picciariello, A.; Altomare, D.F. Relationship between cancer tissue derived and exhaled volatile organic compound from colorectal cancer patients. Preliminary results. *J. Pharm. Biomed. Anal.* **2020**, *180*, 113055. [[CrossRef](#)] [[PubMed](#)]
31. Kabir, K.M.M.; Donald, W.A. Cancer breath testing: A patent review. *Expert Opin. Ther. Patents* **2018**, *28*, 227–239. [[CrossRef](#)] [[PubMed](#)]
32. Politi, L.; Monasta, L.; Rigressi, M.N.; Princivale, A.; Gonfiotti, A.; Camiciottoli, G.; Perbellini, L. Discriminant Profiles of Volatile Compounds in the Alveolar Air of Patients with Squamous Cell Lung Cancer, Lung Adenocarcinoma or Colon Cancer. *Molecules* **2021**, *26*, 550. [[CrossRef](#)]
33. Van De Goor, R.M.G.E.; Leunis, N.; Van Hooren, M.R.A.; Francisca, E.; Masclee, A.; Kremer, B.; Kross, K.W. Feasibility of electronic nose technology for discriminating between head and neck, bladder, and colon carcinomas. *Eur. Arch. Oto-Rhino-Laryngology* **2017**, *274*, 1053–1060. [[CrossRef](#)]
34. Amann, A.; Mochalski, P.; Ruzsanyi, V.; Broza, Y.Y.; Haick, H. Assessment of the exhalation kinetics of volatile cancer biomarkers based on their physicochemical properties. *J. Breath Res.* **2014**, *8*, 016003. [[CrossRef](#)]

35. Haick, H.; Broza, Y.Y.; Mochalski, P.; Ruzsanyi, V.; Amann, A. Assessment, origin, and implementation of breath volatile cancer markers. *Chem. Soc. Rev.* **2014**, *43*, 1423–1449. [[CrossRef](#)]
36. Zhou, W.; Tao, J.; Li, J.; Tao, S. Volatile organic compounds analysis as a potential novel screening tool for colorectal cancer A systematic review and meta-analysis. *Medicine* **2020**, *99*, e20937. [[CrossRef](#)]
37. Van Keulen, K.E.; Jansen, M.E.; Schrauwen, R.W.M.; Kolkman, J.J.; Siersema, P.D. Volatile organic compounds in breath can serve as a non-invasive diagnostic biomarker for the detection of advanced adenomas and colorectal cancer. *Aliment. Pharmacol. Ther.* **2020**, *51*, 334–346. [[CrossRef](#)] [[PubMed](#)]
38. Tian, J.; Xue, W.; Yin, H.; Zhang, N.; Zhou, J.; Long, Z.; Wu, C.; Liang, Z.; Xie, K.; Li, S.; et al. Differential Metabolic Alterations and Biomarkers Between Gastric Cancer and Colorectal Cancer: A Systematic Review and Meta-Analysis. *OncoTargets Ther.* **2020**, *13*, 6093–6108. [[CrossRef](#)] [[PubMed](#)]
39. Peng, G.; Hakim, M.; Broza, Y.Y.; Billan, S.; Abdah-Bortnyak, R.; Kuten, A.; Tisch, U.; Haick, H. Detection of lung, breast, colorectal, and prostate cancers from exhaled breath using a single array of nanosensors. *Br. J. Cancer* **2010**, *103*, 542–551. [[CrossRef](#)] [[PubMed](#)]
40. Haick, H.; Hakim, M. Volatile organic compounds as diagnostic markers for various types of cancer. U.S. Patent No. 9,551,712, 6 January 2011.
41. Altomare, D.F.; Picciariello, A.; Rotelli, M.T.; De Fazio, M.; Aresta, A.; Zambonin, C.G.; Vincenti, L.; Trerotoli, P.; Vietro, N. De Chemical signature of colorectal cancer: Case–control study for profiling the breath print. *BJS Open* **2020**, *4*, 1189–1199. [[CrossRef](#)]
42. Ohta, R.; Yamada, T.; Sonoda, H.; Matsuda, A.; Shinji, S.; Takahashi, G.; Iwai, T.; Takeda, K.; Ueda, K.; Kuriyama, S.; et al. Detection of KRAS mutations in circulating tumour DNA from plasma and urine of patients with colorectal cancer. *Eur. J. Surg. Oncol. (EJSO)* **2021**, *47*, 3151–3156. [[CrossRef](#)]
43. Liu, Y.; Wang, Y.; Cao, Z.; Gao, Y. Changes in the Urinary Proteome in a Patient-Derived Xenograft (PDX) Nude Mouse Model of Colorectal Tumor. *Sci. Rep.* **2019**, *9*, 4975. [[CrossRef](#)]
44. Lalmahomed, Z.S.; Bröker, M.E.; A Van Huizen, N.; Braak, R.R.J.C.V.D.; Dekker, L.J.; Rizopoulos, D.; Verhoef, C.; Steyerberg, E.W.; Luidier, T.M.; Ijzermans, J.N. Hydroxylated collagen peptide in urine as biomarker for detecting colorectal liver metastases. *Am. J. Cancer Res.* **2016**, *6*, 321–330.
45. Erozcenci, L.A.; Böttger, F.; Bijnsdorp, I.V.; Jimenez, C.R. Urinary exosomal proteins as (pan-)cancer biomarkers: Insights from the proteome. *FEBS Lett.* **2019**, *593*, 1580–1597. [[CrossRef](#)]
46. Mallafre-Muro, C.; Llambrich, M.; Cumeras, R.; Pardo, A.; Brezmes, J.; Marco, S.; Gumà, J. Comprehensive Volatilome and Metabolome Signatures of Colorectal Cancer in Urine: A Systematic Review and Meta-Analysis. *Cancers* **2021**, *13*, 2534. [[CrossRef](#)]
47. Erben, V.; Poschet, G.; Schrotz-King, P.; Brenner, H. Comparing Metabolomics Profiles in Various Types of Liquid Biopsies among Screening Participants with and without Advanced Colorectal Neoplasms. *Diagnostics* **2021**, *11*, 561. [[CrossRef](#)]
48. Udo, R.; Katsumata, K.; Kuwabara, H.; Enomoto, M.; Ishizaki, T.; Sunamura, M.; Nagakawa, Y.; Soya, R.; Sugimoto, M.; Tsuchida, A. Urinary charged metabolite profiling of colorectal cancer using capillary electrophoresis-mass spectrometry. *Sci. Rep.* **2020**, *10*, 1–10. [[CrossRef](#)] [[PubMed](#)]
49. Ning, W.; Qiao, N.; Zhang, X.; Pei, D.; Wang, W. Metabolic profiling analysis for clinical urine of colorectal cancer. *Asia-Pacific J. Clin. Oncol.* **2021**, *17*, 403–413. [[CrossRef](#)] [[PubMed](#)]
50. Barichello, S.; Deng, L.; Ismond, K.P.; Loomes, D.; Kirwin, E.M.; Wang, H.; Chang, D.; Svenson, L.W.; Thanh, N. Comparative effectiveness and cost-effectiveness analysis of a urine metabolomics test vs. alternative colorectal cancer screening strategies. *Int. J. Color. Dis.* **2019**, *34*, 1953–1962. [[CrossRef](#)] [[PubMed](#)]
51. Kim, E.R.; Kwon, H.N.; Nam, H.; Kim, J.J.; Park, S.; Kim, Y.-H. Urine-NMR metabolomics for screening of advanced colorectal adenoma and early stage colorectal cancer. *Sci. Rep.* **2019**, *9*, 1–10. [[CrossRef](#)]
52. Zarei, I.; Baxter, B.A.; Oppel, R.C.; Borresen, E.C.; Brown, R.J.; Ryan, E.P. Plasma and Urine Metabolite Profiles Impacted by Increased Dietary Navy Bean Intake in Colorectal Cancer Survivors: A Randomized-Controlled Trial. *Cancer Prev. Res.* **2021**, *14*, 497–508. [[CrossRef](#)]
53. Ang, C.-S.; Baker, M.S.; Nice, E.C. Mass Spectrometry-Based Analysis for the Discovery and Validation of Potential Colorectal Cancer Stool Biomarkers. *Methods Enzymol.* **2017**, *586*, 247–274. [[CrossRef](#)]
54. Gsur, A.; Baierl, A.; Brezina, S. Colorectal Cancer Study of Austria (CORSA): A Population-Based Multicenter Study. *Biology* **2021**, *10*, 722. [[CrossRef](#)]
55. Tikk, K.; Weigl, K.; Hoffmeister, M.; Igel, S.; Schwab, M.; Hampe, J.; Klug, S.J.; Mansmann, U.; Kolligs, F.; Brenner, H. Study protocol of the RaPS study: Novel risk adapted prevention strategies for people with a family history of colorectal cancer. *BMC Cancer* **2018**, *18*, 720. [[CrossRef](#)]
56. Wirbel, J.; Pyl, P.T.; Kartal, E.; Zych, K.; Kashani, A.; Milanese, A.; Fleck, J.S.; Voigt, A.Y.; Palleja, A.; Ponnudurai, R.; et al. Meta-analysis of fecal metagenomes reveals global microbial signatures that are specific for colorectal cancer. *Nat. Med.* **2019**, *25*, 679–689. [[CrossRef](#)]
57. Yang, J.; Li, D.; Yang, Z.; Dai, W.; Feng, X.; Liu, Y.; Jiang, Y.; Li, P.; Li, Y.; Tang, B.; et al. Establishing high-accuracy biomarkers for colorectal cancer by comparing fecal microbiomes in patients with healthy families. *Gut Microbes* **2020**, *11*, 918–929. [[CrossRef](#)]
58. Liang, J.Q.; Li, T.; Nakatsu, G.; Chen, Y.-X.; Yau, T.O.; Chu, E.; Wong, S.; Szeto, C.H.; Ng, S.C.; Chan, F.K.L.; et al. A novel faecal Lachnospirillum marker for the non-invasive diagnosis of colorectal adenoma and cancer. *Gut* **2020**, *69*, 1248–1257. [[CrossRef](#)]

59. Liu, X.; Wen, J.; Li, C.; Wang, H.; Wang, J.; Zou, H. High-Yield Methylation Markers for Stool-Based Detection of Colorectal Cancer. *Am. J. Dig. Dis.* **2019**, *65*, 1710–1719. [[CrossRef](#)] [[PubMed](#)]
60. Vega-Benedetti, A.F.; Loi, E.; Moi, L.; Orrù, S.; Ziranu, P.; Pretta, A.; Lai, E.; Puzzone, M.; Ciccone, L.; Casadei-Gardini, A.; et al. Colorectal Cancer Early Detection in Stool Samples Tracing CpG Islands Methylation Alterations Affecting Gene Expression. *Int. J. Mol. Sci.* **2020**, *21*, 4494. [[CrossRef](#)] [[PubMed](#)]
61. Jin, S.; Ye, Q.; Hong, Y.; Dai, W.; Zhang, C.; Liu, W.; Guo, Y.; Zhu, D.; Zhang, Z.; Chen, S.; et al. A systematic evaluation of stool DNA preparation protocols for colorectal cancer screening via analysis of DNA methylation biomarkers. *Clin. Chem. Lab. Med. (CCLM)* **2020**, *59*, 91–99. [[CrossRef](#)] [[PubMed](#)]
62. Oh, T.J.; Oh, H.I.; Seo, Y.Y.; Jeong, D.; Kim, C.; Kang, H.W.; Han, Y.D.; Chung, H.C.; Kim, N.K.; An, S. Feasibility of quantifying SDC2 methylation in stool DNA for early detection of colorectal cancer. *Clin. Epigenet.* **2017**, *9*, 126. [[CrossRef](#)] [[PubMed](#)]
63. Wang, J.; Liu, S.; Wang, H.; Zheng, L.; Zhou, C.; Li, G.; Huang, R.; Wang, H.; Li, C.; Fan, X.; et al. Robust performance of a novel stool DNA test of methylated SDC2 for colorectal cancer detection: A multicenter clinical study. *Clin. Epigenet.* **2020**, *12*, 1–12. [[CrossRef](#)] [[PubMed](#)]
64. Cheng, Y.-C.; Wu, P.-H.; Chen, Y.-J.; Yang, C.-H.; Huang, J.-L.; Chou, Y.-C.; Chang, P.-K.; Wen, C.-C.; Jao, S.-W.; Huang, H.-H.; et al. Using Comorbidity Pattern Analysis to Detect Reliable Methylated Genes in Colorectal Cancer Verified by Stool DNA Test. *Genes* **2021**, *12*, 1539. [[CrossRef](#)] [[PubMed](#)]
65. Moradi, K.; Babaei, E.; Feizi, M.A.H.; Safaralizadeh, R.; Rezvani, N. Quantitative detection of SRY-Box 21 (SOX21) gene promoter methylation as a stool-based noninvasive biomarker for early diagnosis of colorectal cancer by MethyLight method. *Indian J. Cancer* **2021**, *58*, 217–224.
66. Ahmed, F.E.; Vos, P.; Ijames, S.; Lysle, D.T.; Allison, R.R.; Flake, G.; Sinar, D.R.; Naziri, W.; Marcuard, S.P.; Pennington, R. Transcriptomic molecular markers for screening human colon cancer in stool and tissue. *Cancer Genom. Proteom.* **2007**, *4*, 1–20.
67. Ahmed, F.E.; Jeffries, C.D.; Vos, P.W.; Flake, G.; Nuovo, G.J.; Sinar, D.R.; Naziri, W.; Marcuard, S.P. Diagnostic microRNA markers for screening sporadic human colon cancer and active ulcerative colitis in stool and tissue. *Cancer Genom. Proteom.* **2009**, *6*, 281–295.
68. Ahmed, F.E.; Ahmed, N.C.; Gouda, M.M.; Vos, P.W.; Bonnerup, C. RT-qPCR for Fecal Mature MicroRNA Quantification and Validation. *Methods Mol. Biol.* **2018**, *1765*, 203–215. [[PubMed](#)]
69. Gharib, E.; Nazemalhosseini-Mojarad, E.; Baghdar, K.; Nayeri, Z.; Sadeghi, H.; Rezasoltani, S.; Jamshidi-Fard, A.; Larki, P.; Sadeghi, A.; Hashemi, M.; et al. Identification of a stool long non-coding RNAs panel as a potential biomarker for early detection of colorectal cancer. *J. Clin. Lab. Anal.* **2021**, *35*, e23601. [[CrossRef](#)] [[PubMed](#)]
70. Chauvin, A.; Boisvert, F.-M. Clinical Proteomics in Colorectal Cancer, a Promising Tool for Improving Personalised Medicine. *Proteomes* **2018**, *6*, 49. [[CrossRef](#)] [[PubMed](#)]
71. Komor, M.A.; Bosch, L.J.; Coupé, V.; Rausch, C.; Pham, T.V.; Piersma, S.R.; Mongera, S.; Mulder, C.J.; Dekker, E.; Kuipers, E.J.; et al. Proteins in stool as biomarkers for non-invasive detection of colorectal adenomas with high risk of progression. *J. Pathol.* **2020**, *250*, 288–298. [[CrossRef](#)]
72. Yang, Y.; Misra, B.B.; Liang, L.; Bi, D.; Weng, W.; Wu, W.; Cai, S.; Qin, H.; Goel, A.; Li, X.; et al. Integrated microbiome and metabolome analysis reveals a novel interplay between commensal bacteria and metabolites in colorectal cancer. *Theranostics* **2019**, *9*, 4101–4114. [[CrossRef](#)]
73. Song, E.M.; Byeon, J.-S.; Lee, S.M.; Yoo, H.J.; Kim, S.J.; Chang, K.; Hwang, S.W.; Yang, D.-H.; Jeong, J.-Y. Fecal Fatty Acid Profiling as a Potential New Screening Biomarker in Patients with Colorectal Cancer. *Am. J. Dig. Dis.* **2018**, *63*, 1229–1236. [[CrossRef](#)]
74. Clos-García, M.; García, K.; Alonso, C.; Iruarrizaga-Lejarreta, M.; D’Amato, M.; Crespo, A.; Iglesias, A.; Cubiella, J.; Bujanda, L.; Falcón-Pérez, J.M. Integrative Analysis of Fecal Metagenomics and Metabolomics in Colorectal Cancer. *Cancers* **2020**, *12*, 1142. [[CrossRef](#)]
75. Lin, Y.; Ma, C.; Bezabeh, T.; Wang, Z.; Liang, J.; Huang, Y.; Zhao, J.; Liu, X.; Ye, W.; Tang, W.; et al. ¹H NMR-based metabolomics reveal overlapping discriminatory metabolites and metabolic pathway disturbances between colorectal tumor tissues and fecal samples. *Int. J. Cancer* **2019**, *145*, 1679–1689. [[CrossRef](#)]
76. Hauptman, N.; Glava, D. Colorectal Cancer Blood-Based Biomarkers. *Gastroenterol. Res. Pract.* **2017**, *2017*. [[CrossRef](#)]
77. Rodríguez-Casanova, A.; Costa-Fraga, N.; Bao-Caamano, A.; López-López, R.; Muínelo-Romay, L.; Diaz-Lagares, A. Epigenetic Landscape of Liquid Biopsy in Colorectal Cancer. *Front. Cell Dev. Biol.* **2021**, *9*. [[CrossRef](#)]
78. Gallardo-Gómez, M.; De Chiara, L.; Álvarez-Chaver, P.; Cubiella, J. Colorectal cancer screening and diagnosis: Omics-based technologies for development of a non-invasive blood-based method. *Expert Rev. Anticancer Ther.* **2021**, *21*, 723–738. [[CrossRef](#)] [[PubMed](#)]
79. Petit, J.; Carroll, G.; Gould, T.; Pockney, P.; Dun, M.; Scott, R.J. Cell-Free DNA as a Diagnostic Blood-Based Biomarker for Colorectal Cancer: A Systematic Review. *J. Surg. Res.* **2019**, *236*, 184–197. [[CrossRef](#)] [[PubMed](#)]
80. Qi, J.; Qian, C.; Shi, W.; Wu, X.; Jing, R.; Zhang, L.; Wang, Z.; Ju, S. Alu-based cell-free DNA: A potential complementary biomarker for diagnosis of colorectal cancer. *Clin. Biochem.* **2013**, *46*, 64–69. [[CrossRef](#)]
81. Hao, T.B.; Shi, W.; Shen, X.J.; Qi, J.; Wu, X.H.; Wu, Y.; Tang, Y.Y.; Ju, S.Q. Circulating cell-free DNA in serum as a biomarker for diagnosis and prognostic prediction of colorectal cancer. *Br. J. Cancer* **2014**, *111*, 1482–1489. [[CrossRef](#)] [[PubMed](#)]

82. Wang, J.-Y.; Hsieh, J.-S.; Chang, M.-Y.; Huang, T.-J.; Chen, F.-M.; Cheng, T.-L.; Alexandersen, K.; Huang, Y.-S.; Tzou, W.-S.; Lin, S.-R. Molecular Detection of APC, K-ras, and p53 Mutations in the Serum of Colorectal Cancer Patients as Circulating Biomarkers. *World J. Surg.* **2004**, *28*, 721–726. [[CrossRef](#)]
83. Chen, X.; Sun, J.; Wang, X.; Yuan, Y.; Cai, L.; Xie, Y.; Fan, Z.; Liu, K.; Jiao, X. A Meta-Analysis of Proteomic Blood Markers of Colorectal Cancer. *Curr. Med. Chem.* **2021**, *28*, 1176–1196. [[CrossRef](#)]
84. Kim, G.P.; Colangelo, L.H.; Wieand, H.S.; Paik, S.; Kirsch, I.R.; Wolmark, N.; Allegra, C.J. Prognostic and Predictive Roles of High-Degree Microsatellite Instability in Colon Cancer: A National Cancer Institute–National Surgical Adjuvant Breast and Bowel Project Collaborative Study. *J. Clin. Oncol.* **2007**, *25*, 767–772. [[CrossRef](#)]
85. Lech, G.; Słotwiński, R.; Słodkowski, M.; Krasnodębski, I.W. Colorectal cancer tumour markers and biomarkers: Recent therapeutic advances. *World J. Gastroenterol.* **2016**, *22*, 1745–1755. [[CrossRef](#)]
86. Huang, Z.; Huang, D.; Ni, S.; Peng, Z.; Sheng, W.; Du, X. Plasma microRNAs are promising novel biomarkers for early detection of colorectal cancer. *Int. J. Cancer* **2010**, *127*, 118–126. [[CrossRef](#)]
87. Durán-Vinet, B.; Araya-Castro, K.; Calderón, J.; Vergara, L.; Weber, H.; Retamales, J.; Araya-Castro, P.; Leal-Rojas, P. CRISPR/Cas13-Based Platforms for a Potential Next-Generation Diagnosis of Colorectal Cancer through Exosomes Micro-RNA Detection: A Review. *Cancers* **2021**, *13*, 4640. [[CrossRef](#)]
88. Giessen, C.; Nagel, D.; Glas, M.; Spelsberg, F.; Lau-Werner, U.; Modest, D.P.; Michl, M.; Heinemann, V.; Stieber, P.; Schulz, C. Evaluation of preoperative serum markers for individual patient prognosis in stage I–III rectal cancer. *Tumor Biol.* **2014**, *35*, 10237–10248. [[CrossRef](#)] [[PubMed](#)]
89. Song, Y.F.; Xu, Z.B.; Zhu, X.J.; Liu, J.L.; Gao, F.L.; Wu, C.L.; Song, B.; Tao, X.; Lin, Q. Serum Cyr61 as a potential biomarker for diagnosis of colorectal cancer. *Clin. Transl. Oncol.* **2017**, *19*, 519–524. [[CrossRef](#)] [[PubMed](#)]
90. Bhardwaj, M.; Weigl, K.; Tikk, K.; Benner, A.; Schrotz-King, P.; Brenner, H. Multiplex screening of 275 plasma protein biomarkers to identify a signature for early detection of colorectal cancer. *Mol. Oncol.* **2020**, *14*, 8–21. [[CrossRef](#)]
91. Villar-Vázquez, R.; Padilla, G.; Fernández-Aceñero, M.J.; Suárez, A.; Fuente, E.; Pastor, C.; Calero, M.; Barderas, R.; Casal, J.I. Development of a novel multiplex beads-based assay for autoantibody detection for colorectal cancer diagnosis. *Proteomics* **2016**, *16*, 1280–1290. [[CrossRef](#)] [[PubMed](#)]
92. Hashim, N.A.A.; Ab-Rahim, S.; Ngah, W.Z.W.; Nathan, S.; Ab Mutalib, N.S.; Sagap, I.; Jamal, A.R.A.; Mazlan, M. Global metabolomics profiling of colorectal cancer in Malaysian patients. *BiolImpacts* **2021**, *11*, 33–43. [[CrossRef](#)]
93. Zhang, F.; Zhang, Y.; Zhao, W.; Deng, K.; Wang, Z.; Yang, C.; Ma, L.; Openkova, M.S.; Hou, Y.; Li, K. Metabolomics for biomarker discovery in the diagnosis, prognosis, survival and recurrence of colorectal cancer: A systematic review. *Oncotarget* **2017**, *8*, 35460–35472. [[CrossRef](#)]
94. Hata, T.; Takemasa, I.; Takahashi, H.; Haraguchi, N.; Nishimura, J.; Hata, T.; Mizushima, T.; Doki, Y.; Mori, M. Downregulation of serum metabolite GTA-446 as a novel potential marker for early detection of colorectal cancer. *Br. J. Cancer* **2017**, *117*, 227–232. [[CrossRef](#)]
95. Gu, J.; Xiao, Y.; Shu, D.; Liang, X.; Hu, X.; Xie, Y.; Lin, D.; Li, H. Metabolomics Analysis in Serum from Patients with Colorectal Polyp and Colorectal Cancer by 1H-NMR Spectrometry. *Dis. Markers* **2019**, *2019*, 3491852. [[CrossRef](#)]
96. Nishiumi, S.; Kobayashi, T.; Kawana, S.; Unno, Y.; Sakai, T.; Okamoto, K.; Yamada, Y.; Sudo, K.; Yamaji, T.; Saito, Y.; et al. Investigations in the possibility of early detection of colorectal cancer by gas chromatography/triple-quadrupole mass spectrometry. *Oncotarget* **2017**, *8*, 17115–17126. [[CrossRef](#)]
97. Theodoratou, E.; Thaçi, K.; Agakov, F.; Timofeeva, M.N.; Štambuk, J.; Pučić-Baković, M.; Vučković, F.; Orchard, P.; Agakova, A.; Din, F.V.N.; et al. Glycosylation of plasma IgG in colorectal cancer prognosis. *Sci. Rep.* **2016**, *6*, 28098. [[CrossRef](#)]
98. Doherty, M.; Theodoratou, E.; Walsh, I.; Adamczyk, B.; Stöckmann, H.; Agakov, F.; Timofeeva, M.; Trbojević-Akmačić, I.; Vučković, F.; Duffy, F.; et al. Plasma N-glycans in colorectal cancer risk. *Sci. Rep.* **2018**, *8*, 1–12. [[CrossRef](#)] [[PubMed](#)]
99. Pan, Y.; Zhang, L.; Zhang, R.; Han, J.; Qin, W.; Gu, Y.; Sha, J.; Xu, X.; Feng, Y.; Ren, Z.; et al. Screening and diagnosis of colorectal cancer and advanced adenoma by Bionic Glycome method and machine learning. *Am. J. Cancer Res.* **2021**, *11*, 3002–3020. [[PubMed](#)]
100. Coura, M.D.M.A.; Barbosa, E.A.; Brand, G.D.; Bloch, C.; Sousa, J.B. De Identification of Differential N-Glycan Compositions in the Serum and Tissue of Colon Cancer Patients by Mass Spectrometry. *Biology* **2021**, *10*, 343. [[CrossRef](#)] [[PubMed](#)]
101. Boland, C.R.; Thibodeau, S.N.; Hamilton, S.R.; Sidransky, D.; Eshleman, J.R.; Burt, R.W.; Meltzer, S.J.; Rodriguez-Bigas, M.A.; Fodde, R.; Ranzani, G.N.; et al. A National Cancer Institute Workshop on Microsatellite Instability for cancer detection and familial predisposition: Development of international criteria for the determination of microsatellite instability in colorectal cancer. *Cancer Res.* **1998**, *58*, 5248–5257.
102. Rocker, J.M.; DiPalma, J.A.; Pannell, L.K. Rectal Effluent as a Research Tool. *Am. J. Dig. Dis.* **2015**, *60*, 24–31. [[CrossRef](#)]
103. Heinzlmann, M.; Neynaber, S.; Heldwein, W.; Folwaczny, C. K-ras and p53 mutations in colonic lavage fluid of patients with colorectal neoplasias. *Digestion* **2001**, *63*, 229–233. [[CrossRef](#)]
104. Potter, M.A.; Morris, R.G.; Wyllie, A.H.; Ferguson, A. Detection of Mutations Associated With Colorectal Cancer in DNA From Whole-Gut Lavage Fluid. *JNCI J. Natl. Cancer Inst.* **1998**, *90*, 623–626. [[CrossRef](#)]
105. Shen, W.; Sun, J.; Yao, F.; Lin, K.; Yuan, Y.; Chen, Y.; Han, H.; Li, Z.; Zou, J.; Jiao, X. Microbiome in Intestinal Lavage Fluid May Be A Better Indicator in Evaluating The Risk of Developing Colorectal Cancer Compared with Fecal Samples. *Transl. Oncol.* **2020**, *13*, 100772. [[CrossRef](#)]

106. Yuan, Y.; Chen, Y.; Yao, F.; Zeng, M.; Xie, Q.; Shafiq, M.; Noman, S.M.; Jiao, X. Microbiomes and Resistomes in Biopsy Tissue and Intestinal Lavage Fluid of Colorectal Cancer. *Front. Cell Dev. Biol.* **2021**, *9*. [[CrossRef](#)]
107. Harada, T.; Yamamoto, E.; Yamano, H.-O.; Nojima, M.; Maruyama, R.; Kumegawa, K.; Ashida, M.; Yoshikawa, K.; Kimura, T.; Harada, E.; et al. Analysis of DNA Methylation in Bowel Lavage Fluid for Detection of Colorectal Cancer. *Cancer Prev. Res.* **2014**, *7*, 1002–1010. [[CrossRef](#)]
108. Park, Y.S.; Kim, D.S.; Cho, S.W.; Park, J.W.; Jeon, S.J.; Moon, T.J.; Kim, S.H.; Son, B.K.; Oh, T.J.; An, S.; et al. Analysis of Syndecan-2 Methylation in Bowel Lavage Fluid for the Detection of Colorectal Neoplasm. *Gut Liver* **2018**, *12*, 508–515. [[CrossRef](#)]
109. Brydon, W.G.; Ferguson, A. Haemoglobin in gut lavage fluid as a measure of gastrointestinal blood loss. *Lancet* **1992**, *340*, 1381–1382. [[CrossRef](#)]
110. Namavar, F.; Theunissen, E.B.M.; Vught, A.M.J.J.V.-V.; Peerbooms, P.G.H.; Bal, M.; Hoitsma, H.F.W.; MacLaren, D.M. Epidemiology of the *Bacteroides fragilis* group in the colonic flora in 10 patients with colonic cancer. *J. Med Microbiol.* **1989**, *29*, 171–176. [[CrossRef](#)] [[PubMed](#)]
111. Benson, A.B.; Venook, A.P.; Al-Hawary, M.M.; Arain, M.A.; Chen, Y.-J.; Ciombor, K.K.; Cohen, S.; Cooper, H.S.; Deming, D.; Farkas, L.; et al. Colon Cancer, Version 2.2021, NCCN Clinical Practice Guidelines in Oncology. *J. Natl. Compr. Cancer Netw.* **2021**, *19*, 329–359. [[CrossRef](#)] [[PubMed](#)]
112. Qian, Y.; Daza, J.; Itzel, T.; Betge, J.; Zhan, T.; Marmé, F.; Teufel, A. Prognostic Cancer Gene Expression Signatures: Current Status and Challenges. *Cells* **2021**, *10*, 648. [[CrossRef](#)] [[PubMed](#)]
113. Lin, P.-C.; Yeh, Y.-M.; Chan, R.-H.; Lin, B.-W.; Chen, P.-C.; Pan, C.-C.; Shen, M.-R. Sequential and co-occurring DNA damage response genetic mutations impact survival in stage III colorectal cancer patients receiving adjuvant oxaliplatin-based chemotherapy. *BMC Cancer* **2021**, *21*, 1–11. [[CrossRef](#)]
114. Wills, C.; He, Y.; Summers, M.G.; Lin, Y.; Phipps, A.I.; Watts, K.; Law, P.J.; Al-Tassan, N.A.; Maughan, T.S.; Kaplan, R.; et al. A genome-wide search for determinants of survival in 1926 patients with advanced colorectal cancer with follow-up in over 22,000 patients. *Eur. J. Cancer* **2021**, *159*, 247–258. [[CrossRef](#)]
115. Chiu, J.W.; Krzyzanowska, M.K.; Serra, S.; Knox, J.J.; Dhani, N.; Mackay, H.; Hedley, D.; Moore, M.; Liu, G.; Burkes, R.L.; et al. Molecular Profiling of Patients With Advanced Colorectal Cancer: Princess Margaret Cancer Centre Experience. *Clin. Color. Cancer* **2018**, *17*, 73–79. [[CrossRef](#)]
116. Guinney, J.; Dienstmann, R.; Wang, X.; De Reyniès, A.; Schlicker, A.; Sonesson, C.; Marisa, L.; Roepman, P.; Nyamundanda, G.; Angelino, P.; et al. The consensus molecular subtypes of colorectal cancer. *Nat. Med.* **2015**, *21*, 1350–1356. [[CrossRef](#)]
117. Berg, I.V.D.; Smid, M.; Braak, R.R.J.C.V.D.; van de Wiel, M.A.; van Deurzen, C.H.; de Weerd, V.; Martens, J.W.M.; Ijzermans, J.N.M.; Wilting, S.M. A panel of DNA methylation markers for the classification of consensus molecular subtypes 2 and 3 in patients with colorectal cancer. *Mol. Oncol.* **2021**, *15*, 3348–3362. [[CrossRef](#)]
118. Li, D.-H.; Du, X.-H.; Liu, M.; Zhang, R. A 10-gene-methylation-based signature for prognosis prediction of colorectal cancer. *Cancer Genet.* **2021**, *252*, 80–86. [[CrossRef](#)] [[PubMed](#)]
119. Zhou, Y.; Zang, Y.; Yang, Y.; Xiang, J.; Chen, Z. Candidate genes involved in metastasis of colon cancer identified by integrated analysis. *Cancer Med.* **2019**, *8*, 2338–2347. [[CrossRef](#)] [[PubMed](#)]
120. Gu, L.; Liu, Y.; Jiang, C.; Sun, L.; Zhou, H. Identification and clinical validation of metastasis-associated biomarkers based on large-scale samples in colon-adenocarcinoma. *Pharmacol. Res.* **2020**, *160*, 105087. [[CrossRef](#)] [[PubMed](#)]
121. Li, N.; Xiao, H.; Shen, J.; Qiao, X.; Zhang, F.; Zhang, W.; Gao, Y.; Liu, Y.D. SELE gene as a characteristic prognostic biomarker of colorectal cancer. *J. Int. Med. Res.* **2021**, *49*. [[CrossRef](#)] [[PubMed](#)]
122. Cheng, L.; Han, T.; Zhang, Z.; Yi, P.; Zhang, C.; Zhang, S.; Peng, W. Identification and Validation of Six Autophagy-related Long Non-coding RNAs as Prognostic Signature in Colorectal Cancer. *Int. J. Med. Sci.* **2020**, *18*, 88–98. [[CrossRef](#)]
123. Xi, G.; Ziyu, X.; Yiting, L.; Zonghang, L.; Lifeng, Z. Construction of competing endogenous RNA network and identification of novel molecular biomarkers in colon cancer: A bioinformatic analysis. *Medicine* **2021**, *100*, e25369. [[CrossRef](#)]
124. Buttacavoli, M.; Albanese, N.N.; Roz, E.; Pucci-Minafra, I.; Feo, S.; Cancemi, P. Proteomic Profiling of Colon Cancer Tissues: Discovery of New Candidate Biomarkers. *Int. J. Mol. Sci.* **2020**, *21*, 3096. [[CrossRef](#)]
125. Vasaikar, S.; Huang, C.; Wang, X.; Petyuk, V.A.; Savage, S.R.; Wen, B.; Dou, Y.; Zhang, Y.; Shi, Z.; Arshad, O.A.; et al. Proteogenomic Analysis of Human Colon Cancer Reveals New Therapeutic Opportunities. *Cell* **2019**, *177*, 1035–1049. [[CrossRef](#)]
126. Sethi, M.K.; Kim, H.; Park, C.K.; Baker, M.S.; Paik, Y.; Packer, N.H.; Hancock, W.S.; Fanayan, S.; Thaysen-andersen, M. In-depth N-glycome profiling of paired colorectal cancer and non-tumorigenic tissues reveals cancer-, stage- and EGFR-specific protein. *Glycobiology* **2015**, *25*, 1064–1078. [[CrossRef](#)]
127. Sethi, M.K.; Hancock, W.S.; Fanayan, S. Identifying N-Glycan Biomarkers in Colorectal Cancer by Mass Spectrometry. *Accounts Chem. Res.* **2016**, *49*, 2099–2106. [[CrossRef](#)]
128. Zhang, D.; Xie, Q.; Wang, Q.; Wang, Y.; Miao, J.; Li, L.; Zhang, T.; Cao, X.; Li, Y. Mass spectrometry analysis reveals aberrant N-glycans in colorectal cancer tissues. *Glycobiology* **2019**, *29*, 372–384. [[CrossRef](#)] [[PubMed](#)]
129. Boyaval, F.; van Zeijl, R.; Dalebout, H.; Holst, S.; van Pelt, G.; Fariña-Sarasqueta, A.; Mesker, W.; Tollenaar, R.; Morreau, H.; Wührer, M.; et al. N-Glycomic Signature of Stage II Colorectal Cancer and Its Association with the Tumor Authors N-Glycomic Signature of Stage II Colorectal Cancer and Its Association with the Tumor Microenvironment. *Mol. Cell Proteom.* **2021**, *20*, 100057. [[CrossRef](#)] [[PubMed](#)]

130. Marolla, A.P.C.; Waisberg, J.; Saba, G.T.; Waisberg, D.R.; Margeotto, F.B.; Pinhal, M.A.D.S. Glycomics expression analysis of sulfated glycosaminoglycans of human colorectal cancer tissues and non-neoplastic mucosa by electrospray ionization mass spectrometry. *Einstein* **2015**, *13*, 510–517. [[CrossRef](#)] [[PubMed](#)]
131. Krishn, S.R.; Kaur, S.; Smith, L.M.; Johansson, S.L.; Jain, M.; Patel, A.; Gautam, S.K.; Hollingsworth, M.A.; Mandel, U.; Clausen, H.; et al. Mucins and associated glycan signatures in colon adenoma–carcinoma sequence: Prospective pathological implication(s) for early diagnosis of colon cancer. *Cancer Lett.* **2016**, *374*, 304–314. [[CrossRef](#)] [[PubMed](#)]
132. Hu, W.; Yang, Y.; Li, X.; Huang, M.; Xu, F.; Ge, W.; Zhang, S.; Zheng, S. Multi-omics Approach Reveals Distinct Differences in Left- and Right-Sided Colon Cancer. *Mol. Cancer Res.* **2018**, *16*, 476–485. [[CrossRef](#)]
133. Yang, H.; Jin, W.; Liu, H.; Wang, X.; Wu, J.; Gan, D.; Cui, C.; Han, Y.; Han, C.; Wang, Z. A novel prognostic model based on multi-omics features predicts the prognosis of colon cancer patients. *Mol. Genet. Genom. Med.* **2020**, *8*, e1255. [[CrossRef](#)]
134. Théry, C.; Witwer, K.W.; Aikawa, E.; Alcaraz, M.J.; Anderson, J.D.; Andriantsitohaina, R.; Antoniou, A.; Arab, T.; Archer, F.; Atkin-Smith, G.K.; et al. Minimal information for studies of extracellular vesicles 2018 (MISEV2018): A position statement of the International Society for Extracellular Vesicles and update of the MISEV2014 guidelines. *J. Extracell. Vesicles* **2018**, *7*, 1535750. [[CrossRef](#)]
135. Ruiz-López, L.; Blancas, I.; Garrido, J.M.; Mut-Salud, N.; Moya-Jódar, M.; Osuna, A.; Rodríguez-Serrano, F. The role of exosomes on colorectal cancer: A review. *J. Gastroenterol. Hepatol.* **2018**, *33*, 792–799. [[CrossRef](#)]
136. Bracci, L.; Lozupone, F.; Parolini, I. The role of exosomes in colorectal cancer disease progression and response to therapy. *Cytokine Growth Factor Rev.* **2020**, *51*, 84–91. [[CrossRef](#)]
137. Zhou, J.; Li, X.-L.; Chen, Z.-R.; Chng, W.-J. Tumor-derived exosomes in colorectal cancer progression and their clinical applications. *Oncotarget* **2017**, *8*, 100781–100790. [[CrossRef](#)]
138. Umwali, Y.; Yue, C.-B.; Gabriel, A.N.A.; Zhang, Y.; Zhang, X. Roles of exosomes in diagnosis and treatment of colorectal cancer. *World J. Clin. Cases* **2021**, *9*, 4467–4479. [[CrossRef](#)]
139. Xiao, Y.; Zhong, J.; Zhong, B.; Huang, J.; Jiang, L.; Jiang, Y.; Yuan, J.; Sun, J.; Dai, L.; Yang, C.; et al. Exosomes as potential sources of biomarkers in colorectal cancer. *Cancer Lett.* **2020**, *476*, 13–22. [[CrossRef](#)] [[PubMed](#)]
140. Siveen, K.S.; Raza, A.; Ahmed, E.I.; Khan, A.Q.; Prabhu, K.S.; Kuttikrishnan, S.; Mateo, J.M.; Zayed, H.; Rasul, K.; Azizi, F.; et al. The Role of Extracellular Vesicles as Modulators of the Tumor Microenvironment, Metastasis and Drug Resistance in Colorectal Cancer. *Cancers* **2019**, *11*, 746. [[CrossRef](#)] [[PubMed](#)]
141. He, X.; Zhong, X.; Hu, Z.; Zhao, S.; Wei, P.; Li, D. An insight into small extracellular vesicles: Their roles in colorectal cancer progression and potential clinical applications An insight into small extracellular vesicles: Their roles in colorectal cancer progression and potential clinical applications. *Clin. Transl. Med.* **2020**, *10*, e249. [[CrossRef](#)] [[PubMed](#)]

Y por cierto, el propósito de la vida es aprender a imitar la llamada del tití. Venga, a
vivir.

Trenza del Mar Esmeralda. Bradon Sanderson

